DISCLAIMER

This report was prepared as an account of work sponsored by an agency of the United States Government. Neither the United States Government nor any agency thereof, nor any of their employees, makes any warranty, express or implied, or assumes any legal liability or responsibility for the accuracy, completeness, or usefulness of any information, apparatus, product, or process disclosed, or represents that its use would not infringe privately owned rights. Reference herein to any specific commercial product, process, or service by trade name, trademark, manufacturer, or otherwise does not necessarily constitute or imply its endorsement, recommendation, or favoring by the United States Government or any agency thereof. The views and opinions of authors expressed herein do not necessarily state or reflect those of the United States Government or any agency thereof. Reference herein to any social initiative (including but not limited to Diversity, Equity, and Inclusion (DEI); Community Benefits Plans (CBP); Justice 40; etc.) is made by the Author independent of any current requirement by the United States Government and does not constitute or imply endorsement, recommendation, or support by the United States Government or any agency thereof.

Final Technical Report (FTR)

a. *Federal Agency*	Department of Energy	
b. *Award Number*	DE-EE0009810	
c. *Project Title*	Design Basis Document / Owner's Technical Specification for Nitrate Salt Systems in CSP Projects	
d. *Recipient Organization*	Solar Dynamics LLC	
e. *Project Period*	Start: 05/01/2022	End: 10/31/2025
f. *Principal Investigator (PI)*	Bruce Kelly Senior Engineer Bruce.Kelly@SolarDynLLC.com 707 224-8929	
g. *Business Contact (BC)*	Hank Price Managing Director Hank.Price@SolarDynLLC.com 720 955-6404	

Bruce Kelly — *10/31/2025*

Signature of Certifying Official — *Date*

By signing this report, I certify to the best of my knowledge and belief that the report is true, complete, and accurate. I am aware that any false, fictitious, or fraudulent information, misrepresentations, half-truths, or the omission of any material fact, may subject me to criminal, civil or administrative penalties for fraud, false statements, false claims or otherwise. (U.S. Code Title 18, Section 1001, Section 287 and Title 31, Sections 3729-3730). I further understand and agree that the information contained in this report are material to Federal agency's funding decisions and I have any ongoing responsibility to promptly update the report within the time frames stated in the terms and conditions of the above referenced Award, to ensure that my responses remain accurate and complete.

1. Acknowledgements

This material is based upon work supported by the U.S. Department of Energy's Office of Energy Efficiency and Renewable Energy (EERE) Solar Energy Technologies Office (SETO) submitted under DE-FOA-0002378 Topic Area 4a: CSP: PERFORM, Technical Specifications, Control No: 2378-1549, with Award Number DE-EE0009810.

The subrecipients on the project are the Electric Power Research Institute and Malta.

We would like to acknowledge the contributions provided by the following organizations for their review of the draft report: Alia Energy, Atlantica Yield, Contratos y Diseños Industriales, Cerro Dominador, Crescent Dunes, Fichtner, High Temperature System Designs, National Renewable Energy Laboratory, Sandia National Laboratories, and Vast Energy. Finally, thanks to Shane Powers for his support and guidance on the project.

2. Disclaimer

This report was prepared as an account of work sponsored by an agency of the United States Government. Neither the United States Government nor any agency thereof, nor any of their employees, makes any warranty, express or implied, or assumes any legal liability or responsibility for the accuracy, completeness, or usefulness of any information, apparatus, product, or process disclosed, or represents that its use would not infringe privately owned rights. Reference herein to any specific commercial product, process, or service by trade name, trademark, manufacturer, or otherwise does not necessarily constitute or imply its endorsement, recommendation, or favoring by the United States Government or any agency thereof. The views and opinions of authors expressed herein do not necessarily state or reflect those of the United States Government or any agency thereof.

3. Executive Summary

The number of commercial coal, gas, and nuclear projects built over the past 100 years number in the thousands. As such, there is a large database, available to a wide range of commercial engineering contractors, on proven designs. In essence, unsuccessful designs have, through generations of iterations, been identified and then deleted from further consideration.

In contrast, the number of commercial parabolic trough projects using nitrate salt for the thermal storage media is perhaps 60. Further, the number of commercial central receiver projects using nitrate salt as the working fluid is on the order of 20, including estimates for China. Given the relative immaturity of salt technology, and commercial pressures to successfully bid new solar projects into a mature electricity market, solar projects often promise more than has been delivered.

The Design Basis Document / Owner's Technical Specification is a first step in the iteration process. The report describes the successful features of commercial projects, outlines a

range equipment and system failures in projects that didn't operate as intended, and provides a draft set of design changes intended to correct the known problems.

The product of the study is 3 volumes of technical material; one volume is on parabolic trough technologies; a second is on central receiver technologies, and the third is on potential design changes to parabolic trough and central receiver projects. The 3 volumes, which total some 590 pages, can be found at https://www.solardynllc.com/csp-plant-technologies.

One of the principal topics in the report is the use of functional or prescriptive specifications. Functional specifications describe what the equipment needs to do, consistent with the minimum legal requirements of the local jurisdictions. The details of how this is to be accomplished is developed by the engineering contractor. Prescriptive specifications, which are developed by the Owner, prescribe to the engineering contractor how the functional requirements are to be met. This arrangement ensures that the favorable experience from a previous project is repeated.

One example is the design code for the hot salt tank in central receiver projects. The closest design basis is API Standard 650 Welded Steel Tanks for Oil Storage. However, the maximum design temperature in API 650 is 260 °C. As such, solar projects have typically adopted a hybrid Code approach, in which allowable material stresses are taken from ASME Section II Materials. Further, since the tanks experience daily changes in temperature and in (static) pressure, and since portions of the tank can operate at stresses beyond the elastic range, the low cycle fatigue life of the tank is conducted using the rules of Section VIII Division 2. However, in a recent study by NREL, the principal damage mechanism was identified as creep rather than fatigue. Further, design stresses permitted under Section VIII Division 2, corresponding to a fatigue life of 30 years, result in projected creep lifetimes of only 2 to 5 years. An alternate design approach, prescribed by the Owner, would be based on Code sections intended for high temperature service in the creep regime. A candidate is Section III Division 5. Granted, this is a nuclear code section, and it's use would not likely be mandated by local jurisdictions. However, the effects of creep have been deemed to be of sufficient importance that one nuclear project developer, and one central receiver project developer, have stipulated in the tank design specification that the equipment be designed to the requirements of Section III Division 5.

Table of Contents

1. Acknowledgements 2
2. Disclaimer....2
3. Executive Summary 2
4. Background 12
5. Project Objectives 13
6. Project Milestones 15
7. Functional / Prescriptive Specifications for Parabolic Trough Projects using Organic Working Fluids....23
7.1 Introduction.... 23
7.2 Design Codes and Standards.... 24
7.3 Nitrate Salt Specification 25
7.3.1 Salt Composition.... 25
7.3.2 Grades 26
7.3.3 Allowable Contaminants 27
7.3.4 Supply Options.... 27
7.3.5 Deviations from a 60/40 Mixture 28
7.4 Nitrate Salt Handling and Melting Specification.... 29
7.5 General Salt System Equipment 30
7.5.1 Piping.... 30
7.5.2 Control and Isolation Valves 34
7.5.3 Check Valves.... 36
7.6 Oil to Salt Heat Exchanger 37
7.6.1 Equipment Design.... 37
7.6.2 Process Design.... 37
7.7 Thermal Storage Tank Weld Examinations 38
7.8 Heat Tracing.... 39
7.8.1 System Description.... 39
7.8.2 Scope of Supply.... 40
7.8.3 Electric Heat Tracing System Design Basis.... 41
7.8.4 Equipment Heat Tracing 46
7.9 Salt Pumps.... 50
7.10 Salt Instruments 51
7.10.1 Pressure Instruments.... 51
7.10.2 Flow Instruments 53
7.10.3 Temperature Instruments 54
7.10.4 Level Instruments 55
8. Functional / Prescriptive Specifications for Parabolic Trough Projects using Inorganic Working Fluids....56
8.1 Design Codes and Standards.... 56
8.2 Nitrate Salt Specification 57
8.2.1 Candidate Salt Options.... 57
8.3 Nitrate Salt Handling and Melting Specification.... 63
8.4 General Salt System Equipment 63

8.4.1 Piping 63
8.4.2 Flanges 66
8.5 Heat Tracing 66
8.6 Salt Pumps 67
8.7 Salt Instruments 67
8.8 Collector Field 67
8.8.1 Solar Collector Assemblies 67
8.8.2 Impedance Heating of Receiver Tubes and Flex Hose Assemblies 69
8.8.3 Resistance Heating of the Field Piping 76
8.9 Thermal Storage System 76
8.10 Steam Generation System 77
8.11 Steam Bypass System and Air Cooled Condenser Capacities 77
9. Functional / Prescriptive Specifications for Central Receiver Projects 78
9.1 Design Codes and Standards 78
9.2 Nitrate Salt Specification 79
9.3 General Salt System Equipment 79
9.3.1 Piping 79
9.4 Instruments 80
9.4.1 Flow Measurements 80
9.4.2 Pressure Measurements 81
9.4.3 Level Instruments 81
9.5 Salt Pumps 81
9.5.1 Configuration 81
9.5.2 Installed Redundancy 82
9.6 Receiver System 84
9.6.1 Design Codes 84
9.6.2 Material Selection 85
9.6.3 Tube Clip Design 86
9.6.4 Panel Vent Design 87
9.6.5 Downcomer Design 88
9.6.6 Assembly Location 88
9.6.7 Instruments 89
9.6.8 Non Destructive Examinations 89
9.7 Thermal Storage System 89
9.7.1 Introduction 89
9.7.2 Design Codes 90
9.7.3 Inputs to the Fatigue Analysis 90
9.7.4 Material Selection 91
9.7.5 Determination of the Floor Status Prior to the Start of Commercial Operation 92
9.7.6 Computational Fluid Dynamics Calculations 94
9.7.7 Combined CFD / FEA Calculations 97
9.7.8 Tank Venting 97
9.7.9 Foundations 99
9.7.10 Foundation Cooling 101
9.7.11 Methods for Emptying a Tank 102

9.8 Steam Generator 104
9.8.1 Introduction 104
9.8.2 Design Codes 104
9.8.3 Process Design 105
9.8.4 Material Selection 105
9.8.5 Fouling Factors 107
9.8.6 Feedwater Preheating 107
9.8.7 Evaporator Circulation 108
9.8.8 Fabrication Approaches 108
9.8.9 Commercially Acceptable Rates of Temperature Change 109
9.9 Steam Bypass System and Air Cooled Condenser Capacities 110
10. Oil-to-Salt Heat Exchangers in Parabolic Trough Projects 112
10.1 Configuration 112
10.2 Equipment Location 113
11. Problems and Solutions for Parabolic Trough Projects using Inorganic Heat Transfer Fluids 115
11.1 Temperature Control in the Collector Field During Non-Operating Periods 115
11.1.1 Introduction 115
11.1.2 Loss of Salt Circulation to the Solar Collector Assemblies 115
11.1.3 Loss of Site Electric Power to the Field Piping 115
11.1.4 Heat Trace System 115
11.1.5 Impedance Heating System 116
11.1.6 Continuous Salt Circulation 116
11.1.7 Loss of Circulation Leading to Freezing in Receiver Tubes and Flex Hose Assemblies 117
11.1.8 Freeze Recovery in the Receiver Tubes and Flex Hose Assemblies 118
11.1.9 Loss of Site Electric Power Leading to Salt Freezing in the Field Piping 120
11.1.10 Freeze Recovery in the Field Piping 120
12. Salt Tanks in Parabolic Trough Projects 123
12.1 Material Selection 123
12.2 Corrosion Characteristics 123
12.3 Survival Hypothesis for Carbon Steel Tanks 125
13. Stainless Steel Hot Salt Tanks in Central Receiver Projects 128
13.1 Representative Commercial Design 128
13.1.1 Tank 128
13.1.2 Foundation 128
13.2 Failure Patterns 129
13.3 Consequences of a Leak in the Floor 132
13.3.1 Heat Losses 132
13.3.2 Floor Stresses 133
13.3.3 NOx Production 133
13.3.4 Leak Detection System 134
13.4 Foundation Perimeter Stiffness 135
13.5 Floor Welding 137
13.5.1 Residual Stresses 137

13.5.2 Plate Deformations 138
13.5.3 Stress Relaxation 139
13.5.4 Post Weld Heat Treatment 140
13.6 Hydraulic Tests 141
13.6.1 Plate Stresses 141
13.6.2 Plate Deformations 142
13.7 Radial Temperature Distributions in the Floor 143
13.8 Tank Preheating 146
13.9 Tank Filling 147
13.10 Friction Between the Floor and the Foundation 148
13.10.1 Daily Thermal Cycles 148
13.10.2 Initial Thermal Expansion 149
13.10.3 Maximum Friction Deflections 149
13.10.4 Analytical Solution for Floor Stresses due to Friction 150
13.11 Salt Inlet Flow Distribution 162
13.11.1 Stresses Calculated from Analytical Expressions in Roark 162
13.11.2 Stresses Calculated from Finite Element Models 163
13.12 Operator Actions 166
13.13 Cumulative Effects 167
13.14 Solutions 167
13.14.1 Changes in the Tank Design Codes 167
13.14.2 Methods to Reduce Loads on the Floor 175
13.15 Lifetime Assessment 179
13.15.1 Fatigue Assessment 180
13.15.2 Corrosion Assessment 188
13.15.3 Creep Assessment 189
13.15.4 Subset of Creep Assessment in Weld Regions 190
13.15.5 Subset of Creep Assessment in Buckled Regions 192
13.15.6 Creep Assessment with Consideration of Residual Welding Stresses 194
13.15.7 Relaxation of Residual Stresses Prior to Tank Commissioning 195
13.15.8 Required Relaxation of Residual Stresses to Achieve a 30-Year Creep Life 197
13.15.9 Code Interpretation of Residual Stresses 199
13.15.10 Combined Fatigue and Creep Damage 201
13.15.11 Preliminary Lifetime Assessment 201
13.16 Material Selection 204
13.16.1 Stabilized and Non-stabilized Stainless Steel 204
13.16.2 Stress Relaxation Cracking in Type 347H 208
13.16.3 Stress Relaxation Cracking in Type 316LNB with Lean Austenitic Weld Filler 213
14. Nitrate Salt Steam Generators 214
14.1 Commercial Configuration 214
14.2 Heat Exchanger Location 215
14.3 Cold Reheat Steam Electric Heater 215
14.4 Cyclic Operation 215
14.5 Project Experience 217

14.5.1 Overnight Hold 217
14.5.2 Low Cycle Fatigue 217
14.5.3 Water Chemistry 219
14.5.4 Startup and Shutdown 221
14.6 Changes to the Equipment and the System Design 226
14.6.1 Process Design 226
14.6.2 Startup and Shutdown Procedures 230
14.6.3 Heat Exchanger Fabrication Techniques 237
14.6.4 Material Selection in the Evaporator 239
15. Valves in Salt Service 241
15.1 Valve Types 241
15.2 Stem Sealing 241
15.3 Triple Offset Butterfly Valves 242
15.4 Isolation Valves 243
15.5 Control Valves 243
15.6 Alternates to Globe and Triple Offset Butterfly Valves 243
16. Piping in Salt Service 244
16.1 Type 304H and Type 316H 244
16.2 Type 304L and Type 316L 244
16.3 Type 347H 245
16.3.1 Knife Line Attack 246
16.3.2 Post Weld Heat Treatment of Type 347H 246
16.4 Project Decisions 247
16.5 Pipe Maintenance 248
17. Electric Heat Tracing 249
17.1 Design Criteria 249
17.2 Control Software Location 250
17.3 Cable Redundancy 251
17.4 Control Thermocouples 253
18. Significant Accomplishments and Conclusions 254
18.1 Parabolic Trough Projects using Organic Heat Transfer Fluids 254
18.2 Parabolic Trough Projects using Inorganic Heat Transfer Fluids 254
18.3 Central Receiver Projects 254
19. Path Forward 255
20. Products 256
21. Project Team and Roles 257
22. References 257

List of Figures

Figure 6-1 Melting Point of Binary Nitrate Salt Mixtures 29
Figure 6-2 Pipe Support, Anchor, and Guide 33
Figure 6-3 Heat Trace Arrangement on Pipe at End of Zone 44
Figure 6-4 Typical Heat Trace Cable Arrangement on Valves 46
Figure 6-5 Elevation View of Salt Pump 49
Figure 6-6 Detail of Salt Pump Discharge Head and Bellows 49
Figure 6-7 Pressure Transmitter in a Vertical Process Line 52
Figure 6-8 Pressure Transmitter in a Horizontal Process Line 52
Figure 6-9 Flow Venturi with Diaphragm Pressure Transmitters 53
Figure 7-1 Cross Section of a Representative Ball Joint 68
Figure 7-2 Flex Hose in Shipping Container 69
Figure 7-3 Flex Hose Assembly Installed on a Prototype Collector 70
Figure 7-4 Electrical Resistance Network a Collector Loop 72
Figure 7-5 Midpoint Cable Wiring Arrangement 74
Figure 7-6 Collector Loop in a Potential Commercial Project 75
Figure 7-7 Portable Power Supplies for the Impedance Heating System 75
Figure 7-8 Conceptual Power Distribution with Staggered Polarity 76
Figure 8-1 Rate of Change in the Hot Tank Inventory Temperature Following a Receiver Trip 96
Figure 8-2 Effect of a Crossover Temperature 90 °C Lower than the Inventory Temperature 96
Figure 8-3 Thermal Stress due to Temperature Gradient 104
Figure 12-1 Longitudinal Residual Welding Stress 138
Figure 12-2 Plate Deformations due to Residual Welding Stresses 139
Figure 12-3 Radial Distribution of Heat Flux from the Floor in a Hot Salt Tank 144
Figure 12-4 Differential Element of the Floor 151
Figure 12-5 Radial and Tangential Floor Stresses for Case 0 154
Figure 12-6 Floor Stresses for Case 1: 21 m Tank Radius; 7 mm Floor Thickness 155
Figure 12-7 Initial Floor Stresses for Case 2: 21 m Tank Radius; 7 mm Floor Thickness 156
Figure 12-8 Final Floor Stresses for Case 2: 21 m Tank Radius; 7 mm Floor Thickness 157
Figure 12-9 Floor Stresses for Case 3: 21 m Tank Diameter; 7 mm Floor Thickness 158
Figure 12-10 Floor Stresses for Case 1: 15 m Tank Radius; 14 mm Floor Thickness 159
Figure 12-11 Initial Floor Stresses for Case 2: 15 m Tank Radius; 14 mm Floor Thickness 160
Figure 12-12 Final Floor Stresses for Case 2: 15 m Tank Radius; 14 mm Floor Thickness 161
Figure 12-13 Floor Stresses for Case 3: 15 m Tank Radius; 14 mm Floor Thickness 161
Figure 12-14 Differences in Floor Temperatures versus Time; 90° Circumferential Location 163

Figure 12-15 Differences in Floor Temperatures versus Time; Node 6 Between 45° and 90° 164
Figure 12-16 Differences in Floor Temperatures versus Time; Node 6 Between 90° and 135° 165
Figure 12-17 von Mises Stresses at Node 6 165
Figure 12-18 Larson Miller Diagram for the Stress to Develop 1 Percent Strain 172
Figure 12-19 Hot Tank Temperature Following a Failure of the Cold Tank Diversion Valve 178
Figure 12-20 S-N Curves for Type 316 Stainless Steel 180
Figure 12-21 Centerline Offset Misalignment of Butt Welds in Flat Plates 185
Figure 12-22 Angular Misalignment of Butt Weld Joints in Flat Plates 185
Figure 12-23 Definition of Dimension L in Figure 12-22 185
Figure 12-24 Adjustment Factor for Centerline Misalignment 186
Figure 12-25 Adjustment Factor for Angular Misalignment 186
Figure 12-26 Bulletin 541 Time to Rupture and Stress For Type 316/316H and Type 347H 190
Figure 12-27 Project Omega Time to Rupture and Associated Stress For Type 347H 191
Figure 12-28 Graphical Calculation of Larson Miller Coefficient C_{LMP} 191
Figure 12-29 True Stress as a Function of True Strain for Type 347H at 565 °C 193
Figure 12-30 Time to Rupture as a Function of Stress for Type 347H at 565 °C 194
Figure 12-31 Allowable Combinations of Fatigue and Creep Damage 202
Figure 12-32 Combined Creep and Fatigue Damage for Tank Radii Less than 75 Percent 203
Figure 12-33 Combined Creep and Fatigue Damage for Tank Radii Greater than 93 Percent 203
Figure 12-34 Image of a Precipitate Free Zone in the Weld Metal Near a Grain Boundary 209
Figure 12-35 Three-Step Post Weld Heat Treatment Time and Temperature Schedule 212
Figure 13-1 Salt Pump Arrangement in a Representative Commercial Project 222
Figure 13-2 Intra-Heat Exchanger Salt Valve Arrangement 222
Figure 13-3 Salt Pump Arrangement with Independent Steam Generator Trains 227
Figure 13-4 Intra-Heat Exchanger Salt Valve Arrangement 227
Figure 13-5 Steam Generator Heat Exchanger and Valve Arrangement 230
Figure 13-6 Step 0 - Overnight Hold 232
Figure 13-7 Step 1 - Isothermal Steam Production 233
Figure 13-8 Step 2 - Live Steam and Hot Reheat Steam Production 234
Figure 13-9 Example of Header / Coil Heat Exchanger Fabrication 238
Figure 13-10 Example of an Internal Bore Welded Tube-to-Tubesheet Connection 239

List of Tables

Table 6-1 Milestone Table 16
Table 8-1 Cation Parameters for Calcium, Lithium, Sodium, and Potassium 60
Table 8-2 Oxide Concentrations in Ternary Nitrate Salt Mixtures as a Function of Composition 61
Table 9-1 Salt Pump Fabrication Materials 82
Table 13-1 Stress Relief as a Function of Temperature 139
Table 13-2 Weld Surface Fatigue Strength Reduction Factors - Table 1 of 2 181
Table 13-3 Weld Surface Fatigue Strength Reduction Factors - Table 2 of 2 182
Table 13-4 Equations for Calculating the R Factors in the Equation for ΔS_p 184
Table 13-5 Fatigue Life Knockdown Factors 188
Table 16-1 Allowable Stresses (MPa) for 300-Series Stainless Steel Piping at 565 °C 245

4. Background

The number of commercial coal, gas, and nuclear projects built over the past 100 years number in the thousands. As such, there is a large database, available to a wide range of commercial engineering contractors, on proven designs. In essence, unsuccessful designs have, through generations of iterations, been identified, and then deleted from possible consideration.

In contrast, the number of commercial parabolic trough projects using nitrate salt for the thermal storage media is perhaps 60. Further, the number of commercial central receiver projects using nitrate salt as the working fluid is on the order of 20, including estimates for China. As such, commercial solar technologies have not progressed through the same number of design iterations as fossil and nuclear technologies. This results in 1) the persistence of problems normally seen with first-of-a-kind designs, and 2) a range of problems, yet unresolved, that preclude solar projects from reaching the availabilities required for market acceptance (92+ percent). The problem is compounded by levelized energy prices for solar projects which are often higher than energy prices for fossil projects. This can lead solar project developers to bid projects with low energy prices to attract the capital investment, but the prices are too low to fully reflect the performance risks inherent in an technology that is undergoing iteration.

On a related point, there are likely a range of performance requirements that a plant must satisfy to meet a competitive energy price, but the requirements impose a floor on the design features and the capital cost. One feature is the tube-to-tubesheet connection in a steam generator heat exchanger. As an example, the heat exchanger must tolerate 30,000 daily startup and shutdown cycles, at a temperature change rate of 12 °C/min, if the plant is to meet its annual performance target. Candidate tube-to-tubesheet connections include 1) rolled and strength welded, 2) internal bore welded, and 3) welded header/coil. Option 1 is the least expensive, but it can accommodate rates of temperature change of only 8 to 10 °C/min. Options 2 and 3 incur a cost premium of perhaps 30 percent over Option 1, but both can satisfy the transient requirements. As such, the project must select either Option 2 or Option 3, and reflect the higher capital cost in the energy sales price in the Power Purchase Agreement. If a project is to be successful, it cannot, as has been tried in other commercial projects, bid the low-cost steam generator option and then, through magical thinking, expect to match the projections in the performance model.

The Design Basis Document / Owner's Technical Specification is a first step in the iteration process. The report describes the successful features of commercial projects, outlines a range equipment and system failures in projects that didn't operate as intended, and provides a draft set of design changes intended to correct the known problems.

5. Project Objectives

The work proposed concentrates on a Design Basis Documents / Owner's Technical Specification for parabolic trough and central receiver power plants using nitrate salt as the heat transport fluid and the thermal storage medium. The goals are to:

- Distill the successful experience with nitrate salt systems from as many commercial projects as possible
- Provide technical bases for equipment design/selection that an owner can impose on an EPC contractor set of requirements, above and beyond those in the normal Codes and Standards, on an EPC contractor in an effort to avoid a repeat of past mistakes
- Compile this information in one location to provide guidance on salt systems that is as broadly applicable to as many projects as possible
- Work toward an industry consensus on a Design Basis Document.

If successful, this would allow salt systems to achieve the same levels of reliability and availability as commercial parabolic trough plants using diphenyl oxide / biphenyl (i.e., Dowtherm A, Therminol VP-1) as the heat transfer fluid.

The project deliverable consists of 3 volumes:

- Volume 1 - Specifications for Parabolic Trough Projects
- Volume 2 - Specifications for Central Receiver Projects
- Volume 3 - Narrative

Volumes 1 and 2 include discussions of the following topics:

- Plant functional requirements for the salt systems
- Plant operating states, and transitions between states, for the salt systems
- Risk analysis of the principal salt components
- Plant requirements for the salt systems to meet the functional and the operating requirements
- Type of specification for the principal salt components: functional; or prescriptive

- Current state of the art for salt systems.

Volume 3 discusses a number of cases in which the salt equipment at commercial parabolic trough and central receiver projects has not met the projected levels of reliability and availability. Possible reasons for the sources of the problems are discussed, as is a range of possible alternate designs that could avoid the known problems.

The Final Technical Report includes the following:

- A review of the project milestones

- A subset of the information presented in Volumes 1 and 2, concentrating on the functional and prescriptive specifications.

6. Project Milestones

The primary deliverable in the project is a report, consisting of the 3 volumes noted above. To verify that the report satisfies the goals of the project, a set of 10 milestones was developed. Of the 10 milestones, 8 were associated with the completion of the 8 principal technical tasks. The ninth milestone was an independent review of the draft reports, and the tenth milestone was the submittal of the final report to the OTSI website. A list of the milestones is presented in Table 6-1.

As defined in the Statement of Project Objectives, the independent review group was to consist of 1 project developer, 1 EPC contractor, and 2 other participants in the CSP industry, including project developers, EPC contractors, equipment vendors, and users of nitrate salt technology. The final makeup of the review group included the following organizations:

- Project developer: Vast Energy
- EPC contractors and consultants: Fichtner; Alia Energy; and High Temperature System Designs
- Equipment vendor: Contratos y Diseňos Industriales
- Users of nitrate salt technology: Atlantica Yield; Cerro Dominador; and Crescent Dunes
- National laboratories: National Renewable Energy Laboratory; and Sandia National Laboratories

The reviews of the draft report were conducted under Task 9. The reviews were generally favorable, and included a range of comments and recommendations. The comments and recommendations were incorporated in a revised final report. The revised report was reviewed by DOE, and was judged to have satisfied the Statement of Project Objectives and the End of Project Requirements.

Table 6-1 Milestone Table

Milestone	Performance Metric	Success Value	Assessment Tool / Method of Measuring Success Value	Verification Process	Milestone Confirmation
1	Report contents consistent with current industry versions of DBD/OTS.	DOE concurrence and review of public specifications	Side by side comparison of contents and independent DOE review	3 Tables of Contents provided to DOE for verification	Table of Contents for each Volume accepted by DOE
2.1	Selected information from existing Design Basis Documents. Basis of design are consistent with current commercial parabolic trough projects.	Functions and site conditions to be representative of commercial parabolic trough plants. Design represents 90 percent of commercial plant characteristics.	Third party intermediate project review in Milestone 9.1 agrees that all pertinent functions for parabolic trough plants are covered	Independent CSP industry review in Milestone 9.1	Functions and site conditions reviewed by independent CSP industry participants, and comments incorporated in the final report
2.2	Selected information from existing Design Basis Documents. Basis of design are consistent with current commercial central receiver projects.	Functions and site conditions to be representative of commercial central receiver plants. Design represents 90 percent of commercial plant characteristics.	Third party intermediate project review in Milestone 9.1 agrees that all pertinent functions for central receiver plants are covered	Independent CSP industry review in Milestone 9.1	Functions and site conditions reviewed by independent CSP industry participants, and comments incorporated in the final report
3.1	Selected information from existing Design Basis Documents are consistent with current commercial parabolic trough projects.	Functions and site conditions to be representative of commercial parabolic trough plants. Design represents a nominal 90 percent of commercial plant characteristics.	Third party intermediate project review in Milestone 9.1 agrees that all pertinent functions for parabolic trough plants are covered	Independent CSP industry review in Milestone 9.1	Operating modes and transitions reviewed by independent CSP industry participants, and comments incorporated in the final report

Milestone	Performance Metric	Success Value	Assessment Tool / Method of Measuring Success Value	Verification Process	Milestone Confirmation
3.2	Selected information from existing Design Basis Documents are consistent with current commercial central receiver projects	Functions and site conditions to be representative of commercial central receiver plants. Design represents a nominal 90 percent of commercial plant characteristics.	Third party intermediate project review in Milestone 9.1 agrees that all pertinent functions for central receiver plants are covered	Independent CSP industry review in Milestone 9.1	Operating modes and transitions reviewed by independent CSP industry participants, and comments incorporated in the final report
4.1	Probability * Consequence falls into 1 of 4 categories of importance for parabolic trough plants	Risk assessment conclusions are consistent with parabolic trough industry design experience, failure experience, patterns, and Codes and Standards, where applicable.	Subjective estimates based on public information, EPC experience, and Code guidance on the reliability and availability of salt components in parabolic trough plants.	Independent CSP industry review in Milestone 9.1	Risk assessment reviewed by independent CSP industry participants, and comments incorporated in the final report
4.2	Probability * Consequence falls into 1 of 4 categories of importance for central receiver plants	Risk assessment conclusions are consistent with central receiver industry design experience, failure experience, patterns, and Codes and Standards, where applicable.	Subjective estimates based on public information, EPC experience, and Code guidance on the reliability and availability of salt components in central receiver plants.	Independent CSP industry review in Milestone 9.1	Risk assessment reviewed by independent CSP industry participants, and comments incorporated in the final report
5.1	Public information on commercial parabolic trough projects, plus selected information	Completeness of design assessment, based on other representative parabolic trough	Third party intermediate project review in Milestone 9.1. Justify recommendations based, as much as possible, on	Independent CSP industry review in Milestone 9.1	Plant requirements to meet functional and operating requirements in parabolic trough projects reviewed by independent CSP industry

Milestone	Performance Metric	Success Value	Assessment Tool / Method of Measuring Success Value	Verification Process	Milestone Confirmation
	from existing Design Basis Documents	industry specifications, risk analysis, and a demonstration of which requirements have been successfully met.	commercially proven approaches for parabolic trough plants. Designs should be viewed as avoiding past failures.		participants, and comments incorporated in the final report
5.2	Public information on commercial central receiver projects, plus selected information from existing Design Basis Documents	Completeness of design assessment, based on other representative central receiver industry specifications, risk analysis, and a demonstration of which requirements have been successfully met.	Third party intermediate project review in Milestone 9.1. Justify recommendations based, as much as possible, on commercially proven approaches for central receiver plants. Designs should be viewed as avoiding past failures.	Independent CSP industry review in Milestone 9.1	Summary of commercial central receiver project designs reviewed by independent CSP industry participants, and comments incorporated in the final report
6.1	Those components which require unique design characteristics to meet availability targets for parabolic trough projects, and whose characteristics are not readily known within the broader EPC industry, should be prescriptive.	Prescriptive specifications transfer required information to, and limit flexibility of, EPC contractors new to the solar parabolic trough industry. Address all of the high risk items identified in Task 5.	Third party intermediate project review in Milestone 9.1. Success value is assured when all of the high risk items are discussed.	Independent CSP industry review in Milestone 9.1	Draft list of prescriptive specifications for parabolic trough projects reviewed by independent CSP industry participants, and comments incorporated in the final report
6.2	Those components which require unique design characteristics to meet availability targets for central receiver projects, and whose characteristics	Prescriptive specifications transfer required information to, and limit flexibility of, EPC contractors new to the solar central receiver industry.	Third party intermediate project review in Milestone 9.1. Success value is assured when all of the high risk items are discussed.	Independent CSP industry review in Milestone 9.1	Draft list of prescriptive specifications for central receiver projects reviewed by independent CSP industry participants, and comments incorporated in the final report

Milestone	Performance Metric	Success Value	Assessment Tool / Method of Measuring Success Value	Verification Process	Milestone Confirmation
	are not readily known within the broader EPC industry, should be prescriptive.	Address all of the high risk items identified in Task 5.			
7.1	Public information on commercial parabolic trough projects, plus selected information from existing Design Basis Documents, provides an accurate and complete description of current trough projects.	Completeness of design assessment, based on a industry comparison with existing commercial parabolic trough projects.	Third party intermediate project review in Milestone 9.2.	Independent CSP industry review in Milestone 9.2	The state of the art in commercial parabolic trough projects reviewed by independent CSP industry participants, and comments incorporated in the final report
7.2	Public information on commercial central receiver projects, plus selected information from existing Design Basis Documents, provides an accurate and complete description of current trough projects.	Completeness of design assessment, based on a industry comparison with existing commercial central receiver projects.	Third party intermediate project review in Milestone 9.2.	Independent CSP industry review in Milestone 9.2	The state of the art in commercial central receiver projects reviewed by independent CSP industry participants, and comments incorporated in the final report
8.1	Prescribed, proven, or credible parabolic trough alternates that justify a design change; i.e., avoid trying to fix what might be a fundamental flaw in the current approach	Alternate parabolic trough design has commercial experience regarding reliability and availability.	Public or vendor information on alternate parabolic trough designs; i.e., use at other projects, or prototype development.	Independent CSP industry review in Milestone 9.2	Prescriptive specifications and alternate parabolic trough designs reviewed by independent CSP industry participants, and comments incorporated in the final report

Milestone	Performance Metric	Success Value	Assessment Tool / Method of Measuring Success Value	Verification Process	Milestone Confirmation
8.2	Prescribed, proven, or credible central receiver alternates that justify a design change; i.e., avoid trying to fix what might be a fundamental flaw in the current approach	Alternate central receiver design has commercial experience regarding reliability and availability.	Public or vendor information on alternate central receiver designs; i.e., use at other projects, or prototype development.	Independent CSP industry review in Milestone 9.2	Prescriptive specifications and alternate central receiver designs reviewed by independent CSP industry participants, and comments incorporated in the final report
9.1	Formalized review assessment conducted at the completion of Tasks 2, 3, 4, 5, and 6	Review board to consist, as a minimum, of 1 project developer, 1 EPC contractor, and 2 other entities	Third party review determines that the functional description, operating modes, risk analysis, and plant requirements are complete and reasonable. Differences in opinions will be discussed and resolved to the extent possible.	Participation in the review by interested parties in the CSP industry	Drafts of Volumes 1 and 2 reviewed by independent CSP industry participants, and comments incorporated in the final report
9.2	Formalized review assessment conducted at the completion of Tasks 7 and 8	Review board to consist, as a minimum, of 1 project developer, 1 EPC contractor, and 2 other entities	Third party review determines that the current design description, and proposed alternate designs, are complete and reasonable. Differences in opinions will be discussed and resolved to the extent possible.	Participation in the review by interested parties in the CSP industry	Draft of Volume 3 reviewed by independent CSP industry participants, and comments incorporated in the final report
11	Submission of final report to OSTI.gov, and presentation of	Final report with identifiable e-link number, and presentations	Final report made available to the public within 90 days of project end date, and	DOE approval of final report, and DOE notification of	

Milestone	Performance Metric	Success Value	Assessment Tool / Method of Measuring Success Value	Verification Process	Milestone Confirmation
	results in public forums	conducted for conferences and webinars	presentation materials made available to the public	public presentations	
11.1	After DOE approval, final report is submitted to OSTI.gov	Final report is accepted by OTSI, with an identifiable e-link number	Available to public within 90 days of project end date. Verified and revised by SETO technology manager. Complete accounting of learnings over the life of the project. Citations to all public information created over the life of the project within the report.	DOE approval of final report	
11.2	Preliminary and final results are presented in public forums	Presentations are made at a minimum 1 conference and 1 webinar	Presentation materials are made available to the public	DOE invitation to, and notification of, public presentations	
EOP	Inclusion of all principal design and operating characteristics for commercial parabolic trough and central receiver projects. Risk analysis of principal salt components. Defining functional or prescriptive specifications for principal salt components. Analyzing current designs in terms of annual availability, and	Industry review, with a group consisting of 1 project developer, 1 EPC contractor, and 2 other participants in the CSP industry, including project developers, EPC contractors, equipment vendors, and users of nitrate salt technology.	Interest in the CSP industry to develop a common Design Basis Document for commercial plant designs	CSP industry participating in the review process	Drafts of Volumes 1, 2, and 3 reviewed by DOE and independent CSP industry participants, and comments incorporated in the final report

Milestone	Performance Metric	Success Value	Assessment Tool / Method of Measuring Success Value	Verification Process	Milestone Confirmation
	recommending possible design changes to reach availability targets. Work toward an industry concurrence on successful design features, and recommendations on alternate designs.				

7. Functional / Prescriptive Specifications for Parabolic Trough Projects using Organic Working Fluids

7.1 Introduction

Plant and equipment specifications fall into two broad categories:

- Functional specifications describe what the system or the equipment needs to do, consistent with the minimum legal requirements of the local jurisdictions. The details of how this is to be accomplished is developed by the engineering contractor. This allows the engineering contractor to define the process and the equipment designs such that the functional requirements can be met at the lowest cost

- Prescriptive specifications, which are developed by the Owner, prescribe to the engineering contractor how the functional requirements of the project are to be met. Prescriptive elements include items such as the process design, Code Section selection, fabrication techniques, materials selection, and component details. This arrangement ensures that the favorable experience from a previous project is repeated, and helps to avoid situations in which an inexperienced contractor repeats mistakes from earlier projects.

It can be noted that the use of prescriptive specifications often requires the following:

- The Owner must have a thorough understanding of the process and the technical features of the plant. For example, the heat trace designs in commercial projects often use 1 dual-element thermocouple in each zone as the input to the temperature set point controller. However, a heat trace design, which reflects the experience from previous projects, might use 2 to 4 thermocouples, distributed along the length of the zone, as inputs to the controller. This arrangement can help to detect defects in the insulation, local areas with temperatures below the freezing point of the salt, local areas which are receiving too much heat input from adjacent zones, and leakage past isolation valves.

- The Owner is prepared to accept what is likely to be an increase in the capital cost as a means of achieving the goals set in the performance and in the financial models. For example, the Owner may require the use of all-welded construction in salt heat exchangers. This fabrication approach is more expensive than the conventional approach; i.e., tube rolling followed by strength welding of the tube to the tubesheet. However, an all-welded design is more tolerant of the transient stresses associated with 1) daily startup and shutdown, and 2) mistakes made by the operators. In turn, the improvement in plant availability more than compensates for the marginal increase in the cost of the heat exchangers due to an all-welded design.

In the sections below is a list of the Design Codes and Standards, followed by a discussion of recommended prescriptive specifications.

7.2 Design Codes and Standards

For the salt components and equipment in a commercial project, reference codes and standards are listed below for the US market. If the plant is constructed outside of the US, an equivalent matrix will need to be developed for the host country.

Designation	Title
API	Standard 650, Welded Steel Tanks for Oil Storge
ASME	B31.1, Power Piping
ASME	Section I, Rules for the Construction of Power Boilers
ASME	Section II, Materials
ASME	Section V, Non Destructive Examination
ASME	Section VIII, Division 1, Rules for the Construction of Pressure Vessels
ASME	Section VIII, Division 2, Alternative Rules for the Construction of Pressure Vessels
ASTM	A105, Specification for Forgings, Carbon Steel, for Piping Components
ASTM	A181, Specification for Forgings, Carbon Steel for General Service
ASTM	A182, Specification for Forged or Rolled Alloy-Steel Pipe Flanges, Forged Fittings, and Valves and Parts for High-Temperature Service
ASTM	A192, Specification for Seamless Carbon Steel Boiler Tubes for High-Pressure Service
ASTM	A193, Specification for Alloy-Steel and Stainless Steel Bolting Materials for High-Temperature Service
ASTM	A194, Specification for Carbon and Alloy Steel Nuts for Bolts for High-Pressure and High-Temperature Service
ASTM	A213, Specification for Seamless Ferritic and Austenitic Alloy-Steel Boiler, Superheater, and Heat Exchanger Tubing
ASTM	A216, Specification for Steel Castings, Carbon, Suitable for Fusion Welding, for High-Temperature Service
ASTM	A240, Specification for Heat-Resisting Chromium and Chromium-Nickel Stainless Steel Plate, Sheet, and Strip for Pressure Vessels
ASTM	A312, Specification for Seamless and Welded Austenitic Stainless Steel Pipe
ASTM	A325, Specification for Structural Steel Bolts, Steel, Heat Treated, 120/125 ksi Minimum Tensile Strength
ASTM	A351, Specification for Castings Austenitic Austenitic-Ferritic (Duplex) for Pressure-Containing Parts
ASTM	A36, Specification for Carbon Structural Steel
ASTM	A387, Specification for Pressure Vessel Plates, Alloy Steel, Chromium-Molybdenum
ASTM	A403, Specification for Wrought Austenitic Stainless Steel Piping Fittings

ASTM	A500, Specification for Cold-Formed Welded and Seamless Carbon Steel Structural Tubing in Rounds and Shapes
ASTM	A506, Specification for Steel, Sheet and Strip, Alloy, Hot-Rolled and Cold-Rolled, Regular Quality and Structural Quality
ASTM	A516, Specification for Pressure Vessel Plates, Carbon Steel, for Moderate- and Lower-Temperature Service
ASTM	A53, Specification for Pipe, Steel, Black and Hot-Dipped, Zinc-Coated Welded and Seamless
ASTM	A556, Specification for Seamless Cold-Drawn Carbon Steel Feedwater Heater Tubes
HEI	Heat Exchange Institute
NEC	National Electric Code
NEMA	National Electrical Manufactures Association
NFPA	National Electric Code (NEC), National Fire Protection Association (NFPA)
TEMA	Tubular Exchanger Manufacturers Association, 8th Edition TEMA Standards
IBC	International Building Code

7.3 Nitrate Salt Specification

7.3.1 Salt Composition

Thermal storage systems in parabolic trough projects are an indirect design, in which the working fluid in the collector field (Therminol) is different than the working fluid in the storage system (an inorganic salt).

There are a wide range of inorganic salts suitable for use as the storage medium, including the following 6 candidates:

- Binary nitrate salt (solar salt) mixture, which is 60 weight percent sodium nitrate ($NaNO_3$) and 40 weight percent potassium nitrate (KNO_3)

- Ternary nitrate salt mixture, which, with contributions of 30 weight percent lithium nitrate ($LiNO_3$), 18 weight percent sodium nitrate ($NaNO_3$), and 52 weight percent potassium nitrate (KNO_3), offers the lowest melting point.

- Ternary nitrate/nitrite salt mixture, the most common of which is Hitec®, with contributions of 7 weight percent sodium nitrate ($NaNO_3$), 40 weight percent sodium nitrite ($NaNO_2$), and 53 weight percent potassium nitrate (KNO_3)

- A ternary nitrate salt mixture, Hitec XL®, with contributions of 42 weight percent calcium nitrate ($Ca(NO_3)_2$), 15 weight percent sodium nitrate ($NaNO_3$), and 43 weight percent potassium nitrate (KNO_3)

- A quaternary nitrate salt mixture, reviewed by Sandia National Laboratories, with contributions of 22 weight percent lithium nitrate ($LiNO_3$), 17 weight percent calcium nitrate ($Ca(NO_3)_2$), 18 weight percent by weight sodium nitrate ($NaNO_3$), and 43 weight percent potassium nitrate (KNO_3)

- A quinary nitrate/nitrite salt mixture, patented by Sandia National Laboratories, with contributions of 13 weight percent lithium nitrate ($LiNO_3$), 10 weight percent by weight sodium nitrate ($NaNO_3$), 12 weight percent potassium nitrate (KNO_3), 29 weight percent sodium nitrite ($NaNO_2$), and 36 weight percent potassium nitrite (KNO_2).

The ideal salt would have 1) a high upper temperature limit in terms of thermal stability, 2) a low freezing point, and 3) be inexpensive. As one might expect, none of the candidate salts fulfill all of the ideal requirements.

In a parabolic trough project, representative cold tank and hot tank temperatures are 292 °C and 385 °C, respectively. Each of the 6 candidate salts have upper temperature limits of at least 450 °C, and can readily satisfy the thermal stability requirements at the temperatures characteristic of the hot tank.

The cold tank temperature is dictated by the 1) final feedwater temperature of the Rankine cycle (~225 °C), 2) the approach temperature at the cold end of the steam generator economizer (55 to 60 °C), and the approach temperature at the cold end of the oil-to-salt heat exchanger (7 to 8 °C). The ternary nitrate salt, Hitec, Hitec XL, the quaternary nitrate salt, and the quinary nitrate/nitrite salt have freezing points which are 100 to 150 °C lower than the freezing point of the 60/40 salt mixture. However, the lower freezing points cannot be exploited in the storage system because the lowest system temperature (290 °C) is at least 50 °C higher than the candidate salt with the highest freezing point (~235 °C for the 60/40 mixture).

As such, the choice among the 6 candidate salts distills to one of cost, and the 60/40 mixture will always offer the lowest commodity pricing.

7.3.2 Grades

Sodium nitrate is available in refined, technical, and industrial grades, and potassium nitrate is available in refined and technical grades. The refined grades have the lowest impurities and the highest cost, while the industrial grades have the highest impurities and the lowest cost.

The principal impurity of interest are the chlorides, either in the form of chloride ions or the perchlorate. The mechanism for corrosion by chlorine and chloride was suggested

by Grabke et al [1]. Specifically, chlorine forms at the surface of the metal in contact with the salt. Through diffusion, chlorine congregates at the boundary between the inside of the corrosion scale and the parent metal. The chlorine reacts with the metallic elements, forming metal chlorides. The metal chlorides, which have high vapor pressures, evaporate and diffuse back out through the corrosion scale layer [2]. The metal chlorides, in contact with the salt, are oxidized to various metal oxides. This releases the chlorine to repeat the corrosion process. The chlorides act, in effect, as catalysts to accelerate the oxidation rates of the parent metal. In the paper by Grabke, the process was explained specifically in reference to iron based alloys, where various oxides, such as hematite (Fe_2O_3) or magnetite (Fe_3O_4), are formed.

In general, the technical grades of nitrate salt are suitable for parabolic trough applications, offering an acceptable compromise between purity, chloride corrosion rate, and cost.

A typical technical grade specification should include the following items:

- Minimum nitrate concentration of 99 percent by weight
- Maximum total chloride ion concentration from all sources of 0.2 percent by weight.

7.3.3 Allowable Contaminants

Maximum contamination from all sources, by weight, will be:

Nitrite: < 0.02 percent
Carbonate: < 0.10 percent
Sulfate: < 0.01 percent
Hydroxyl alkalinity: < 0.20 percent
Perchlorate: < 0.085 percent
Magnesium: < 0.035 percent.

The specification should also state that notification shall be provided for any contaminants not listed above which exceed a concentration of 0.04 percent by weight.

7.3.4 Supply Options

The salt may be supplied in one of two forms:

Option 1: The sodium nitrate is delivered in separate bags from the potassium nitrate. The project is responsible for mixing the two components in the required 60/40 mixture, melting the solid mixture, and loading in salt in the storage system

[1] Grabke, H.J., E. Reese, and M. Spiegel, *Effects of chlorides, hydrogen chloride, and sulfur dioxide in the oxidation of steels below deposits*. Corrosion Science, 1995. 37(7): p. 1023-1043
[2] Williams, D.F., *Assessment of Candidate Molten Salt Coolants for the NGNP/NHI Heat-Transfer Loop*, 2006, Oak Ridge National Laboratory

Option 2: The salt supplier mixes the components, melts the solid mixture, solidifies the liquid mixture in the form of a prill, and delivers the prills to the site. The project is responsible for melting the prills and loading the salt in the storage system.

Option 1 can offer a slight discount in the price of the salt. However, the material handling requirements and costs can be substantial. In addition, the project must have the equipment to treat a one-time emission of oxides of nitrogen. Specifically, all commercial grades of salt contain trace amounts of magnesium. Magnesium is soluble in nitrate salt, appearing as magnesium nitrate. Upon heating, the magnesium nitrate decomposes via the following irreversible reaction:

$$Mg(NO_3)_2 \Rightarrow MgO + 2\ NO_2 + \tfrac{1}{2}\ O_2$$

The magnesium oxide is insoluble in the salt, and forms a solid precipitate. The NOx has a very low solubility in the salt, and essentially all of the NOx appears as a gas in the ullage space above the liquid level. A typical commercial project might require 30,000 metric tons of salt. The magnesium concentration in the technical grade of the salt is a nominal 0.035 percent by weight, which translates to about 10,000 kg (410 kg mole) of magnesium. The decomposition reaction produces 2 moles of NOx per mole of magnesium, which results in the generation of about 38,000 kg of NOx. Some form of NOx capture and treatment system will be required to both meet environmental regulations and to ensure worker safety. The least complex approach is probably a water spray column, in which water reacts with NOx to form nitric acid, N_2NO_3. The acid is neutralized with a base, and then shipped offsite for disposal.

Under Option 2, the process of melting and mixing the components to form prills will promote the magnesium decomposition reaction. As such, the one-time production and treatment of NOx will be the responsibility of the salt supplier rather than the responsibility of the project. This division of responsibility will be reflected in the cost of the salt delivered to the project.

As part of the procurement process, the engineering contractor will need to conduct an economic analysis to determine which of the two supply options offers the lowest total cost to the project.

7.3.5 Deviations from a 60/40 Mixture

Under either Option 1 or Option 2, the final composition is likely to vary slightly from the desired 60/40 mixture. In principle, property tables and relationships could be developed for the exact salt mixture at the project. However, the properties are not strongly influenced by mixture fractions, which are often in the range of 58/42 to 62/48 for commercial projects. An example is the melting point, as shown in Figure 7-1.

Other properties, specifically the density, can be estimated by adjusting the 60/40 properties based on molar volumes, as described by Bradshaw [3].

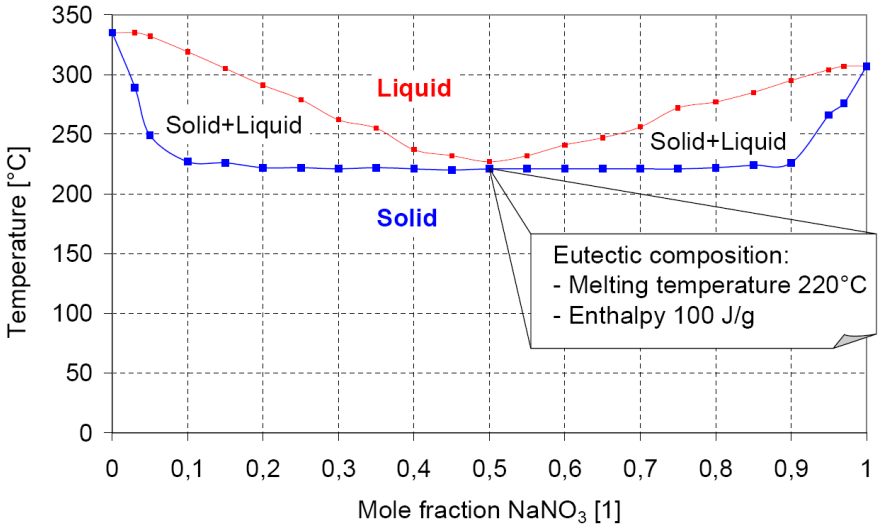

Figure 7-1 Melting Point of Binary Nitrate Salt Mixtures

7.4 Nitrate Salt Handling and Melting Specification

Nitrate salt is hygroscopic, and absorbs moisture from the air during transit and when stockpiled for melting.

In trough projects, the design temperature of the hot salt tank is on the order of 395 °C. During the salt melting process, the temperature of the liquid salt is raised to something less than the design temperature of the hot tank; perhaps, 350 °C.

The salt, as delivered, contains 0.01 to 0.05 percent magnesium nitrate, depending on the purity. At temperatures of 550 °C and above, the magnesium nitrate, in a period of several days, decomposes via the following reaction:

$$Mg(NO_3)_2 \rightarrow MgO + 2\ NO_2 + \tfrac{1}{2}\ O_2$$

The magnesium oxide precipitates as a solid, and the NO_2 and the O_2 leave the salt as gases.

The magnesium nitrate concentration is only a fraction of a percent; however, each mole of magnesium nitrate produces two moles of NO_2. For a plant with a storage mass

[3] Bradshaw, R. W., (Sandia National Laboratories, Albuquerque, New Mexico), "Effect of Composition on the Density of Multi-Component Molten Nitrate Salts", Sandia Report SAND2009-8221, December 2009

of 35,000 metric tons, the total NO_2 production will range from 2,000 to 11,000 kg, depending on the purity of the salt.

In a trough project, the salt, after melting, is loaded into the storage tanks. However, the temperature of the salt is perhaps in the range of 275 to 350 °C, depending on the capacity of the tank electric heaters. As such, the magnesium decomposition rate is much slower than would occur at a temperature of 550 °C; certainly on the time span of months. Further, the water that is adsorbed by the salt in transit and in storage does not leave the salt during, and immediately after, the melting process. Anecdotal evidence suggests that the time required to release the water from the salt is measured in weeks. As such, within the liquid inventory of the salt, NO_2 produced from magnesium decomposition comes into contact with H_2O released from the salt. The two combine to form nitric acid, H_2NO_3. The nitric acid is released from the salt in the form of a gas. Further, the gas can condense on any surface with temperatures below about 80 to 90 °C. Since nitric acid has a dew point higher than water vapor, any warm surface on which the vapor condenses will essentially be pure acid. Nitric acid samples collected from a commercial project during commissioning showed pH values in the range of 1 to 2.

With the exception of the heat transfer surfaces in the oil-to-salt heat exchanger, essentially everything in the storage system is fabricated from carbon steel. Nitric acid in contact with carbon steel results in high corrosion rates, with the highest rates measured in mm per month.

The specification for salt handling and melting must include the following provisions:

- To prevent damage to the carbon steel equipment which is exposed to the ullage gas in the storage tanks, the equipment must be maintained at a temperature of at least 250 °C for a period of several months after the salt is loaded into the storage tanks. A temperature of 250 °C prevents the condensation of both nitric acid and salt vapors.

- If the equipment cannot be maintained at a temperature of 250 °C, then the equipment must be fabricated from a material which is resistant to nitric acid corrosion, such as stainless steel.

7.5 General Salt System Equipment

7.5.1 Piping

Design Codes

The nitrate salt piping can be designed to the requirements of either ASME B31.1 - Power Piping or ASME B31.3 - Process Piping.

B31.1, compared with B31.3, is more conservative in terms of material specifications, stress intensity factors, stress design factors, and radiographic inspections. In the interests of providing reliable piping systems, at least two commercial central receiver projects have selected B31.1 as the design code for the salt piping in the receiver system. This includes the cold salt pump discharge piping, the riser, the inter-panel piping, the vent lines, the drain lines, and the downcomer.

In a parabolic trough plant using an organic heat transfer fluid, the salt piping is limited to the thermal storage system. The pipe lengths and quantities are relatively small, and the potential cost premium between selecting B31.1 or B31.3 is likely to be modest. However, the design temperatures and the rates of temperature change in the trough storage system are modest compared to central receiver projects. To some extent, these characteristics could influence the decision regarding the design code for the piping. At least one commercial parabolic trough project has selected B31.3 for the design of the salt piping in the storage system.

Materials

The cold salt and the hot salt piping is typically ASTM A106 Gr B or Gr C, with a nominal corrosion allowance of 1.6 mm (1/16 in.).

Connections, Sizes, and Schedules

End connections for salt piping will be butt welded joints, except in the following locations:

- Salt pump discharge nozzles. Flanged connections using ring-type joints are permitted.

- Salt tank nozzle connections to the gas space inside the roof.

The minimum system piping diameter shall be DN 100 (4 in.) to reduce the potential for salt freezing due to damaged insulation or due to reduced heat trace capacity.

For both cold salt and hot salt service, the minimum schedule for DN 100 (4 in.) lines is Schedule 40. The goal is to provide sufficient bending stiffness to limit sagging and to prevent sections in the line which may not fully drain.

For lines larger than DN 100, the minimum Schedule is 20. The goal is to provide enough stiffness at the ends of pipe such that normal handling of the pipe does not cause the ends to become oval, which would make lineup and fitment prior to welding problematic.

All pipe will be specified as seamless to provide as much resistance to fatigue damage as possible.

Flanges

Flanges in salt service may be of the following types: ring type joint; or hub type. No other types of flanges, such as raised face flanges, will be used due to the potential for relaxation of the bolted connection and leakage past the gasket due to the excellent wetting characteristics of the salt. Ring type joint gaskets and hub rings will be ASTM A182 Gr F21.

Stud bolts used at temperatures below 400 °C will be specified as ASTM A193 Gr 7.

Fittings

Butt weld fittings will be used in salt service in all pipe sizes.

The following fittings are not suitable for salt service:

- Compression fittings. Salt in contact with the threads and the ferrules will develop corrosion layers. Over time (months), the corrosion layers will merge, which will make disassembly of the fitting impossible

- Flat face and raised face flanges. The flanges rely on a gasket to provide the seal. However, salt is an excellent wetting agent, and no gasket material has yet been identified that is impervious to salt intrusion and seepage. Further, should salt come into contact with the flanges bolts and nuts, corrosion between the threaded regions will make disassembly impossible

- Socket welded connections. The wall thickness of the socket is the roughly the same as the wall thickness of the adjacent piping. As such, the combined wall thickness of the pipe / socket is nominally double the wall thickness of the piping. The plant operates under daily thermal cycles, with rates of temperature change as high as 360 °C/min. A pipe / socket combination subject to a thermal transient will establish a radial temperature gradient through the pipe / socket. The gradient will be the largest near the bottom of the socket due, in part, to the air gap between the outside of the pipe and the inside of the socket. The gradient will be the smallest at the weld connecting the outside of the pipe and the end of the socket. The cyclic radial temperature gradients will establish cyclic longitudinal gradient in the fitting, which will impose longitudinal sheer and bending stresses on the welds. Over time, this can result in a low cycle fatigue failure of the fitting weld.

Pipe Supports, Anchors, and Guides

Pipe supports, anchors, and guides are subjected to daily thermal expansion and contraction cycles.

At the Solar Two project, insulated pipe supports, using an external metal clamp with a calcium silicate insert between the pipe and the clamp, had an effective life of perhaps 1 year before the insert worked loose from the clamp. Alternate designs, using a radial fin to positively locate the insert within the clamp, also failed due to fracturing of the insert.

Following the Solar Two project, changes have been made to insulated pipe supports, including the use of refractory inserts with a higher crush strength. If a project plans to use insulated pipe supports, then surveys should be conducted of commercial projects where the proposed pipe supports are already in use. This will assist the engineering contractor in 1) determining which locations are suitable for insulated supports, and 2) specifying the refractory materials for the support.

Nonetheless, there are likely to be locations where insulated supports will not provide the required stiffness, strength, or cyclic lifetime in locations which are difficult to access (i.e., along the length of the downcomer). An alternate design for the supports, anchors, and guides uses a metal web, welded directly to the pipe. The web, in turn, is welded to a base plate. A portion of the web is removed to reduce conduction heat transfer through the web. The basic design is illustrated in Figure 7-2.

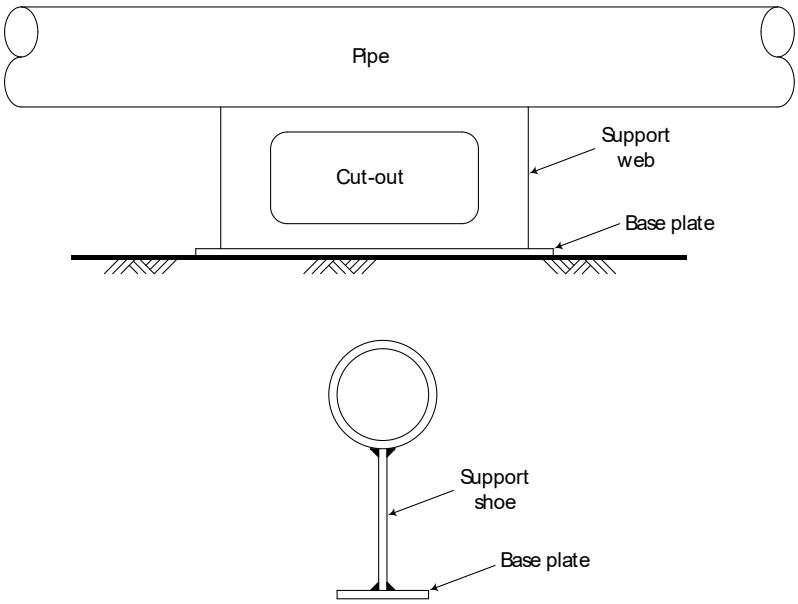

Figure 7-2 Pipe Support, Anchor, and Guide

The heat losses at the support will be greater than the heat losses in the adjacent pipe. As such, additional heat trace will need to be provided at the supports to ensure adequate pipe temperatures.

For pipe supports handling strictly vertical loads, without the possibility of a lateral component, conventional spring hangers are recommended.

7.5.2 Control and Isolation Valves

In general, the use of control and isolation valves in salt service should be held to the minimum.

Process Design

In general, valves in salt service are a major contributor to plant forced outages. One of the principal goals of the process design is to develop an equipment arrangement that uses as few salt valves as possible.

Extended Bonnets

Valves for service at temperatures above 350 °C will be specified with extended bonnets to ensure that the packing temperature does not exceed 200 °C in the absence of supplemental heat from the bonnet heat trace system. A heat trace zone, dedicated to the bonnet region, maintains the packing temperature in the desired range of 275 °C to 300 °C.

Valve Types

A salt corrosion layer develops on the plugs and the seats of all valves. For gate and ball valves, the two sealing surfaces slide across one another. When the corrosion layers develop, particularly with the valves in the closed position, the corrosion layers can lead to binding and erratic valve motion. As such, gate and ball valves are not suitable for salt service. For globe and offset butterfly valves, the plugs move perpendicular to the seats, and the development of the corrosion layers are less likely to interfere with the motion of the valve.

Globe and offset butterfly valve seats and disks will have Stellite® faces. Nonetheless, hardened surfaces will corrode in salt service. Over time, the valve will fail to provide leak-tight service, and the equipment downstream of the valve must be able to operate safely with a small, but continuous, flow of salt. For example, vent valves for heat exchangers should be located at the top of the vent line to allow leakage past the valve to drain to a storage tank.

A number of items can be noted from the experience with salt valves at commercial projects:

- The commercial experience with triple offset butterfly valves in isolation service has been decidedly mixed. The valves have a low ratio of 'thickness to diameter'. Pipe loads transferred to and through the valve body can be higher

than expected due, for example, to 1) forcing the pipe into alignment with the valve body prior to welding, or 2) deteriorations in the pipe supports, anchors, or guides. This, in turn, can lead to flexing and distortion of the valve seat, in which case the valve can develop an internal leak. At one commercial project, leakage rates after about 2 years of service were such that the triple offset valves were replaced by globe valves

- In general, globe valves provide more consistent sealing characteristics because the valve body is rigid, which 1) reduces deflections of the body and the seat due to piping forces, and 2) keeps the plug and the seat in alignment.

- For a given pipe size, globe valves are likely to be more expensive, and in some cases much more expensive, than triple offset butterfly valves. However, if the plant experiences a forced outage to replace one or more triple offset butterfly valves, then the lost revenue can be on the order of $1,000,000 per week. In general, the improvement in the plant availability associated with selecting globe valves during the design phase will justify the marginal increase in the capital cost for the globe valves.

Stem Seals

For globe valves, the preferred stem seal, by a considerable margin, is a metal bellows. The bellows, although expensive, provide a hermetic stem seal. Hermetic seals are important, as leakage past the valve stem will expose the heat trace cables on the valve body and the adjacent piping to salt. The cables operate at temperatures which are high enough (> 650 °C) to decompose the salt. Several of the decomposition products are various oxides, which aggressively corrode the outer metal covering on the heat trace cables. Corrosion lifetimes are often measured in weeks. Once the covering corrodes, the internal heating cables are exposed to moisture, and can fail in a matter of days. Failed cables lead to immovable valves and frozen salt piping, which can necessitate forced outages, lasting hours to days. A project economic analysis will often show that the marginal improvement in plant availability and revenue, due to a properly functioning heat trace system, justifies the marginal expense for bellows stem seals.

The bellows should have a minimum fatigue life of 10,000 cycles, and should be replaceable with the valve in place. The bellows region will require both heat tracing and insulation. If available, a pre-engineered bellows enclosure should be procured from the valve supplier.

The bellows is designed to withstand the maximum salt pressure expected in the valve body. In some applications, the maximum pressure may occur following a tube leak in a heat exchanger.

The primary bellows stem seal should be supplemented with a backup conventional stem packing, as described below.

For offset butterfly valves, bellows stem seals are not an option, and a conventional stem packing must be used. However, carbon and graphite materials used in standard bonnet packings are only marginally acceptable in salt service. The salt is an oxidizing material, and reacts with the carbon and graphite to form CO_2. To date, the valve stem packing which offers the longest, but nonetheless marginal, service life consists of alternating layers of the following:

- Wire-reinforced graphite braid packing over a fiberglass core: Style 1200-PBI from Garlock Engineering, or Style 387I from John Crane, Inc.

- Fiberglass-filled Teflon® washers.

The allowable temperature range for the materials is 260 °C to 315 °C. The lower temperature limit is to prevent salt from freezing; the upper limit is to prevent the Teflon from decomposing. Teflon, as it decomposes, produces fluorine gas, which aggressively attacks the valve stem material. Note that the stem packing relies on graphite, and will require periodic replacement, regardless of the valve temperature.

Bonnet Gaskets

For split-body globe valves, the bonnet gaskets should be either metallic ring type (carbon core with a soldered silver sheath), or welded spiral wound.

7.5.3 Check Valves

A conventional check valve can be provided in the discharge line of a salt pump for the following purposes:

- Should a pump trip, the check valves prevents a reverse flow through the pump, and protects against an overspeed condition in reverse rotation

- During steam generator startup, hot salt is blended with cold salt by operating the hot salt pump in parallel with the cold salt attemperation pump. At the start of the blending process, the pressure at the discharge of the hot salt pump is slightly lower than the pressure at the discharge of the attemperation pump. The speed of the hot salt pump is then increased until the discharge pressure of the hot salt pump is a few Pa higher than the discharge pressure of the attemperation pump. A check valve at the discharge of the hot salt pump 1) prevents a reverse flow though the hot salt pump when the discharge pressure of the hot salt pump is less than the discharge pressure of the attemperation pump, and 2) helps to accurately control the relative flow rates of hot salt and cold salt when the hot salt pressure is only slightly greater than the cold salt pressure.

As with all salt valves, corrosion layers will develop on the flap, the seat, and the pivot of the check valve. If the valve remains in the closed position for an extended period of time (weeks to months), then the corrosion layers on the internal components can merge, which would leave the check valve immovable.

As with globe and triple offset butterfly valves, the flap in the check valve moves perpendicular to the seat, which reduces the potential for the corrosion layers on the flap and the seat to merge. Nonetheless, the only effective means of preventing problems with corrosion is to periodically open and close the valve.

7.6 Oil to Salt Heat Exchanger

7.6.1 Equipment Design

The oil-to-salt heat exchanger necessarily undergoes a daily startup and shut down cycle. Further, the higher the allowable transient heating and cooling rate (°C/min) and the higher the allowable thermal shock value, (°C), the more thermal energy can be stored each day for electric power production.

The heat exchanger concept with the highest tolerance for cyclic thermal stresses is perhaps an all-welded design. Examples include the header/coil approach, and the internal bore welded design, each of which are discussed in Section 9.8.8, Fabrication Approaches.

7.6.2 Process Design

To ensure that the heat exchanger reaches its projected fatigue life, the process design must ensure that the transient heating and cooling rates, and the thermal shocks, are maintained within the limits set by the vendor. To this end, the process design should include the following set of features:

- During Hold periods, cold salt is supplied to the cold end of the heat exchanger. The flow of Therminol through the heat exchanger is suspended to reduce the potential for cold Therminol from the collector field freezing salt in the heat exchanger. As such, no heat transfer occurs, and the salt leaving the hot end of the heat exchanger is returned to the cold tank through a recirculation line.

- Included in the design is a Therminol mixing at the hot end of the heat exchanger. At the beginning of a charge cycle, cold Therminol from the discharge of the Therminol pumps is mixed with hot Therminol from the collector field at the mixing station. The blending process controls the rate of temperature increase in the heat exchanger during the transition from Hold to Charge, and reduces the magnitude of any thermal shocks.

- Also included in the design is a salt mixing station at the hot end of the heat exchanger. At the end of a Discharge period, cold salt from the cold salt pump is mixed with hot salt from the hot salt pump at the mixing station. The blending process controls the rate of temperature decrease in the heat exchanger during the transition from Discharge to Hold.

- During the Hold period, the flow rate of salt is set to a value which is equal to, or greater than, the minimum flow rate specified by the vendor. During normal operation, the heat exchanger is always operated at a combination of salt flow rate and Therminol flow rate that satisfies the vendor flow rate requirement. As a consequence, the minimum flow rate criterion on the salt side is automatically satisfied both during the Hold period, and during the transition from Discharge to Hold.

- Included in the design is a bypass line on the Therminol side of the heat exchanger. During heat exchanger startup, the bypass line would operate as follows:

    - For collector field outlet temperatures less than the cold salt temperature, the isolation valve in the bypass line is open, and the flow of Therminol bypasses the heat exchanger
    - When the collector field outlet temperature reaches the cold salt temperature, the isolation valve is closed, and a flow of Therminol is established in the heat exchanger. The flow rate is large enough to satisfy the minimum flow rate specified by the vendor. Since the temperature of the salt is equal to the temperature of the Therminol, no heat transfer occurs. As a result, during the period in which the flow rate of Therminol increases from an initial value of zero to a final value equal to the minimum flow rate, the heat exchanger is operating under isothermal conditions. As such, the potential for developing damaging transient thermal stresses is very low.

7.7 Thermal Storage Tank Weld Examinations

The floors in the thermal storage tanks are constructed from an array of rectangular plates. The nominal plate dimensions are 2.5 m by 12.5 m. Representative plate thicknesses are in the range of 7 to 10 mm, and two weld passes are typically required.

The allowable tolerances on the dimensions of the plates are presented in ASTM A568/A568M-19a, Standard Specification for Steel, Sheet, Carbon, Structural. Since all of the plates are not exactly the same size and shape, the dimensions of the gaps between adjacent plates will vary. To provide consistent inter-plate welds, backing strips are welded to the backs of alternating plates prior to arranging the plates on the foundation.

The storage tanks are subjected to daily thermal cycles, which results in cyclic loads on the floor generated by friction and radial temperature gradients. For the tanks in parabolic trough projects, it's not clear if a low cycle fatigue analysis is required. However, if such an analysis is justified, then the fatigue properties of the weld are subject to a weld fatigue strength reduction factor. The topic is discussed in Section 5.13.2, Fatigue Strength Reduction Factors, of Volume 3 - Narrative.

To improve the calculated fatigue life of the floor, the reduction factors should be a low as practical. The smallest reduction factors (1.0) are achieved by 1) machining the weld surface, 2) confirming the weld quality through the use of ultrasonic tests (radiographic examinations are not practical on the floor), and 3) examining the weld surface through a combination of visual, magnetic particle, or dye penetrant tests.

The largest reduction factors (4.0) occur on the back sides of welds that cannot be observed or are otherwise non-definable. This characteristic applies to the bottom of the root pass in contact with the top of the backing strip.

The Owner must coordinate with the tank fabricator to reach an agreement on the welding procedures and the weld examinations to ensure a consistent treatment among the cost of the tank floor, the calculated fatigue life, and the expected fatigue life in commercial service.

7.8 Heat Tracing

7.8.1 System Description

The electric heat trace system thermally conditions equipment prior to initiating salt flow, and provides freeze protection on all salt equipment.

Although not specifically discussed in the Design Basis Document, electric heat trace systems may also be used for the overnight temperature control of large steam valves and the steam turbine casing.

The heat trace system is integrated system with the master control system as part of the distributed control system. The heat trace can be directly linked with other process control functions such that thermal conditioning is fully automated.

There are three approaches for the control of the heat trace system:

1. The heat trace vendor supplies a dedicated controller to the heat trace system. The controller, and the software, are typically proprietary to the vendor. The controller receives inputs from the control thermocouples, and sends on/off control signals to the electronic contactors that provide electric power to the heat trace circuits. The duty of the heat trace circuit is controlled by pulse width modulation of the output signal

2. Inputs from the circuit control thermocouples are received by the distributed control system, the distributed control system calculates the required pulse width of the heat trace circuit, and then sends the on/off control signals to the circuit contactors

3. A hybrid approach, in which 1) the standard controller is provided by the vendor to control the heat trace circuits, and 2) a communication link is provided between the vendor controller and the distributed control system such that distributed control system can monitor all aspects of the heat trace system.

The first approach is the most common. However, the controller typically has a dedicated station for the operator, which can make tailoring the operation of the heat trace system to the plant operating mode a tedious process. Further, the temperature signals from the heat trace control thermocouples are not available to the data historian, which can make system diagnosis a more complicated process.

The second approach 1) makes available to the distributed control system all of the information from the heat trace system, and 2) allows the operation of the heat trace circuits to be automatically adjusted to the plant operating mode. However, the number of input signals to, and output signals from, the distributed control system is a large number, and this will increase the cost of the distributed control system.

This third approach can combine the benefits, and minimize the liabilities, of the first and the second approaches. However, it will require the cooperation of the heat trace vendor regarding project access to the vendor's proprietary hardware and software.

The approach selected in a commercial project will depend on the preferences of the Owner, plus the willingness of the heat trace vendor to allow the project access to vendor equipment.

7.8.2 Scope of Supply

The electric heat trace equipment will be purchased as a system that encompasses the zone definitions, heat transfer calculations, cable arrangements, sensor locations, cable fabrication, installation, and acceptance testing. Zone definitions, and locations of the temperature sensors, will be developed in cooperation with the project engineering contractor. The scope of supply will encompass all materials and hardware, including the heat trace cables, splice kits, power supply junction boxes, temperature sensors, sensor junction boxes, and all installation hardware.

Fabrication and assembly of each heat trace cable will be performed by the supplier in the field. This is to ensure the cables are cut to match the as-built configuration of the equipment. Normally, fabrication of the cables at the vendor's shop is preferred, as the quality of the hot-to-cold junctions can be more closely controlled. However, the project schedule does not allow the preparation of factory cables after the salt equipment has

been installed. The vendor will be required to supply cables, manufactured in the field, to have the same quality and reliability as cables manufactured at the vendor's shop.

The heat trace system design and supply should include the solid state circuit contactors. However, the electric power distribution, installation of the solid state contractors, and connections of the temperature sensors to the instrument junction boxes should be provided by the site electrical contractor.

7.8.3 Electric Heat Tracing System Design Basis

Zone Definitions

The boundaries of the heat trace zones will be defined by the equipment geometries, the system operating modes, and liquid locations within the equipment. Also, zone temperature set points will vary by state and transition. As such, the definition of the zones will need to be determined by the project engineering contractor, and not by the heat trace vendor. The heat trace vendor will collaborate with the engineering contractor to set limits, as needed, on practical zone dimensions. As an example, transitions between operating modes can result in certain pipe segments changing from flowing salt to stagnant salt. The zone boundaries, and the location of the temperature sensors, must be selected such that the full lengths of the stagnant zones, which change with the mode, are always protected. In addition, the temperature sensors must monitor the temperatures only in the stagnant zones, not in the flowing zones.

In general, zone lengths for piping should be as long a possible. Plant availability is improved by 1) reducing in the number of cables, contactors, controllers, and communication lines; 2) reducing the number of alarms monitored by the operators; and 3) reducing the number of potential operating modes which are not used correctly. The division of a piping circuit into multiple zones tends to decrease the plant availability, as the loss of one zone is equivalent to the loss of the complete circuit. The potential availability penalty associated with lengthy outages to remove and replaced failed cables in long heat trace zones is offset by increasing the number of installed spare cables.

Any significant change in the mass per unit length in a zone, such a valve in a pipe, requires a separate zone.

Any significant change in heat loss per unit length in a zone, such as a valve bonnet, requires a separate zone.

Any pipe section or instrument location, in which a zone of stagnant salt is intentionally formed for temperature control, requires a separate zone. Examples are illustrated in Figure 7-7 Pressure Transmitter in a Vertical Process Line, and in Figure 7-8 Pressure Transmitter in a Horizontal Process Line.

Thermal losses at pipe and equipment supports will be much higher than in the adjacent pipe or equipment. The geometry of the supports will need to be analyzed by the engineering contractor to determine if separate zones are required at the supports.

If different operating modes subject a pipe or a vessel to different static fluid heights, then the boundary between the zones must end above the liquid level. For example, recirculation from a salt pump at a demonstration solar project produced a static height of about 9 m in a riser. If the heat trace zone in the lower section of the riser had ended below an elevation of 9 m, then the stagnant salt above the top of the zone would have frozen in a matter of a few hours. Further, if the zone spans a region which is not exposed to salt at the top, but is flooded below, then a heat transfer analysis must be conducted to confirm that the temperature in the upper portion of the zone does not exceed safe levels.

Zone Thermal Capacities

The thermal capacity in each zone is determined by the following factors:

- An economic analysis, comparing the capital cost of the heat trace capacity with the system startup time. One example is a salt line, which is normally drained at the end of an operating day. Prior to startup the following day, the temperature of the piping must be increased to the salt fill temperature. If the line has a high heat trace capacity, then the preheat time will be short, the preheat energy will be low, but the capital cost will be high. (The reverse also applies.) As such, there is an optimum heat trace capacity that minimizes the sum of (the equivalent capital cost of the preheat energy) and (the capital cost of the heat tracing).

- An Owner's assessment of the degree to which the heat trace capacity must accommodate an expected degradation in the cable heating capacity or an increase in the heat losses through the equipment insulation

- An Owner's assessment of the reliability of the heat trace cables, and the requirement for spare installed cables.

The nominal set of design parameters include the following:

- Empty salt pipes, empty valve bodies, and valve bonnets can be preheated from ambient temperature to 275 °C in 12 hours

- Empty salt heat exchangers can be preheated from ambient temperature to 275 °C in 36 hours. Preheating energy will be provided by a combination of electric heat trace cables on the shells and the channels, and an electric recirculation water heater.

The calculations will be performed using the design minimum ambient temperature and a concurrent wind speed of 14 m/sec.

Allowances of 5 percent will be added to the zone capacities for simple geometries (pipe sections) and 30 percent for complex geometries (valve bodies, valve bonnets, pipe supports, guides, and anchors).

Control and Set Point Temperatures

The minimum system set point temperatures, for both the cold and the hot salt equipment, is a nominal 275 °C.

The controller temperature dead band is selected to limit contactor cycling; i.e., -10 °C to +10 °C.

Component Redundancy

The required number of heat trace cables to satisfy the preheat requirements will be calculated as noted above. The number of installed cables will be equal to the number of required cables, plus the following allowances for spare cables:

- 100 percent for cables on the piping from the heat exchangers. This segment of piping operates under daily thermal cycles, and the failure rates of the heat trace cables are expected to be 'moderate to high'

- 50 percent for cables on 1) the salt piping to the heat exchangers, 2) the nitrogen vent lines to the salt tanks, and 3) the vent and drain lines for the heat exchangers. This equipment operates under essentially steady state temperatures, and the failure rates of the heat trace cables are expected to be 'low'.

The spare cables will accommodate failures of the original cables without the need to remove the insulation. The spare cables will be labeled as such, but not connected to the electric power supply.

To the extent possible, large valves will have spare heat trace cables installed. For small valves, and for the bonnets on both large and small valves, the installation of spare cables is not practical. As such, spare cables, fabricated to the dimensions of the original cables, will be assembled and kept in the warehouse for future maintenance.

For each temperature sensor installed on a pipe, valve body, valve bonnet, or instrument, an installed spare shall be provided. Dual element thermocouples satisfy the redundancy requirement.

Component Requirements

The recommended cable type is mineral insulated, with dual conductor heating elements, a welded sheath, and magnesium oxide insulation. A welded sheath is preferrable to a brazed joint, as the latter can be subject to cracking due to differential thermal expansion between different metals. The cables can be supplied with either an Inconel or a 300-series stainless steel sheath. The latter is less expensive than the former, and offers a similar resistance to corrosion should the cables be exposed to salt following a leak.

Two cable diameters are recommended: $^{5}/_{16}$-inch (nominal 8 mm) for 600 V service for long piping zones; and $^{3}/_{16}$-inch (nominal 5 mm) for 120 V service on valves and line devices. The conductor resistance will vary, depending upon the length of the cable. Cable power density should be limited to 160 W/m to reduce the potential for corrosion of the sheath in the event of a salt leak.

The cables are secured to the pipe using stainless steel tie wires or straps. A typical installation, showing the end of a zone, is illustrated in Figure 7-3. A stainless steel foil layer is installed over the cables, followed by a flexible blanket insulation approximately 25 mm thick. The foil prevents the flexible blanket from potentially lodging underneath the cables, which would cause the cables to overheat. A rigid block insulation is installed over the blanket. The blanket conforms to the uneven surfaces produced by the cables, the ties, and the corrugated tubes at the end of the zone. This, in turn, reduces the potential for convection heat flows under the rigid insulation.

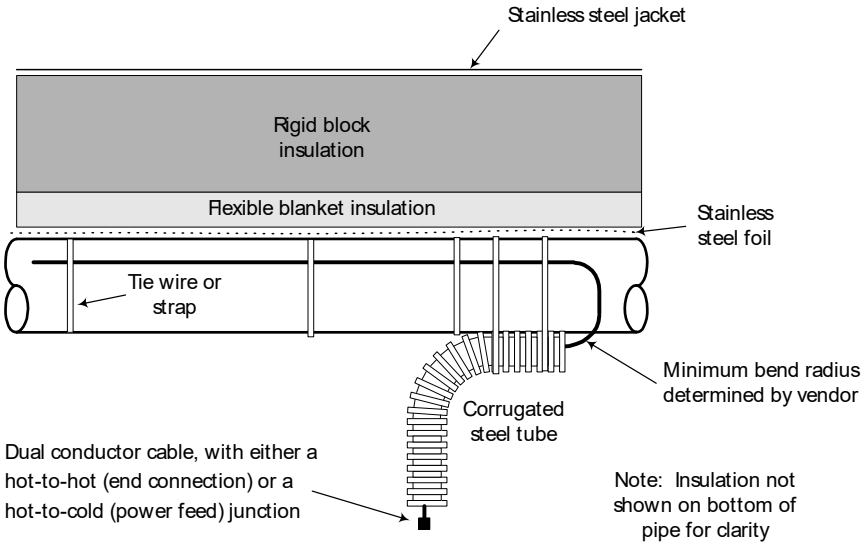

Figure 7-3 Heat Trace Arrangement on Pipe at End of Zone

For zone temperature measurement, either thermocouples or resistance temperature detectors are acceptable. Whichever type is selected, they will be standard across the entire facility.

Valve Zones

The heat trace for a valve will be independent of the heat trace for the adjacent pipe, for three reasons:

- The unit mass, in kg/m, of a valve body is much higher than the unit mass of the adjacent pipe. As such, if a time is specified to preheat the piping system to 275 °C, the heat input per meter for a valve body must be much higher than the heat input per meter for the pipe

- The type of insulation on a valve body is often different from the type of insulation on the adjacent pipe. As such, under steady state conditions, the heat loss per meter of valve body will be different than the heat loss per meter of the pipe

- The unit heat losses, in W/m^2, from the valve bonnet are much higher than the unit heat losses from the valve body. Also, the temperature of the bonnet must be maintained within a narrow range of 275 °C to 300 °C if a stem packing is used. The lower value ensures the salt will not freeze in the bonnet. The upper value ensures that Teflon or other organic materials in the stem packing, if used, do not decompose.

A typical cable installation on a valve is illustrated in Figure 7-4. The power rating for cable on the valve body is selected based on the required system preheat time. If the valve body is large enough, redundant cables can be installed.

The power rating for the cable on the valve bonnet is selected to maintain metal temperatures in the range noted above, under the worst combination of wind speed and ambient temperature. In general, limited space is available on valve bonnets, and only one cable can be provided.

Since the heat trace circuit for the valve body operates independently of the heat trace circuit for the valve bonnet, separate thermocouples are required for the two zones.

Check valves do not have extended bonnets. If the insulation thickness on the check valve is the same as the insulation thickness on the adjacent pipe, then the unit heat loss for the valve should be essentially the same as the unit heat loss for the pipe. Consequently, treating the pipe and a check valve as a contiguous zone is an acceptable design practice.

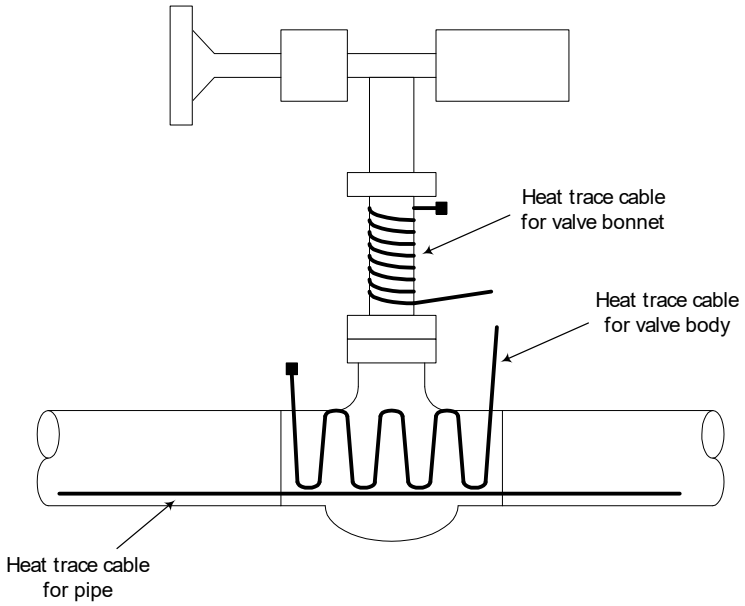

Figure 7-4 Typical Heat Trace Cable Arrangement on Valves

Temperature Sensor Installation

Sensor elements are to be welded or banded to the pipe or equipment, and then covered with a stainless steel tent to reduce convection heat losses from the sensor.

The number of sensors in a zone will depend on the geometry of the zone, as follows:

- For zones of limited dimensions, such as instrument stubs, one dual-element thermocouple is adequate

- For long pipes, operating in cyclic service, as many as 6 to 8 dual-element thermocouples may be needed to understand the temperature distribution throughout the zone. The heat trace circuits would be controlled based on a low select feature

- For pipes operating with salt flowing in some modes, but switching to static salt in other modes, a minimum of 2, and as many as 6, dual-element thermocouples may be needed to maintain set point temperatures during all of the modes.

7.8.4 Equipment Heat Tracing

Heat tracing requirements unique to major equipment items are described below.

Pressure Safety Valves

All pressure relief valves in salt service will have electric heat tracing. However, the springs are subject to relaxation, even those fabricated from high temperature materials such as Inconel. As such, the heat trace cable locations and the valve insulation must be designed to 1) maintain a valve body temperature of at least 275 °C, and 2) maintain the spring temperature as low as practical. In general, separate zones will be provided for the valve body, the inlet piping, and the outlet piping.

The discharge line from the valve must have heat tracing over the entire length of the pipe.

A weep hole at the low point in the valve discharge line should be provided to indicate that 1) the valve is leaking, and 2) the valve should be removed for lapping of the seat and the plug during the next scheduled plant outage. Leakage from the discharge line can be collected in metal containers, allowed to freeze, and returned to the storage tanks through the manway.

Vortex Shedding Flow Meters

Vortex shedding flow meters reside in fittings, which are generally the same diameter as the pipe. As such, the meter and the adjacent pipe can be treated as a contiguous zone. Nonetheless, the meter has a small boss which houses the vibration sensor, and the boss extends through the pipe insulation. The boss is not insulated due to temperature limits on the piezoelectric sensor. Therefore, the boss acts like a fin and cools the top of the fitting.

At the one solar project, a loop in the shape of an "S" with a length of 30 cm, was added to each cable on the 150 mm flow meters to compensate for the convection losses from the boss. With a unit rating of 130 Watts per meter, and 2 active cables, the loops increased the heat input to the meter by 80 Watts over that which would have been provided by the cables on the adjoining pipe.

Tank Vents

Each of the storage tanks has a vent in the roof, which is open to the atmosphere. To prevent the condensation of salt vapors in the vent, the entire length of the line is heat traced and insulated.

Further, the heat losses from the vent are relatively high because 1) the end of the vent is exposed to the atmosphere, and 2) ambient air enters the vent whenever the level in the tank is decreasing. As such, the heat trace circuit on the vent line is treated as a separate zone.

Tank Vacuum / Pressure Relief Valves

The vacuum / pressure relief valve are attached to the roof tank, and the valves are insulated. However, the combination of convection and radiation heat transfer from the liquid inventory to the valves is not always sufficient to maintain the temperature of the valves above the salt freezing point. This is particularly the case if the insulation on the valve has been damaged or degraded. As such, the valves are heat traced, and each valve is treated as a separate zone.

In general, inventory levels in the storage tanks decrease only slowly. As such, the mass flow rate of air entering the tank, either through the vent or through the vacuum relief valve, is a relatively low value. Although the air entering the tank is at ambient temperature, the cooling effect on the vent and the relief valve is modest, and the likelihood that salt vapors from the ullage space will freeze on, and eventually plug, the vent or the relief valve is vanishingly small.

Tank Level Gauges

Air supply lines to bubbler level gauges will have electric heat tracing. The purpose is to prevent any residual moisture, which might be present in the instrument air, from freezing and plugging the lines on cold days. However, the heat tracing equipment on the air lines is different from the heat tracing equipment on the salt lines. The air lines use self-regulating heat trace cables, in which the electric current varies inversely, and passively, with the cable temperature. Representative maintenance temperatures range from 65 to 75 °C.

Capillary Lines for Diaphragm Pressure Transmitters

The capillary fluid is the eutectic NaK mixture, which has a freezing point is about -12 °C. As such, no electric heat trace is required for the capillary line.

Salt Pumps

The salt pumps are supported on a platform above the storage tanks, and draw suction from near the bottom of the tanks. An elevation view of the general arrangement is shown in Figure 7-5. The gap between the top of the tank and the bottom of the support structure is spanned with a metal bellows, as shown by the arrow in Figure 7-6. Electric heat trace will be installed on the bellows.

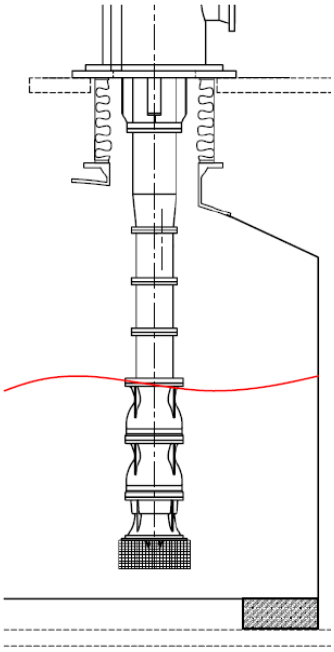

Figure 7-5 Elevation View of Salt Pump

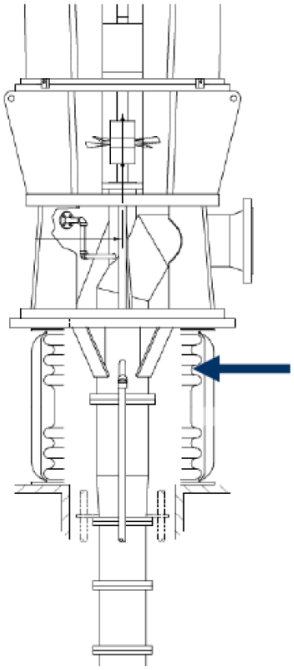

Figure 7-6 Detail of Salt Pump Discharge Head and Bellows

Depending on the pump geometry, it may also be possible to install heat tracing in the region above the bellows and adjacent to the discharge flange. If not, this portion of the

pump must be thoroughly insulated to prevent salt from freezing on the shaft, and, depending on the location of the bearings, lock the rotor to the housing.

Essentially all salt pumps use a stuffing box near the top of the pump shaft. The stuffing box reduces the vertical migration of salt up the shaft due to surface tension effects. The stuffing box is provided with either service or instrument air to 1) develop a slight positive pressure near the top of the pump, and 2) cool the packing in the box. The air lines to the box must have electric heat tracing to prevent salt vapors from condensing in the lines. (When the pump is idle, the air flow to the stuffing box is stopped to limit cooling at the top of the shaft.)

7.9 Salt Pumps

The pumps are a vertical turbine design, with the bearings lubricated by the salt. The pumps are located on structures above the salt tanks, and draw suction from a point near the bottom of the tank.

Commercial tank designs have volumes on the order of 17,000 m^3. The mass of steel in the tank, and to a first order the price, reaches a minimum value with a height-to-diameter ratios of 1. As such, the optimum tank would have a height and a diameter of 28 m. However, API 650-style tanks are supported by the parent soil beneath the foundation base mat. A representative allowable soil bearing load at many project locations is 240 kPa (5,000 lb_f/ft^2), which effectively limits the allowable salt inventory depth to about 12 m. As such, overall pump shaft lengths of 14 to 16 m are expected.

Representative fabrication materials, for both the cold salt and the hot salt pumps, include the following:

- Column - Carbon steel
- Shaft - Alloy steel
- Bowls - Carbon steel
- Impellers - Stainless steel
- Shaft bearings - Cast iron.

An insulated bellows, illustrated in Figure 7-5, 1) bridges the space between the top of the pump and the bottom of the support structure, and 2) allows for differential movement between the tank and the support structure.

The pump discharge connection may be either a ring type joint or a hub type flange. The ring gasket or hub ring shall be Type 321H or 347H stainless steel.

The pumps use variable speed motor drives. The pump will be capable of operating from minimum speed through rated speed with no restrictions on speed.

Installed Redundancy

In the thermal storage system, one 100-percent pump is provided for each process requirement. No installed redundancy is provided because 1) the reliability of salt pumps is excellent, and 2) the isolation and control valves associated with redundant pumps in parallel often exhibit a mediocre-to-poor reliability.

To quantify the effect, each pump requires 3 valves: a discharge isolation; a discharge control; and a minimum flow recirculation. The mean time between failures for salt valves is on the order of 4,000 hours, with a mean time to repair of 12 hours. Each valve must be in service for the pump to operate, which translates to an equipment-in-series availability of 0.991. In contrast, a salt pump has a mean time between failure of 10,000 hours, and a mean time to repair of 48 hours. This translates to an availability of 0.999.

7.10 Salt Instruments

7.10.1 Pressure Instruments

The pressure instrument with the fewest liabilities is a diaphragm unit in combination with a remote transducer. A capillary tube, filled with NaK, connects the diaphragm with the transducer. NaK is the preferred capillary fluid. It has a very low vapor pressure, which reduces the potential for changes in the diaphragm temperature to influence the pressure readings. The fluid also has a low freezing point (-12 °C), which eliminates the need to heat trace the capillary tube. Nonetheless, temperature compensation is still required for accurate readings.

The diaphragm should be located in a position, in combination with a dedicated heat trace zone and thermal insulation, which maintains a constant temperature of 275 °C during all operating modes.

An example of an installation in a vertical process line is shown in Figure 7-7. The dimensions of the external loop are selected such that a diaphragm temperature of 275 °C is maintained, even if the temperatures in the process line reaches 385 °C. During normal operation, the isolation valve is closed. If it is necessary to drain the system, the valve is opened.

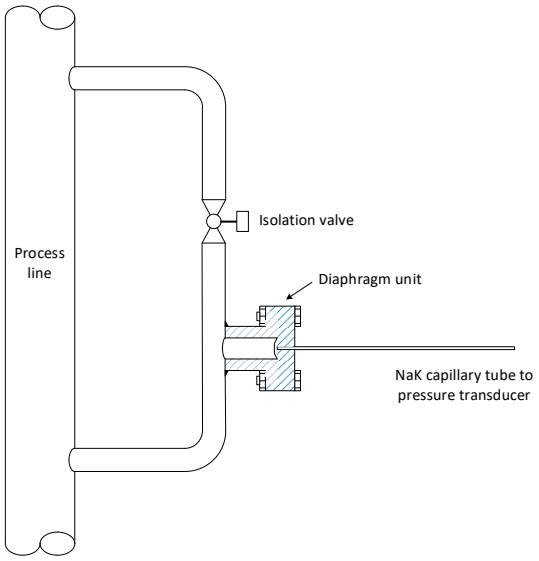

Figure 7-7 Pressure Transmitter in a Vertical Process Line

An example of an installation in a horizontal process line is shown in Figure 7-8. The dimensions of the standoff line are selected such that a diaphragm temperature of 275 °C is maintained, even if the temperatures in the process line reaches 395 °C. During normal operation, the isolation valve is open. If it is necessary to perform maintenance on the diaphragm unit, the process line is drained and the isolation valve is closed.

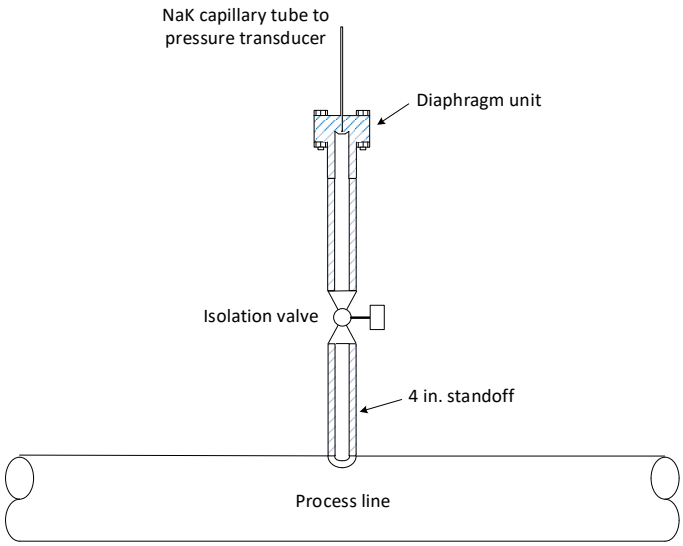

Figure 7-8 Pressure Transmitter in a Horizontal Process Line

In both the vertical and the horizontal installations, compressed air, rather than salt, is likely to be in contact with the diaphragm. Rapid changes in the pressure in the salt are likely to be damped by the trapped air. However, for process control, the installation geometries have proven satisfactory.

7.10.2 Flow Instruments

Candidate Designs

Vortex shedding flow meters have shown good reliability and availability in salt service. Meters are available in sizes up to 400 mm (16 in.), with a maximum process temperature of 450 °C.

Ultrasonic flow meters are suitable for use at all salt temperatures. For pipe sizes of 75 mm and smaller, the refraction angles may need to be increased to achieve the desired accuracy.

In principle, the pressure transmitters described above in Section 7.10.1 can be used in combination with a differential pressure transducer to measure flow based on differential pressure. The differential pressure can be developed using conventional flow devices, including venturis, flow nozzles, and orifice plates. A potential design of a flow venturi in combination with diaphragm pressure transmitters is shown in Figure 7-9.

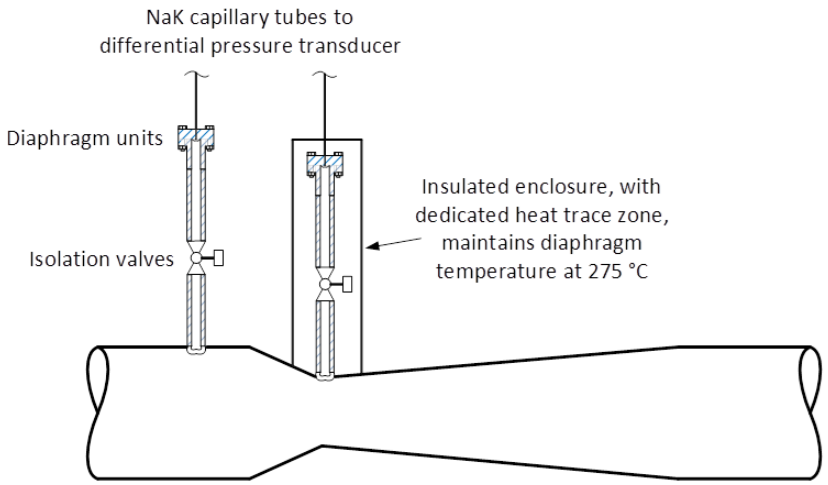

Figure 7-9 Flow Venturi with Diaphragm Pressure Transmitters

Venturis, flow nozzles, and orifice plates are available from a number of commercial vendors, and can operate over the full range of temperatures and flow rates expected in a commercial project. However, it not known if a vendor has combined a conventional flow device with diaphragm units and NaK capillary tubes to develop a differential

pressure flow device for use in salt service. In principle, the reliability and the accuracy of such a device should be suitable for commercial use, and could offer an alternate to ultrasonic flow meters in high temperature (> 450 °C) service.

Accuracy and Reliability

In general, the reliability and the accuracy of flow instruments, particularly ultrasonic units, tends to be in the range of 'fair' to 'good'. For process control, in which accurate flow meters readings are important for equipment protection, redundant instruments can be placed in series, and a 1-out-of-2 voting logic employed. Clearly, this will increase the cost of the project to provide the necessary straight pipe lengths upstream and downstream of the meters. However, the marginal cost of the piping must be evaluated in terms of the reduced risk to the equipment.

7.10.3 Temperature Instruments

Either thermocouples or resistance temperature detectors can be used for temperature measurements. However, the accuracy of thermocouples is generally sufficient for process control in commercial projects. The additional accuracy that may be provided by resistance temperature detectors generally does not warrant the additional expense of the detectors.

Dual element thermocouples are commonly used to reduce repair times should one of the elements fail.

Industry standard thermowells, with thermocouples or resistance temperature detectors, will be used for fluid temperature measurements. External thermocouples, pushed against the outside of the pipe or equipment by a spring, are not acceptable. The small, but inevitable, natural convection air flows around the outside of the thermocouple housing lead to inaccurate measurements.

Temperature measurements in various locations will not be amenable to the use of thermowells. Examples include the shells of heat exchangers and the outside of a pipe for heat trace control. In these cases, the thermocouple will be welded to the pipe or equipment by means of a welding tab. The thermocouple is covered with a stainless steel tent, which is then tack-welded to the equipment.

Electric heat trace temperature sensors, either thermocouple or resistance temperature detector, are acceptable, but must be standardized across the entire project.

For temperature measurements taken directly from the tank inventories, immersion thermocouples may be used.

Thermocouple extension wire used with salt components must use high temperature ceramic fiber insulation.

7.10.4 Level Instruments

Bubbler level gauges may be used in both cold and hot tanks and vessels, operating at essentially any pressure.

Radar level detectors are suitable for both cold salt service and hot salt service in tanks operating at atmospheric pressure.

8. Functional / Prescriptive Specifications for Parabolic Trough Projects using Inorganic Working Fluids

8.1 Design Codes and Standards

For salt equipment and components, reference codes and standards are listed below for the US market. If the plant is constructed outside of the US, an equivalent matrix will need to be developed for the host country.

Designation	Title
API	Standard 650, Welded Steel Tanks for Oil Storge
ASME	B31.1, Power Piping
ASME	Section I, Rules for the Construction of Power Boilers
ASME	Section II, Materials
ASME	Section III, Division 1, Subsection NH, Class 1 Components in Elevated Temperature Service
ASME	Section V, Non Destructive Examination
ASME	Section VIII, Division 1, Rules for the Construction of Pressure Vessels
ASME	Section VIII, Division 2, Alternative Rules for the Construction of Pressure Vessels
ASTM	A105, Specification for Forgings, Carbon Steel, for Piping Components
ASTM	A181, Specification for Forgings, Carbon Steel for General Service
ASTM	A182, Specification for Forged or Rolled Alloy-Steel Pipe Flanges, Forged Fittings, and Valves and Parts for High-Temperature Service
ASTM	A192, Specification for Seamless Carbon Steel Boiler Tubes for High-Pressure Service
ASTM	A193, Specification for Alloy-Steel and Stainless Steel Bolting Materials for High-Temperature Service
ASTM	A194, Specification for Carbon and Alloy Steel Nuts for Bolts for High-Pressure and High-Temperature Service
ASTM	A213, Specification for Seamless Ferritic and Austenitic Alloy-Steel Boiler, Superheater, and Heat Exchanger Tubing
ASTM	A216, Specification for Steel Castings, Carbon, Suitable for Fusion Welding, for High-Temperature Service
ASTM	A240, Specification for Heat-Resisting Chromium and Chromium-Nickel Stainless Steel Plate, Sheet, and Strip for Pressure Vessels
ASTM	A249, Specification for Welded Austenitic Steel Boiler, Superheater, Heat Exchanger, and Condenser Tubes
ASTM	A312, Specification for Seamless and Welded Austenitic Stainless Steel Pipe
ASTM	A325, Specification for Structural Steel Bolts, Steel, Heat Treated, 120/125 ksi Minimum Tensile Strength
ASTM	A351, Specification for Castings Austenitic Austenitic-Ferritic (Duplex) for Pressure-Containing Parts
ASTM	A36, Specification for Carbon Structural Steel
ASTM	A387, Specification for Pressure Vessel Plates, Alloy Steel, Chromium-Molybdenum

ASTM	A403, Specification for Wrought Austenitic Stainless Steel Piping Fittings
ASTM	A500, Specification for Cold-Formed Welded and Seamless Carbon Steel Structural Tubing in Rounds and Shapes
ASTM	A506, Specification for Steel, Sheet and Strip, Alloy, Hot-Rolled and Cold-Rolled, Regular Quality and Structural Quality
ASTM	A516, Specification for Pressure Vessel Plates, Carbon Steel, for Moderate- and Lower-Temperature Service
ASTM	A53, Specification for Pipe, Steel, Black and Hot-Dipped, Zinc-Coated Welded and Seamless
ASTM	A556, Specification for Seamless Cold-Drawn Carbon Steel Feedwater Heater Tubes
HEI	Heat Exchanger Institute
NEC	National Electric Code
NEMA	National Electrical Manufactures Association
NFPA	National Electric Code (NEC), National Fire Protection Association (NFPA)
TEMA	Tubular Exchanger Manufacturers Association, 8th Edition TEMA Standards
IBC	International Building Code

8.2 Nitrate Salt Specification

8.2.1 Candidate Salt Options

As discussed in Section 7.3, there is a range of inorganic salt options for use as the working fluid in the collector field, the storage system, and the steam generator system. The options include the following:

- Binary nitrate salt (solar salt) mixture, which is 60 weight percent sodium nitrate ($NaNO_3$) and 40 weight percent potassium nitrate (KNO_3)

- Ternary nitrate/nitrite salt mixture, the most common of which is Hitec®, with contributions of 7 weight percent sodium nitrate ($NaNO_3$), 40 weight percent sodium nitrite ($NaNO_2$), and 53 weight percent potassium nitrate (KNO_3)

- A ternary nitrate salt mixture, Hitec XL®, with contributions of 42 weight percent calcium nitrate ($Ca(NO_3)_2$), 15 weight percent sodium nitrate ($NaNO_3$), and 43 weight percent potassium nitrate (KNO_3)

- A ternary nitrate salt mixture, which, with contributions of 30 weight percent lithium nitrate ($LiNO_3$), 18 weight percent sodium nitrate ($NaNO_3$), and 52 weight percent potassium nitrate (KNO_3), offers the lowest melting point among the ternary nitrate mixtures (~120 °C)

- A quaternary nitrate salt mixture, reviewed by Sandia National Laboratories, with contributions of 22 weight percent lithium nitrate ($LiNO_3$), 17 weight percent calcium nitrate ($Ca(NO_3)_2$), 18 weight percent sodium nitrate ($NaNO_3$), and 43 weight percent potassium nitrate (KNO_3)

- A quinary nitrate/nitrite salt mixture, patented by Sandia National Laboratories, with contributions of 13 weight percent lithium nitrate ($LiNO_3$), 10 weight percent sodium nitrate ($NaNO_3$), 12 weight percent potassium nitrate (KNO_3), 29 weight percent sodium nitrite ($NaNO_2$), and 36 weight percent potassium nitrite (KNO_2).

The ideal salt would have 1) a low freezing point, 2) a high upper temperature limit in terms of thermal stability, and 3) be inexpensive. As one might expect, none of the candidate salts fulfill all of the ideal requirements.

The collector field in a commercial project will require several kilometers of piping, both in the collector receiver tubes and in the field headers. All of the piping must be protected from freezing, either in the form of impedance heating on the receiver tubes or electric resistance heating on the field piping. Electric heating, in general, is expensive, and selecting a working fluid with a low freezing temperature reduces the duty, and the cost, of the heating system. Of the candidate salts, the quaternary nitrate salt mixture had the lowest freezing point (~100 °C), followed by the quinary nitrate/nitrite mixture (105 °C), followed by the ternary nitrate mixture (120 °C), Hitec XL (133 °C), Hitec (142 °C), and the 60/40 mixture (235 °C).

With an organic working fluid in the collector field, the maximum temperature is limited to a nominal 392 °C based on the thermal stability of the oil. With an inorganic working fluid, the maximum temperature of the working fluid must be greater than 392 °C to offset the complexity and the cost of the electric heating system. The benefits of the higher temperature are 1) an increase in the efficiency of the Rankine cycle, 2) a reduction in the unit cost of the storage system, in $/kWht, due to an increase in the difference between the cold tank and the hot tank temperatures, and 3) a reduction in the cost of the storage system due to a switch from an indirect system to a direct system; i.e., eliminating the oil-to-salt heat exchangers. Previous studies have shown that the collector field outlet temperature should be at least 450 °C to offset the cost of the electric heating systems [4].

Binary Nitrate Salt

Of the candidate salts, the binary nitrate salt mixture offers the highest thermal stability, with an upper temperature limit of about 600 °C. It is also the least expensive mixture, as it does not require lithium or nitrite contributions. However, it is the most problematic in terms of freeze protection, as it has the highest melting point.

Hitec

If the collector field outlet temperature is 450 °C, then a representative film temperature in the collector receiver tubes is on the order of 465 to 470 °C. At these temperatures, the nitrite anion component of Hitec undergoes the following decomposition reaction:

$$2\ NO_2^- \rightarrow 2\ NO + 2\ O^{--}$$

[4] Kearney, D., et. al., (Kearney & Associates, Vashon, Washington), 'Engineering Evaluation of a Molten Salt HTF in a Parabolic Trough Solar Field', National Renewable Energy Laboratory Contract NAA-1-30441-04, January 2001

The decomposition reaction is more problematic in Hitec than in a 60/40 salt mixture because the nitrite concentration in Hitec (40 weight percent) is at least an order of magnitude greater than the equilibrium concentration of nitrite in a 60/40 mixture. This applies, even under conditions in which binary salt temperature in central receiver projects is a nominal 565 °C.

The nitrite decomposition reaction is largely irreversible, as the NO produced is vented from the storage tanks as part of the daily charge/discharge cycle. As with the calcium nitrate decomposition (discussed below), NO emissions can represent a health hazard. Also, the oxide species (O^{--}) are chemically aggressive in terms of corrosion in carbon, ferritic, and austenitic steels. Further, the decomposition and the loss of the nitrite ions effectively increases the concentration of the more stable nitrate ions. This, in turn, raises the freezing point of the mixture, and removes some of the motivation to select Hitec as the working fluid.

In general, the use of Hitec at a maximum working temperature of 450 °C is marginally acceptable; at working temperatures above 450 C, Hitec is likely unsuitable.

Hitec XL

At the working temperatures in the receiver tubes, the calcium nitrate in Hitec XL thermally decomposes via the following reactions:

$$Ca(NO_3)_2 \rightarrow Ca^{++} + 2\ NO_3^-$$

$$NO_3^- \rightarrow NO_2^- + \tfrac{1}{2}\ O_2$$

$$2\ NO_2^- \rightarrow 2\ NO + 2\ O^{--}$$

$$Ca^{++} + O^{--} \rightarrow CaO$$

The calcium oxide (CaO) is largely insoluble and forms a precipitate. The NO is released from the salt as a gas, and can represent a health hazard to the plant personnel. The decomposition reaction results in an inventory mass loss on the order of 1+ percent per year, and the cost to replenish the inventory can represent a significant operating expense to the project. In addition, calcium nitrate is available commercially as the tetrahydrate. The high water content of the hydrate results in a lengthy and a cumbersome dehydration and melting process. In general, the operating problems with Hitec XL are not offset by the benefits of a relatively low melting point.

On a related point, the relative stability of salt mixtures containing lithium nitrate ($LiNO_3$) (discussed in the section below) is greater than mixtures containing calcium nitrate ($Ca(NO_3)_2$), as indicated by the maximum temperature at which decomposition products became appreciable. The trend in stability of ternary mixtures followed the correlation for single salts established by Stern [5]. This correlation is based on a parameter of the cation species consisting of the square root of the covalent metallic radius, r, divided by the effective nuclear

[5] Stern, K. H., Journal of Physical Chemistry, Reference Data 1 (1972), 747

charge, Z. Stability increases as the cation parameter increases, which implies that electrostatic effects between the cations and the polyatomic nitrate anions are important. The values of this parameter for the alkali and alkaline earth metals of interest are given in Table 8-1.

Table 8-1 Cation Parameters for Calcium, Lithium, Sodium, and Potassium

Cation	$r^{0.5} / Z$
Ca^{++}	0.38
Li^{+}	0.45
Na^{+}	0.53
K^{+}	0.62

The stability of ternary mixtures appears to be determined primarily by the least stable constituent. The types of cations in the salt mixtures had relatively little effect on the nitrate / nitrite / oxygen equilibrium reaction (i.e., $NO_3^- \leftrightarrow NO_2^- + ½\ O_2$) over the range of compositions investigated. In contrast, decomposition to form corrosive oxide ions was strongly influenced by the types of cations present. This suggests that cations may interact more strongly with nitrite or oxide ions than with nitrate ions.

Ternary Nitrate Salt

The ternary nitrate salt composition should offer an improved thermal stability, compared to Hitec and to Hitec XL, for the following reasons:

- There are no nitrite contributions to the mixtures
- As noted in Table 8-1, lithium has a higher cation parameter than calcium.

Nonetheless, as summarized in Table 8-2, ternary mixtures containing $LiNO_3$ can produce significant concentrations of oxide ions [6]. As a point of reference, the 60/40 binary salt reportedly contains less than $1 * 10^{-2}$ molal total oxide ions under similar conditions of temperature and atmosphere.

It should be noted that the above data were developed with an ullage gas composition of 100 percent O_2. This was done to prevent the formation of lithium carbonate from the CO_2 normally present in atmospheric air. However, if O_2, rather than air, is used as the ullage gas, this forces the following equation to the left:

$$NO_3^- \leftrightarrow NO_2^- + ½\ O_2$$

[6] Nissen, D. A., and Meeker, D. E., Inorganic Chemistry 22, (1983) 716

Table 8-2 Oxide Concentrations in Ternary Nitrate Salt Mixtures as a Function of Composition

$LiNO_3$:$NaNO_3$:KNO_3, weight percent	Melting point, °C	Operating temperature, °C	NO_2^- concentration, 10^{-2} molal	Oxide concentration, 10^{-2} molal
12 : 18 : 70	200	500	8.5	1.1
		550	20.6	1.2
20 : 28 : 52	160	500	11.1	1.2
		550	30.0	2.9
27 : 33 : 40	150	500	12.6	7.6
		550	27.8	11.0
30 : 18 :52 [1]	120	500	12.4	11
		550	27.0	20

Note 1: Eutectic mixture

This, in turn, reduces the concentration of nitrite ions, which, in turn reduces the formation of oxide reactions via the following reaction:

$$2\ NO_2^- \rightarrow 2\ NO + 2\ O^{--}$$

In central receiver projects, the long term nitrite concentration is in the range of 2 to 3 weight percent [7], and the associated oxide concentrations (which, to some degree, are unknown) result in acceptable corrosion rates for carbon, ferritic, and austenitic steels. A nitrite concentration of 2.5 percent by weight is equivalent to a molal concentration of $5.2 * 10^{-2}$. As indicated in Table 8-2, to achieve comparable corrosion rates between a ternary nitrate salt (using an ullage cover gas of O_2) and the 60/40 binary nitrate salt (using an ullage cover gas of air), the lithium contribution in the ternary salt must be held to values less than 20 percent. This in turn, results in a melting point in the range of 180 to 200 °C.

In addition, the ternary nitrate salt is more expensive than the 60/40 binary nitrate salt because the unit cost of lithium nitrate is approximately 9 times the price of both the sodium nitrate and the potassium nitrate. The cost of the 12 : 18 : 70 ternary salt mixture translates to an increase in the unit cost of storage ($/kWht) on the order of 50 to 60 percent.

Quaternary Salt

The quaternary salt does not contain nitrite salts, and therefore should avoid the thermal stability limits associated with Hitec. However, the mixture does contain calcium nitrate; as such, the quaternary salt is likely to be constrained to the same upper temperatures limit as Hitec XL. Further, the mixture contains 22 percent by weight lithium nitrate, which translates to

[7] Pacheco, J. E. (Sandia National Laboratories, Albuquerque, New Mexico), 'Final Test and Evaluation from the Solar Two Project', Sandia Report SAND2002-0120, January 2002

an increase in the unit cost of the storage system, relative to the 60/40 mixture, of at least 200 percent.

Quinary Salt

The quinary salt has a nitrite contribution of 65 percent by weight. This value is larger than the nitrite contribution in Hitec (40 percent); as such, the thermal stability limit of the quinary salt is likely to be lower than the thermal stability limit of Hitec. In addition, the unit cost of the quinary mixture will be greater than the unit cost of the 60/40 binary nitrate salt because 1) the quinary mixture contains 13 percent by weight lithium nitrate, and 2) the unit cost of sodium nitrite and potassium nitrite is approximately 50 percent higher than the unit cost of sodium nitrate and potassium nitrate. The cost factors translate to an increase in the unit price of the storage system, relative to the 60/40 mixture, of approximately 150 percent.

Salt Selection

As noted above, the minimum collector field outlet temperature for a trough project using an inorganic working fluid is on the order of 450 °C. This temperature limit essentially eliminates Hitec, Hitec XL, the quaternary nitrate mixture, and the quinary nitrate/nitrite mixture from consideration in a commercial project.

The remaining candidate salts include the following:

- The 60/40 binary nitrate salt mixture, with a low cost and a high thermal stability, but with a high freezing point of 235 °C

- The ternary nitrate mixture, with a freezing point of 180 to 200 °C (depending on the composition), a favorable thermal stability limit of about 540 °C, but with a unit cost of storage that is 50 to 60 percent higher than the unit cost of storage with the 60/40 binary salt.

To select between the two salts, a detailed economic analysis of the combined cost of the thermal storage system and the freeze protection system would be needed. To a zeroth order, the analysis is likely to favor the 60/40 binary mixture, for the following reasons:

- The cost for freeze protection in a plant with a fluid melting point of ~190 °C is not significantly lower than the cost for freeze protection in a plant with a fluid melting point of 235 °C

- There is a considerable data base, totaling several hundred plant years, on the use of the binary salt in commercial service

- The 60/40 binary salt is immune from the swings in the commodity prices of lithium carbonate seen in the past few years.

For the 60/40 binary salt mixture, details on the salt characteristics are presented in the following sections:

- Grades: Section 7.3.2
- Allowable Contaminants: Section 7.3.3
- Supply Options: Section 7.3.4
- Deviations from a 60/40 Mixture: Section 7.3.5.

8.3 Nitrate Salt Handling and Melting Specification

An outline of the salt handling and melting procedures for the 60/40 binary mixture are presented in Section 7.4.

8.4 General Salt System Equipment

Section 7.5 includes a discussion of salt piping, flanges, fittings, pipe supports, pipe anchors, pipe guides, and valves. However, the discussion is limited to low temperature (< 390 °C), carbon steel salt piping in the thermal storage system.

A description of the high temperature (500+ °C), stainless steel piping for trough projects using inorganic heat transfer fluids is discussed below.

8.4.1 Piping

Design Codes

The nitrate salt piping can be designed to the requirements of either ASME B31.1 - Power Piping or ASME B31.3 - Process Piping, subject to approval from the local jurisdictional agencies.

Collector Field Piping

The salt piping in commercial central receiver projects, which is typically designed to B31.1, has experienced very few, if any, failures associated with material specification, low cycle fatigue, or weld cracking. To some degree, this would argue for the selection of B31.1 for the design of the collector field piping in a trough project using an inorganic heat transfer fluid for the following reasons:

- The design temperatures of the hot salt piping in a trough project using an inorganic heat transfer fluid (510 to 540 °C) are similar to the design temperature of the hot salt piping in a central receiver project (565 °C)

- If a project is to meet the availability values typically adopted for project financing, then the field piping in a trough project must have an availability comparable to the availability of the salt piping in a central receiver project; i.e., at least 99.5 percent.

However, in a parabolic trough project using an inorganic heat transfer fluid, the total length of the salt piping in the collector field is comparable to the total length of the Therminol piping in the collector field of a parabolic trough plant using an organic heat transfer fluid; i.e., considerably more than the salt piping in a central receiver project. As such, selecting B31.3 rather than B31.1 for the field piping should offer a lower project cost, due to the following considerations:

- The weld examinations are less rigorous

- The stress intensity factors and the stress design factors permit fewer expansion loops, or expansion loops with smaller dimensions (assuming that the allowable nozzle loads on equipment connected to the salt piping can be satisfied).

Nonetheless, there is no operating experience with large commercial trough projects using inorganic heat transfer fluids. To some degree, it remains an open topic as to whether B31.3 is an acceptable design code for the field piping.

Steam Generation System and Rankine Cycle

B31.1 is the required design specification for boiler external piping; i.e., the piping upstream of, or downstream from, a steam generator to the first flanged or welded connection. As a practical matter, the following piping is also often designed to B31.1:

- The cold salt and the hot salt piping to, within, and from the steam generator

- The water/steam piping segments in and around the steam generator and the turbine-generator, which operate at combinations of high temperature and high pressure.

Materials

9. The cold salt piping is typically ASTM A106 Gr B or Gr C, with a nominal 30-year corrosion allowance of 1.6 mm (1/16 in.). The hot salt piping is a 300-series stainless steel, with a nominal corrosion allowance of 0.7 mm (1/32 in.). Candidate materials include both L-grade (Type 304L and Type 316L) and H-grade (Type 304H, 316H, and 347H) steels. Recent commercial projects have generally selected Type 347H, but this may not always be the preferred choice. A discussion of the advantages, and the disadvantages, of each option is presented in Section 1,

Piping in Salt Service.

Stainless Steel Material Specification

All stainless steel materials are to be supplied in a solution annealed condition.

Stabilization Heat Treatment of Type 347H Piping

The pipe shall conform to ASME SA-312, Grade TP347H.

After solution annealing of the pipe, an additional stabilization heat treatment is to be performed per ASME SA-312 Supplementary Requirement S6. The stabilization process occurs at a temperature which is lower than the temperature which dissolves niobium carbide, but it is higher than the temperature which dissolves chromium carbides, such as $Cr_{23}C_6$. The material is held at the stabilization condition for a period which is long enough to promote the formation of the desired niobium carbides at the expense of the undesired chromium carbides.

The stabilization steps are as follows:

- Raise the temperature to the stabilization temperature at a minimum rate of 280 °C/hour
- Hold at the stabilization temperature of 885 °C ± 14 °C for a minimum period of 2 hours
- Remove the pipe section from the heat source and allow the assembly to air cool to ambient conditions.

The stabilization step may be performed during the ramp down cycle of the solution annealing process.

Stabilization Heat Treatment of Type 347H Wrought Fittings

All wrought stainless steel pipe fittings shall conform to ASME SA-403, WP347H, Class S (Seamless) per ASME SA-403.

After solution anneal of the fittings, an additional stabilization heat treatment shall be performed per ASME SA-403 Supplementary Requirement S2, except it shall be done in a temperature range of 845 to 870 °C and the fittings cooled in air.

The stabilization step may be performed during the ramp down cycle of the solution annealing process.

Stabilization Heat Treatment of Type 347H Forged Flanges and Fittings

All forged stainless steel pipe flanges and fittings shall conform to ASME SA-182, F347H.

After solution anneal of the fittings, an additional stabilization heat treatment shall be performed per ASME SA-182 Supplementary Requirement S10, except it shall be done in a temperature range of 845 to 870 °C and the fittings cooled in air.

The stabilization step may be performed during the ramp down cycle of the solution annealing process.

Post Weld Heat Treatment of Type 347H Pipe and Fittings

It is acceptable for the stabilized piping and fittings to receive an additional stabilization treatment during the post weld heat treatment of spool assemblies in the shop, and during the post weld heat treatment of the field weld that attach to these pipes and fittings

It can be noted that post weld heat treatment of stabilized stainless steel pipe and fitting is not required by the ASME Code. The use of a post weld heat treatment is a decision to be made by the Owner as a means of reducing, but not eliminating, the potential for intergranular stress corrosion cracking in the heat affected zones of the welds. To make an informed decision regarding the use of post weld heat treatment, the Owner must, to some extent, be an expert in the Owner's technology.

9.1.1 Flanges

Flanges in salt service may be of the following types: ring type joint; or hub type. No other types of flanges, such as raised face flanges, will be used due to the potential for relaxation of the bolted connection and leakage past the gasket due to the excellent wetting characteristics of the salt. Ring type joint gaskets and hub rings will be ASTM A182 Gr F21 for low temperature service, and ASTM A240 Gr 304 for high temperature service.

Stud bolts used at temperatures below 400 °C will be specified as ASTM A193 Gr 7. For temperatures above 400 °C, or pressure containing components with external heat tracing, stud bolts will be specified as ASTM A193 Gr B8R, with ASTM A194 Gr 8R heavy hex nuts.

9.2 Heat Tracing

Section 7.8 presents a discussion of scope of supply, zone definitions, zone thermal capacities, control and set point temperatures, component redundancy, component requirements, valve zones, temperature senso installation, and installation details for pressure safety valves, vortex shedding flow meters, tank level gauges, capillary lines for diaphragm pressure transmitters, and salt pumps.

Cable Redundancy

The required number of heat trace cables to satisfy the preheat requirements will be calculated as described in Section 7.8. The number of installed cables will be equal to the number of required cables, plus the following allowances for spare cables:

- 100 percent for the cables 1) on the hot salt piping from the collector field, and 2) the hot salt piping to the steam generator. These segments of piping operate under daily thermal cycles, and the failure rates of the heat trace cables are expected to be 'moderate to high'

- 50 percent for cables on 1) the cold salt piping to the collector field, 2) the cold salt piping from the steam generator, and 3) the vent and drain lines for the steam generator heat exchangers. These segments of piping operate under essentially steady state temperatures, and the failure rates of the heat trace cables are expected to be 'low'.

The spare cables will accommodate failures of the original cables without the need to remove the insulation. The spare cables will be labeled as such, but not connected to the electric power supply.

9.3 Salt Pumps

The basic features of salt pumps are discussed in Section 7.9. However, the hot salt temperatures in projects using nitrate salt as the collector field working fluid are approximately 125 °C higher than the hot salt temperatures in projects using Therminol as the collector field working fluid. This requires a change in the fabrication materials for the hot salt pump, as follows:

- Column - Stainless steel

- Shaft - Stainless or nickel alloy steel

- Bowls - Stainless steel

- Impellers - Stainless steel

- Shaft bearings - Cobalt chromium alloy; i.e., Stellite.

9.4 Salt Instruments

Pressure instruments, flow instruments, temperature instruments, and level instruments are discussed in Section 7.10.

9.5 Collector Field

9.5.1 Solar Collector Assemblies

The hardware used in the collector field of a plant with an inorganic heat transfer fluid is essentially the same as the hardware used in the collector field of a plant with Therminol as the heat transfer fluid. This hardware includes the foundations, the support structure, the drive, the mirrors, the heat collection elements, and the local controllers.

The principal differences in the hardware lie in the connections between the rotating heat collection elements and the fixed piping. In a project using Therminol, the most common connection is a ball joint. A cross section of a representative design is shown in Figure 9-1. A threaded retainer loads the two seals against the inner ball. A packing material, consisting of grease and graphite flakes, is injected between the two seals to form a liquid-tight boundary. However, all of the candidate salts discussed in Section 8.2 are oxidizing materials. Over time (days to months) the salt reacts with the grease and the graphite to form CO_2. The packing eventually disappears, and the joint begins to leak. Considerable research effort has been devoted to finding either an organic or an inorganic packing material that compatible with salt and provides a liquid-tight boundary, but to date this has proven unsuccessful.

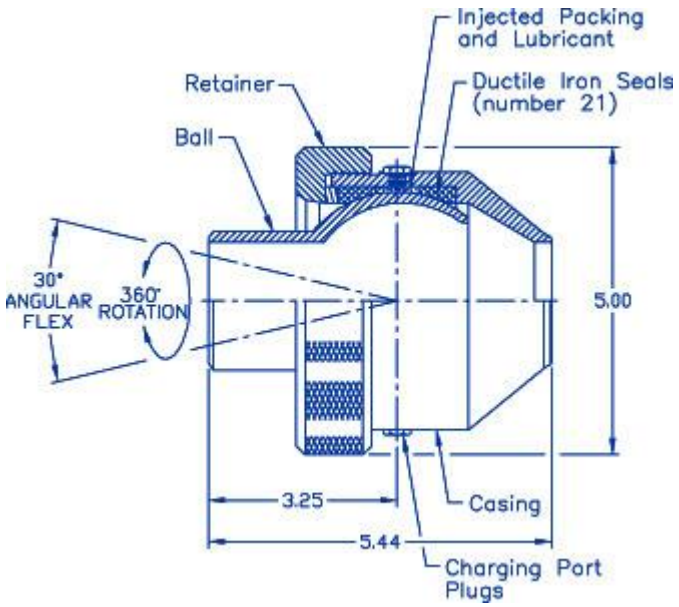

Figure 9-1 Cross Section of a Representative Ball Joint

Instead, the industry has adopted a flex hose arrangement to accommodate 1) the axial thermal expansion and contraction of the receiver tubes, and 2) the rotation between the fixed field piping and the rotating collector assembly. The hose consists of the following:

- An inner bellows, which forms the pressure boundary
- A wire braid, over the inner bellows, to prevent the bellows from crimping
- An outer bellows to protect and to support the wire braid.

A representative flex hose assembly, in its shipping container, is shown in Figure 9-2. The flex hose assembly, installed on a prototype collector, is shown in Figure 9-3. The upper portion accommodates the thermal expansion and contraction of the receiver tubes, and the two lower section accommodate the collector rotation by bending.

9.5.2 Impedance Heating of Receiver Tubes and Flex Hose Assemblies

The absorber tube for the receiver is enclosed in a glass envelope, and a vacuum is drawn in the annular space between the receiver tube and the glass envelope. The receiver tubes require some form of heat addition, other than from solar radiation, for the following purposes:

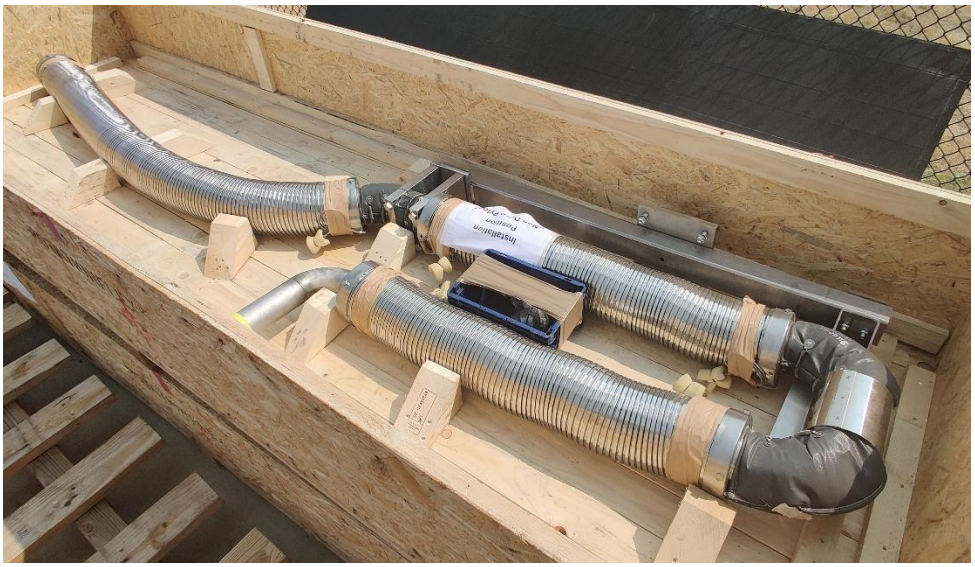

Figure 9-2 Flex Hose in Shipping Container

Figure 9-3 Flex Hose Assembly Installed on a Prototype Collector

- The receiver tubes must be preheated prior to filling with salt to prevent a thermal shock which could break the glass-to-metal seal

- Should salt freeze in the receiver tubes, heat must be added to melt the frozen sections.

Two forms of electric heating have been considered for design of the receiver:

- A conventional heat trace cable, installed on the non-illuminated inside of the receiver tube

- A direct current power supply, which passes a high current through the receiver tubes. The current is converted to heat by the familiar I^2R effect.

The industry has generally not pursued the first approach, for the following reasons:

- The electric cable providing power to the heat trace cable must penetrate the vacuum boundary. The seal for the cable must remain vacuum-tight for decades under thermally cycling conditions. To date, a suitable design for the seal has yet to be identified

- There is a commercial market for parabolic troughs using Therminol as the working fluid; however, there is no commercial market for parabolic troughs using salt as the working fluid. As such, the limited number of commercial receiver suppliers have little motivation to develop a reliable seal for the electric connection.

The impedance heating approach is feasible for receiver tubes due to a combination of a small metal cross section area and a relatively high resistivity for stainless steel. However, based on local jurisdictional requirements, the maximum voltage is limited to either 80 V, based on IEEE requirements [8], or is limited to 50 V, based on NEC Article 110.27 [9].

The low voltage allowances result in the following features of an impedance heating system:

- A representative power input to the receiver tubes is 250 W/m. This translates to electric currents in the range of 400 to 600 Amps, depending on the receiver diameter and the wall thickness. The large electric currents result in large transformers, switchgear, and electric cables for the distribution of power to the trough structures, compounded by the need to keep the voltage drops in the range of only a few Volts. For example, a representative size of the electric power cables is illustrated at the top of Figure 9-3, where the combined cross section areas of the three cables approaches the diameter of the receiver tube

- The receiver tube and the flex hose connections are supported by the collector structure. The structure has a much lower electric resistivity than the receiver tubes and the flex hoses. As such, the electric isolation of the receiver tubes and the flex hoses must be essentially perfect. Otherwise, the heating currents will shunt around the receiver tubes and the flex hoses, which decreases the heat input to the receiver tubes and the flex hoses

It can be noted that the electric resistance of the receiver tubes is different than the electric resistance of the flex hose assembly. If the receiver tubes and the flex hoses are to be preheated at the same rate, then separate power supplies, operating at different currents and voltages, will be required for the receiver tubes and the flex hose assemblies.

Design Requirements

As the design of the impedance heating system is fundamentally an electrical problem, each collector loop is considered as a series of electrical resistance elements. The impedance heating system may connect at any point between the resistance elements shown in Figure 9-4, and may be composed of one or multiple power supplies based on the geometry

[8] "IEEE Recommended Practice for Electrical Impedance, Induction, and Skin Effect Heating of Pipelines and Vessels", Institute of Electrical and Electronics Engineers, Inc., Standard 844-1991, March 1991
[9] 2017 NEC edition of NFPA 70, '110.27(A) Live Parts Guarded Against Accidental Contact'

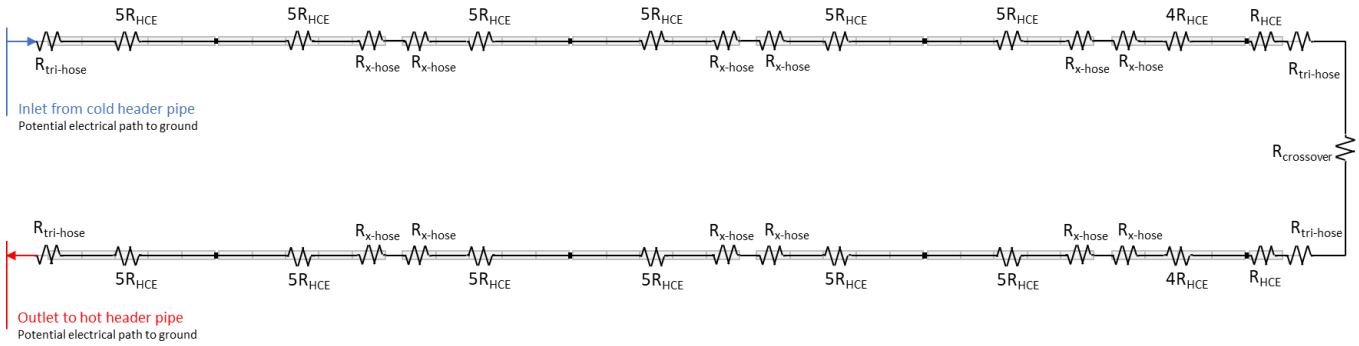

Figure 9-4 Electrical Resistance Network a Collector Loop

The main challenge with impedance heating systems is eliminating paths to ground. The receiver tubes, the flex hose assemblies, and the fixed piping that compose the electrical circuit in Figure 9-4 have numerous paths to ground through the collector structure, and all of the paths need to be electrically isolated. In addition, the field header piping represents additional paths to ground that cannot be easily isolated, but must be considered in the wiring configuration.

Permanent Systems

A commercial parabolic trough plant may be made up of several hundred collector loops. In principle, permanent impedance systems can be installed on each loop, and the plant could recover from a freeze event in approximately 3 weeks by heating the field piping, the receiver tubes, and the flex hose assemblies simultaneously. In practice, such a system would be limited by the capacity of the plant auxiliary transformers to distribute power from the grid to the various electric heating loads. One study estimates that a maximum of 10 collector loops could be melted at any one time based on the typical capacity of auxiliary transformers in commercial projects [10]. This would result in a freeze recovery time approaching 100 days for the very largest solar fields.

As might be expected, given the large sizes of the electric equipment required for impedance systems, the estimated capital cost to provide a permanent system on each loop is quite high, and may approach \$80/m^2. This is approximately 50 percent of the unit cost of the collector field, and would render the approach infeasible.

Mobile Systems

An alternate approach to a permanent impedance heating system is a mobile system. The system consists of a number of trailers towed by trucks. On each trailer is a generator, a step-down transformer, and electric cables stored on a series of reels. The cables provide

[10] C. Prieto, A. Rodríguez-Sánchez, F. J. Ruiz-Cabañas and L. F. Cabeza, "Feasibility study of freeze recovery options in parabolic trough collector plants working with molten salt as heat transfer fluid", *Energies*, vol. 12, no. 12, pp. 1-20, 2019

temporary connections between the step-down transformer and permanent electrical connection points in the collector loop.

The truck and each trailer have a common ground bus for connecting the collector structure to the generator neutral. A ground cable also connects to a local permanent grounding well that is bonded to the plant permanent grounding grid.

The estimated cost of a mobile system is on the order of $1,500,000 [11]. An economic analysis will determine the optimum combination of the number of impedance heating systems and the time to recover from a frozen collector field. For the complete plant, the estimated unit cost of the mobile heating systems is on the order of $5 to $10/m^2 of collector area.

Electric Power Supply Arrangements

The arrangement of the electric connections between the power supply and the receiver tubes, or between the power supply and the flex hose assemblies, has, as its principal goal, the elimination of current leakage into the supporting structure. Two configurations have been considered in an effort to reach this goal; midpoint cable; and staggered polarity.

Midpoint Cable The midpoint cable wiring method, illustrated in Figure 9-5, is described in a conceptual design study developed for NREL [12], and it is described in a freeze protection study which considers a reduced order model to estimate the melt time [12]. This method involves

[11] Shininger, R. (Solar Dynamics LLC, Broomfield, CO), "Simplified Melting and Rotation Joint Technology", DOE SunShot Technology to Market Award Number DE-EE0008140, August 2022
[12] K. &. Associates, "Engineering & Evaluation of a Molten Salt HTF in a Parabolic Trough Solar Field," NREL Contract No. ANN-30441-04, Final Report, 2002

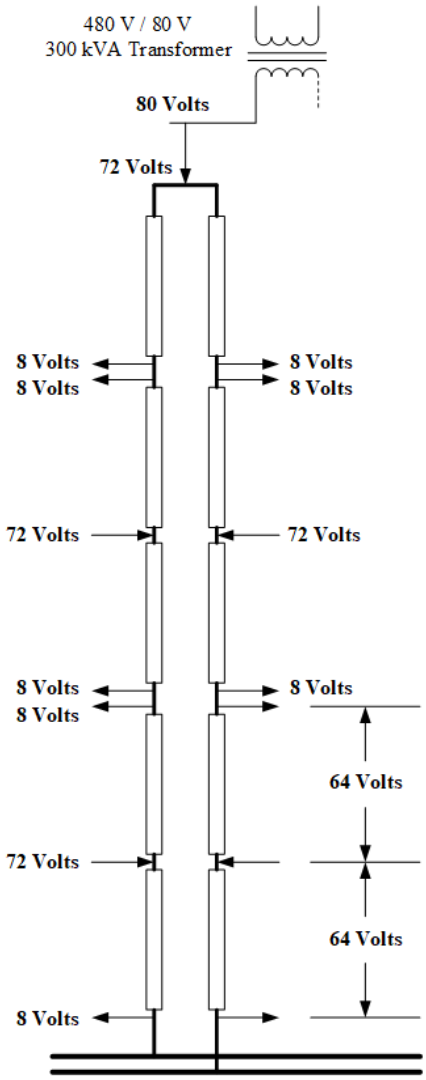

Figure 9-5 Midpoint Cable Wiring Arrangement

wiring the positive terminal in the middle of the element to be heated, and splitting the negative terminal between the two ends. In this fashion, the ends of two adjacent circuit will always be at the minimum voltage, and the maximum voltage is at the electrical center of the circuit. This wiring configuration can also be advantageous for avoiding current leaks to ground.

In the figure, the difference between the supply voltage (80 V) and the voltage supplied to the receiver tubes (72 V) is the volage drop in the electric cables between the power supply and the receiver tubes. Similarly, the difference between the outlet voltage from the receiver tubes (8 V) and the voltage at the power supply (0 V) is the voltage drop in the electric cables between the receiver tubes and the power supply.

Staggered Polarity The staggered polarity method is described in a report looking into alternate methods for freeze protection and recovery [17]. This method involves wiring multiple

power supplies in series with opposing polarity to limit the maximum voltage of the total circuit. Only the output terminal of the power supply immediately adjacent to the header piping is grounded. With the staggered polarities and voltage drop of the interconnecting portable cables, the maximum voltage from any section of piping to ground is less than the maximum voltage across any of the power supply terminals.

To illustrate the concept, a collector loop in a potential commercial project is shown in Figure 9-6.

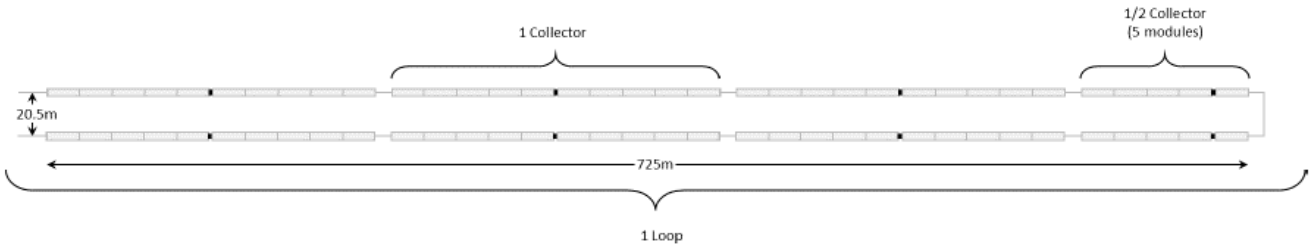

Figure 9-6 Collector Loop in a Potential Commercial Project

The electric resistance of the loop is represented above in Figure 9-4. A series of portable power supply trailers are placed within the loop, as shown in Figure 9-7.

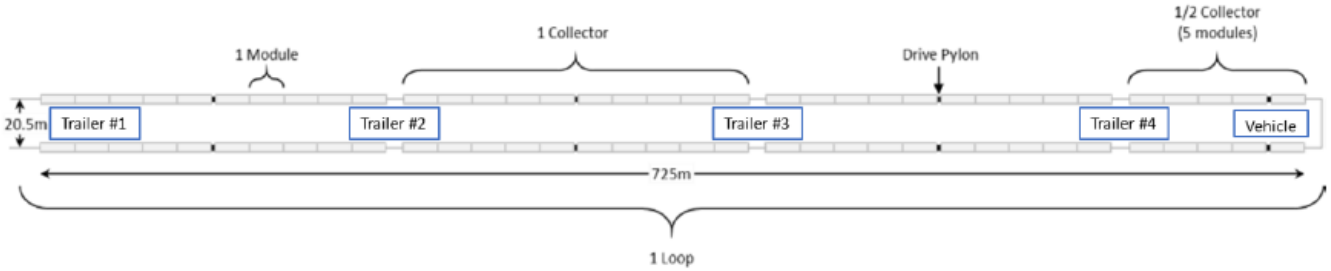

Figure 9-7 Portable Power Supplies for the Impedance Heating System

A conceptual arrangement for the power distribution is shown in Figure 9-8. The green outlines represent the trailers shown in Figure 9-7.

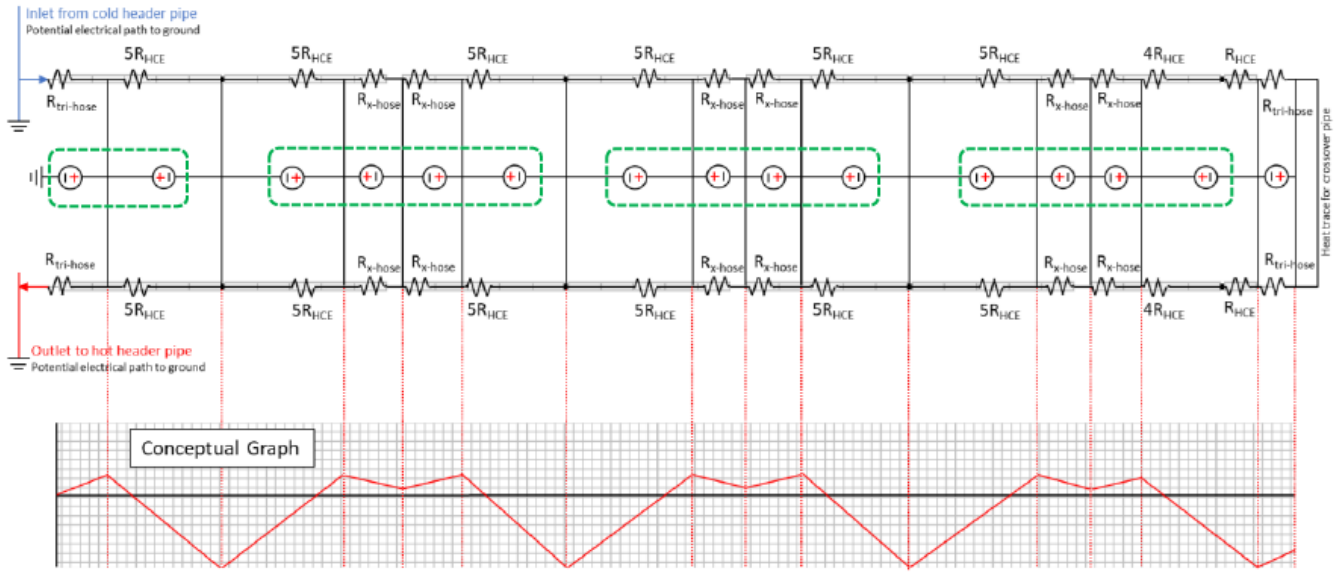

Figure 9-8 Conceptual Power Distribution with Staggered Polarity

9.5.3 Resistance Heating of the Field Piping

The resistance heating system for the field piping follows the basic design approach discussed in Section 7.8.

As discussed in Section 12.1, the field piping will, at some point in the life of the project, be required to recover the field piping from a frozen condition. This process, as one might imagine, is rather lethargic, with thaw periods ranging from 1 week to 1 month, depending on the diameter of the piping.

Heat tracing is expensive, and the design duty of the system is never generous. As such, the heating rate of the pipe is sensitive to the condition of the pipe insulation. In the plant design phase, an economic analysis will be conducted to determine the optimum combination of the design duty of the heat trace system and the recovery time from a frozen condition. The uncertainties in the analysis are likely be high, as there are no data on the frequency of the freezing events in commercial projects. Nonetheless, the design capacity of the heat tracing should assume some level of degradation in the thermal resistance of the pipe insulation. This is to prevent large deviations between the expected thawing period and the actual thawing period due to slow, but expected, degradation in the quality of the insulation.

9.6 Thermal Storage System

The thermal storage system in a trough project using an inorganic heat transfer fluid is nominally the same as the thermal storage system in a central receiver project. A discussion of the specifications for the thermal storage equipment is presented in Section 6.10 of Volume 2 - Specifications for Central Receiver Projects.

9.7 Steam Generation System

The steam generation system in a trough project using an inorganic heat transfer fluid is nominally the same as the steam generation system in a central receiver project. A discussion of the specifications for the steam generator equipment is presented in Section 6.12 of Volume 2 - Specifications for Central Receiver Projects.

9.8 Steam Bypass System and Air Cooled Condenser Capacities

The criteria for selecting the capacities of the steam bypass system and the air cooled condenser in a trough project using an inorganic heat transfer fluid is nominally the same as the criteria used in a central receiver project. A discussion of the specifications for the steam bypass system and the air cooled condenser is presented in Section 6.14 of Volume 2 - Specifications for Central Receiver Projects.

10. Functional / Prescriptive Specifications for Central Receiver Projects

10.1 Design Codes and Standards

Reference codes and standards are listed below for the US market. If the plant is constructed outside of the US, an equivalent matrix will need to be developed for the host country.

Designation	Title
API	Standard 650, Welded Steel Tanks for Oil Storge
ASME	B31.1, Power Piping
ASME	Section I, Rules for the Construction of Power Boilers
ASME	Section II, Materials
ASME	Section III, Division 1, Subsection NH, Class 1 Components in Elevated Temperature Service
ASME	Section V, Non Destructive Examination
ASME	Section VIII, Division 1, Rules for the Construction of Pressure Vessels
ASME	Section VIII, Division 2, Alternative Rules for the Construction of Pressure Vessels
ASTM	A105, Specification for Forgings, Carbon Steel, for Piping Components
ASTM	A181, Specification for Forgings, Carbon Steel for General Service
ASTM	A182, Specification for Forged or Rolled Alloy-Steel Pipe Flanges, Forged Fittings, and Valves and Parts for High-Temperature Service
ASTM	A192, Specification for Seamless Carbon Steel Boiler Tubes for High-Pressure Service
ASTM	A193, Specification for Alloy-Steel and Stainless Steel Bolting Materials for High-Temperature Service
ASTM	A194, Specification for Carbon and Alloy Steel Nuts for Bolts for High-Pressure and High-Temperature Service
ASTM	A213, Specification for Seamless Ferritic and Austenitic Alloy-Steel Boiler, Superheater, and Heat Exchanger Tubing
ASTM	A216, Specification for Steel Castings, Carbon, Suitable for Fusion Welding, for High-Temperature Service
ASTM	A240, Specification for Heat-Resisting Chromium and Chromium-Nickel Stainless Steel Plate, Sheet, and Strip for Pressure Vessels
ASTM	A249, Specification for Welded Austenitic Steel Boiler, Superheater, Heat Exchanger, and Condenser Tubes
ASTM	A312, Specification for Seamless and Welded Austenitic Stainless Steel Pipe
ASTM	A325, Specification for Structural Steel Bolts, Steel, Heat Treated, 120/125 ksi Minimum Tensile Strength
ASTM	A351, Specification for Castings Austenitic Austenitic-Ferritic (Duplex) for Pressure-Containing Parts
ASTM	A36, Specification for Carbon Structural Steel
ASTM	A387, Specification for Pressure Vessel Plates, Alloy Steel, Chromium-Molybdenum
ASTM	A403, Specification for Wrought Austenitic Stainless Steel Piping Fittings

ASTM	A500, Specification for Cold-Formed Welded and Seamless Carbon Steel Structural Tubing in Rounds and Shapes
ASTM	A506, Specification for Steel, Sheet and Strip, Alloy, Hot-Rolled and Cold-Rolled, Regular Quality and Structural Quality
ASTM	A516, Specification for Pressure Vessel Plates, Carbon Steel, for Moderate- and Lower-Temperature Service
ASTM	A53, Specification for Pipe, Steel, Black and Hot-Dipped, Zinc-Coated Welded and Seamless
ASTM	A556, Specification for Seamless Cold-Drawn Carbon Steel Feedwater Heater Tubes
ASTM	B443, Specification for Nickel-Chromium-Molybdenum-Columbium Alloy (UNS NO6625) Plate, Sheet and Strip
ASTM	B444, Specification for Nickel-Chromium-Molybdenum-Columbium Alloy (UNS NO6625) Pipe and Tube
ASTM	B446, Specification for Nickel-Chromium-Molybdenum-Columbium Alloy (UNS NO6625) Rod and Bar
NEC	National Electric Code
NEMA	National Electrical Manufactures Association
NFPA	National Electric Code (NEC), National Fire Protection Association (NFPA)
TEMA	Tubular Exchanger Manufacturers Association, 8th Edition TEMA Standards
UBC	Uniform Building Code

10.2 Nitrate Salt Specification

The component salts are available in refined, technical, and industrial grades. The refined grades have the lowest impurities and the highest cost, while the industrial grades have the highest impurities and the lowest cost. The technical grades are generally suitable for central receiver applications, offering an acceptable compromise between purity and cost.

A typical technical grade specification should include the following items:

- Minimum nitrate concentration of 99 percent by weight
- Maximum total chloride ion concentration from all sources of 0.2 percent by weight.

10.3 General Salt System Equipment

10.3.1 Piping

Design Codes

The nitrate salt piping can be designed to the requirements of either ASME B31.1 - Power Piping or ASME B31.3 - Process Piping.

Receiver System

B31.1, compared with B31.3, is more conservative in terms of material specifications, stress intensity factors, stress design factors, and radiographic inspections. In the interests of providing reliable piping systems, at least two commercial central receiver projects have selected B31.1 as the design code for the salt piping in the receiver system. This includes the cold salt pump discharge piping, the riser, the inter-panel piping, the vent lines, the drain lines, and the downcomer.

Steam Generation System and Rankine Cycle

B31.1 is the required design specification for boiler external piping; i.e., the piping upstream of, or downstream from, a steam generator to the first flanged, welded, or threaded connection. As a practical matter, the following piping is also often designed to B31.1:

- The cold salt and the hot salt piping to, within, and from the steam generator
- The water/steam piping segments in and around the steam generator and the turbine-generator, which operate at combinations of high temperature and high pressure.

10.4 Instruments

10.4.1 Flow Measurements

Flow meter options include vortex shedding, ultrasonic, and venturi.

Vortex shedding meters are generally preferred over ultrasonic meters due to higher reliabilities, less signal noise, and lower instances of dropped signals. However, vortex meters are limited to a maximum process temperatures of 450 °C, and a maximum pipe size of DN 400. As such, the meters are restricted to use on the cold side of the system.

Ultrasonic meters do not have a restriction on maximum pipe diameter, and can be used on both the cold side and the hot side of the system. For pipe sizes of 75 mm and smaller, the refraction angles may need to be increased to achieve the desired accuracy.

Accuracy and Reliability

To compensate for the (at times) lower availability of ultrasonic flow meters, one of two design approaches can be followed:

- Ultrasonic meter vendors can provide 2 or 3 independent transmitter / receiver combinations in a single pipe spool piece. A 1 out of 2, or a 2 out of 3, voting logic can be used to obtain a flow signal
- Different types of flow meters can be arranged in series; i.e., a vortex unit in series with an ultrasonic unit. In this way, a 1 out of 2 voting logic can be used to compensate for dropped signals or an obvious problem with calibration.

The latter arrangement will, of course, be met with resistance on the part of the engineering contractor, as it will increase the total length of pipe for the required diameters upstream, and the diameters downstream, of the meters. However, the control logic for the receiver likely includes a provision to trip both the heliostat field and the receiver on a loss of flow to the inlet vessel, or a loss of flow to either of the two flow circuits. If the receiver is tripped, then the receiver is typically drained. Resetting a trip of the heliostat field, and restarting the receiver, will lead to an outage lasting at least 90 minutes and as much as 3 hours. Since this type of trip happens several times a year, the marginal cost to install redundant flow meters, or different flow meters in series, can likely be recovered by the improvements in plant availability, electric output, and annual revenues.

10.4.2 Pressure Measurements

The pressure instrument with the fewest liabilities is a diaphragm unit in combination with a remote transducer. A capillary tube, filled with NaK, connects the diaphragm with the transducer. The diaphragm should be located in a position, in combination with a dedicated heat trace zone and thermal insulation, which maintains a constant temperature of 275 °C during all operating modes.

Experience at commercial projects indicates that using globe valves, rather than triple offset butterfly valves, in the external loops provides better isolation characteristics. This, in turn, helps to prevent damage to the diaphragm unit from overheating.

As an alternate approach, there are commercial diaphragm units designed for operation at temperatures as high as 600 °C (https://www.badotherm.com/products/diaphragm-seal-systems/). At two commercial projects, the Badotherm units have operated as intended.

10.4.3 Level Instruments

Bubbler level gauges may be used in both cold and hot tanks operating at atmospheric pressure, and in pressure vessels operating at elevated pressures.

For vessels operating at pressures greater than about 7 bar (i.e., the inlet vessel of a receiver), a supplemental air compressor, operating at pressures in the range of 30 to 50 bar, is required to supply air at the required pressure to the bubbler controller.

Radar level detector are suitable for use in both cold salt and hot salt tanks operating at atmospheric pressure.

10.5 Salt Pumps

10.5.1 Configuration

Representative fabrication materials for the cold salt and the hot salt pumps are shown in Table 10-1.

Table 10-1 Salt Pump Fabrication Materials

	Cold Salt	Hot Salt
Column	Carbon steel	Stainless steel
Shaft	Alloy steel	Stainless or nickel alloy steel
Bowls	Carbon steel	Stainless steel
Impellers	Stainless steel	Stainless steel
Bearings	Cast iron	Cobalt chromium alloy (Stellite)

10.5.2 Installed Redundancy

Essentially all commercial projects provide some level of installed pump redundancy.

A typical arrangement for the pumps in the steam generation system include three 50-percent capacity hot salt pumps, and two 100-percent capacity cold salt attemperation pumps. The pump arrangement is based on two 50-percent heat exchanger trains supplied from 1) the 3 hot salt pumps, which are on a common header, and 2) the 2 attemperation pumps, which are on a common, but separate, header.

A typical arrangement for the receiver system uses four 33-percent capacity cold salt pumps supplying a common riser.

Steam Generator Pump Redundancy

There is a range of benefits associated with independent steam generator trains. Since the trains are hydraulically independent, three options are available for supplying salt to the heat exchangers:

- Option 1) One 100-percent capacity installed hot salt pump, with a spare pump in the warehouse, and one 100-percent capacity installed attemperation pump, with a spare pump in the warehouse. For both spare pumps, the spare consists of only the pump; a spare motor and a spare variable frequency drive are not provided

- Option 2) Two 100-percent capacity installed hot salt pumps, and two 100-percent capacity installed attemperation pumps

- Option 3) Two 50-percent capacity installed hot salt pumps, with a spare pump in the warehouse, and two 50-percent capacity installed attemperation pumps, with a spare pump in the warehouse. For both spare pumps, the spare consists of only the pump; a spare motor and a spare variable frequency drive are not provided.

<u>Option 1</u>

Option 1 should provide the best combination of availability and capital cost. On the order of 150 salt pumps with extended shafts are in commercial service, and the reliability has been

excellent. Further, the time required to remove and replace a pump can, in principle, be as short as 24 to 48 hours. An outage period of 1 to 2 days is comparable to the outage periods discussed below for Option 2. As such, Option 1 does not necessarily impose an inherent availability penalty relative to Option 2.

Option 2

In theory, Option 2 could offer an improvement in availability over Option 1. However, the problems with salt pumps are generally not associated with the pump; the problems are typically associated with the ancillary equipment for the pump. These problems include:

- Sticking or erratic movement of the discharge control and the discharge isolation valves
- Leakage of salt from the stem seals of the discharge control or the discharge isolation valves. The salt contaminates the insulation on the valves and the adjacent piping, which can lead to piping temperatures in stagnant lines falling below the freezing point of the salt. Once the salt in a line freezes, the heat trace is no longer capable of thawing the line. To restore the system, the insulation will need to be removed, the stem seals on the valves replaced, the insulation replaced, and the heat trace returned to service. The time required to thaw a line is a function of the pipe diameter, and can range from hours for a small line to days for a large line.
- Sticking or erratic movements of the vent valves which remove air from the pump column
- Incorrect or erratic readings from the flow and pressure instruments at the pump discharge, leading to unnecessary trip signals or incorrect judgement calls on the part of the operator
- Incorrect timing of the supply of instrument air to the shaft packing, leading to salt freezing in the gland and binding of the pump
- Problems with the heat tracing on each of the above items, leading to low equipment temperatures (salt freezing) or high equipment temperatures (corrosion of carbon steel components).

Although counterintuitive, two 100-percent capacity pumps can result in a decrease in system availability relative to one 100-percent capacity pump because redundant pumps require twice the ancillary equipment. Stated another way, there are a finite number of maintenance hours available to maintain the equipment in working order. If the number of ancillary items is reduced by a factor of 2, then it is more likely that the equipment will receive the required maintenance to reach the projected levels of availability.

Lastly, Option 1 requires four pumps, two motors, and two variable frequency drives, while Option 2 requires four pumps, four motors, and four variable frequency drives. As such, Option 1 should be slightly less expensive than Option 2.

Option 3

As noted in the introductory paragraph, a typical steam generator pump arrangement includes three 50-percent hot salt pumps, and two 100-percent attemperation pumps, with the 5 pumps supplying two 50-percent steam generator trains. As such, for each train, there is one 100-percent hot salt pump and one 200-percent capacity attemperation pump. In contrast, Option 1 refines this approach by providing one 100-pecent capacity hot salt pump and one 100-percent capacity attemperation pump, which should be the preferred arrangement.

In addition, Option 1 requires four pumps, two motors, and two variable frequency drives, while Option 3 requires six pumps, four motors, and four variable frequency drives. As such, Option 1 should be somewhat less expensive than Option 3.

Receiver Pump Redundancy

As with the steam generation system, the majority of the problems with salt pumps are associated with the ancillary equipment. To this end, the availability of the receiver pump system can be improved by using three, rather than four, 33-percent capacity pumps.

It can be noted that some commercial projects will operate four 33-percent capacity pumps during those hours in which the solar radiation is particularly high. Nonetheless, to some extent, this operating approach is adopted because the pumps cannot meet their required combination of flow and head; i.e., a 33-percent capacity pump cannot provide one-third of the required flow. The solution to this problem is not to provide a margin on the flow and head characteristics of the three pumps by starting a fourth pump. The preferred approach is to specify the necessary margins as part of the procurement process, and obligate the vendor to correct any performance deficiencies identified in the water flow tests. The margins should reflect uncertainties in items such as the effect of corrosion on the friction factors in the riser and the absorber.

10.6 Receiver System

10.6.1 Design Codes

The receiver is not a fired heater; as such, the selection of ASME Section I as the design code is not a mandatory jurisdictional requirement. (Nonetheless, Boeing selected Section I as the design code for the salt receiver at the 10 MWe Solar Two demonstration project in California. Of the Code options, this approach was judged to be the most stringent, and Boeing wished to avoid potential problems with the local Authorized Inspector regarding the eventual selection of the design code.)

ASME Section VIII Division 2 is often selected as the design code, as it includes methods for estimating low cycle fatigue life in cyclic service. Division 2 also includes provisions for design by analysis, including methods for estimating effects such as combined creep-fatigue damage using visco-plastic analyses. However, Section VIII is applicable only for section thicknesses of 3.2 mm (1/8 in.) and above. In contrast, all commercial salt receivers use tubes with wall

thicknesses in the range of 1.5 to 1.65 mm, and Section VIII is not strictly applicable. To avoid this limitation, SolarReserve adopted ASME B31.1, Power Piping, as the design code for the receiver at the Crescent Dunes project.

10.6.2 Material Selection

The materials of choice for the receiver in a commercial project include the following:

- Alloy 230 for the absorber tubes
- Alloy 230 or Type 347H stainless steel for the panel headers
- Type 347H stainless steel for the outlet vessel and the high temperature piping
- Carbon steel for the inlet vessel and the low temperature piping.

Intergranular Stress Corrosion Cracking of Alloy 230

Alloy 230 is a high nickel alloy, and is generally viewed as immune to intergranular stress corrosion cracking. Nonetheless, leaks in the steam generator introduce water into the storage tanks. Steam released from the salt can travel up the receiver vent line, and condense in the receiver panels at night. At one commercial project, cracks developed in the Alloy 230 receiver tubes, and an examination of the tubes showed evidence of water condensation and intergranular stress corrosion cracking.

It is optimistic to expect that leaks will never develop in the steam generator. One method to prevent steam condensation in the receiver is to purge the receiver with dry, or with heated dry, air at night. The source of the dry air is the instrument air system. This approach was adopted at the 10 MWe Solar Two demonstration project. At this project, the receiver tubes were fabricated from Type 316H stainless steel. Intergranular stress corrosion cracking was judged to be largely inevitable, and supplying dry air to the receiver at night was done to extend, as much as possible, the life of the receiver.

Post Weld Heat Treatment of Type 347H Piping

Type 347H stainless steel is nominally Type 304H stainless steel with niobium added as an alloying element. The niobium bonds with the carbon to form niobium carbide. As such, free carbon, normally present in Type 304H, is not available to react with chromium to form chromium carbide. Since chromium carbide is a necessary precursor to intergranular stress corrosion cracking, Type 347H offers an improved resistance to intergranular stress corrosion cracking than either Type 304H or Type 316H.

Nonetheless, the improved corrosion resistance is degraded during welding. Metal temperatures during welding are high enough to dissolve the niobium carbide. As the weld cools, there are regions of the weld zone that favor the reformation of niobium carbide, but there are also regions in which the time-temperature progression favor the formation of

chromium carbide. Typically, there are narrow zones, on either size of the heat affected zone, that are rich in chromium carbide, and these zones are susceptible to intergranular stress corrosion cracking.

One solution to this weld feature is to perform a post weld heat treatment. The heat treatment process consists of a series of steps in which 1) the temperature is raised to a point which dissolves the chromium carbide, 2) the temperature is raised to a new value which favors the reaction of the now-available carbon with niobium to form niobium carbide, and 3) the temperature is quickly reduced through the point which favors the reaction of the remaining carbon with chromium to form chromium carbide.

It can be noted that the theoretical benefits of a post weld heat treatment are not assured, for the following reasons:

- The work is performed in the field, and there are inherent variations in the ambient weather conditions and the skills of the personnel

- If the required time-temperature profiles are not followed accurately, then the full transition from chromium carbide to niobium carbide may not be achieved. As a result, the weld region may still be susceptible to intergranular stress corrosion cracking

- Depending on the weld filler material and the time-temperature profile, there is the potential to form a range of intermetallic compounds, such as Fe-Cr, Fe-Mo, and $(FeNi)_x(CrMo)_y$. These compounds increase the strength, but reduce the ductility, of the weld region.

Different engineering contractors have different opinions as to the value of post weld heat treatment of Type 347H piping. At one commercial project, the vendor for the receiver performed a post weld heat treatment of all of the stainless steel piping in the receiver, while the engineering contractor for the balance of the plant (i.e., everything outside of the scope of the receiver) did not perform a post weld heat treatment of any of the stainless steel piping.

In general, the solar industry has yet to reach a consensus on the value of, and the need for, the post weld heat treatment of Type 347H piping. Early in the design phase, the project should consult with a materials specialist and a welding engineer to develop an approach to post weld heat treatment that will be applied on a consistent basis throughout the plant.

10.6.3 Tube Clip Design

Each tube is supported at the top by a panel, and is periodically guided over the length of tube by a series of independent clips. The clips maintain the tubes parallel to each other, and in the plane of the absorber, while allowing unrestricted vertical movement for thermal expansion and contraction.

The clips are designed to allow one tube to be removed from the panel for replacement.

The clip-to-tube weld procedure must limit the penetration of the tube wall to the minimum amount necessary for complete fusion. Full penetration welds are not permitted.

The tube clips must slide freely in the support frame guides, while allowing for unrestricted thermal growth of the tubes. Unrestricted is defined as the change in tube length due to a change in temperature from ambient to the melting point of the material.

The tube clip must provide a low cycle fatigue life of 30,000 cycles at a rate of temperature change of 360 °C/min.

The tube clip acts as a heat sink. As such, the clip cannot be located at the edge of the oven box structure. Otherwise, the tube clip would not be properly heated by either the radiant heaters in the oven box or by the preheat flux from the heliostat field. Tube clips must be located outside of the oven box envelope over the full range of tube thermal expansions.

10.6.4 Panel Vent Design

Air must be vented from the absorber panels during the daily fill process. Two options are available for the venting arrangement:

- A vent line is connected to the top of the upper crossover line between two adjacent panels, and an orifice is installed in the vent line. The orifices discharge to a header which is common to the panels in that flow circuit. An isolation valve is installed at the end of each vent header, and the discharge from the two isolation valves connect to the side of the outlet vessel.

- A vent line is connected to the top of the upper crossover line between two adjacent panels, and an isolation valve is installed in the vent line. The valves discharge to a location on the side of the outlet vessel that is above the normal liquid level

The first approach reduces the number of isolation valves, and this generally offers a meaningful improvement in system availability. However, the static pressure in the crossover line between Panels 1 and 2 is higher than the static pressure in the crossover line between Panels 3 and 4. As such, there is a small flow of salt which passes from the 1-2 crossover line to the 3-4 crossover line. Since the salt temperature at the outlet of Panel 1 is lower than the salt temperature at the outlet of Panel 3, the bypass flow in the vent line reduces the salt temperature at the inlet of Panel 4. The attemperation effect occurs along the length of the circuit, and reduces the outlet temperature from the last panel by about 5 °C. As such, the set point for the receiver outlet temperature must be set to 570 °C to achieve a temperature in the downcomer of 565 °C. This has a small, but measurable, effect on the receiver efficiency and the low cycle fatigue life of the panels near the end of the flow circuit.

The second approach avoids the performance penalties, but increases the number of valves. The reliability of valves in salt service, including the reliability of the heat trace and the insulation on the valves, is such that commercial projects generally accept the loss in performance associated with the vent orifices.

10.6.5 Downcomer Design

There are two principal approaches to the design of the downcomer:

- Flooded, with the level in the receiver outlet vessel controlled by throttle valves at the base of the downcomer
- Partially flooded, with the static head dissipated by orifice plates located along the length of the downcomer. Neither an outlet vessel, nor throttle valves, are required.

The most common approach is the flooded downcomer, as the hydraulic performance is fully predictable.

With a flooded downcomer, the outlet vessel must be vented to the atmosphere to provide a predictable level control signal to the downcomer throttle valves. However, the vented vessel can overflow if there are control upsets in the downcomer. To protect the receiver from damage should the outlet vessel overflow, a vent line connects the top of the outlet vessel with the top of the hot salt tank. The vent line must normally operate empty due to Code requirements for a vented vessel. As such, when salt enters the vent line, the velocity increases at a rate of 9.8 m/sec^2. When the salt reaches the first elbow in the first expansion loop, some of the velocity head is converted to a momentum load on the elbow. Momentum loads are difficult to estimate, as the flow is a mixture of salt and air, and the relative proportions of the two fluids change at different locations in the vertical and the horizontal sections of the vent line. Nonetheless, the momentum loads are expected to be high, with values in the range of 75,000 to 150,000 N. A robust set of pipe guides and anchors will be required to transfer these loads from the piping to the tower. The principal design risk is underestimating the loads, and then having to retrofit larger guides and anchors in a location where access is difficult.

To some degree, the complexity in analyzing the flows in a partially flooded downcomer with orifice plates is nominally the same order of magnitude as analyzing the flows in a partially flooded vent line. These considerations may influence the choice between a flooded downcomer and a partially flooded downcomer.

10.6.6 Assembly Location

There are two locations options for the assembly of the receiver:

- At the top of the tower. Components are lifted by crane, and then assembled at an elevation of about 200 m.

- At grade. The receiver is assembled at grade, moved to a position inside the tower through a large opening on the side of the tower, and then lifted by jacks supported by the tower. The opening on the side of the tower is then closed and reinforced.

The former approach is perhaps the more common, but it can incur certain liabilities, as follows:

- A penalty in labor productivity due to a need for all of the craft workers to commute on an elevator with a finite capacity

- Limited areas for the staging of materials and equipment

- Wind speeds are higher than at grade, which can reduce the number of hours suitable for welding.

The latter approaches reduces the above liabilities, but requires a tower design which can safely withstand wind and seismic loads with a large opening in the side.

The engineering contractor will need to conduct an economic analysis of the two options to determine the preferred construction approach.

10.6.7 Instruments

Instruments in salt service are typically problematic. There has a been a wealth of experience gained over the past two decades at commercial projects; some of it good, and much of it bad. As such, the selection of the type, and the method for the installation, of the instruments should be prescriptive. Details of the recommended instruments are presented above in Section 10.4.

10.6.8 Non Destructive Examinations

All tube and header welds require non-destructive examination to verify weld quality and integrity. Each panel will be hydrotested to 1.5 times the operating pressures in accordance with ASME code requirements. In addition, each panel will be pressurized with helium to TBD bar, and the panel assembly helium leak tested, in accordance with ASME Section V. Molten nitrate salt is an excellent wetting agent and will penetrate porous surfaces and minute cracks that will not be apparent with a hydrotest.

10.7 Thermal Storage System

10.7.1 Introduction

Specifications for the storage tanks in commercial projects are a mix of functional and prescriptive requirements. The functional aspects deal with items such as thermal capacity, allowable heat losses, and maximum soil temperatures. The prescriptive aspects include the following:

- Type of tank; i.e., flat bottom with a self-supporting dome roof

- Design codes and standards

- Materials

- Methods for emptying a tank.

However, at least 6 failures of the hot salt tanks in commercial projects have occurred in the past decade. Further, the number of hot tanks in commercial service (outside of China) is very limited: Gemasolar, Crescent Dunes, Noor III, and two at Cerro Dominador. This translates to a probability of failure of essentially 100 percent. As such, the format of the current set of functional and prescriptive specifications is not adequate for the needs of the industry. Outlined below are some recommendations regarding additional prescriptive requirements to the specification.

10.7.2 Design Codes

A specific design code for flat bottom tanks, operating at high temperatures and under cyclic thermal conditions, is under development but is not yet approved for public distribution. As such, the closest applicable code is American Petroleum Institute Standard 650, Welded Steel Tanks for Oil Storage. However, the Standard applies only to process temperatures of 260 °C and below, and does not consider low cycle fatigue conditions. To date, commercial projects have used the following codes, in combination with API 650, for the design of the tank:

- ASME Section II for allowable material stresses

- ASME Section VIII Division 2 for calculating the low cycle fatigue life associated with stresses during commissioning and operation.

Nonetheless, if the tanks, designed to API 650 / Section II / Section VIII Division 2, are failing, is this combination of design codes appropriate for the service conditions? Specifically, at the temperatures of interest in the hot tank (> 550 °C), stainless steel is subject to the effects of creep. Due to the cyclic nature of plant operation, in combination with multi-hour periods at high liquid inventories (high stresses), the hot tank should be designed to withstand the combined effects of fatigue and creep.

The topic is discussed in Section 5.14.1, Changes in the Tank Design Codes, of Volume 3 - Narrative. The recommended approach is to use Section III Division 1 Subsection NH, or alternately Section III Division 5, to develop values for the allowable stresses consistent with limits on accumulated damage due to creep and fatigue. In addition, residual welding stresses should be included in the assessment of creep damage, as discussed in Section 5.15.9, Code Interpretation of Residual Stresses, of Volume 3 - Narrative.

10.7.3 Inputs to the Fatigue Analysis

The floors in the thermal storage tanks are constructed from an array of rectangular plates. The nominal plate dimensions are 2.5 m by 12.5 m. Representative plate thicknesses are in the range of 7 to 10 mm, and two weld passes are typically required.

The allowable tolerances on the dimensions of the plates are presented in ASTM A480/A480M-22a, Standard Specification for General Requirements for Flat-Rolled Stainless

and Heat-Resisting Steel Plate, Sheet, and Strip. Since all of the plates are not exactly the same size and shape, the dimensions of the gaps between adjacent plates will vary. To provide consistent inter-plate welds, backing strips are welded to the backs of alternating plates prior to arranging the plates on the foundation.

The storage tanks are subjected to daily thermal cycles, which results in cyclic loads on the floor generated by friction and radial temperature gradients. For the tanks in parabolic trough projects, it's not clear if a low cycle fatigue analysis is required. However, if such an analysis is justified, then the fatigue properties of the weld are subject to a weld fatigue strength reduction factor. The topic is discussed in Section 5.13.2, Fatigue Strength Reduction Factors, of Volume 3 - Narrative.

To improve the calculated fatigue life of the floor, the reduction factors should be a low as practical. The smallest reduction factors (1.0) are achieved by 1) machining the weld surface, 2) confirming the weld quality through the use of ultrasonic tests (radiographic examinations are not practical on the floor), and 3) examining the weld surface through a combination of visual, magnetic particle, or dye penetrant tests.

The largest reduction factors (4.0) occur on the back sides of welds that cannot be observed or are otherwise non-definable. This characteristic applies to the bottom of the root pass in contact with the top of the backing strip.

The Owner must coordinate with the tank fabricator to reach an agreement on the welding procedures and the weld examinations to ensure a consistent treatment among the cost of the tank floor, the calculated fatigue life, and the expected fatigue life in commercial service.

10.7.4 Material Selection

Hot Tank

For design temperatures above 538 °C, the H grades of stainless steel, with a minimum carbon content of 0.04 percent, are required by the ASME Code. The carbon helps to pin the metal grains, which provides the required resistance to creep.

Candidate materials include Type 304H, Type 316H, and Type 347H stainless steel. At the Solar Two demonstration project, the hot tank was fabricated from Type 304H. However, to avoid potential problems with intergranular stress corrosion cracking, the solar industry has adopted Type 347H, a stabilized stainless steel, in the current generation of projects.

Nonetheless, the choice of Type 347H as the stabilized stainless steel is not without a known set of risks. The principal problem is the use of niobium as the stabilizing element, which can lead to a phenomenon known as stress relaxation cracking. The topic is discussed in some detail in Section 5.12 of Volume 3 - Narrative.

In future commercial projects, the engineering contractor must perform a risk analysis between potential tank materials, neither of which offers a perfect solution:

- Type 304H and Type 316H essentially avoid the potential for stress relaxation cracking due to the absence of niobium. However, the materials are susceptible to intergranular stress corrosion cracking should the tank be exposed to liquid water in combination with chlorides. This can happen under the following conditions:
    a. A pumped heat storage project is planned for a coastal location. The tank, after fabrication but prior to commissioning, can be exposed to salt spray from the ocean.
    b. After the tank has been in commercial service, the tank is drained for maintenance and inspection. If the temperature of the metal drops below the dew point, then moisture can condense on either the inside or the outside of the tank. (A potential solution is to introduce dry, heated, air into the tank such that the metal temperatures never fall below the dew point. To what extent this can be guaranteed by the maintenance company is perhaps an open topic.)

- Type 347H reduces the potential for intergranular stress corrosion cracking, but introduces the potential for stress relaxation cracking. The cracking mechanism is a function of the metal thickness, the number of welding passes, the stress distribution, and the time / temperature history of the tank. If the development rate of the cracking can be predicted with the necessary accuracy, then it may be possible to fabricate a tank in Year 0 of the project, and then fabricate a replacement tank to be placed into service, for example, in Year 10 of the project. However, if the development rate of the cracking cannot be predicted with the required certainty, then the project may be obligated to build two tanks in Year 0 in preparation for an expected failure at some undefined point in the future.

Cold Tank

The cold tank is fabricated from a conventional carbon steel, such as A 516 Grade 60 or 70.

10.7.5 Determination of the Floor Status Prior to the Start of Commercial Operation

Fabricating the floor, preheating the tank, and filling the tank for the first time has the potential to introduce a set of plastic deformations in the floor. The engineering contractor must define the three-dimensional shape of the floor at the time of initial filling. The shape of the floor can be determined by lidar scans from the roof of the tank, or by inelastic finite element calculations of the buckling patterns. The initial shape of the floor is a principal input to a subsequent stress analysis of the floor. The stress analysis will consider loads due to friction, radial and circumferential stresses due to radial temperature gradients, and transient stresses due to receiver startup, shutdown, and trips. The stress analysis, in turn, will define operating permissives, to be programmed in the distributed control system, regarding allowable combinations of inventory depth, downcomer temperature, and downcomer flow rate.

Deformations Produced in the Floor During Welding

The floor consists of a pattern of rectangular plates. Welding the plates produces compressive stresses at each edge. The stresses produce plastic deformations, which convert the flat plates into shallow domes.

The combination of high spots near the center of each plate, and low regions at the edges, results in a plate which has already buckled. The floor is, in essence, a large thin plate, and if the plate has already buckled, then it's resistance to further buckling is very low.

Deformations Produced During the Hydraulic Test

The floor, after welding, has developed something of a waffle pattern. As such, tracing the distance along either the top or the bottom of all of the plates in the floor results in a dimension which is greater than the diameter of the tank.

The radial stiffness of the bottom course of the tank is several orders of magnitude greater than the radial stiffness of the floor. The floor plates are relatively thin (7 to 10 mm), and when the tank is filled with water during the hydraulic test, the slightly domed plates are pushed down into contact with the foundation. (The hydrostatic forces required to deform the plates are discussed in Section 5.8.1, Plate Stresses, in Volume 3 - Narrative.) This changes the dimension of the floor, from one which was slightly larger than the diameter of the bottom course to a new dimension which is equal to the diameter of the bottom course.

The change in dimension will appear as some combination of elastic and additional plastic deformation in the floor. When the water is removed from the tank, the floor will develop a new shape, based, in part, on the residual stresses associated with any new plastic deformations.

An assessment of the plastic deformations made during the hydraulic test can be made by measuring the shape of the floor before and after the test.

Deformations Produced in the Floor During Preheating

During preheating, combustion gases from an air heater enter the tank through a nozzle suspended from the roof. The gases move the tank in a somewhat uncontrolled manner, and leave the tank through a manway in the roof opposite the inlet nozzle.

The temperature distribution in the tank is a function of the gas flow pattern, the local heat transfer coefficients, heat transfer to the foundation, the thermal inertia of the foundation, heat transfer to the tank external insulation, and the thermal inertia of the wall, the roof, and the external insulation. Almost by definition, the metal temperatures will not increase at the same rate throughout the tank. This, in turn, will establish thermal stresses within the tank.

The magnitude of the stresses must be estimated to determine the effect on the fatigue life of the tank, and to determine if additional plastic deformations have occurred during preheating.

For example, radial temperature gradients in the floor of 35 °C and higher have the potential to plastically deform the floor near the center of the tank.

Deformations Produced in the Floor During Initial Filling with Salt

During preheating, additional deformations, both elastic and plastic, can be produced in the floor due to temperature gradients within the tank. After preheating is complete, the floor is likely to retain something of a waffle shape. Some form of buckles may also be present, depending on the stresses associated with welding, hydraulic testing, and preheating.

As with the hydraulic test, the floor will be pushed down against the foundation when the hydrostatic pressure reaches a nominal value of 7 kPa. This occurs with a salt depth of about 0.4 m. However, the structural stiffness of the buckles, if present, is much higher than the bending stiffness of the plates. As such, the buckles, once formed, become a permanent feature of the floor.

Deforming the plates during filling will result in a new combination of stresses and deformations. The new combination becomes the starting point for the creep and fatigue characteristics of the tank associated with the daily cyclic operation of the plant.

10.7.6 Computational Fluid Dynamics Calculations

The salt flow enters the tank through a distribution header located just above the floor. Due to the large dimensions of commercial tanks (~ 40 m diameter), the temperature distribution in the inventory is necessarily non-uniform during transient conditions. Non-uniform temperature distributions produce thermal stresses, and the magnitude of the stresses need to be defined to calculate the low cycle fatigue life of the tank.

Cold Tank Thermal Cycles during Commercial Operation

The cold tank is subjected to a number of temperature cycles over the course of a year. The most common is the daily startup of the receiver. At the beginning of the startup, the temperature of the salt leaving the receiver is the cold salt temperature (290 °C), and the flow in the downcomer returns to the cold salt tank. Over the next 15 to 20 minutes, the temperature at the salt leaving the receiver increases from 290 °C to the design value of 565 °C. At some point in the progression, the flow in the downcomer switches from the cold tank to the hot tank. A typical crossover temperature is 520 °C, but the crossover value can change, depending on the initial levels and the inventory temperatures in the cold tank and the hot tank. As such, the cold tank experiences a slow cooling rate during the evening shutdown period, followed by a modest heating cycle during each receiver startup.

Similarly, during a weather outage period, the cold tank experiences a slow cooling cycle, followed by a modest heating cycle when the receiver is placed back in service. However, the inventory temperatures, and the rates of temperature change, are somewhat different than the daily receiver startup cycles due to the different hold times.

Cold and Hot Tank Status During Outage Periods

Friction forces between the floor and the foundation develop, in part, due to changes in the inventory temperature during hold and outage periods (Section 5.10.4 in Volume 3 - Narrative). If the inventory is at, or near, the minimum level, then floor stresses remain well within allowable values for all changes in the inventory temperature. However, if the inventory is at, or near, the design level, then changes in the inventory temperature must be limited to values in the range of 2 to 3 °C to maintain floor stresses within acceptable values.

During extended outages, the tank temperatures can change, as follows:

- The temperature in the cold tank can decay by as much as 30 °C, which is followed by an increase of 30 °C during a return to commercial service
- The temperature in the hot tank can decay by as much as 290 °C, which is followed by an increase of 290 °C during a return to commercial service.

Changes in the inventory temperature of 30 to 290 °C are large enough to establish the full potential friction forces on the floor. As such, to reduce the friction forces during, and at the end of, the extended outage period, the inventory levels in both the cold and the hot tank should be set to, and maintained at, 50 percent.

Atypical Transient Conditions

A range of atypical conditions can arise, which will subject the tanks to conditions outside of those expected during normal operation. Two examples include the following:

Receiver Trip A possible, and not unreasonable, scenario is one in which the hot tank is close to the minimum inventory, the receiver trips, and then the following single failure occurs: the downcomer diversion valve to the cold tank fails to open. The receiver outlet temperature decays at the projected rate of 360 °C/min, and the entire inventory of the receiver inlet vessel is directed to the hot tank. The estimated rate of change in the tank inventory temperature is shown in Figure 10-1.

The peak rate of temperature change in the bulk inventory is -360 °C/hr, which is approximately 6 times the typical rate allowed by the tank supplier. Depending on the effectiveness of the distribution ring, local rates of temperature change at the floor could exceed -360 °C/hr, which has the potential for permanently damaging the floor.

Selected Crossover Temperature As discussed in Section 10.7.6, the downcomer crossover temperature can be reset by the operator at any time. In the interests of capturing as much energy from the receiver as possible for electric power production, the operator may select a crossover temperature that is considerably lower than the inventory temperature in the hot tank. The effect of selecting a crossover temperature that is 90 °C lower than the inventory temperature is illustrated in Figure 10-2.

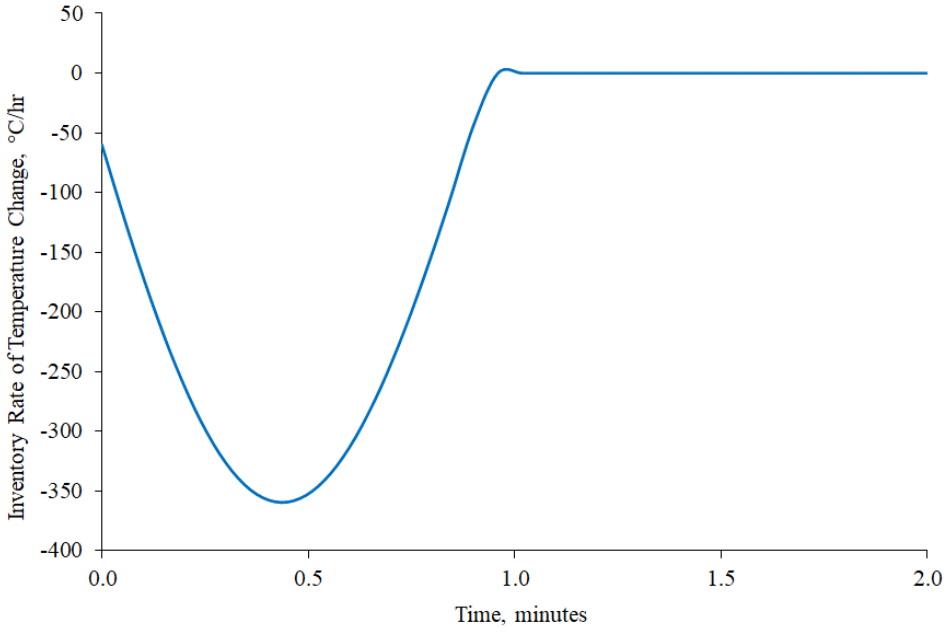

Figure 10-1 Rate of Change in the Hot Tank Inventory Temperature Following a Receiver Trip

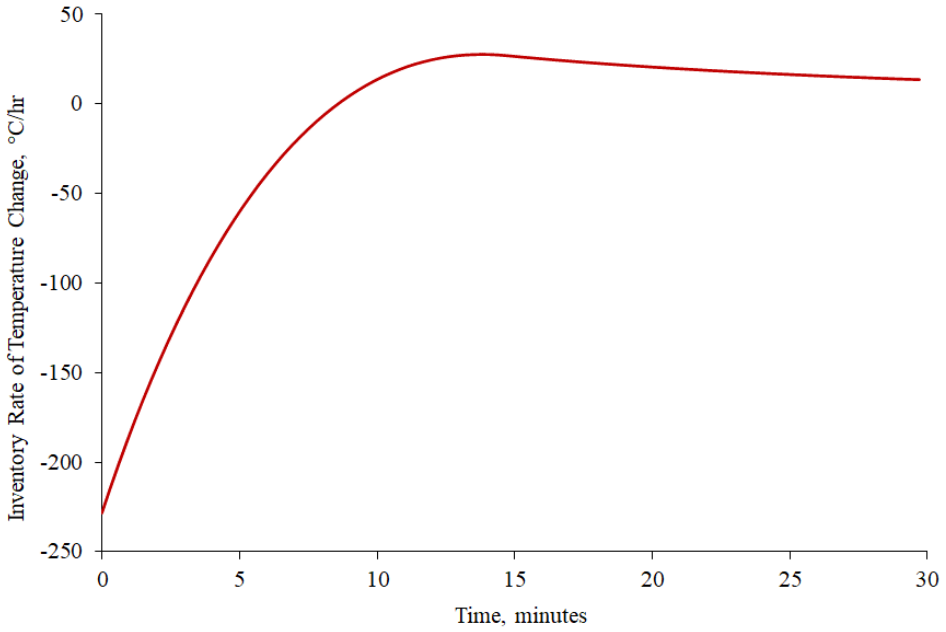

Figure 10-2 Effect of a Crossover Temperature 90 °C Lower than the Inventory Temperature

The result is a peak rate of temperature change of -230 °C/hr, which is about 4 times the typical allowable rate.

Each of these atypical transient conditions has the potential to significantly reduce the low cycle fatigue life of, or causing immediate damage to, the tank. Since both of these conditions are possible, and perhaps probable, the project must identify approaches to avoid damage to the tank. Potential approaches include the following:

- Develop an inlet distribution system that isolates, as much as possible, the floor from the rapid changes in the inlet temperature
- Train the operating staff in the basic principles of transient thermal stresses and low cycle fatigue
- Mandate limits on acceptable crossover temperatures as a function of the tank level.

10.7.7 Combined CFD / FEA Calculations

The engineering contractor, having defined the initial stress distributions and the deformations in the floor after filling with salt, must determine the stress distributions in the tank expected during daily operating sequences. The sequences include both normal operation and emergency conditions, such as a receiver trip.

The calculations must include the effects of the following:

- Friction between the floor and the foundation, including the non-uniform friction effects due to the weld backing plates attached to the bottom of the floor
- Deformations of the floor, including the potential for continued yielding and ratcheting.

The engineering contractor must demonstrate to the Owner that the selected design approach of a flat bottom tank has a fatigue life at least equal to, and preferably longer than, the duration of the project.

10.7.8 Tank Venting

Nitrate salt, as delivered to the project, is approximately 99 percent nitrate (NO_3^-). Once the project has been in commercial operation for perhaps 1 to 2 years, the nitrate ion reaches an equilibrium condition with the nitrite ion (NO_2^-) and oxygen in the ullage gas in the storage tanks based on the following reaction:

$$NO_3^- \leftrightarrow NO_2^- + ½\ O_2$$

The equilibrium concentration of the nitrite ion is on the order of 3 to 5 percent, depending on the operating characteristics of the receiver and the storage volume.

Cover Gas

As such, air is the preferred cover gas. Specifically, using an alternate cover gas, such as nitrogen, would cause the above the equation to always shift to the right. This, over time, would increase the nitrite ion concentration at the expense of the nitrate ion concentration, and promote the following non-equilibrium reaction:

$$NO_2^- \rightarrow O^- + NO$$

The non-equilibrium reaction is undesirable, for two reasons:

- The oxide ions (O^-) remain in solution, and are aggressive corrosive agents
- The NO is released from the liquid in the form of a gas, and produces various forms of NOx in contact with the ambient.

Inter-tank Vent Line

During a discharge cycle, salt moves from the hot tank to the cold tank. If there is an inter-tank vent line, then ullage gas, at a temperature of 295 °C, moves from the cold tank to the hot tank. The cold gas, in contact with the inner surfaces of the hot tank, is heated. To prevent the ullage pressure in the hot tank from exceeding the design pressure, a portion of the ullage gas moving from the cold tank to the hot tank must be vented to the atmosphere.

The process is reversed during a charge cycle, in which ambient air must be added to the cold tank to prevent the ullage pressure in the cold tank from falling below the design vacuum rating.

An inter-tank vent reduces the mass of air which must be vented from the hot tank, and added to the cold tank, over the course of a charge / discharge cycle. This, in turn, reduces one source of thermal losses from the storage system. However, the use of an inter-tank vent line incurs two liabilities:

- The line must be continuously heat traced to prevent the condensation of salt vapors in the line. A calculation shows that the annual energy required to maintain the vent line at a minimum temperature of 275 °C is greater than the marginal energy lost due to simply venting the tanks to the ambient
- If the heat tracing and the insulation on the vent line are not in perfect working order, then it is possible to condense enough salt vapors from the storage tanks to completely plug the line. This is not a theoretical problem, as this condition developed at the Solar Two demonstration project. The defect was a section of the vent line, approximately 200 mm long, between the end of one heat trace zone and the start of the next heat trace zone. Over the course of about 2 years, the DN250 line became fully blocked. With the vent line blocked, and with the pressure/vacuum relief valve on the hot tank partially blocked due to a small defect in the valve insulation, filling the hot tank during

the morning startup of the receiver forced the tank floor into a convex shape, which lifted the tank from the foundation. The relief valve (eventually) lifted, which dropped the tank back down onto the foundation. This situation had the potential to rupture the tank.

The preferred approach to venting the tanks is to provide, on each tank, an open goose neck which is vented directly to the atmosphere. The full length of the goose neck is heat traced and insulated to prevent the condensation of salt vapors. The goose neck is installed in parallel with the tank pressure / vacuum relief valves required by the API 650 Standard.

10.7.9 Foundations

Floor Insulation

The vertical loads on the foundation are a function of the radial position in the foundation. Near the perimeter of the tank, the principal vertical load is the dead weight of the wall and the roof. These loads are distributed into the foundation by an annular plate, approximately 1 m wide, located just below the wall. Inside the inner radius of the annular plate, the principal vertical load on the foundation is the static head of the salt inventory.

The principal insulating material under the floor of the tank is either an expanded clay (Utelite) or an expanded glass (FoamGlas). Design information for both expanded clay and Utelite show allowable compressive stresses that are higher than the anticipated foundation loads, both at the perimeter of the tank and at the center of the tank. As a result, a number of commercial projects have adopted expanded clay as the sole foundation material due to its low cost, low thermal conductivity, and acceptable strength. However, in all of these projects, the expanded clay has not performed as expected. In particular, the particles of clay are prone to shifting and movement as the tank undergoes cyclic expansion and contraction cycles. The movement of the clay is due to two effects:

- At the perimeter of the tank is an annular plate, which is thicker than the floor. The plate 1) transmits the concentrated weight of the roof, the wall, and the tank insulation down into the foundation, and 2) ensure that the displacements in bending are at acceptable levels. The annular plate also carries some of the static hydraulic loads from the salt inventory. However, the compressive loads just inside the perimeter of the plate must be matched by tensile loads just outside the perimeter of the plate. Expanded clay has only a limited capacity to transmit tensile loads. Further, periodic fill and drain cycles in the tank establish periodic tensile loads in the expanded clay. These two conditions cause the clay to move out, up, and away from the perimeter of the foundation.

- Daily thermal cycles of the tank cause the annular plate to push the clay out from the perimeter as the tank expands, but the clay does not return to its original position as the tank contracts.

As a result, the outer edge of the annular plate loses its vertical support. The plate has only a limited capability for accommodating bending loads, and the concentrated vertical load from

the wall and the roof plastically deforms the plate in a downward arc. This is a dangerous condition, as plastic deformation of the wall-to-floor welds seriously compromises the low cycle fatigue life of the tank.

To prevent this situation, the foundation materials directly beneath the wall must be sufficiently rigid to prevent any angular deflections of the annular plate. Two design options have been adopted for this purpose:

- A refractory material, either in the form of bricks or a large casting, is placed in the space between the top of the concrete base mat and the bottom of the tank.

- Metal slip plates are located on top of the expanded clay to prevent direct contact between the floor and the expanded clay.

The first option was successfully used at the 10 MWe Solar Two demonstration project, it was adopted and is in use at one commercial project, and it has been adopted as the design basis for a plant under construction. To date, no problems have been reported from the commercial project in operation.

The second option has been adopted at two commercial central receiver projects, and at least one commercial parabolic trough project. However, the results are somewhat mixed for the hot tanks in the central receiver projects. Specifically, the annular plate and the slip plate must necessarily be stainless steel. However, stainless steels in sliding contact are prone to galling, and this can lead to effective coefficients of friction which are greater than 1. This in turn, can produce two undesirable characteristics:

- When the tank expands, high compressive forces can be transferred from the annular ring to the floor, and the floor already has a poor resistance to buckling

- When the tank either expands or contracts, high radial forces are developed on the annular plate, and some form of an anchor must be provided for the annular plate. However, the anchor is necessarily located beneath the floor, and there is essentially no access for inspection, maintenance, or repair.

In general, the use of a refractory material to support the weight of the wall and the roof represents, perhaps, the smallest sum of liabilities.

It can be noted that refractory materials carry their own set of design liabilities, as follows:

- The materials, either as brick or cast, are not inexpensive

- Some of the refractories can react with nitrate salt, leading to a loss of strength. As such, the refractories must be isolated from potential leaks, as discussed below

- There is a significant degree of uncertainty in the coefficient of friction between refractories and stainless steel at temperatures of 500 °C and above. Preliminary

experimental data shows coefficients to be greater than 0.3, and perhaps as high as 1.0. This may, in effect, obligate the use of a solid lubricant between the annular ring and the refractory.

Solid Lubricant

The most common solid lubricant is sand, as it is inexpensive and thermally stable. Nonetheless, the coefficient of friction between stainless steel and sand is poorly defined. The industry, for better or worse, has assumed nominal coefficients to be in the range of 0.3 to 0.4, but there are little data to corroborate this assumption.

Ideally, the project Owner would commission an experiment, early in the project development phase, to determine a defensible value. This value would then be used by the engineering contractor in the analysis of floor friction loads.

Drip Pan

Nitrate salt is an excellent wetting agent. Should a leak develop in either the wall or in the floor, salt will permeate the materials in the foundation. As discussed in Section 5.3 of Volume 3 - Narrative, contamination of the foundation with salt will lead to an increase in thermal losses, the potential to produce NOx emissions, and the potential to decrease the strength of refractory materials. To limit these consequences, a continuous drip pan must be installed under the layer of solid lubricant. The pan will direct any leakage to safe areas beyond the edge of the foundation.

10.7.10 Foundation Cooling

Soil temperatures beneath the concrete base mat must be maintained at values less than about 75 °C. These temperatures limit the desiccation of the soil, and to limit the oxidation of organic materials in the soil. The goal is limit the shrinkage and the settlement of the soil to values which are consistent with the normal allowances for the settlement of the tank.

To control the soil temperatures, heat is removed from the base mat by means of active cooling. Two cooling options are available: forced air cooling, and water circulation. The solar industry has universally adopted forced air cooling, for the following reasons:

- The heat flux into the foundation is perhaps 60 to 70 W/m^2. This is a modest value, and the flux can be readily transferred to a flow of air with an acceptable temperature rise along the diameter of the foundation.

- Unlike a water circuit, leakage in the air duct does not materially affect the cooling capacity.

10.7.11 Methods for Emptying a Tank

The salt pumps are located on structures above the roofs of the tanks. As such, the top of the pump is located in a fixed position. However, the location of the bottom of the pump is a function of the thermal expansion of the pump column. In the hot tank at one commercial project, the distance between the bottom of the pump and the top of the floor is 430 mm with the equipment at ambient temperature; the distance is reduced to 230 mm with the equipment at the design temperature.

At this particular project, the minimum submergence of the pump is 400 mm. As such, if the tank must be emptied, the pumps can only draw suction down to inventory levels between 630 mm (inventory at the design temperature) and 730 mm (inventory at the minimum salt temperature). After the pumps could no longer draw suction, this would leave something on the order of 1,700 metric tons of salt in the tank.

Pump Tail Pieces

To remove a portion of the remaining salt, one approach is to remove one of the pumps from the tank, install a tail piece on the suction bell, reinstall the pump, and pump down to a level that is as low as the pump can safely operate without vibration. Nonetheless, this approach carries two liabilities:

- All of the salt cannot be removed from the tank due to the flow characteristics of the salt at the entrance to the suction bell; i.e., some minimum submergence will always be required to prevent two-phase flow at the pump inlet

- The time required to withdraw, and reinstall, the pump is at least 16 hours.

Ring Header with Eductors

One possible approach to remove essentially all of the salt is to install a dedicated ring header on the floor at the point of the lowest elevation; i.e., the tank perimeter. The ring header will have a series of eductors, which draw suction from points essentially on the floor.

The motive salt for the ring header in the cold tank is provided by salt from one of the hot salt pumps. The piping connection between the discharge of the hot salt pump and the inlet to the ring header is by a dedicated line, which has blind flanges at each end. The blind flanges are removed only when it is necessary to drain the tank. The discharge of the ring header returns to the hot salt tank.

Similarly, the motive salt for the ring header in the hot tank is provided by one of the attemperation pumps. The discharge from the ring header returns to the cold salt tank.

The motive salt for the eductors in the cold tank is hot salt. However, the hot salt flows only through the venturi; the high temperature salt does not come into contact with the cold tank wall or floor. A similar condition applies to the cold salt supplied to the eductors in the hot tank.

It can be noted that the proposed approach is only conceptual; it has yet to be demonstrated in a commercial project.

Temporary Drain Pump

One approach that has been adopted in 4 commercial projects to remove the last 0.5 m of salt is the following:

- A DN100 hole is drilled in the side of the tank. A pipe is inserted through the hole, and the dimensions of the pipe are such that the end of the pipe reaches the floor
- A temporary cantilever salt pump and sump are installed outside of the tank, at an elevation somewhat below the elevation of the floor
- A second section of temporary pipe is installed, which reaches the bottom of the sump
- The sump is filled with salt, and the pump is started. A partial vacuum is drawn in the temporary line, which establishes a siphon flow in the line
- The discharge from the temporary pump is directed to a catch basin, where the salt is allowed to freeze.

The approach is effective in removing essentially all of the salt from the tank.

It can be noted that installing temporary drain equipment in response to a leak requires the removal of a section of insulation on the tank wall. This results in 1) a wall temperature that is relatively high beneath the insulation to the left of the section where the insulation has been removed, 2) a wall temperature that is relatively low where the insulation has been removed, and 3) a wall temperature that is relatively high beneath the insulation to the right of the section where the insulation has been removed. For a flat plate, subjected to a temperature gradient of high - low - high, the thermal stress can be estimated using the equations shown in Figure 10-3.

Using representative properties for Type 347H stainless steel, a temperature gradient of 27 °C results in a peak stress equal to the ASME allowable value, and a gradient of 58 °C results in a peak stress equal to the yield stress. These gradients are quite moderate; as such, the potential for damaging the tank wall by removing the insulation is fairly high.

As an alternate approach, the equipment required to drain the last 0.5 m of the inventory can be classified as permanent equipment, which is installed when the storage system is constructed. In this way, the equipment is 1) pre-installed to limit the exposure of plant personnel to unexpected hazards, and 2) insulated to control thermal stresses.

A rectangular plate or strip $ABCD$ (Fig. 15.5) is heated along a transverse line FG uniformly throughout the thickness and across the width so that the temperature varies only along the length

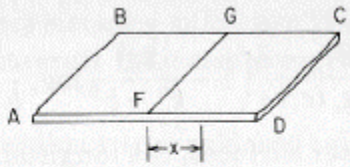

Figure 15.5

with x. At FG the temperature is T_1; the minimum temperature in the plate is T_0. At any point along the edges of the strip where the temperature is T, a tensile stress $\sigma_x = E\gamma(T - T_0)$ is developed; this stress has its maximum value at F and G, where it becomes $E\gamma(T_1 - T_0)$. Halfway between F and G, a compressive stress σ_y of equal intensity is developed along line FG (Ref. 7).

Figure 10-3 Thermal Stress due to Temperature Gradient

10.8 Steam Generator

10.8.1 Introduction

The specification for the steam generator is largely a functional one. Requirements are set for a broad range of items, such as live steam pressure-temperature-flow, reheat steam pressure-temperature-flow, feedwater pressure-temperature-flow, and steam quality. The details of the design, such as heat transfer areas and pressure drops, are then selected by the vendor.

10.8.2 Design Codes

The steam generator is not considered a fired heater; as such, the requirements of ASME Section I are not considered mandatory. The most common design code is ASME Section VIII. Both Division 1 and Division 2 of Section VIII can apply, depending on the locations in the heat exchanger which are subjected to relatively high levels of transient stresses. Nonetheless, it can be noted that California and the city of Albuquerque, New Mexico, have determined that new steam generators, whether fired or unfired, must be designed to the requirements of Section I.

Allowable material stresses are derived from Section II of the ASME Code.

Depending on the process conditions and the dimensions of the heat exchangers, the requirements of the Tubular Equipment Manufacturers Association may also apply.

10.8.3 Process Design

The heat transfer areas, and the pressure drops, in each of the steam generator heat exchangers are selected based on the design point requirements. However, the steam generator necessarily undergoes a startup and a shutdown each day. At the low flow rates characteristic of startup and shut down, the pressure drops on both the shell- and the tube-sides are very low. Low pressure drops generally lead to non-uniform flow distributions. Non-uniform flow distributions produce non-uniform temperature distributions, which, in turn, can lead to unpredictable, and potentially high, local stresses. To a first order, the majority of the heat exchanger failures experienced in solar projects are due to high stresses, typically in the tubesheet, generated during the startup and the shutdown cycles.

In general, it is difficult to calculate, with certainty, the flow and the temperature distributions in the heat exchangers during transient conditions. As a result, it is difficult to predict, with any reasonable certainty, the low cycle fatigue life of the equipment. To prevent these problems, a process design must be developed which ensures that acceptable temperature distributions are known to be present in each of the heat exchangers at a continuous thermal duty equal to 1 percent of the design duty.

An alternate approach is to establish a set of flows and temperatures in each heat exchanger that are not proven to be safe on a local level, but are known to be safe on a global level. One example is the preheater. Early in the startup process, feedwater flow rates are in the range of 1 to 10 percent of the design flow rate. In this range, it is unlikely that the flow will be distributed uniformly among the ~900 tubes in the heat exchanger. However, it is possible to artificially increase the feedwater volume flow rate by recirculating saturated water from the steam drum to a mixing point upstream of the cold end of the preheater. As an example, the volume flow rate can be increased to 25 percent of the design volume flow rate. The flow distribution will still not be known on a local basis. However, the volume flow rate satisfies the vendor's lower limit on the minimum flow rate (typically 16 percent). As such, the flow and the temperature distributions in the heat exchanger are known to be safe on a global level, and the preheater can safely operate, on a continuous basis, at feedwater flow rates in the range of 1 to 10 percent of the design value.

10.8.4 Material Selection

Preheater

Due to a relatively low design temperature (400 °C), the preheater is typically fabricated from a carbon steel. The choice of the alloy for specific section of the heat exchanger, such as the tubes, will be made by the vendor based on availability, allowable stresses, and ease of fabrication.

Evaporator

The solar industry has generally defaulted to the use of Type 347H as the material for the tubes, the shell, the channel, and the tubesheet in the evaporator. At the design temperatures

in the evaporator, Type 347H offers a favorable combination of high strength and good resistance to salt corrosion. Nonetheless, the material is not without potential liabilities. The steam generator is not a fired heater, and as such, does not need to comply with the requirements of Section I of the ASME Code. However, austenitic materials are prohibited in Section 1 for heat exchangers in boiling service due to the potential for chloride stress corrosion cracking.

A range of ferritic materials offer the required resistance to salt corrosion at the design temperature of the evaporator (510 °C). These include 5 Cr - 1 Mo and 9 Cr - 1 Mo, particularly if vanadium is included as an alloying element. The evaporator at the Solar Two project was fabricated using T91 tubes, and performed satisfactorily until the tube bundle ruptured as the result of an error in the process design. The ferritic materials do not use nickel as an alloying element, which makes the material essentially immune to chloride stress corrosion cracking. The ferritic materials are also much less susceptible to pitting corrosion should solid iron oxide materials be transported from the condensate system, and accumulate in the evaporator. Pitting corrosion in stainless steel evaporator tubes is a known problem in commercial plants.

Superheater and Reheater

The tubes, the shell, and the tubesheet are fabricated from stainless steel to provide the required resistance to corrosion from salt. The channel is not exposed to salt, but it is also typically fabricated from stainless steel. All of the components are fabricated from an 'H' grade of stainless steel, with a minimum carbon content of 0.04 percent, due to Code requirements for design temperatures above 538 °C.

In principle, the fabrication material could be a non-stabilized stainless steel, such Type 304H or Type 316H, or a stabilized stainless steel, such as Type 321H or Type 347H. However, the non-stabilized materials are subject to intergranular stress corrosion cracking should the heat exchangers, during a maintenance period, be exposed to liquid water. The most likely sources of water would be condensation of moisture in the air if the metal temperatures fell below the dew point, or a hydro test after a tube inspection or after inserting a tube plug. To avoid the potential for intergranular stress corrosion cracking, the solar industry has generally adopted a stabilized stainless steel for the tubes, the channel, the tubesheet, and the shell. The most common choice is Type 347H due to its availability in the shapes required.

It can be noted that the potential problems with stress relaxation cracking of Type 347H in hot salt tanks may not be as prevalent in a heat exchanger. Similar to the bottom course in a hot tank, the heat exchanger requires the welding of thick metal sections to one another. The thickest connection is the weld between the channel and the tubesheet. This requires the use of multiple welding passes, similar to the number of passes in the welds of a hot tank. In terms of stress relaxation cracking, both of these weld regions produce a high risk due to the large residual stresses. However, the heat exchanger, after fabrication, can be heat treated in an oven to reduce the residual stresses. Further, the rates of heating, and the hold times at the required temperatures, can be carefully controlled, which reduces the potential for hot reheat cracking.

10.8.5 Fouling Factors

Fouling factors on the water/steam side of the heat exchangers are generally well known, based on decades of experience with solar steam generators in commercial projects. Values recommended by the vendor are likely the best choice. However, there is little published information, either experimental or theoretical, on the recommended factor for the salt side. The industry has often adopted a default value of 0.000088 m^2-°C/W (1/2000 Btu/hr-ft^2-°F), but the value should be viewed as an allowance. In a commercial project, the engineering contractor should request the vendor to develop designs based on values of 0.00018, 0.000088, and 0.000059 m^2-°C/W (1/1000, 1/2000, and 1/3000 Btu/hr-ft^2-°F), and then perform a risk analysis to determine the best combination of long-term heat exchanger performance and capital cost.

On a related point, the fouling factors selected for the water side of the preheater and the water/steam side of the evaporator are likely to assume that the feedwater chemistry remains within the design values for pH and dissolved oxygen. However, a number of commercial projects have experienced problems with water chemistry due to operators errors, inadequate operator training, or improperly calibrated monitoring equipment. In a commercial project, the engineering contractor should evaluate the potential for a similar situation to occur, and conduct a risk assessment to determine the best combination of fouling factor, long-term heat exchanger performance, and capital cost.

10.8.6 Feedwater Preheating

The temperature of the feedwater at the cold end of the preheater must always be high enough to prevent salt from freezing in the heat exchanger. At the design point, the final feedwater temperature is always high enough (~ 240 °C) to satisfy this requirement. However, during turbine startup and low load operation, final feedwater temperatures are in the range of 180 to 230 °C, and freezing is likely to occur. To prevent this, one of two forms of feedwater preheating are used in commercial projects:

- A startup feedwater heater is located between the last extraction feedwater heater and the steam generator preheater. The heat source for the startup heater is typically live steam. The live steam is throttled and attemperated prior to delivery to the heater.

- Saturated water from the steam drum is recirculated to the cold end of the preheater. Direct contact heat exchange between the saturated water and the final feedwater raises the temperature of the mixed feedwater flow to the required values.

The first approach is the most common, as it effective and avoids the need for a recirculation pump. However, using live steam for feedwater heating is thermodynamically inefficient, and this form of feedwater heating has a measurable negative effect on the gross cycle efficiency at loads in the range of 60 to 90 percent.

The second approach incurs a smaller thermodynamic penalty than the first, and it avoids the need for an additional heat exchanger. Specifically, the startup heater is exposed to large

temperature changes each day, and it is subjected to rapid temperature changes in response to a turbine trip. A leak in the startup heater, or a failure in the instruments associated with the startup heater, will likely lead to a forced outage. However, the second approach requires a recirculation pump, which is not needed in the first approach.

The decision between the two approaches will depend, to some degree, on the selection of the circulation concept for the evaporator. If the evaporator uses forced circulation, then the second approach requires only the addition of a set of preheater recirculation pumps in parallel with the evaporator circulation pumps. However, if the project or the vendor selects a natural circulation evaporator to avoid the need for circulation pumps, then the first approach to feedwater preheating is likely to be preferred.

10.8.7 Evaporator Circulation

Commercial projects have successfully used both natural and forced circulation for the evaporator. The decision is normally based on the preferences of the steam generator vendor. Nonetheless, there is an incentive to select a forced circulation design. The benefits are associated with actively controlling temperature profiles in the heat exchangers during startup and low load operation.

The approach to temperature control relies, in part, on the recirculation of saturated water from the steam drum to the cold end of the preheater. As such, the second approach to feedwater preheating, discussed above in Section 10.8.6, would be the clear choice.

It can be noted that recirculating water from the steam drum the cold end of the preheater increases the volume flow rate through the preheater. The engineering contractor will need to evaluate each step in the startup of the Rankine cycle to determine the volume flow rate to the preheater at each combination of load, final feedwater temperature, feedwater flow rate, and recirculation flow rate. There may be a stage in the startup process that results in volume flow rate which is larger than the volume flow rate at the 100 percent load condition. If so, the design condition for the preheater may be during an intermediate turbine load, rather than at full load.

10.8.8 Fabrication Approaches

There are several methods available for distributing flow to the tubes in each heat exchanger:

- Conventional, with a flat tubesheet. The tubes are strength welded to the face of the tubesheet, and the tubes are then plastically expanded into the tubesheet in a rolling operation.

- Internal bore welding, with a flat tubesheet. Nozzles are machined from the face of the tubesheet. The ends of the tubes are butt welded to the ends of the nozzle using an internal bore welder.

- Header/coil, with a circular tubesheet. Holes are drilled in a section of pipe, nozzles are welded at each hole, and the ends of the tubes are welded to the ends of the nozzle.

The first approach is the most common, as it is typically the most economical. However, the steam generator necessarily operates through daily temperature cycles. The heat exchanger consists of metal sections which range from thin (1.65 mm for the tube wall) to thick (200 mm for the tubesheet). During transient conditions, temperature gradients are established, which lead to stress gradients. The stress gradients can result in flexing of the tubesheet, which causes relaxation of the friction connection between the tube and the tubesheet. If the friction bond is broken, then cyclic loads on the tube-to-tubesheet weld often cause the weld to fail, which leads to leakage from the channel (water/steam) into the shell (salt).

The integrity of the tube-to-tubesheet connection can be maintained if the heat exchangers are operated within the transient limits defined by the vendor. Representative limits include a maximum rate of temperature change of 10 °C/min and a maximum thermal shock of 100 °C. Thermal shock is defined as the difference in temperature between the fluid entering the heat exchanger and the metal temperature in the heat exchanger. The value can be either positive or negative. In general, one thermal shock per day is permitted.

It can be noted that these limits, although specified by the vendor, have been difficult to satisfy in many commercial projects.

The internal bore welding and the header/coil approaches typically result in an increase the capital cost of the heat exchanger; perhaps on the order of 20 to 30 percent. However, each approach offers the following benefits regarding reliability:

- The connections between the tube and the tubesheet are welded, which should be a more robust connection than a friction connection

- The nozzles between the tubesheet and the tubes are typically tapered, and the transition in thickness between the tubesheet and the tube reduces the thermal stresses in this region during transient conditions.

Should a heat exchanger develop a leakage rate that requires a shutdown for tube plugging, the outage period to cool the heat exchangers, effect the repairs, and preheat the equipment in preparation for filling with salt is at least 1 week. The weekly revenue of a typical commercial project is on the order of $1,000,000. If the selection of an all-welded fabrication approach reduces the number of plant shutdowns required for heat exchanger repair by even one during the 30-year life of the project, the marginal capital cost for all-welded construction is likely to be justified.

10.8.9 Commercially Acceptable Rates of Temperature Change

The allowable rate of temperature change is defined by the vendor, and is generally the result of a low cycle fatigue analysis of the heat exchanger geometry. Representative values range from 8 to 12 °C/min.

As noted above, some commercial projects have had difficulty meeting a requirement of 10 °C/min. If the heat exchangers have a limit which is lower than 10 °C/min, this will compound the problem. In general, an allowable rate of 8 °C/min is probably too low for commercial consideration.

The engineering contractor must develop a process design that can satisfy, with some margin, the vendor limits on rate of temperature change. To the extent that the engineering contractor has confidence in the control authority of the proposed process design, this may determine the minimum allowable rate specified the procurement package.

10.9 Steam Bypass System and Air Cooled Condenser Capacities

During normal operation, the air cooled condenser rejects heat from the Rankine cycle to the environment. To a first order, a plant with a 125 MWe turbine, operating with a gross cycle efficiency of 0.43, requires an air cooled condenser capacity of 165 MWt.

Tripping the steam generator, in response to a turbine trip, should be avoided if possible. However, if the steam generator were to remain in operation at full load following a turbine trip, then the duty of the condenser would increase to 290 MWt.

Clearly the project would like to avoid a situation in which the design capacity of the condenser must be 75 percent greater than the normal operating duty.

There is also a second-order problem with the capacity of the steam bypass system. Specifically, the bypass system consists of a high pressure throttle valve, a high pressure water spray attemperator, a low pressure throttle valve, and a low pressure water spray attemperator. The latent heat transfer in the high pressure attemperator mimics the live steam enthalpy drop across the high pressure turbine, and the latent heat transfer in the low pressure attemperator mimics the hot reheat steam enthalpy drop across the intermediate / low pressure turbine. Spray water for the high pressure attemperator is provided by the feedwater pump, and spray water for the low pressure attemperator is provided by the condensate pump.

The latent heat duty of the low temperature attemperator is such that required spray water flow rate plus the condensate flow rate from the condenser is about 130 percent of the condensate flow rate with the turbine operating at the design point. The condensate pump can be sized for the 130 percent condition. However, the pump would then be operating at approximately the 75 percent flow condition throughout the life of the project.

To avoid this situation, the capacity of the steam bypass system can be selected such that the required spray water flow rate to the low pressure attemperation plus the condensate flow rate is equal to the condensate flow rate when the turbine is operating at the design point. This can be accomplished if the live steam flow rate following a turbine trip is reduced to about 70 percent of the design flow rate.

The live steam flow rate can be reduced to 70 percent of the design value by reducing the flow rate of hot salt to the steam generator by 30 percent; i.e., to 70 percent of the design value.

The salt flow rate can be changed in manner of seconds, as the temperature profile along the steam generator flow path remains unchanged. However, the allowable rate at which the salt flow rate can be reduced is likely governed by level stability considerations for the steam drum.

If the live steam flow rate is reduced to 70 percent of the design value, then the condenser duty will be on the order of 200 MWt. This is about 20 percent greater than the design duty. However, by raising the saturation pressure in the condenser somewhat above the design value, the log mean temperature difference with the ambient increases, which increases the duty of the heat exchanger.

It can be noted that a steam bypass flow capacity equal to 70 percent of the design live steam flow rate is only a notional value. The actual value will be determined by the following:

- Transient level characteristics in the steam drum
- The potential availability of control valves, acting as pressure relief valves, on the steam drum to accommodate short term (on the order of minutes) increases in the drum pressure
- The ability of the air cooled condenser to accommodate saturation pressures above the design value.

11. Oil-to-Salt Heat Exchangers in Parabolic Trough Projects

11.1 Configuration

Shell and Tube

The industry has generally adopted shell-and-tube heat exchangers for oil-to-salt heat exchangers. The designs include 1) fixed tubesheet with U-tube bundles, 2) floating tubesheet with straight-tube bundles, and 3) header/coil arrangements with circular tubesheets.

The combination of the heat transfer properties of salt and the optimum approach temperatures require long heating lengths, which, in turn, often results in 3 to 6 heat exchangers in series. For the heat exchangers at the low temperature end of the series, the shell and tube materials can be carbon steel. For the heat exchangers at the high temperature end of the series, the tubes are stainless steel to provide the required corrosion resistance to the chlorides in the salt.

Flat Plate

Rather than shell and tube designs, two commercial projects selected a flat plate design. Stainless steel plates are stamped to provide the desired flow pattern. A group of plates are stacked, and then seal welded at the edges. Distribution boxes at each end of the exchanger align the salt flow and the oil flow in alternating, counterflow layers. An external steel box frame provides the required resistance to bowing of the plates generated by the fluid pressures.

The design offers a favorable combination a large heat transfer area in a small footprint, and low pressure drops on both the oil- and salt-sides. The principal liability is a significant difference in the low thermal inertia of the plates, and the relatively high thermal inertias of the perimeter plate welds and the external frame. To limit the stresses in the transitions between the thin metal sections and the thick metal sections, the allowable rate of temperature change is typically restricted to values (~ 1.5 to 2 °C/min) which are lower than values for shell and tube designs (~ 10 °C/min). Unfortunately, a rate of 2 °C/min is impractically restrictive for equipment that receives heat directly from the solar field. In commercial service, the heat exchangers developed cracks after only a few years in operation. The cracks allowed Therminol, at a pressure of 10 bar, to leak into the salt side, at a pressure of perhaps 2 bar. A pressure of 2 bar is less than the vapor pressure of Therminol at the design temperature. As a result, the Therminol flashes on the salt-side of the heat exchangers, carrying Therminol vapor into the ullage space of the storage tanks. Some of the Therminol eventually makes its way to the atmosphere, which represents both an emissions problem and a financial penalty to replace the lost Therminol.

On a point related to the leaks, it is difficult to access the portions of the heat exchangers where the cracks develop. The experience with leak repair has been decidedly mixed, and in some cases, the only method to repair the leak is to replace the heat exchanger.

11.2 Equipment Location

The heat exchangers are large and heavy pieces of equipment. The lowest cost approach to supporting the equipment is to place the heat exchangers at grade. However, commercial projects have located the equipment in one of the following two locations:

- On an elevated platform between the storage tanks, with a height slightly above the mid-point of the wall height of the tank

- On an elevated platform between the tanks, at a height above the top of the wall of the tanks.

These approaches are not inexpensive, as 1 to 1.5 kg of structural steel are required to support each kg of equipment. In addition, the wind loads on an elevated structure translate to higher foundation costs. Nonetheless, the benefits associated with elevating the equipment are judged to outweigh the costs, for the following reasons:

- With the heat exchangers located at grade, a drain tank, located below grade, is required. The drain tank requires a pit, electric heat tracing, thermal insulation, a range of instruments, and two drain pumps. This approach will incur a cost (but it will be less than the cost of an elevated structure)

- The drain pumps in the drain tank will have a certain capacity, which in turn, defines the time required to drain the heat exchangers. If the heat exchangers must be drained quickly in an emergency, then the drain pumps may not have the desired capacity unless large, and expensive, pumps are initially selected

- If the height of the elevated platform is at least the height of the mid-point of the tank walls, then the heat exchangers can be drained by opening a valve to the tank with the lowest inventory level. This passive drain approach is more reliable, and has a higher availability, than the active drain method associated with a drain tank and drain pumps. It can be noted that the mass of salt in the heat exchangers and in the associated piping is 'small' relative to the mass of salt in a storage tank, even with the tank at the minimum level. Assuming that adequate mixing occurs between the inventory in the tank and the salt entering the tank, then the thermal transient experienced by the tank during a drain sequence will be well within the limits set by the tank supplier.

- Most importantly, the heat exchangers, at some point in the life of the project, will need to be drained for inspection and maintenance. If the heat exchangers are located above the storage tanks, then there is no method by which salt can enter the heat exchangers after the equipment has been drained, and expose the maintenance personnel to potential harm. Similarly, if the heat exchangers are located at the mid-point of the tank wall height, and if the inventory levels in both tanks are set the same, then there is no method for salt to enter the heat exchangers. This is a subtle point regarding safety. There have been instances in which pipes were allowed to cool to ambient temperature, forming frozen plugs in the lines. The project staff knew, with certainty, that there was

no danger to the personnel working downstream of the frozen equipment. In separate cases, the frozen plugs thawed, resulting in severe injury in one case and death in a second. Locating the equipment on an elevated platform is, in effect, a form of insurance. And like all insurance, it is a complete waste of money, until it is needed.

12. Problems and Solutions for Parabolic Trough Projects using Inorganic Heat Transfer Fluids

Current problems with the use of inorganic heat transfer fluids in parabolic trough projects, and possible solutions, are outlined in the sections which follow.

12.1 Temperature Control in the Collector Field During Non-Operating Periods

12.1.1 Introduction

Prior to filling with salt, the field piping, the receiver tubes, and the flex hose assemblies are preheated to a nominal temperature of 300 °C. This is to prevent thermally shocking the receiver tubes, and to prevent local freezing in the smaller lines. The field piping is preheated using the electric heat trace system (Section 12.1.4). The receiver tubes and the flex hose assemblies are preheated using a number of portable impedance heating systems (Section 12.1.5).

Once the system is filled, the primary means of temperature control is continuous circulation of cold salt during those periods in which the collector field is not in normal operation (Section 12.1.6).

12.1.2 Loss of Salt Circulation to the Solar Collector Assemblies

If salt circulation stops, then temperature control of the field piping is performed with the electric heat trace system. However, there is no permanent equipment to maintain control of the temperature of the receiver tubes and the flex hose assembles. Since it is not feasible to rapidly drain the equipment in the collector field (i.e., within hours), a loss of circulation necessarily results in salt freezing in the receiver tubes and in the flex hose assemblies. Conceptual methods to recover from freezing in the receiver tubes and in the flex hose assemblies is described in Section 12.1.8.

12.1.3 Loss of Site Electric Power to the Field Piping

At some point in the life of the project, electric power could be lost at the site. This could occur due to the simultaneous loss of imported electric power from the grid, the loss of emergency power from the standby Diesel generator, or the loss of the transformer supplying electric power to the emergency bus. Should this happen for a period of a few days, then salt will begin to freeze in the field piping. The process for recovering from freezing in the field piping is discussed in Section 12.1.10.

12.1.4 Heat Trace System

All of the fixed salt piping in the collector field will use electric heat tracing, for the following purposes:

- Preheating the equipment prior to filling with salt

- Temperature maintenance during periods when the salt is not circulating

- Freeze recovery.

The design of the heat trace system is identical to the systems described in Section 9.8 and Section 10.6 of Volume 1 - Parabolic Trough Specifications, and in Section 6.8 of Volume 3 - Central Receiver Specifications.

12.1.5 Impedance Heating System

Impedance heating system operates on "Joule heating", allowing electricity to flow through the pipe network, generating heat from the energy dissipated in the resistance of each component. The impedance heating system is intended for three primary functions:

1. Preheat a collector loop before initial filling with salt (in addition to subsequent filling operations following any maintenance tasks that require draining)

2. Freeze protection for a collector loop which has experienced a loss of flow

3. Freeze recovery of a collector loop which has experienced a loss of flow for an extended period.

The design of the impedance heating system is discussed in Section 10.9.2 of Volume 1, Specifications for Parabolic Trough Projects.

12.1.6 Continuous Salt Circulation

As with the Therminol in commercial trough projects, once the field piping and receiver tubes are filled, the system remains filled throughout the life of the project. This is the case because there is no on-site storage equipment with sufficient volume to hold the entire inventory of the working fluid.

It can be noted that the salt tanks in the storage system are in one of two conditions: one is empty, and the other is full; or both are partially filled. In principle, there is a large permanent volume to accept salt drained from the collector system. However, if collector system is being drained, then the temperature of the salt from the collector system is likely to be 'low'. Introducing low temperature salt into the hot tank, or transferring salt from the cold tank to the hot tank to make space available in the cold tank, has the potential to thermally shock, and permanently damage, the hot tank. As such, the volume available in the storage tanks is not available to drain the collector field.

The basis operating mode for the collector field is continuous circulation, for the following reasons:

- Since there are no provisions for draining the entire system, the principal means of freeze protection in the field piping and in the receiver tubes is continuous circulation

during non-sunny periods [13]. Salt is circulated from the cold tank, through the collector field, and returned to the cold tank. Representative heat losses are on the order of 11 W/m^2 of collector aperture area.

- The inventory in the receiver tubes cools at a faster rate than the inventory in the field piping. Should the circulation stop for some period of time (say, hours), the temperature of the inventory in the field piping will be higher than the temperature of the inventory in the receiver tubes. When circulation resumes, there is the potential for thermally shocking the receiver tubes by introducing relatively warm salt from the field piping into the receiver tubes.

As such, the cold salt pumps must operate, essentially without interruption, for some 300,000 hours during the life of the project.

Thermal energy to compensate for the heat losses from the field piping and the receiver tubes is provided by the cold salt tank. If the temperature of the cold tank falls below a pre-determined value, then supplemental energy is supplied to the tank from external electric salt heaters. Electric power for the heaters is supplied from the grid, or should connection to the grid be lost, from standby Diesel generators.

12.1.7 Loss of Circulation Leading to Freezing in Receiver Tubes and Flex Hose Assemblies

In commercial projects, the reliability of the cold salt pumps, the electric salt heaters, and the standby Diesel generators is generally excellent, and the probability that continuous salt circulation can be maintained is regarded as high. Nonetheless, there are a number of conditions that could result in a loss of circulation, as follows:

- The switchgear supplying electric power to the cold salt pumps fails
- A crack develops, almost anywhere, in the headers of the field piping
- A defect in the insulation on the flex hose assemblies or the loop crossover piping leads to a frozen plug
- Salt isolation valves must be moved periodically to prevent sticking associated with corrosion. The isolation valve could move from open to closed, but then fails to re-open
- Operation of the salt pumps may require permissiveness from flow meters, pressure transmitters, or isolation valve positioners. If the signals from the flow meters, the

[13] Salt can be drained from individual loops by 1) closing isolation valves at the ends of the loop, 2) connecting a vacuum tank, located on the bed of a truck, to one end of the loop, 3) opening a vent valve at the other end of the loop, and 4) pushing salt from the loop into the vacuum tank by means of air flowing into the vent valve. Salt can be returned to individual loops by 1) closing the vent valve, 2) connecting the loop to the vacuum tank, 3) drawing a vacuum in the loop, 4) opening a vent valve on the vacuum tank to push salt into the loop, and 5) opening the isolation valves at the ends of the loop to establish salt circulation.

pressure transmitters, or the valve positioners are lost, then the pump will trip. If it appears that repairs to the flow meters, pressure transmitters, or valve positioners will require a period that could challenge the freezing time of a receiver tube in the worst-case condition (broken glass envelope), then the control system logic could be changed to bypass the permissive. At this time, the pumps could be restarted. However, having a qualified controls engineer at the site to revise the logic is not a certainty, particularly at night, on the weekends, and during holiday periods

- The pumps develop a mechanical problem, such as a broken coupling, or there is a problem with the variable frequency drive for the motors

- An operator, in an attempt to reduce the auxiliary power demand of the salt circulation pumps, operates the pumps at too low of a flow (leading to overheating), too low of a speed (leading to vibration), or beyond the run-out point (leading to vibration). Overheating and vibration will damage a pump, which then requires the pump to be removed for repair.

It is difficult to quantify the above effects, but the probability that one of the above, or something similar to the above, will occur during the life of the plant is a value approaching 100 percent. Depending on the source of the problem, and depending on the number and the location of the isolation valves in the field piping, something in the range of $^{1}/_{16}$ to $^{16}/_{16}$ of the salt in the receiver tubes and flex hose assemblies could freeze.

12.1.8 Freeze Recovery in the Receiver Tubes and Flex Hose Assemblies

Impedance Heating of Receiver Tubes

Previous studies looking at impedance heating of molten salt parabolic trough plants considered power densities up to 250 W/m for freeze recovery of the solar field [14]. A recent set of computational fluid dynamics calculations of the melting process show a total melt time of 12.0 hours for heat collection elements in which the vacuum space is intact [15]. (Melt times for receiver tubes with a lost vacuum or a broken glass envelope are the subject of separate studies.) The difference in heat losses between the bellows and receiver tube results in an acceptable maximum difference in temperature of 12 °C along the length of the receiver. Finite element calculations from the same study show a heat input of 250 W/m produces stresses of 40 MPa in the receiver tube and 9.5 MPa in the glass envelope, which are well below the yield strength of the absorber tube (205 MPa) and the glass envelope (27 MPa), respectively. The calculated stress values noted above assume the salt is free to expand during melting, as noted in previous freeze-thaw tests [16].

[14] D. Kearney, B. Kelly, and U. Herrmann, "Engineering aspects of a molten salt heat transfer fluid in a trough solar field," Energy, Vol. 29, No. 5-6, pp. 861-870, 2004
[15] Shininger, R., Imponenti, L., Kattke, K., and Marcotte, P. SMART: Simplified Melting And Rotation-joint Technology. United States: N. p., 2022. Web. doi:10.2172/1882508.
[16] G. Kolb, C. Ho, B. Iverson, T. Moss, and N. Siegel, "Freeze-thaw tests on trough receivers employing a molten salt working fluid", Proceedings of ASME Energy Sustainability, 2010

Another recent study considers a reduced order modeling approach to model and optimize a freeze recovery system for a commercial molten salt parabolic trough plant. In this case, the impedance heating system is limited by the cost of electrical utilities required to switch the plant from a 240 MW source to a 150 MW sink [17]. Depending on the size of the project, the ambient conditions, and the capacities of the electric heating systems, the cost constraints resulted in estimated melt times for the entire solar field in the range of 100 to 300 days.

In order to avoid challenges with electrical infrastructure and reduce the capital cost of impedance heating systems for the plant, a mobile heating system has been proposed and evaluated [18]. The mobile concept can be completely housed in trailers that can be moved by vehicle, each trailer would have a diesel generator and several DC power supplies depending on the plant geometry. It is estimated such a mobile system could significantly reduce the capital cost compared to fixed impedance heating circuits permanently installed at every collector.

During freeze recovery, salt in the headers and the flex hose assemblies should be melted prior to solar heating of the receiver tubes to allow the salt to expand in the axial direction. In a commercial system, there are many factors that cause salt to melt unevenly in a receiver tube (damaged glass envelopes, lost vacuum, broken mirrors, etc.), so it is possible that sections of the solar field could experience constrained salt expansion during freeze recovery. Modeling this phenomenon is very difficult. In addition, the initial conditions after freezing, in terms of void space in the receiver tubes, are not necessarily known. For these reasons, any freeze recovery system will have to be demonstrated at full scale (i.e., a complete loop) before commercial application. To date, demonstrations of freeze protection by impedance heating have occurred in 2-collector and loops operating with design temperatures of 500 °C [19], and freeze recovery has only been demonstrated on a smaller string of heat collection elements [3].

Solar Heating of Receiver Tubes

The solar heating method, or controllable solar flux heating, uses solar energy for freeze protection and recovery. Recent studies suggest it is possible to thaw frozen salt in the receiver tubes if the heat input is attenuated to reasonable levels [Imponenti et al, 2020]. One method to accomplish this is via a solar 'pass-through', i.e., cyclically moving the mirrors back and forth through the focal point of the collector. The heat input to the receiver tubes is adjusted by pausing the mirrors in the off-focus position before completing the next pass-through cycle. This method is attractive as it requires no additional hardware; however, additional testing is required before the technology can be considered commercially viable.

[17] C. Prieto, A. Rodríguez-Sánchez, F. J. Ruiz-Cabañas, and L. F. Cabeza, "Feasibility study of freeze recovery options in parabolic trough collector plants working with molten salt as heat transfer fluid," Energies, vol. 12, no. 12, 2019
[18] Shininger, Ryan, Imponenti, Luca, Kattke, Kyle, and Marcotte, Patrick. SMART: Simplified Melting And Rotation-joint Technology. United States: N. p., 2022. Web. doi:10.2172/1882508.
[19] Gaggioli, W., Fabrizi, F., Rinaldi, L., D. Ascenzi, "Experimental tests about the cooling/freezing of the molten salts in the receiver tubes of a solar power plant with parabolic trough", AIP Conference Proceedings 1850, 2017

The main problems regarding solar heating involve local non-uniform heat inputs and losses from the following effects:

- Receiver tubes with lost vacuum or broken glass envelopes
- Non-illuminated portions of the receiver tubes at the end of a collector at low sun incidence angles
- Broken or missing mirrors.

Additional aspects include the time and the weather conditions required for a full freeze recovery, which may restrict the effectiveness to the summer months at many plant locations. While modeling studies have shown the stress levels in the receiver tubes to be well below allowable values, no analyses have been performed on the collector drives to determine if the continuous back and forth motion effects the lifetime of this component.

Since solar heating is only applicable for the illuminated portions of the receiver tubes, an impedance heating system will still be required for both the receiver tubes and the flex hose assemblies. Solar heating may be used to supplement the impedance heating systems, allowing capital and operational cost savings.

12.1.9 Loss of Site Electric Power Leading to Salt Freezing in the Field Piping

As noted above, salt freezing in the field piping requires the simultaneous loss of imported electric power from the grid and emergency power from the standby Diesel generator. The probability that both sources of electric power would be simultaneously lost is low. However, the project lenders will assign a non-zero probability to the condition, and the project will need to specify, and evaluate, a method for recovery.

12.1.10 Freeze Recovery in the Field Piping

Technical Considerations

In commercial solar projects, the electric heat tracing performs the following functions:

- Preheat an empty pipe from an initial temperature of about 25 °C to the required salt fill temperature of 275 °C. The preheat period, which determines the heat input to the pipe, ranges from 8 to perhaps 16 hours
- Once the pipe is filled, but there is no flow in the pipe, maintain the temperature of the line at a value of at least 275 °C to prevent freezing.

As one might imagine, the thermal input to the pipe to meet the preheat requirement can be fairly modest, as the thermal mass of the system is limited to the thermal mass of the metal, plus a nominal one-half of the thermal mass of the insulation. However, there will be instances in which the heat trace system will be required to thaw the salt in the field piping. In this case,

the thermal mass of the system increases substantially; i.e., by the sum of the sensible heat required to increase the temperature of the salt from ambient to the melting point, plus the latent heat required to convert the solid salt to a liquid.

The time required to thaw a frozen line is a function of the diameter of the line. As the diameter of the line increases, the surface to volume ratio decreases, which generally increases the thawing period. In a commercial project, the largest line size is about DN 600 (24 in.). If the heat trace is designed to preheat an empty line in a period of 8 hours, then the required duty is a nominal 700 W/m. If the line, after filling, becomes frozen, then the time required to thaw the line is approximately 10 days.

If the heat trace system is operated with a duty cycle of 100 percent over a period of 10 days, then the pipe will reach a steady state temperature; in this case, a value of just over 600 °C. For a hot salt header, fabricated from stainless steel, this metal temperature is acceptable. However, for a cold salt header fabricated from carbon steel, the maximum metal temperature should be limited to 400 °C to prevent high metal corrosion rates. Doing so limits the allowable thermal input from the heat trace system to a nominal 400 W/m, which, in turn, increases the thawing period to about 20 days.

The 10 and 20 days thawing periods are based on 7 in. of calcium silicate insulation in an as-new condition. However, the quality of the insulation is expected to degrade over time due to 1) gaps developing in the insulation from daily thermal expansion and contraction cycles, 2) moisture intrusion, and 3) insulation compaction due to foot traffic. If the thermal conductivity of the insulation increases by 20 percent, then the thawing periods increase to about 12 days for the stainless steel lines and 24 days for the carbon steel lines.

A worst case condition be associated with local damage to the insulation which increased the thermal conductivity by a value of 50 percent. The damage could be due to personnel walking on the salt piping, incomplete repairs to the insulation, or salt leakage from a failed valve packing saturating the insulation. Should these conditions occur, the time to thaw a carbon steel header is on the order of 1 month.

The time to recover from a frozen collector field is in the range of 35 to 60 days. In practice, the time to recover may be longer, depending on the condition of the field piping insulation, the availability of the mobile impedance heating systems, and whether electric power to the field piping is interrupted during the freeze recovery process.

Financial Considerations

It is not unreasonable to expect that the first commercial projects will freeze salt in the collector field more often than expected, and the recovery times will be longer than expected. A potential, but not implausible, scenario might be one in which salt freezes in the field once in each of the first 5 years of commercial operation, and the recovery time in each case is 75 days. This would result in an availability in the first 5 years of commercial service of 70 to 75 percent, rather than the expected 90 percent. A worst case scenario might be on in which salt

freezes twice in the first year of commercial service, and the recovery time in each case is 90 days. This would result in an availability of 50 percent in the first year of service.

Plant availabilities in this range, particularly early in the life of the project, will have a noticeable, and detrimental, effect on the return on investment to the equity providers. In principle, the equity providers can compensate for the availability risks by increasing the return on investment. However, this will increase the levelized cost of energy. At some point, the risk premium for the use of an inorganic heat transfer fluid will offset the benefits of using an inorganic fluid; i.e., a reduction in the unit cost of the storage system, and an increase in the gross Rankine cycle efficiency. The economics of a plant using an inorganic fluid may essentially be a on par with the economics of a plant using Therminol as the working fluid. In this case, the investment community would, in their own interests, continue with the current state of the art in trough technology, and the commercial potential of the advanced working fluid may not be realized.

13. Salt Tanks in Parabolic Trough Projects

13.1 Material Selection

A range of corrosion studies have shown acceptable corrosion characteristics of carbon steel, at temperatures up to 400 °C, with chloride contents up to 0.6 percent [20,21]. As a result, all commercial parabolic trough projects fabricate the cold tank and the hot tank from carbon steel.

13.2 Corrosion Characteristics

At least one commercial project has experienced problems with significant corrosion in the salt tanks. The repairs involved suspending the tank on external supports, and replacing a portion of the bottom course in the tank wall.

An examination of the sections removed showed evidence of stress corrosion cracking. This form of corrosion is different than the uniform surface corrosion processes observed in the Abengoa and the Sandia studies.

Stress corrosion cracking is a combined mechanical and electro-chemical corrosion process which results in cracking of certain materials [22]. The mechanism is not simply an overlapping of corrosion and mechanical stresses, but an auto-catalytic, self-accelerating process leading to high metal dissolution rates. The process includes an oxidation reaction:

$$Fe \rightarrow Fe^{++} + 2\ e^{-}$$

The oxidation reaction is accompanied by a reduction reaction, typically involving the oxygen and water:

$$O_2 + 2\ H_2O + 4\ e^{-} \rightarrow 4\ OH^{-}$$

Further reactions can then occur, including:

$$Fe^{++} + 2\ OH^{-} \rightarrow Fe(OH)_2$$

$$2\ Fe(OH)_2 + H_2O + \tfrac{1}{2}\ O_2 = 2\ Fe(OH)_3$$

The hydrated oxides can lose water during dry periods, and revert to anhydrous oxides, including ferrous oxide (FeO) and ferric oxide (Fe_2O_3, hematite).

---

[20] Sanchez, L., and Madina, V. (Abengoa Solar NT, Sevilla, Spain), 'Estudio de corrosion del acero A516Gr70 en tanques piloto. Tiemp 1', Documento 12-0106-IN-641-000, July 2009

[21] Bradshaw, R. W., and Clift, W. M. (Sandia National Laboratories, Livermore, California), 'Effect of Chloride Content of Molten Nitrate Salt on Corrosion of A516 Carbon Steel', Sandia Report SAND2010-7594, November 2010

[22] Corrosion in Carbon Steels – IspatGuru

Initially, a small pit is formed at the surface, and develops into a crack due to applied or residual stresses in the material. The crack formation opens up a new active (non-passive) metal surface, which corrodes very easily. This leads to further crack propagation and exposure of new highly active metal surfaces in the crack. Metal dissolution in the crack advances rapidly until mechanical failure occurs. Brittle failure can occur in normally ductile metals at stress levels which are less than the yield strength. Internal stresses in a material can be sufficient to initiate an attack of stress corrosion cracking.

Stress corrosion cracking of carbon steel is rare compared with stress corrosion cracking of stainless steel. One potential source of cracking in carbon steel is the exposure of the metal to liquid water in the presence of nitrates. One hypothetical failure mechanism is as follows:

- The outside of the tank is exposed to nitrate salt. The source of the salt could be 1) vapor condensation from ullage gases passing through a vacuum / pressure relief valve, or 2) salt leakage from pumps, valves, instruments, or piping above the tanks

- Water comes into contact with the outside of the tank. The source of the water could be 1) site flooding during a particularly heavy rain, 2) rainwater entering gaps in the tank insulation, or 3) maintenance personnel using wash water to remove the salt

- As noted above, process conditions (i.e., hydrostatic loads) can produce stresses, which are 1) within the ASME allowable values, but 2) high enough to initiate cracking. Additional stresses can be generated should water come into contact with the tank. Heat transfer will produce local temperature gradients, which, in turn, can generate local thermal stresses. Temperature gradients on the order of 45 °C can produce stresses equal to the ASME allowable value, and a gradient of approximately 115 °C can cause the material to yield.

Should the above combination of conditions occur, then a failure due to stress corrosion cracking may be the result.

To limit the potential for stress corrosion cracking, the following approaches can be adopted:

- If frozen salt is to be removed from the metal, methods should be limited to mechanical abrasion or media blasting

- To prevent runoff, following heavy rains, from coming into contact with the bottom of the tank, a comprehensive drainage system can be provided. Alternately, the tanks can be elevated above grade; however, this approach can be more expensive than a drainage system.

- Ensure that the metal jacket covering the insulation is always free of gaps and defects

- To the extent possible, locate equipment, such as pumps, valves, instruments, and fittings, away from the top of the tank

- Substitute a ferritic material, such as 2¼ Cr - 1 Mo, for the carbon steel. The chromium offers a more robust surface passivation layer than can be provided by carbon steel, and the absence of nickel in the alloy limits the potential for stress corrosion cracking. It can be noted that 1) the reliability of salt tanks fabricated from carbon steel has been excellent, and 2) the occurrences of stress corrosion cracking in carbon steel are rare, and the sources of the corrosion are both understood and preventable. Selecting a ferritic material would only apply to rare cases where carbon steel would be routinely, and unavoidably, exposed to combinations of salt and liquid water.

13.3 Survival Hypothesis for Carbon Steel Tanks

The cold tanks in central receiver projects, and the hot and the cold tanks in parabolic trough projects, are fabricated from carbon steel. Known failures in carbon steel tanks include weld defects (1 tank) and stress corrosion cracking from water/salt mixtures on the tank exterior (several tanks). However, in contrast to stainless steel tanks, there have been no known failures due to leaks in the floor.

The similarities between carbon steel tanks, and the stainless steel hot salt tanks in central receiver projects, are numerous. The common features include the following:

- The system geometries are essentially identical: flat bottom tank with a self-supporting domed roof; insulated foundation with cooling air passages; and inlet salt flow distribution by means of a distribution ring header
- The floors consist of a staggered array of thin (7 to 8 mm) rectangular plates. The plates are connected to one another by butt welds. The floor deforms during the welding process, producing an array of shallow domes

- Prior to filling with salt, the tanks are preheated using combustion gases. Less-than-perfect control over the flow distribution of the combustion gases can produce radial temperature gradients in the floor, which are of sufficient magnitude to potentially buckle the floor

- When the tank is filled, hydrostatic forces push the floor flat against the foundation

- Residual stresses due to welding and floor deformations tend to persist; i.e., stress relaxation is moderate due to the low operating temperatures

- Radial temperature gradients are an inherent characteristic of the tank and the foundation design, and the gradients have the potential to damage the floor

- Daily reversals in floor friction forces, due to daily thermal cycles, are also an inherent characteristic, and have the potential to damage the floor.

Nonetheless, there are important differences with the hot salt tanks in projects operating at design temperatures above 500 °C, as follows:

- The coefficient of thermal expansion for carbon steel (11 to 12 10^{-6} /°C) is approximately 70 percent of the coefficient of expansion for stainless steel (16 to 17 10^{-6} /°C). For a given temperature differential, the thermal stresses due to self-restraint in a carbon steel tank are about 30 percent lower than the thermal stress due to self-restraint in a stainless steel tank. This characteristic is important in reducing the effects of radial temperature gradients in the floor

- The thermal conductivity of carbon steel (40 to 45 W/m-°C) is at least a factor of 2 higher than the thermal conductivity of stainless steel (15 to 20 W/m-°C). The higher conductivity has a second-order, but useful, effect in terms of reducing thermal stresses during transient conditions

- For carbon steel, at 370 °C, the stress amplitude associated with a fatigue life of 40,000 cycles is 209 MPa. For stainless steel, at 540 °C, the stress amplitude associated with a fatigue life of 40,000 cycles, is 159 MPa. For a given stress amplitude, carbon steel accumulates fatigue damage at a lower rate than stainless steel

- In a central receiver project, during transient conditions, the salt flow enters the cold tank at a temperature that is higher than the bulk inventory. Due to density differences, the incoming flow rises, rather than sinks. This reduces the potential for local temperature gradients in the floor, and the associated thermal stresses

- The temperature gradients in the tank are a function of the inventory temperature, the thermal resistance of the insulation, and the degree to which the properties of the insulation have degraded over time. In a parabolic trough project, the inventory temperature in the hot tank is approximately 180 °C lower than the inventory temperature in the hot tank of a central receiver project. The lower temperatures reduce the potential to produce large temperature gradients, and thereby large thermal stresses, in the tank, particularly in cases in which the insulation has degraded or been subject to mechanical damage.

- The response time of the collector field in a trough project is longer than the response time of the heliostat field / receiver in a central receiver project. As such, the rates of temperature change in the hot tank of a trough project are relatively slow. This reduces the potential for non-isotropic temperatures in the bulk inventory, and reduces the magnitude of intra-tank thermal stresses due to self-restraint

- Both the cold tank and the hot tank in parabolic trough plants operate at temperatures below which creep damage can start to develop. The opposite applies to the hot tanks in central receiver projects

- The niobium in Type 347H generates niobium carbonitrides. The non-uniform precipitation of the carbonitrides, as discussed in Section 14.16.2, leads to non-uniform strength distributions, stain localization, internal cracks, internal voids, and eventually external cracks. The precipitation characteristics are the most pronounced in areas of high strains; i.e., the tops of buckles. The floors in carbon steel tanks likely experience

similar deformations and areas of high strains. However, unlike Type 347H stainless steel, the strength and the ductility of carbon steel do not decay over time.

In general, if a carbon steel tank can survive the first 3 years of service, then it is likely to survive the full 30 years.

14. Stainless Steel Hot Salt Tanks in Central Receiver Projects

14.1 Representative Commercial Design

14.1.1 Tank

A representative storage quantity for a commercial project is 30,000 to 40,000 metric tons of salt. Since the salt has an extremely low vapor pressure (< 1 kPa at 600 °C), the lowest cost storage approach is a vertical tank with a flat bottom and a self-supporting roof. Due to the chemical stability of the salt, the tank can be vented directly to the atmosphere.

Design standards for this type of tank, operating at temperatures up to 600 °C, have yet to be developed. In the interim, the closest design standard is American Petroleum Institute Standard 650, Welded Tanks for Oil Storage. However, the Standard only considers operating temperatures up to 260 °C, and low cycle fatigue conditions are not part of the Standard. As a result, a hybrid design approach has typically been adopted, as follows:

- For design temperatures above 260 °C, allowable material stresses are derived from Section II of the ASME Code
- For the evaluation of low cycle fatigue, the methods described in Section VIII, Division 2, of the Code are often adopted.

It can be noted that, in some project jurisdictions, an evaluation of the fatigue life using Section VIII Division 2 is not required. However, this can present a substantial risk to the project in terms of the reliability of the storage system. A discussion of the recommended design codes is presented in Section 14.14.1.

For design temperatures above 538 °C, the H grades of stainless steel, with a minimum carbon content of 0.04 percent, are required by the ASME Code. Candidate materials include Type 304H, Type 316H, and Type 347H stainless steel. At the 10 MWe Solar Two demonstration project, the hot tank was fabricated from Type 304H [23]. However, to avoid potential problems with intergranular stress corrosion cracking, the solar industry has adopted Type 347H, a stabilized stainless steel, in the current generation of projects.

14.1.2 Foundation

The foundation consists of the following elements, moving from the top down:

- A layer of solid lubricant; candidate materials include sand, perlite, and calcium silicate
- The primary tank support / insulating layer under the floor. Candidate materials include expanded clay, expanded glass, and refractory bricks

[23] Pacheco, James (Sandia National Laboratories, Albuquerque, New Mexico), 'Final Test and Evaluation Results from the Solar Two Project', Sandia report SAND2002-0120, January 2002

- A concrete base mat below the insulating layer

- A concrete ring wall to retain the insulating layer underneath the tank.

The foundation base mat has a series of cooling air pipes embedded in the concrete. Air flow in the cooling passages is established by fans or by natural convection. The air flow rate is set to maintain the soil temperature, directly beneath the foundation base mat, at values no higher than 75 °C. The goal is to limit the desiccation of the soil, and the oxidation of organic materials, to values that prevent unpredictable settlements of the tank.

14.2 Failure Patterns

The number of commercial central receiver projects in service, excluding those in China, is six: Gemasolar, Cerro Dominador, Crescent Dunes, Noor III, Redstone, and Noor Energy 1. The first four plants have been in service for some number of years, and the last two have recently entered service.

Among the first four, the hot salt tank at Gemasolar has failed, and a replacement tank has been built alongside the first tank. Also, the hot salt tank at Crescent Dunes has developed leaks in the floor on three occasions, and problems have developed with two other projects. For the plants which have been in service for more than 1 year, the failure rate, for all intents and purposes, is essentially 100 percent. Given the limited number of commercial projects the failure rate of hot salt tanks is not commercially sustainable.

With the limited number of cases, it is difficult to define a generic or a typical failure mechanism. Nonetheless, all of the tanks share a common set of characteristics which, when combined, are potential sources of future problems. The common design and operating characteristics include the following:

- The floor is fabricated from an array of rectangular plates. Welding the plates to one another generates residual welding stresses which are equal to, or higher, than the yield stress (see Section 14.5). Weld shrinkage establishes tensile stresses at the top of the plates, which are balanced by compressive stresses at the bottom of the plates. The stresses cause the plates to bow upward at the center, and the plates take on the shape of a shallow dome. The height of the dome is in the range of 50 to 150 mm. It can be noted that the floor is a large, thin sheet. The sheet, having been deformed by the welding process, has a low structural stability in terms of its ability to tolerate compressive stresses

- The tank is filled with water for the hydraulic tests. When the hydrostatic pressure reaches a value of about 7 kPa (approximately 1 m of water), the plates are pushed flat against the foundation (see Section 14.6). Changing the shape of the plates from domed to flat generates compressive stresses at the edge of the plates that are at, or above, the yield stress. When the water is removed at the end of the hydraulic tests, the plates revert from flat back toward the original domed shapes. However, the

residual stresses and the shape of the floor after the hydraulic tests will be different than the residual stresses and the shape of the floor before the hydraulic tests

- Radial temperature gradients in the floor are an inherent characteristic of a flat bottom tank on an insulated foundation (See Section 14.7). Specifically, the conduction heat transfer into the foundation near the center of the tank is 'low' due to the long conduction heat path from the center of the foundation to the ambient. In contrast, the conduction heat transfer into the foundation, and to environment, near the perimeter of the tank is 'higher' due to the relatively short conduction heat paths to the ambient. A radial temperature gradient establishes a combination of radial and tangential stresses in the floor. At some value for the gradient (yet to be defined, but perhaps 30 to 40 °C), the combination of radial and tangential stresses can reach the yield value near the center, and at the perimeter, of the tank

- The tank is preheated using combustion gases from a fired air heater (see Section 14.8). The gas flow patterns inside the tank are determined by the arrangement of the inlet duct and the outlet chimney. However, high temperature air is a relatively poor mechanism for convection heat transfer, and the uniformity of the gas flow pattern inside the tank is determined by the sophistication of the duct and chimney arrangement. Further, the thermal inertia of the floor is lower than the thermal inertia of the wall, and the thermal inertia of the floor is several orders of magnitude lower than the thermal inertia of the foundation. This combination of features has the potential to establish radial temperature gradients in the floor which are high enough to establish compressive stresses at, and above, the yield point. Should this happen, the floor, due to its low structural stability in compression, has the potential to develop further deformations. Preliminary finite element calculations show that the floor can develop a set of orthogonal buckles, which span the diameter of the tank, during the preheating process

- Three items can be noted regarding a finite elements analysis of the floor after the preheating process:
    - Static analyses will not reproduce the buckles seen in the floor; a quasi-static or a dynamic analysis is needed
    - The shape and the dimensions of the buckles are highly influenced by the shape and the dimensions of the initial deformations produced during welding and following the hydraulic tests
    - The deformations produced in the floor during welding, and the associated residual stresses, vary across the floor. The characteristics follow a statistical pattern, but they also contain random elements. Since the shape and the dimensions of the buckles are a function of the welding deformations and the residual stresses, the characteristics of the buckles (length, height, width, residual stress, and residual strain) also contain random elements. As such, developing a generic, or a typical, analysis predicting the creep-fatigue properties of the buckled regions is difficult. Nonetheless, it is possible to state that the creep-fatigue life of the buckled regions will be considerably less than the life of the project.

- When the tank is filled with salt, hydrostatic loads are sufficient to push the plates down flat against the foundation (see Section 14.9) for a second time. This removes the domed deformations that exist after the hydraulic tests (but does not remove any buckles which may have formed during the hydrostatic tests and the preheating process). When the plates transition from a domed shape to a flat shape, the edges of the plates are again placed into compression. The radial stiffness of the wall is several orders of magnitude greater than the radial stiffness of the floor, and some fraction of the compressive loads on the plates can be translated into additional deformations at the buckles, if present

- The rectangular plates used to fabricate the floor do not all have the same dimensions, the plates are not perfectly square, and the plates have some level of curvature. To accommodate the variations in the horizontal and the vertical gaps between plates, weld backing strips are typically used. The backing plates are intentionally welded to the bottom of the floor, and become a permanent feature of the tank. When the tank is heated from ambient to the design temperature for the first time, the backing strips push the sand in the top layer of the foundation toward the edge of the tank. This leads to 1) local portions of the floor which are unsupported, which generates bending stresses in the floor, and 2) local variations in the friction forces generated between the floor and the foundation

- After the tank enters commercial service, the temperature of the inventory increases during the day, and decreases during the evening and during shutdown periods. The thermal expansion and contraction of the tank generates friction forces on the floor, and these forces oscillate between compression and tension (see Section 14.10). Under certain conditions, the tank can be close to full and the temperature of the inventory can increase. The calculated compression stresses near the center of the tank can exceed the yield value. This, in turn, can produce additional plastic deformations, particularly if the displacements occur near buckles in the floor. The difficulty of analyzing this effect is compounded by the non-uniform distribution of friction resulting from the use of weld backing strips

- The flow entering the tank is mixed with the bulk inventory by means of a distribution header located about 1 m above the floor (see Sections 14.11 and 14.12). However, the distance between the center of the tank and the distribution header, and the distance between the distribution header and the wall of the tank, is on the order of 8 to 12 m. As such, non-isotropic temperature distributions in the inventory, on the time scale of minutes, can develop during transient conditions. Further, daily transient conditions (i.e., receiver startup) consist of relatively cold salt entering the hot tank. The difference in temperature between the salt entering the tank and the bulk inventory is ideally small (< 10 °C). However, depending on decisions made by the operator, the difference can be as large as 100 °C. Under these conditions, cold salt will descend toward the floor due to density differences, which, in turn, can lead to local depressions in the temperature of the floor. Local variations in temperature on the order of 40 °C can generate thermal stresses at, or above, the yield point. The associated strains can add to, or subtract from, the strains already present in the floor

- The commercial hot salt tanks built to date use Type 347H stainless steel. This material is a stabilized stainless steel, which provides additional resistance to intergranular stress corrosion cracking compared to the H grades of Type 304 and Type 316. The stabilizing element added to the alloy is niobium. However, thermodynamic considerations lead to the precipitation of niobium carbonitrides (see Section 14.16.2). Within the grain boundaries, a fine-grained precipitate of niobium carbonitride forms; at the grain boundaries, a coarse-grained precipitate is formed. On a time scale of years, a precipitate-free zone can develop between the grain boundaries. The strength of the coarse-grained precipitate is lower than the strength of the fine-grained precipitate, and the strength in the precipitate-free zone is lower still. When the material is subjected to tensile stresses, the material develops strains, but the strains are concentrated in the area with the lowest strength (precipitate-free zones). This leads to internal cracking, micro-void formation, or a combination of the two. The defects eventually progress to the exterior. The process is known as stress relaxation cracking, and it is accelerated by temperature and strain

- Any section of the floor which has buckled is a region of high strain, with the highest strains occurring at the top of the buckle. The strains at these locations are also influenced by friction forces between the floor and the foundation. The friction forces, which are highest near the center and at the perimeter of the tank, reverse direction daily due to the cyclic thermal expansion and contraction of the tank

- Stress relaxation cracking will proceed most quickly in the regions of the highest strains; i.e., the tops of the buckles. Further, these sections of the tank are 1) subjected to cyclic loading, and 2) the fatigue life of material subjected to previous plastic strains is generally quite low. As such, the area of the tank most prone to failure, through a combination of stress relaxation cracking and low cycle fatigue, is the top of the buckles near the center of the tank. It can be noted that the cracks seen to date in the floors of commercial tanks have occurred at this location.

14.3 Consequences of a Leak in the Floor

Salt has a low surface tension, and as such, it is an effective wetting agent. Expanded clay is an effective thermal insulation due to its large number of extremely small internal cavities. These material characteristics lead to a situation in which salt, when in contact with clay, fills the internal cavities with salt. The saturation process requires a period of days to weeks; however, once the clay is saturated, there is no practical mechanism for removing the salt from the clay.

14.3.1 Heat Losses

The thermal conductivity of salt (0.55 W/m-°C) is about 2.5 times the thermal conductivity of expanded clay (0.22 W/m-°C). As such, exposing the clay to salt increases the thermal conductivity of the clay, with the increase a function of the degree of saturation. However, there are little, and often conflicting, data on the increase. A representative value for the increase is on the order of 1.5.

If exposure of the expanded clay to salt increases in the thermal conductivity of the foundation insulation by a factor of 1.5, then the heat transfer through the foundation will increase by a similar factor. As a consequence, the temperature of the soil can rise above the design value of 75 °C. To limit the possibility of unpredictable tank settlements, the capacity of the foundation cooling fans will need to be increased. If higher fan capacities are insufficient to maintain soil temperatures below 75 °C, air chillers can be added at the inlet to the cooling fans.

14.3.2 Floor Stresses

As discussed in Section 14.7, even moderate radial temperature gradients in the floor can produce stresses at, or above, the allowable values in Section II of the ASME Code.

Should the tank develop a leak, the heat flux into the foundation will increase. An increase in the heat flux will change the radial temperature gradient in the floor. This, in turn, has the potential to either decrease or increase the radial and tangential stresses in the floor. Further, the distribution of the salt in the foundation may be random and change over time. As a result, the heat flux into the foundation, the temperature distribution in the floor, and the stress distribution in the floor could also be random and change over time. As such, the potential exists for new, and unexpected, radial and circumferential temperature distributions to develop in the floor.

In principle, an estimate could be made of the changes in the stress distribution in the floor due to a leak if the radial and the circumferential temperature distributions in the floor were known. However, there are typically a limited number of thermocouples installed on the floor; perhaps 8 to 12. This number of temperature readings may not be enough to accurately predict a stress distribution in the floor. If so, it may not be possible to estimate the potential for plastic collapse, or the remaining creep and fatigue life, of the floor. The Owner may decide that the risks associated with this situation are not acceptable. Unfortunately, the only solution is to remove the foundation material exposed to salt, and replace with foundation with new material. However, due to the size of the tank, replacing the foundation requires that the floor be removed, the tank elevated by means of a jacking system, the foundation excavated, and the floor replaced with a new floor.

14.3.3 NOx Production

A more significant problem is the chemical reaction of expanded clay with salt. Nitrate salt is an oxidizing agent. The expanded clay, during its production, is fired at temperatures high enough to form an oxide. However, one oxide species can react with an oxidizing agent to form another oxide species. At the temperatures seen in the foundation of a hot tank, clay can undergo the second oxidation step. The oxidation is accompanied by a series of reduction reaction in the salt, as follows:

$$NO_3^- \rightarrow NO_2^- + \frac{1}{2}O_2$$
$$NO_2^- \rightarrow NO + O^-$$

The NO leaves the clay in the form of a gas, and, upon exposure to the atmosphere, can react with oxygen to form NO_2.

The oxidation / reduction reactions are not particularly fast. However, due to the large quantities of clay in a tank foundation, and due to the large surface-to-volume ratios inside the clay structure, the NOx emitted from a foundation can be on the order of kg/day. Emission rates this high can present a health hazard to maintenance personnel, and may cause the project to exceed allowable emissions. Further, the NOx production should, in principle, continue until either all of the clay has been oxidized to its new oxidation state, or all of the salt has been reduced to NOx. Given the dimensions of the foundation in a commercial plant, this process could involve decades.

14.3.4 Leak Detection System

Identification of Leak Location

At the Solar Two demonstration project, the perimeter of the foundation used hard refractory bricks to support the concentrated load of the roof and the wall. However, the strength of the selected refractory would be reduced if the bricks were exposed to nitrate salt. To help ensure the integrity of the foundation following a leak, a continuous metal sheet was installed between the solid sand lubricant and the refractory. A leak would percolate horizontally through the sand layer, and then fall onto the soil outside of the foundation.

As might be imagined, a leak would percolate through the sand in essentially all directions, and the point on the soil where the leak accumulated may not be a good indication of the radial location of the leak. To help identify the source of the leak, an array of collection troughs or channels could be located at the top of the foundation.

One potential arrangement is an array of orthogonal channels. The channels would slope down from the center of the foundation to the perimeter; i.e., similar to that of the floor. A leak would flow primarily into 2 channels, and cross-correlating the positions on the perimeter where the leak appeared would provide an indication of the leak in the floor.

A second potential arrangement is an array of radial and tangential channels. A leak entering a radial channel would be directed to the perimeter of the foundation. However, some portion of the leak could enter a tangential channel, and then flow to one or more of the associated radial channels. This collection arrangement would provide information on the circumferential location of the leak, but only limited information on the radial location.

It should be noted that the effectiveness of the leak detection system requires that the foundation directly beneath the floor be as impervious to salt as possible. Specifically, if the material beneath the floor is pervious (i.e., sand), then the leak would flow horizontally as well vertically, and the leak would not be confined to only one or two channels. This, in turn, implies the following:

- The material at the top of the foundation is either a metal slide plate or a hard refractory

- If the material is a refractory, then the selected material must be chemically and structurally stable if exposed to salt. In addition, the coefficient of friction between the floor and the refractory will be different, and perhaps higher, than the coefficient of friction between steel and sand

- If the material is a metal plate, then the following applies:
  - The selected plate material must be resistant to galling with the stainless steel floor in the hot tank
  - A common approach to welding the floor is to tack weld a backing strip along the bottom edge of a plate, locate the adjacent plate, and perform a root pass in the space defined by the edges of the adjacent plates and the backing plate. The backing plate will be lower than the bottom of the floor; however, space for the backing plate is provided by movement of the sand beneath the floor. In contrast, with a metal plate beneath the floor, backing strips can no longer be used. This may require modifications to the floor welding procedure to ensure that the root pass only fuses with the floor plates and not with the plate beneath the tank
  - The floor, after welding, will have depressed sections at the weld seams and elevated sections near the centers of the plates. This will produce non-uniform contact between the floor and the slide plate, which will produce 1) regions of locally high friction forces, and 2) friction forces which vary radially and tangentially in a non-uniform manner. To what extent this influences the stresses in the floor, and the consequent effect on the creep lifetime, will require FEA analyses
  - After the tank enters commercial service, the residual welding stresses in the floor will start to relax. The will change the dimensions of the depressed and the elevated sections, which will change the distribution of the friction forces between the floor and the sliding plate.

Isolation of Foundation Insulation

Even if the collection channels can provide only a qualitative location of a leak, the collection equipment provides an important secondary function. Specifically, some fraction, and perhaps a majority, of the leak will be captured by the collection system. This will reduce the net flow rate of salt into the foundation insulation, which will 1) provide the operators with additional time to drain the tank, and 2) reduce the increase in the heat losses through the foundation due to adding salt (with a relatively high conductivity) to the foundation insulation (with a relatively low conductivity).

14.4 Foundation Perimeter Stiffness

The vertical loads on the foundation are a function of the radial location in the foundation. The highest loads occur at the perimeter of the tank, where the weight of the wall and the weight of the roof must be supported.

At the Solar Two demonstration project, the nominal diameters of the storage tanks were 12 m. The perimeters of the tank foundations were constructed by stacking, and mortaring, a group of refractory bricks. The bricks formed a ring wall, which carried the vertical loads of the wall and the roof down into the concrete mat foundation below. During the 3-year life of the project, no differential or unexpected settlements in either the hot tank or the cold tank were observed. A postmortem examination of the inside of both tanks showed no unexpected deformations of the floors or the walls [24].

Not too surprisingly, the construction of a ring wall using refractory bricks is a labor intensive exercise. Further, refractory bricks are expensive relative to other potential foundation materials. Commercial projects, both parabolic trough and central receiver, after the Solar Two project pursued less expensive approaches to the foundation design. A common approach used expanded clay, such as Utelite, as the primary foundation material under the entire tank. The expanded clay both supported the tank and provided the primary thermal insulation under the floor.

Allowable stress values for the expanded clay showed that the material could safely support the vertical loads at the tank perimeter due to the weight of the wall and the roof. However, during tank fabrication at one commercial project, depressions in the foundation were observed at the perimeter of the tanks even before the tanks were filled with salt. At another commercial project, depressions in the perimeter foundation were observed after the tanks were filled with salt, and then exposed to a number of thermal expansions and contractions. The depressions were produced by the movement of clay particles relative to one other, and the inability of the particles to remain in fixed positions over an extended period of time when exposed to cyclic loads. An hypothesis for this effect is based on the following:

- Finite element calculations of the foundation show that compressive loads at the perimeter of the tank can safely be accommodated by the foundation insulation. However, at a distance slightly beyond the edge of the floor, the compression loads drop to zero

- The foundation, by definition, does not move. As such, compressive forces in the foundation at the edge of the floor must be balanced by tensile forces in the foundation just outside the edge of the floor. The tensile forces are established by friction between adjacent particles in the expanded clay. However, the tank fills and drains daily, which results in a pattern of cyclic compressive loads on the foundations. This, in turn, results in cyclic tensile loads on the expanded clay. However, the clay particles are not bonded to one another, and cyclic loadings can result in particles moving relative to one another. The path of least resistance is a movement of particles out, up, and away from the zone immediately below the edge of the tank.

[24] Pacheco, James (Sandia National Laboratories, Albuquerque, New Mexico), 'Final Test and Evaluation Results from the Solar Two Project', Sandia report SAND2002-0120, January 2002

- The movement of the clay particles leaves the perimeter of the floor unsupported. The floor is not designed to withstand the bending loads generated by the weight of the wall and the roof, and the floor plastically deforms down in response.

The plastic deformations at the perimeter of the floor produce two undesirable effects:

- The high strains associated with plastic deformations significantly reduce the low cycle fatigue life of the floor at this location

- As the tank expands and contracts, the curved perimeter of the tank tends to push the expanded clay, rather than slide over the expanded clay. This increases the depth of the depression, which 1) increases the effective coefficient of friction between the floor and the foundation, and 2) promotes further plastic deformation of the annular floor plate.

In general, the use of expanded clay as the foundation material near the perimeter of the tank has been shown to not be an acceptable approach. Some form of a rigid material, such as refractory bricks or refractory castings, at the perimeter is required.

For existing tanks with clay foundations, inserting metal plates, between the bottom of the tank and the top of the clay, at the tank perimeter has been adopted as a corrective measure. However, the long term effectiveness of this approach is something of an unknown.

14.5 Floor Welding

In commercial salt tanks, the floor is typically fabricated from large rectangular plates. The plates are arranged on the foundation, and then butt welded along each face.

The plates, as supplied by the mill, are not all exactly the same dimensions and are not all exactly the same shape. This results in a variation in the gaps between plates. To assist in the welding process, weld backing strips are attached to the bottom of alternating plates. The backing strips also help to control the gas chemistry in the weld region.

The floor plates have a thickness in the range of 6 to 11 mm, depending on the tank vendor. The number of welding passes ranges from 1 to 3.

14.5.1 Residual Stresses

For a floor plate weld requiring 2 passes, the residual welding stresses are a function of the weld length, as illustrated by the red line in Figure 14-1 [25]. Residual stresses in the range of

[25] Osorio, J. (National Renewable Energy Laboratory, Golden, Colorado), Failure Analysis for Molten Salt Thermal Energy Tanks for In-Service CSP Plants, DOE Award Number DE-EE00038475

300 to 700 MPa are well above the yield stress, which leads to plastic strains in the vicinity of the weld [26].

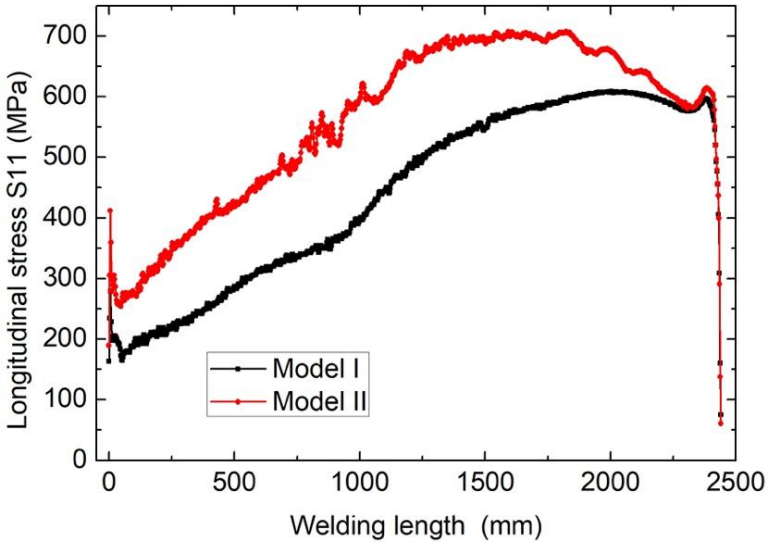

Figure 14-1 Longitudinal Residual Welding Stress

As the weld cools, the metal shrinks, which establishes tensile stress at the top of the weld. This is matched by compressive stresses at the bottom of the weld.

14.5.2 Plate Deformations

The deformation associated with the residual stresses for a subset of the floor welds is illustrated in Figure 14-2. The view shows the edge of two adjacent plates, with the weld located at the mid-point of the curve; i.e., at the lowest point. The overall displacement between the ends of the two plates and the low point at the weld zone is 86 mm.

When all of the welding for the floor plates is completed, each plate takes on the shape of the top of a shallow sphere with a large radius. The low points in the floor are along the weld seams, and the high points in the floor are the centers of the plates.

It can be noted that the floor, after welding, is no longer flat; i.e., the floor has, in effect, buckled at each of the plate seams. This has important implications for the stability of the floor once the tank has been commissioned and is placed into commercial service.

[26] Huang, Hui, (Oak Ridge National Laboratory, Oak Ridge, Tennessee), 'Finite Element Analysis and In-Situ Measurement of Out-of-Plane Distortion in Thin Plate TIG Welding', UT-Battelle, LLC, under DOE Contract DE-AC05-00OR22725, January 2019

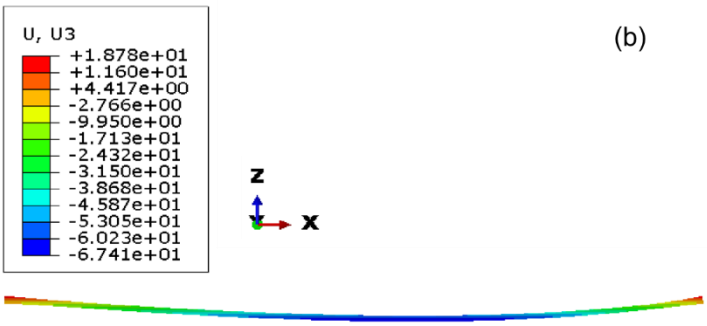

Figure 14-2 Plate Deformations due to Residual Welding Stresses

14.5.3 Stress Relaxation

Stresses in the weld region, either due to welding or due to plate deformations, have values at or above the yield stress. This would normally result in creep lifetimes on the order of 2 to 3 years. However, the stresses do not persist due to stress relief. The effect is illustrated in Table 14-1 for 300-series stainless steels [27].

Table 14-1 Stress Relief as a Function of Temperature

Temperature, °C	Stress relief, percent
200 to 400	40 (peak)
550 to 650	35
850 to 900	55
950 to 1,050	95

Several months after the start of commercial service, the residual stresses have relaxed to a steady state value of about 125 MPa, as described in Section 14.15.8. This stress is permanent, and other stresses due to friction, radial temperature gradients, and transient thermal stresses can add to, or subtract, from this value.

It can be noted that stainless steels typically have sufficient uniaxial ductility to accommodate the plastic strains associated with the level of stress relaxation above. However, if the material is constrained, then strains can develop in multiple axes of the heat affected zones. Stainless steels with a high carbon content have a multiaxial failure ductility as low as 1 percent. The creep strain that occurs during the relaxation of the weld residual stresses could be sufficiently large to exceed the multiaxial failure ductility, and cracks could develop in the weld zone.

[27] Peckner, D. and Bernstein, I., Handbook of Stainless Steel, Chapter 4, Table 25, ISBN 0-07049147-X, 1977

To a first order, the potential to damage the tank is perhaps the largest at the start of commercial service. As the weld and the plate stresses relax over the first 100 hours or so of operation at the design temperature, the residual stresses approach a lower, steady state value. To this end, it may be beneficial to heat treat the tank, at a nominal temperature of at least 550 °C for 100 to 200 hours, to remove some fraction of the residual stresses.

On a related point, the salt inventory at the Solar Two project was melted and then placed in the hot tank. In the hot tank, the inventory was heated to 540 °C over a period of 10 days, and then maintained at that temperature for 20 days. The purpose of the heating phase was to promote the thermal decomposition of the magnesium nitrate in the salt to magnesium oxide and various nitrogen oxides; i.e.,

$$Mg(NO_3)_2 \rightarrow MgO + 2\ NO_2 + ½\ O_2$$

The decomposition process, which was a one-time event, released the NOx gas in the hot tank. This avoided potential problems with releasing the gas in the receiver, which may have had a detrimental effect on the heat transfer rates. Interestingly, the 20-day decomposition period may have had an inadvertent, but beneficial, effect of relaxing a portion of the residual welding stresses prior to the start of the test and evaluation program. In new commercial projects, it may be worthwhile to give some consideration to a similar process in which the hot tank is heated to a temperature close to the design temperature, and then held at that temperature for a period which is long enough to relax some portion of the stresses associated with fabrication, preheating, and the initial filling.

14.5.4 Post Weld Heat Treatment

One method for reducing residual welding stresses is a post weld heat treatment. A representative process is described in Section 17.3.2. The heat treatment process requires accurate control over heating rates, hold times, and cooling rates to achieve the desired combination of metal chemistry and stress reduction.

There are specialty contractors who provide heat treating services for large field equipment, such as the wall of a salt tank. However, the floor of the tank is more problematic. Specifically, 1) the floor can only be heated from one side, and 2) the floor is in contact with the foundation. The floor is relatively thin, and achieving the required heating rates and hold times should be feasible. However, with a hold time on the order of 1 hour, the temperature of the foundation directly beneath the weld will increase to a value approaching the treatment temperature. During the cooling period, the foundation will return some of this heat back to the weld, and it may not be possible to achieve the required cooling rate.

Further, should the tank develop a leak, the foundation will absorb some of the salt. Repairs could be made to the floor by draining the tank, removing the damaged sections, and welding in new sections. If the original floor required a post weld heat treatment, then the replacement sections should also receive a post weld heat treatment. However, the heat treatment temperatures are high enough to thermally decompose the salt absorbed by the foundation. The decomposition process releases NOx, which can be a hazard to plant personnel, and the

decomposition also generates a range of oxide species. The oxides will produce very high corrosion rates, both during the heat treatment period and after the tank returns to commercial service.

In summary, it may not be feasible to conduct a post weld heat treatment on the tank floor, either during construction or following a repair. As such, the creep and fatigue life assessment of the floor will need to be based on the following:

- The metal properties and the metal chemistry at the boundaries of the plates in the as-welded condition
- A limited relaxation of residual stresses due to metal temperatures no higher than the design tank temperature.

14.6 Hydraulic Tests

A common commercial plate dimension is 2.44 m by 9.75 m (8 ft. by 32 ft.). A representative tank diameter in a commercial project is 42 m. As such, a nominal 13 rows of plates are required to span the diameter of the tank.

As discussed in Section 14.5, the plates in the floor are forced into the shape of the top of a sphere with a large radius. The deformations noted in Figure 14-2 are consistent with evidence from tanks in commercial projects which show deformation at the center of the plate on the order of 50 to 100 mm.

14.6.1 Plate Stresses

When the tank is filled with water for the hydraulic tests, hydrostatic loads on the plates push the plates down toward a flat shape. The deformation at the center of a flat plate, with a uniform loading and fixed at the edges, is given by the following equation from Roark:

$$y_{max} = \frac{\alpha q b^4}{E t^3}$$

where σ is a coefficient based on the length-to-width ratio of the plate [ ] (i.e., dimensionless), q is the pressure loading [MPa], b is the width of the plate [m], E is the modulus of elasticity [MPa], and t is the thickness of the plate [m]. The floor plates in commercial projects have a representative length of 10.0 m, a width of 2.50 m, and a thickness of 0.00715 m. The length-to-width ratio is 4, which results in a value for σ of 0.0284.

To reach a displacement of 100 mm for y_{max}, the required static pressure is 6,800 Pa, which corresponds to a water depth of 0.8 m. As such, soon after the tank begins to fill, the floor goes from a domed shape to a flat shape.

The peak stress in the plate occurs at the center of the long edge, and is given by the following equation from Roark:

$$\sigma_{max} = \frac{\beta q b^2}{t^2}$$

where β is a coefficient based on the length-to-width ratio of the plate [ ], q is the pressure loading calculated in the equation above [0.0068 MPa], b is the width of the plate [m], and t is the thickness of the plate [m]. For a plate with a length-to-width ratio of 4, β has a value of 0.5, and the peak stress is calculated to be 416 MPa. This value exceeds the yield stress at ambient temperature, which means that yielding occurs in a section of the weld region near the center of the plate, which relieves some portion of the imposed stress.

When the plate changes shape from domed to flat, the stress in the center of the plate can be estimated using the following equation from Roark:

$$\sigma_{max} = -\frac{\beta q b^2}{t^2}$$

where β is a coefficient based on the length-to-width ratio of the plate [ ], q is the pressure loading calculated in the equation above [0.0068 MPa], b is the width of the plate [m], and t is the thickness of the plate [m]. For a plate with a length-to-width ratio of 4, β has a value of 0.25, and the compressive stress is estimated to be 208 MPa.

14.6.2 Plate Deformations

If the center of the plate is raised by 100 mm, then the width of each plate is reduced by about 4 mm. When the tank is filled, hydrostatic loads push down on the plates, and change the shape of the plates from curved to flat. As such, the width of each plate will increase by 4 mm. Across the diameter of the tank, the total change in the width of the plates is 13 * 4 mm = 52 mm.

The radial stiffness of the wall is several orders of magnitude greater than the radial stiffness of the floor, particularly if the plates have already buckled due to welding. As such, the 52 mm increase in plate dimensions is converted into some combination of elastic and inelastic deformations. The deformations will be determined, in part, by the residual stresses produced during welding. Since the residual stress distribution is difficult to predict, and somewhat random, the additional plate deformations will also be difficult to predict and somewhat random.

When the water is removed at the end of the hydraulic tests, the hydrostatic loads are also removed. Residual stresses in the plates will cause the plate to return toward the domed shapes produced during the welding process. However, any plastic deformations produced in the plates when the tank was full will result in a different floor shape after the hydraulic tests than before the hydraulic tests.

To support a finite element calculation of the stresses in the floor, measurements can be taken of the floor shape before and after the hydraulic tests.

14.7 Radial Temperature Distributions in the Floor

Commercial salt storage tanks are placed on a foundation, which typically consists of the following elements:

- A concrete base mat, which is the lowest level of the foundation. A series of parallel cooling air pipes is located in the mat, and a flow of air is forced through the pipes by means of a fan. The air flow removes the majority of the heat flux (> 90 percent) passing from the tank into the foundation. The heat removal from the base mat maintains the soil temperature beneath the base mat to a maximum temperature of about 75 °C. This temperature ensures that the desiccation of the soil, and the oxidation of organic materials in the soil, do not reach levels which could cause settlement of the tank.

- A primary insulating layer, beneath the majority of the floor. The insulating material can be an expanded clay, such as Utelite®, or an expanded glass, such as FoamGlas®.

- A ring wall, composed of a hard refractory material, at the perimeter of the tank. The refractory provides the foundation stiffness needed to support the concentrated weight of the wall and the roof.

- A solid lubricant, such as sand, on top of the primary insulating layer and the refractory ring wall.

Near the center of the tank, conduction heat transfer from the floor into the foundation is primarily one-dimensional; i.e., straight down. The thermal resistance to conduction heat transfer is largely the thermal resistance of the primary insulating material. The overall thermal resistance in this direction is 'large'. Conversely, near the perimeter of the tank, conduction heat transfer from the floor is a combination of vertical heat transfer through the refractory material and horizontal heat transfer through the soil surrounding the refractory ring wall. The thermal conductivity of many refractories is about double the thermal conductivity of expanded clay, and the thermal conductivity of soil is a factor of 4 to 5 times the thermal conductivity of expanded clay. As such, the heat flux from the floor to the environment is a function of the radial position in the floor, as illustrated in Figure 14-3.

Due to mixing within the tank inventory, the temperature of the inventory is largely isotropic. As such, if the heat flux from the floor to the foundation is a function of the radial position, then the temperature of the floor must also be a function of the radial position.

A two-dimensional, steady-state conduction heat transfer model of the foundation was developed to explore this effect. The model is simplified by simulating the convection heat transfer within the inventory as follows:

- Case 1 - The convection heat transfer is simulated by multiplying the thermal conductivity of the salt by a factor of 100

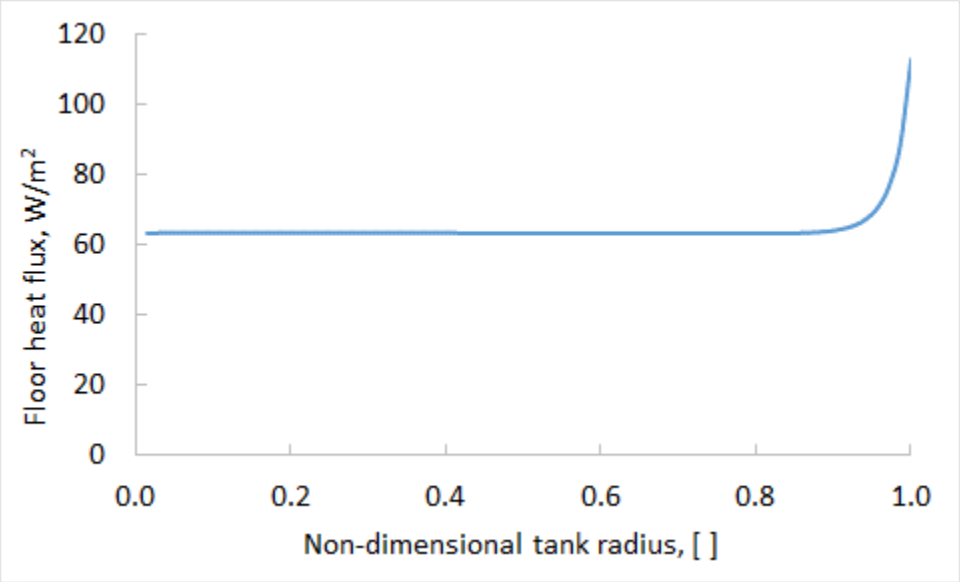

Figure 14-3 Radial Distribution of Heat Flux from the Floor in a Hot Salt Tank

- Case 2 - The convection heat transfer is simulated by multiplying the thermal conductivity of the salt by a factor of 10

- Case 3 - The convection heat transfer is simulated by multiplying the thermal conductivity of the salt by a factor of 1. This represents a case in which the salt is completely stagnant. Such a condition can occur when 1) the temperature of the inventory is, say, 500 °C, 2) the plant starts an extended shutdown, and 3) the electric salt heaters do not start operation until the temperature of the inventory has decayed to, say, 300 °C.

In each of the three Cases, the depth of the salt inventory is taken to be 3.5 m, and the temperature at the top of the inventory is assumed to be a constant value of 560 °C.

In Case 1, the radial temperature gradient in the floor is a modest 4 °C.

For an unconstrained circular plate, subject to a radial temperature gradient, the radial stress and the tangential stress are given by the following formula in Roark [28]:

$$\sigma_r = \gamma E \left(\frac{1}{R^2} \int_0^R Tr\, dr \; - \; \frac{1}{r^2} \int_0^r Tr\, dr \right)$$
$$\sigma_t = \gamma E \left(-T \; + \; \frac{1}{R^2} \int_0^R Tr\, dr \; - \; \frac{1}{r^2} \int_0^r Tr\, dr \right)$$

where γ is the coefficient of thermal expansion (1/°C), E is the modulus of elasticity (kg/m-sec^2), R is the radius of the disc (m), and T is the temperature at any point a distance *r* from

[28] Young, W. C., and Budynas, R. G., 'Roark's Formulas for Stress and Strain', Seventh Addition, 2002

the center minus the temperature of the coldest part of the disc (°C). The radial and the tangential stresses are combined using the following formula:

$$\sigma_{Combined} = \sqrt{\sigma_r^2 \; - \; \sigma_r \; * \; \sigma_t + \sigma_t^2}$$

In Case 1, with the convection modeled as 100 times the thermal conductivity of the salt, the peak stress in the floor is 12 MPa and it occurs at the perimeter (the calculated stress at the center is infinite, as the equation involves a division by zero). This value is approximately 11 percent of the allowable stress listed in Section II of the ASME Code for Type 347H stainless steel at 560 °C, and approximately 10 percent of the allowable stress associated with a creep lifetime of 300,000 hours as defined in API 579-1 / ASME FFS-1 (see Section 14.15.3).

Repeating the calculations for Case 2, in which the convection is modeled as 10 times the thermal conductivity of the salt, the radial temperature gradient has increased to 33 °C, and the peak stress has increased to 107 MPa. This value is nominally equal to the ASME allowable stress, and approximately 85 percent of the allowable stress associated with a creep lifetime of 300,000 hours. Informal discussions with other organizations developing finite element models of the floor have reached similar results.

Repeating the calculations for Case 3, in which the inventory is assumed to be stagnant, produces a radial temperature gradient on the order of 175 °C due to the relatively low thermal conductivity of the salt.

Clearly, Case 3 represents something of a worst case condition, as 1) the time required to develop the steady-state temperature profile could be several weeks, and 2) the operators are likely to recognize the problem, and establish some form of circulation in the tank, before salt temperatures reach values this low. Nonetheless, the calculated temperature profile indicates the potential for two significant problems:

1. The calculated stresses at the perimeter are the same order of magnitude as the tensile strength, and rupture of the floor cannot be discounted.

2. The temperature of the metal at the perimeter of the tank (330 °C) is perhaps 100 °C above the freezing point of the salt. Nonetheless, there is the potential for salt to freeze 1) if there are local defects in the insulation, 2) if the insulation has become wetted by salt due to leakage from the pumps, valves, and instruments above the tank, or 3) if water has infiltrated the insulation due, for example, to heavy rains. If frozen salt develops in the floor near the perimeter of the tank, then the salt will be thawed by recirculating the inventory within the tank. In the regions beneath the frozen salt, the heat flux into the metal will be defined by the thermal conductivity of the solid salt. However, in the regions adjacent to the frozen salt, the heat flux into the metal will be defined by the convection heat transfer coefficients of the circulating salt. The two heat fluxes could differ by an order of magnitude, which, in turn, could produce local temperature gradients large enough to damage the tank. Unfortunately, the freeze / thaw progression would be largely random and beyond the control of the project. As

such, it may be impossible to assess the potential damage to the tank from a freeze / thaw cycle.

Clearly, the steady-state model only mimics the effect of convection within the salt inventory. Nonetheless, the calculations show that a radial temperature gradient about 35 °C establishes stresses equal to the ASME allowable value, and a gradient of approximately 50 °C produces stresses at the yield value. Further, should the inventory becomes stagnant for even a moderate period of time (i.e., days), then permanent damage to the floor may be inevitable.

Should the floor plastically deform due to a radial temperature gradient, and the gradient is then removed, the stress distribution in the floor will be a combination of the new temperature gradient, plus a hysteresis effect from the plastic deformation. Further, the magnitude of the hysteresis effect will be difficult to both calculate and verify.

14.8 Tank Preheating

Prior to filling the tank with salt, the tank and the top of the foundation are preheated to a nominal temperature of 320 °C to prevent a thermal shock to the tank. The heating medium is hot air from a propane- or a natural gas-fired direct air heater. The hot air is directed through a manway in the roof, flows down a short (2 m) temporary gas duct suspended from the roof, enters the tank with the flow directed nominally toward the center, and then exits through a second manway in the roof.

The preheating period ranges from 7 to 20 days. The allowable rate of temperature change is limited; values in the range of 1.5 to 2 °C/hr are typical. Limits are also placed on the intra-tank temperature differential; however, the allowable differentials are relatively high. In one commercial project, differences in temperature as high as 33 °C between the center of the tank and any wall location are permitted.

The preheating process is one in which damage could occur to the tank, as follows:

- Due to non-uniform heat losses from the tank, radial temperature gradients of 25+ °C can be established in the floor

- The flow of preheating air enters the tank at only one location, and the air flow path is dictated by the location and the shape of the inlet duct. As such, the air flow path is known on a gross basis, but is largely beyond the control of the operators. Further, air at high temperatures has a low density, and is generally a poor mechanism for heat transfer. The combination of inexact control over the air flow and the low heat transfer coefficients can result in unavoidable non-uniform temperature distributions in the tank

- The allowable measured intra-tank temperature differentials are the same order of magnitude as the radial temperature gradient (35 °C in Case 2 above). A radial gradient of 35 °C, particularly in combination with the friction forces between the floor and the foundation, has the potential to plastically deform the floor

- The thermocouples located in the tank may not be in the exact locations required to measure the maximum intra-tank temperature differentials. As such, the measured maximum differential might be 33 °C, but the actual maximum differential could be in excess of 33 °C. (One method to avoid this limitation would be to monitor the temperature of the floor and the wall using an infrared thermometer. The measuring portions of the instrument will need to tolerate temperatures as high as 400 °C.)

The floor, at the start of the preheating phase, has already deformed due to the welding processes. During preheating, a radial temperature gradient in the floor will develop, with the highest temperature near the center and the lowest temperature at the perimeter. If the gradient exceeds some threshold value, probably on the order of 35 to 50 °C, then compression stresses near the center of the tank can exceed the yield value. The buckling resistance of the floor will be very low due to 1) the preexisting plate deformations, and 2) the absence of stabilizing hydrostatic forces from the salt. As such, the floor could develop permanent buckles (ridges) even prior to the start of commercial service. As with every metal, the stresses associated with plastic deformation will have a significant detrimental effect on the creep life and the low cycle fatigue life.

As noted above in Section 14.2, the characteristics of the buckled regions (length, height, width, residual stress, and residual strain) are functions of the welding deformations and residual stresses. These characteristics will have some random features, and it is difficult to develop a generic analysis which applies to all buckled regions. However, the creep-fatigue life of a buckled region is always expected to be less than the 30-year life of the project.

14.9 Tank Filling

Following the completion of the tank preheating, the shape of the floor will consist of a combination of domed sections (generated at the end of the hydraulic tests) and perhaps some buckled regions. The salt melting process begins. As the tank is filled with salt, hydrostatic loads will push the floor plates down against the foundation for a second time. The required hydrostatic pressure is on the order of 7 kPa, which corresponds to a salt depth of about 0.4 m. Since the minimum salt level in the tank is 1.0 m during commercial operation, the floor remains flat against the foundation for the life of the tank.

Changing the shape of the plates from domed to flat will generate stresses at both the edges and at the center of the plates. The deflection of the plates will depend on the shape of the floor at the completion of both the hydrostatic tests and the preheating. However, the shape of the floor at the end of preheating may not be known, or it may be difficult to measure. As such, estimating the stresses at the edges of the plates, and at the centers of the plates, after the fill process is likely to involve large uncertainties. Nonetheless, some portions of the plate edge and the plate center stresses will remain as permanent stresses. Under various conditions, the permanent stresses could add to, or subtract from, other stresses generated by friction, radial temperature gradients, and transient temperature conditions.

From a review of the plate deformations, two observations can be made:

- The vertical dimensions of the buckles seen in commercial tanks are larger than the cumulative changes in the plate widths discussed above. However, there are a number of mechanisms, discussed in the Sections below, which can produce ratcheting, the starting point of which are the buckles produced during filling (and likely preheating)

- Buckles, once produced, are permanent. Specifically, there are only 2 mechanisms that could, in principle, remove a buckle:
    - Hydrostatic forces. The maximum hydrostatic load of approximately 250 kPa occurs when the tank is full. However, the stiffness of a triangular, or a semi-circular, buckle is such that a load of 250 kPa produces vertical deflections in the buckle that are much smaller than the height of the buckle
    - Inverted radial temperature gradients. If the floor is placed in tension, the tensile forces will pull on the sides of the buckles, which causes the height of a buckle to decrease. However, for the buckles to permanently deform, the tensile stresses on the buckle must exceed the yield value. This can occur if the temperature of the floor at the perimeter of the tank is 40 °C, or more, above the temperature of the floor at the center of the tank. However, the heat loss pattern in the tank, plus the flow distribution inside the tank, will not allow this condition to occur. Further, to remove the buckle, the height of the buckle would need to be converted into a linear, plastic, compression of the floor. But it is not possible to simultaneously subject local portions of the floor to compression stresses and other portions of the floor (i.e., the buckles) to tensile stresses.

14.10 Friction Between the Floor and the Foundation

14.10.1 Daily Thermal Cycles

Over the course of a typical operating day, the hot tank undergoes the following cycle:

- In the afternoon, the inventory level and the inventory temperature reach their maximum values

- Early in the evening, the inventory level reaches its minimum value. Heat losses from the tank cause the temperature of the inventory to decay

- Early in the morning, the receiver is started. Over the next 20 minutes or so, both the flow rate and the outlet temperature from the receiver increase. At a pre-defined downcomer temperature, salt flow is directed to the hot tank. The crossover temperature is on the order of 30 to 60 °C lower than inventory temperature. The goal is to capture as much useful thermal energy from the receiver as possible for electric power production. Note that this phase of the receiver startup results in a decay in the inventory temperature

- Once the receiver reaches its normal design temperature, the temperature of the hot tank inventory starts to increase

- The continuous heat losses from the tank, in combination with a maximum salt inlet temperature of 565 °C, mean that 1) the temperature of the inventory ranges daily between a minimum value of about 540 °C and a maximum value of about 560 °C, and 2) the inventory temperature never reaches the design receiver outlet temperature of 565 °C.

As such, the tank is subjected to a daily condition, typically in the afternoon, in which the level and the temperature of the inventory both increase. If the temperature of the inventory increases, then the tank will expand. Friction between the tank and the foundation, in turn, places the floor into compression. As discussed in the sections above, the floor has a low buckling resistance due to the plate deformations associated with welding, and due (potentially) to the plate deformations associated with preheating.

14.10.2 Initial Thermal Expansion

As an example of the thermal expansion, a hot salt tank in a representative commercial project has a nominal diameter, at ambient temperature, of 42 m. As the temperature of the tank is increased from ambient conditions to the normal design temperature of 565 °C, the radius of the tank increases by $\delta = R * \gamma * \Delta T = 0.219$ m, where R is the tank radius [m], γ is the coefficient of thermal expansion [1/°K], and ΔT is the change in metal temperature [°K]. Thus, at the design temperature, the radius of the tank is 21.219 m.

14.10.3 Maximum Friction Deflections

As noted above, the tank experiences daily thermal cycles, and the movement of the tank is constrained by friction forces between the floor and the foundation. The maximum amount which the floor can be radially deflected by static friction (i.e., before the tank starts to slide) is given by the following expression:

$$\delta = \frac{(1-\nu)\,\mu\,\rho\,H\,g\,R^2}{3\,E\,t_p}$$

where δ is the deflection of the floor, m
v is Poisson's ratio, [ ]
μ is the coefficient of friction, [ ]
ρ is the density of the salt, kg/m^3
H is the depth of the salt, m
g is the acceleration due to gravity, m/sec^2
R is the outer radius of the tank, m
E is the modulus of elasticity for stainless steel, MPa
t_p is the thickness of the floor, m

With a representative maximum salt height of 11.5 m, and assuming that the coefficient of friction is 0.3, then the maximum deflection is 0.0055 m.

Along this line of thought, if the tank is at a condition where the friction loads are zero, and the temperature of the inventory increases, then the tank will expand by an amount equal to R * γ * ΔT. If the expansion amount is set equal to the maximum deflection possible due to static friction, then the associated change in inventory temperature is 15 °C. Stated another way, if the tank is full, and if the temperature of the inventory increases by 15 °C, then the maximum friction force will be applied to the foundation.

Operating experience from commercial plants shows that the hot tank experiences multiple cycles each year in which the tank is full, or nearly full, and the temperature of the inventory increases by at least 15 °C. One such situation in which this can occur is as follows:

- The receiver starts in the morning, but the skies are partially cloudy, and the receiver outlet temperature is set to a value less than 565 °C to prevent temperature overshoots during cloud transients
- The steam generator is not started until noon, which means that the inventory level in the hot tank is rising throughout the morning
- In the afternoon, the steam generator demand is close to the receiver output, and the level in the hot tank remains essentially constant
- The weather clears, and the receiver outlet temperature is increased to the design value of 565 °C.

As such, the floor is exposed to some number of cycles in each year in which the floor starts in a state with a low stress (i.e., the tank close to empty) and then the stress in the floor reaches the maximum value possible due to friction.

14.10.4 Analytical Solution for Floor Stresses due to Friction

The tank expands and contracts due to daily changes in the temperature of the inventory. The friction force, kg-m/sec^2 (i.e., N), which can be applied by the tank to the foundation is as follows:

$$\tau_{Friction} = -\mu\ \rho\ H\ g\ A$$

where μ is the coefficient of friction, [ ]
ρ is the density of the salt, kg/m^3
H is the depth of the salt, m
g is the acceleration due to gravity, m/sec^2
A is the floor area, m^2

The shear force, kg-m/sec^2, that the foundation applies to the tank is given by the following:

$$\tau_{Foundation} = \frac{G * u * A}{t_{Foundation}}$$

where G is the shear modulus of the foundation, kg/m-sec^2
u is the deflection of the foundation, m
A is the floor area, m^2
$t_{Foundation}$ is the thickness of the foundation, m

A differential element of the floor is illustrated in Figure 14-4.

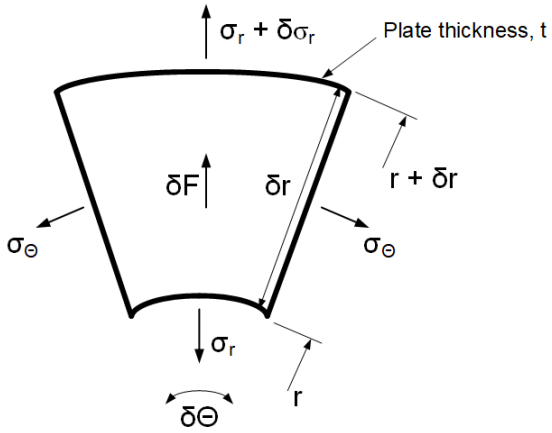

Figure 14-4 Differential Element of the Floor

Setting the force balance to zero yields the following:

$$2\,\sigma_\Theta \sin\left(\frac{\delta\vartheta}{2}\right)\delta r\, t - \sigma_r\,\delta\Theta\, r\, t + (\sigma_r + \delta\sigma_r)(r + \delta r)\,\delta\Theta\, t + \delta F = 0$$

Using a small angle approximation $\sin\left(\frac{\delta\vartheta}{2}\right) \approx \frac{\delta\vartheta}{2}$, setting $\delta A = \delta r\, r\, \delta\Theta$, dividing by $\delta A / t$, and setting $\tau = \frac{\delta F}{\delta A}$ yields:

$$\frac{\delta\sigma_r}{\delta r} + \frac{1}{r}(\sigma_r - \sigma_\Theta) = -\frac{\tau}{t_p}$$

where σ_r is the radial stress, kg/m-sec^2 (i.e., Pa)
r is the radius, m
σ_Θ is the tangential stress, kg/m-sec^2
τ is the unit shear force between the floor and the foundation, kg/m-sec^2
t_p is the thickness of the floor, m

In an axisymmetric plate, the radial strain, [ ], is:

$$\varepsilon_r = \frac{\delta u}{\delta r}$$

the tangential strain, [ ], is:

$$\varepsilon_\theta = \frac{u}{r}$$

the radial stress, kg/m-sec^2, is:

$$\sigma_r = \frac{E}{(1-\nu^2)}(\varepsilon_r + \nu\varepsilon_\theta)$$

where v is Poisson's Ratio, [ ]

and the tangential stress, kg/m-sec^2, is:

$$\sigma_\theta = \frac{E}{(1-\nu^2)}(\varepsilon_\theta + \nu\varepsilon_r)$$

Substituting in the equations above results in a second order differential equation for the deflection:

$$\frac{d^2u}{dr^2} + \frac{1}{r}\frac{du}{dr} - \frac{1}{r^2}u + \frac{(1-\nu^2)}{E}\frac{\tau}{t_P} = 0$$

The solution involves a number of terms, including the following:

- Concentrated vertical load of the wall and the roof, carried down to the perimeter of the floor
- Coefficients of friction, which can have different values for area under the majority of the floor and the area under the annular plate beneath the wall
- Thermal expansion and contraction of the tank due to daily changes in the temperature of the inventory
- Shear stiffness of the foundation
- Radial location in the floor where the shear force reaches a maximum.

The solution is subject to a boundary condition, in which the radial stress at the center of the floor is equal to the tangential stress at the center of the floor.

The location in the floor where the shear force reaches a maximum is designated r_2. For radial locations greater than r_2, the radial stress in the floor is given by:

$$\sigma_r = \frac{W_{Wall}\, g\, C_{F_{Perimeter}}}{2\,\pi\, R\, t_P} + \frac{(3+\nu)}{3}\frac{(\,C_{F_{Floor}}\rho\, g\, H)}{t_P}\,(R-r)$$

where W is the weight of the wall and the roof, kg
$C_{F_{Perimeter}}$ is the coefficient of friction beneath the annular plate, [ ]
$C_{F_{Floor}}$ is the coefficient of friction beneath the majority of the floor, [ ]
R is the tank radius, m
r is the radius at which the stress is calculated, m

and the tangential stress is given by:

$$\sigma_\Theta = \frac{W_{Wall}\, g\, C_{F_{Perimeter}}}{2\,\pi\, R\, t_P} + \frac{1}{3}\frac{(\, C_{F_{Floor}} \rho\, g\, H)}{t_P}\,((3+\nu)R - (1+3\nu)r)$$

For radial locations less than r_2, the expressions for the radial and the tangential stresses are as follows:

$$\sigma_r = \frac{W_{Wall}\, g\, C_F}{2\,\pi\, R\, t_P} + \frac{(3+\nu)}{3}\frac{(C_F\, \rho\, g\, H\, R)}{t_P} - \left(\frac{5}{24}\right)\frac{(3+\nu)\,(C_F\, \rho\, g\, H)^2}{(t_P\, g_F\, \alpha\, \Delta T)} - \left(\frac{1}{8}\right)\frac{(3+\nu)\,(g_F\, \alpha\, \Delta T)\, r^2}{t_P}$$

$$\sigma_\theta = \frac{W_{Wall}\, g\, C_F}{2\,\pi\, R\, t_P} + \frac{(3+\nu)}{3}\frac{(C_F\, \rho\, g\, H\, R)}{t_P} - \left(\frac{5}{24}\right)\frac{(3+\nu)\,(C_F\, \rho\, g\, H)^2}{(t_P\, g_F\, \alpha\, \Delta T)} - \left(\frac{1}{8}\right)\frac{(1+3\nu)\,(g_F\, \alpha\, \Delta T)\, r^2}{t_P}$$

Coefficient of Friction Values

A common solid lubricant used under the floors of commercial tanks is sand. A paper by Uesugi [29] summarizes the results of experiments to measure the coefficient of friction between a steel plate and sand.

The coefficient is a function of the surface roughness of the plate, the size of the sand particles, the vertical loading on the sand, and the number of strain reversals. However, the coefficients generally fall within a fairly narrow range of 0.5 to 0.7.

Representative Results for a Commercial Tank

For the purposes of the discussion, stresses due to friction were calculated using the following parameters:

- Tank radius of 21.0 m at ambient temperature
- Coefficient of friction of 0.6 between the floor and the sand
- Coefficient of friction of 1.0 between the perimeter of the floor and refractory bricks beneath the perimeter of the floor

[29] Uesugi, Morimichi, et. al., (Department of Architectural Engineering, Chiba University, Japan), 'Friction Between Sand and Steel under Repeated Loading', Soils and Foundation Volume 29, No. 3, 127-137, September 1989, Japanese Society of Soils Mechanics and Foundation Engineering

- Floor thickness of 7.14 mm
- Foundation shear stiffness of 320,000,000 kg/m^2-sec^2.

Case 0

Case 0 corresponds to the following transition: 1) the tank is empty, at a temperature of 20 °C, followed by 2) the tank is preheated to a temperature of 320 °C over the course of several days.

A plot of the radial and the tangential stresses is shown in Figure 14-5. Negative values correspond to compressive stresses; i.e., the expansion of the floor is resisted by the shear stiffness of the foundation.

Since the tank is empty, the vertical loads on the floor are largely determined by the weight of the floor; i.e., close to zero. The radial and the tangential stresses, which are determined by the friction forces at the perimeter of the tank due to the weight of the wall, the roof, and the insulation, have nominally the same values.

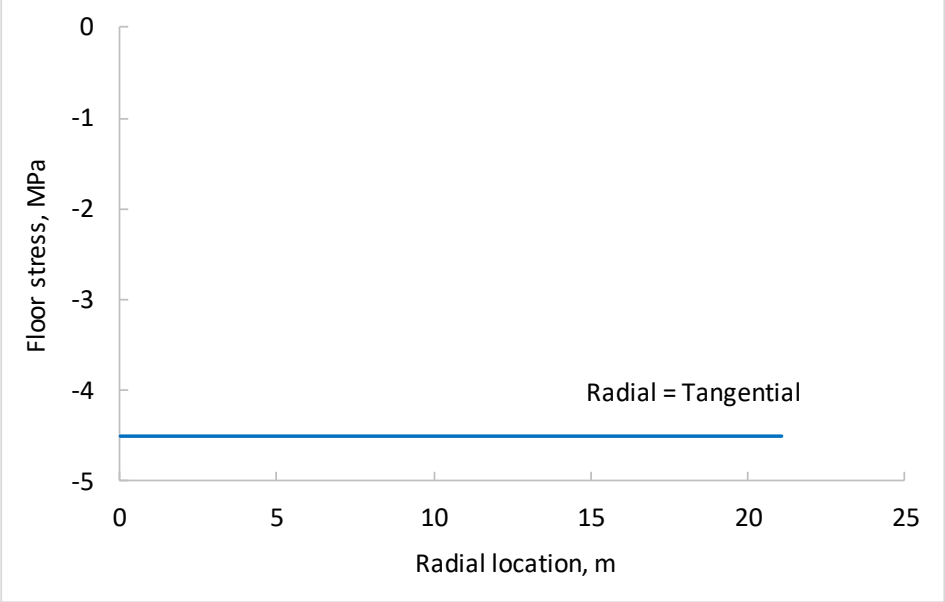

Figure 14-5 Radial and Tangential Floor Stresses for Case 0

Case 1

Case 1 corresponds to a condition in which 1) salt, at a nominal temperature of 320 °C, is loaded into the tank to a depth of 1.5 m after the tank has been preheated, followed by 2) the inventory temperature is raised to a value of 565 °C over the course of several days. The

inventory depth remains at 1.5 m during this multi-day process to minimize the friction loads between the floor and the foundation.

With the inventory depth at the minimum, the radial and the tangential stresses in the floor, as a function of the radial location, are shown in Figure 14-6. Negative values for the stresses correspond to compressive loads.

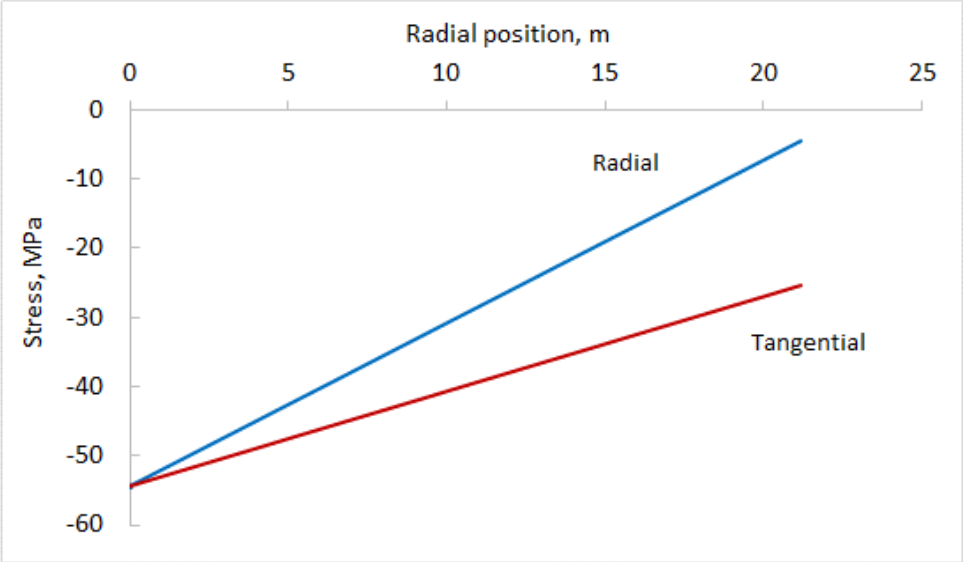

Figure 14-6 Floor Stresses for Case 1: 21 m Tank Radius; 7 mm Floor Thickness

The radial stress at the perimeter of the tank is not equal to zero due to the friction forces generated at the perimeter by the weight of the wall, the roof, and the insulation.

Case 2

In Case 2, the plant is in normal commercial service. At the beginning of the day, the inventory depth is 1.5 m. Over the course of the day, the inventory depth increases to 10.5 m. The inventory temperature remains constant at 565 °C. Since the tank neither expands nor contracts, the stresses in the floor remain constant at the profiles shown in Figure 14-6.

The project decides to postpone the startup of the turbine for a period of 8 hours to take advantage of higher energy sales prices. During this period, the tank cools from an initial temperature of 565.0 °C to a new temperature of 562.9 °C (ΔT = -2.1 °C). The temperature decays causes the tank to contract, and a ΔT of -2.1 °C represents the largest temperature change which can occur before the tank begins to slide on the foundation.

The floor stresses generated by this condition are shown in Figure 14-7. Positive values correspond to tensile loads.

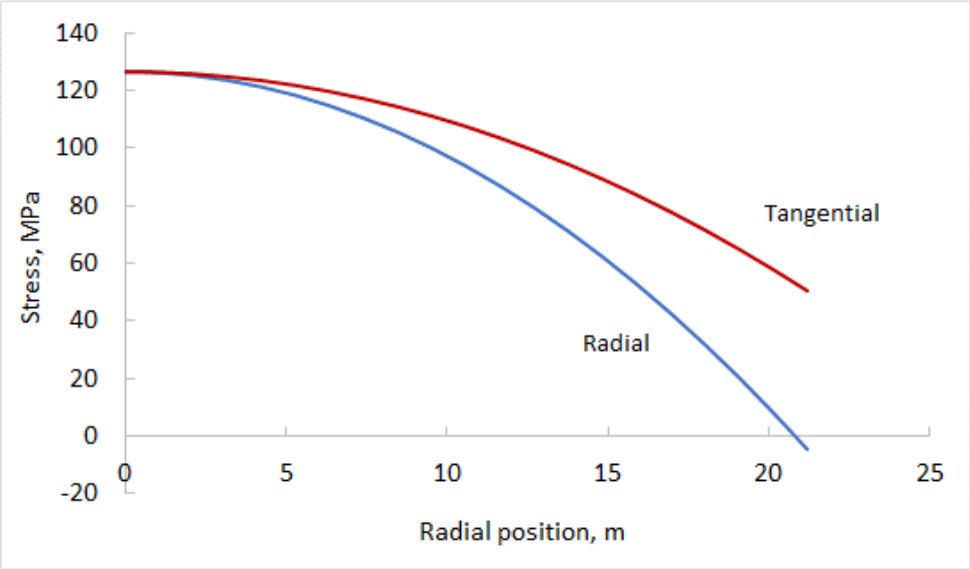

Figure 14-7 Initial Floor Stresses for Case 2: 21 m Tank Radius; 7 mm Floor Thickness

The stresses shown in Figure 14-7 assume that the floor starts in an unstressed condition. However, this is not the case, as the floor starts with the stress distribution shown in Figure 14-6. The stresses shown in Figure 14-6 can be combined with the stresses shown in Figure 14-7 if the change in shear stress with radius is a constant value; i.e., the tank has not yet started to slide. The linear superposition of stresses (i.e., Figure 14-6 + Figure 14-7) is shown in Figure 14-8.

Of note in Figure 14-8 are 1) the stress values, and 2) a situation in which a change in the inventory temperature of small as 2 °C can produce stresses within 80 percent of the allowable stresses listed in Section II of the Code.

Case 3

In Case 3, the tank begins the day with an assumed inventory temperature of 550 °C and an inventory level of 10.5 m. The inventory level in the morning is initially a high value in anticipation of meeting a high demand for electric energy during the day.

In the morning, the steam turbine is placed in service. Over the course of the day, the thermal power supplied by the receiver is nominally similar to the thermal power demand of the steam generator. As such, the inventory level in the hot tank largely remains constant at 10.5 m. However, the inventory temperature can increase above 550 °C if the solar radiation conditions are favorable and the receiver can operate for several hours at the design temperature of 565 °C.

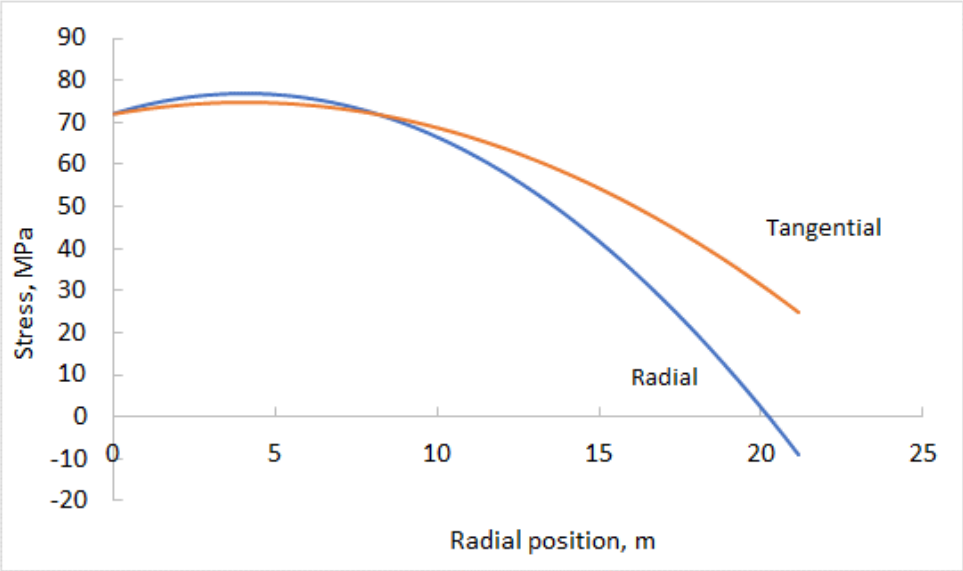

Figure 14-8 Final Floor Stresses for Case 2: 21 m Tank Radius; 7 mm Floor Thickness

Assuming that the inventory temperature reaches the design value of 565 °C, the stresses produced in the floor due to the expansion of the tank are shown in Figure 14-9. The combination of a high inventory level (10.5 m) and an increase in the inventory temperature (15 °C) places compressive loads on the floor near the center of the tank, and these stresses exceed the yield value. Similarly, if the tank has a high inventory level, but cools by 15 °C, then the tank will contract, generating a mirror image (tensile, rather than compressive) of the floor stresses.

Several items can be noted in this discussion:

- The combination of a high inventory level and an increase in the inventory temperature is not a hypothetical condition. It has been observed in commercial projects, when the project is trying to tailor electric energy deliveries to the needs of the local utility

- Similarly, the combination of a high inventory level and a decrease in the inventory temperature can occur if an afternoon with intermittent clouds results in a series of receiver start / stop cycles, each of which adds relatively cold salt to the hot tank

- The stresses shown in Figure 14-9 assume that the tank starts in condition with zero initial stress. Clearly, this will not be the case, as the stresses at any particular time will be determined by the temperature / level history of the tank up to that point. As might be imagined, 1) the history of the tank will largely be unknown, or 2) even if the history was known, it's unlikely that the project could develop a running calculation of the floor stresses which had a meaningful accuracy. To bound the problem, the stresses shown in Figure 14-6 (Case 1) represent a case in which 1) the inventory is at, or near, the minimum level (1.5 m), and 2) the tank has been sliding over the entire floor area,

except for a small area near the center of the tank. This, in turn, should produce, in essence, a baseline stress at an inventory level of 1.5 m. As such, with inventory depths at or near the minimum, the stresses at the center of the tank should oscillate between two baseline values: -55 MPa (tank expanding); and +55 MPa (tank contracting). To a zeroth-order, the 55 MPa baseline stresses at the center of the tank will either add to, or subtract from, the stresses at the center of the tank developed at other combinations of level and temperature; i.e., those shown in Figure 14-9. The exact value for the stress at the center of the tank will require a more sophisticated calculation than the analytical solution noted above. Nonetheless, stresses well above the yield value are expected, particularly if compressive (tensile) stresses developed during the day add to baseline compressive (tensile) stresses carried over from when the tank was last at the minimum level.

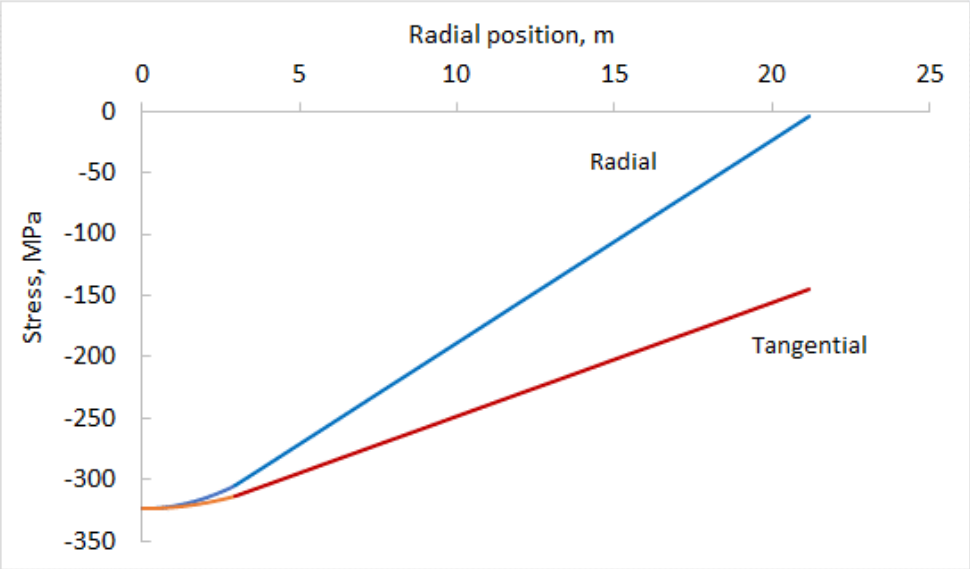

Figure 14-9 Floor Stresses for Case 3: 21 m Tank Diameter; 7 mm Floor Thickness

Parametric Tank Designs

The friction stresses in a representative tank (21.0 m radius; 7 mm floor thickness), operating through typical daily and annual thermal cycles, are likely to be well above values which could be considered consistent with a creep lifetime of 30+ years.

To prevent potentially damaging stresses in the floor, the temperature of the inventory must be controlled to values in the range of perhaps ±2 °C of a reference value. However, the transient nature of the plant operations, plus conditions outside the project's control (i.e., forced outages), are likely to exceed the ±2 °C operating constraint on a regular basis.

One possible method for reducing the friction stresses in the floor is to make change changes to the tank design. As an example, one 100-percent capacity hot tank could be replaced by

two 50-percent capacity tanks, and the thickness of the floor could be doubled from the minimum specified in API 650 (i.e., 2 x (6.35 mm + corrosion allowance)). This would result in a tank radius of 14.9 m and a floor thickness of 14.3 mm.

For this analysis, the balance of the design parameters, including the coefficient of friction between the floor and the foundation (0.6), the coefficient of friction between the annular perimeter plate and the foundation (1.0), and the shear modulus of the foundation (320,000,000 kg/m^2-sec^2), are assumed to remain unchanged.

Case 1

As in the previous section, Case 1 corresponds to a condition in which 1) the tank is preheated to 300 °C, 2) salt, at a nominal temperature of 320 °C, is loaded into the tank to a depth of 1.5 m, and 3) the inventory temperature is raised to 565 °C over the course of several days.

With the inventory at the minimum depth, the radial and the tangential stresses in the floor, as a function of the radial location, are shown in Figure 14-10. Negative values correspond to compressive loads.

To a first order, reducing the tank radius from 21 m to 15 m, and doubling the floor thickness from 7 mm to 14 mm, reduces the peak stresses at the center of the tank by about 60 percent (55 MPa down to 21 MPa).

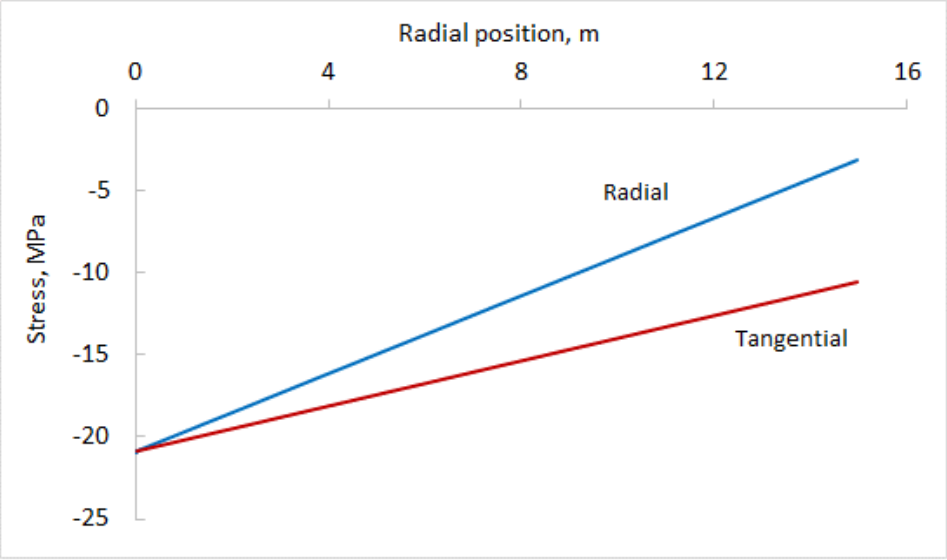

Figure 14-10 Floor Stresses for Case 1: 15 m Tank Radius; 14 mm Floor Thickness

Case 2

Similar to Case 2 above, the tank cools from an initial temperature of 565.0 °C down to a new temperature of 562.0 °C (ΔT = -3.0 °C). The temperature decays causes the tank to contract, and a ΔT of -3.0 °C represents the largest temperature change which can occur before the tank begins to slide on the foundation. The associated stresses are shown in Figure 14-11. Positive values represent tensile stresses.

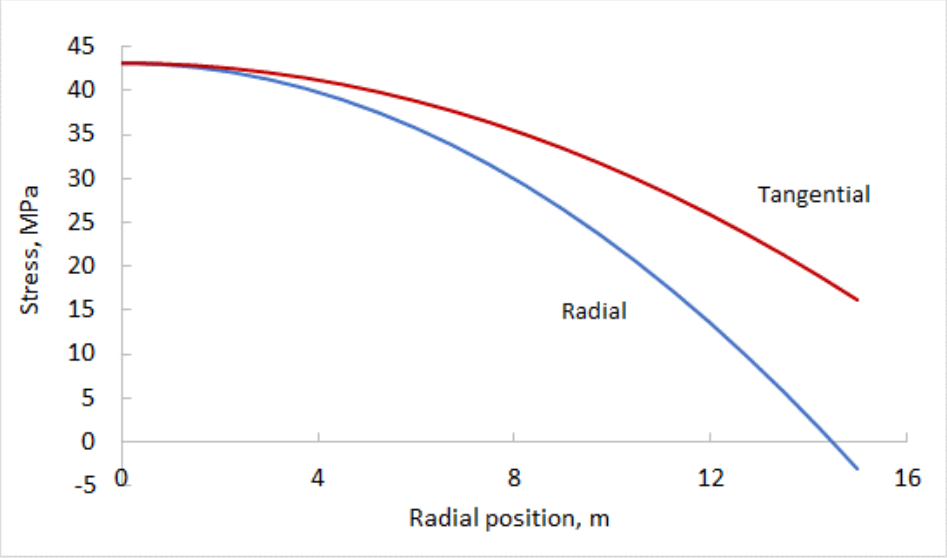

Figure 14-11 Initial Floor Stresses for Case 2: 15 m Tank Radius; 14 mm Floor Thickness

As above, the compressive stresses shown in Figure 14-10 can be combined with the tensile stresses shown in Figure 14-11 using linear superposition. The results are shown in Figure 14-12. To a first order, reducing the tank diameter by a factor of 2 and doubling the floor thickness reduces the peak stresses at the center of the tank by a nominal 65 percent (78 MPa down to 25 MPa).

Case 3

Similar to Case 3, the tank begins the day with an assumed inventory temperature of 550 °C and an inventory level of 10.5 m. The inventory level remains constant during the day; however, the inventory temperature rises by 15 °C to a value of 565 °C by late in the afternoon. The associated stresses are shown in Figure 14-13.

Reducing the tank diameter by a factor of $\sqrt{2}$ and doubling the floor thickness reduces the peak stresses at the center of the tank by a nominal 65 percent (320 MPa down to 115 MPa). Importantly, the values are now the same order of magnitude as the allowable stresses listed in Section II of the Code.

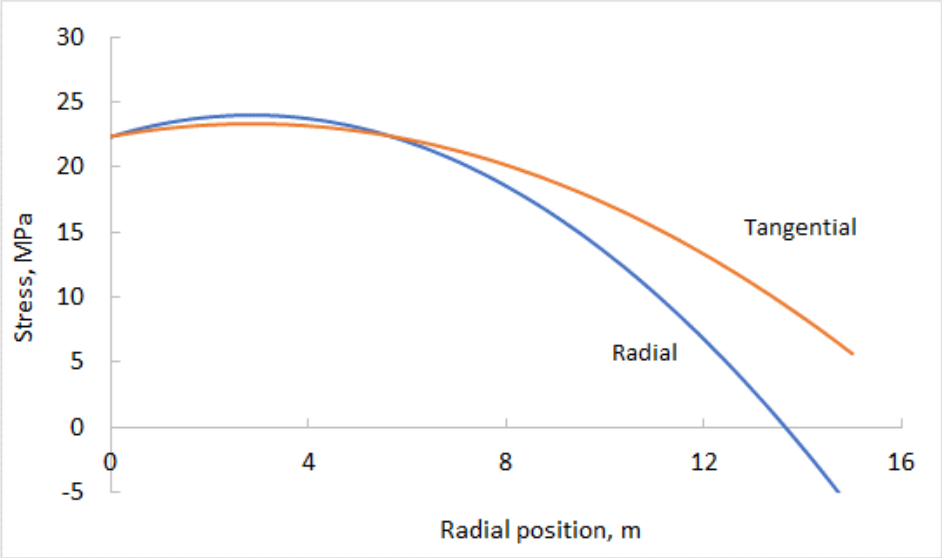

Figure 14-12 Final Floor Stresses for Case 2: 15 m Tank Radius; 14 mm Floor Thickness

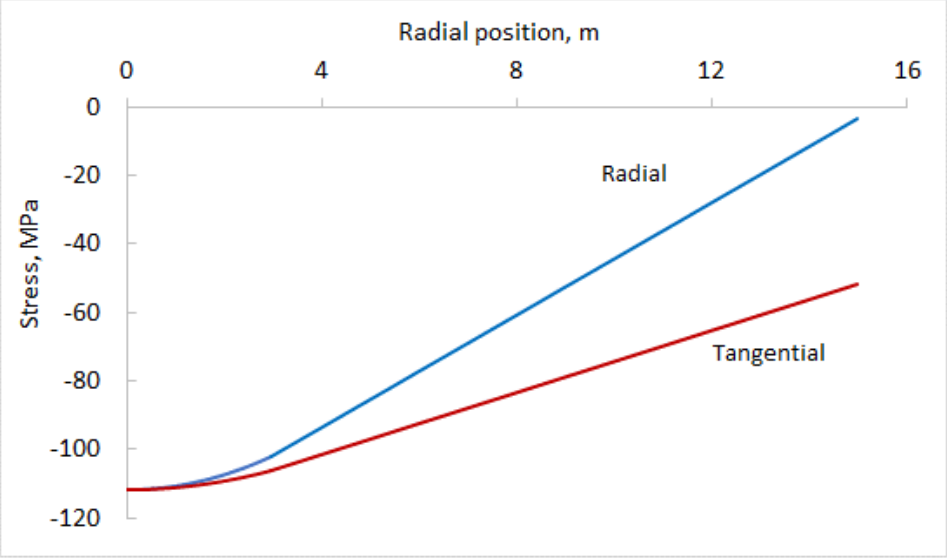

Figure 14-13 Floor Stresses for Case 3: 15 m Tank Radius; 14 mm Floor Thickness

As noted above in the discussion for the 21 m tank, an accurate estimate of the floor stresses for the 15 m tank will require 1) a more sophisticated approach than an analytical solution, and 2) analyzing the history of the floor stresses prior to the condition of interest. As such, it's not possible to state that the floor stresses for the 15 m tank will always be less than the allowable stresses listed in Section II of the Code. Nonetheless, it is apparent that there is likely a combination of tank diameters and floor thicknesses that result in stresses due to friction, in combination with stresses due to temperature gradients (Section 14.7), that satisfy the allowable limits discussed in Section 14.14.1.

14.11 Salt Inlet Flow Distribution

The salt flow entering the tank is typically distributed by means of a single ring header. The circumference of the header is in the range of 40 to 60 percent of the circumference of the tank. The header has either a series of holes or a group of eductors to distribute the incoming flow with the main inventory.

The distribution arrangement is simple and offers a low cost. However, it can suffer various performance liabilities, as follows:

1. The effectiveness of the mixing is dependent on the velocity of the salt leaving the distribution ring. At low receiver flow rates, the salt velocities in the header will be low, and the extent of the mixing will be limited. Imperfect mixing can either add to, or subtract from, the existing radial temperature gradient in the floor. Any operating condition which increases the radial temperature gradient carries the risk of adding creep or fatigue damage to the floor.

2. During receiver startup, or following a trip of the receiver, both the temperature and the flow rate of the salt can be well below design values. A condition can occur in which relatively cold salt leaves the distribution ring, and the salt sinks to the floor due to buoyancy effects. This, in turn, can lead to a non-uniform temperature distribution in the floor immediately below the distribution ring.

14.11.1 Stresses Calculated from Analytical Expressions in Roark

The stresses associated with this flow condition can be estimated using the following expression from Roark:

> A thin circular disk at uniform temperature has the temperature changed ΔT throughout a comparatively small central circular portion of radius a. Within the heated part there are radial and tangential compressive stresses $\sigma_r = \sigma_t = \frac{1}{2} \Delta T \gamma E$. At points outside the heated part, a distance r from the center of the disk but still close to the central portion, the stresses are $\sigma_r = \frac{1}{2} \Delta T \gamma E a^2/r^2$ (compression) and $\sigma_t = \frac{1}{2} \Delta T \gamma E a^2/r^2$ (tension); at the edge of the heated portion, there is a maximum shear stress $\sigma_r = \frac{1}{2} \Delta T \gamma E$.

Using representative values for the modulus of elasticity, E, and the coefficient of thermal expansion, γ, for stainless steel, a local temperature depression of 54 °C results in a stress equal to the allowable stress for stainless steel at 560 °C. A local temperature depression of 87 °C produces stresses equal to the yield stress. The local stresses can either add to, or subtract from, the stresses normally present in the floor.

It can be noted that differences between the temperature of the salt in the distribution ring and the temperature of the bulk inventory can differ, during transient conditions, by values up to at least 90 °C.

14.11.2 Stresses Calculated from Finite Element Models

A computational fluid dynamics / finite element model has been developed for a hot salt tank at a commercial project. Using historical operating data from the project for inventory temperatures, flow conditions into the tank (flow rate, temperature), and flow conditions out of the tank (flow rate, temperature), floor temperatures have been calculated for a number of radial and circumferential locations as a function of time.

Using data from one particular day, which included a number of cloud transients, the differences in floor temperatures at two radial locations are shown in Figure 14-14. The two locations are as follows:

- Between Node 2 (17 percent of the tank radius) and Node 3 (33 percent of the tank radius)
- Between Node 5 (67 percent of the tank radius) and Node 6 (85 percent of the tank radius)

The circumferential location is 90° clockwise from North.

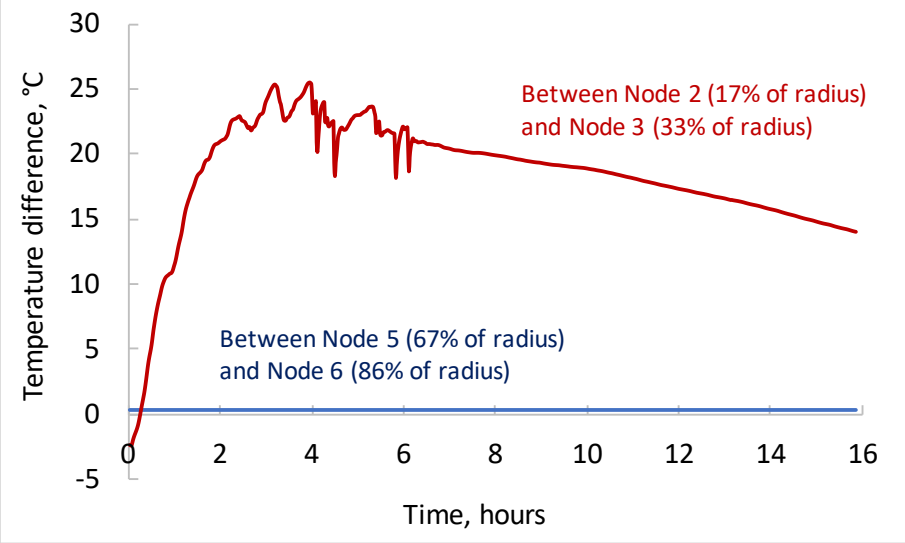

Figure 14-14 Differences in Floor Temperatures versus Time; 90° Circumferential Location

The radial temperature difference is concentrated near, and somewhat inside, the location of the distribution header (between Nodes 2 and 3). Near the perimeter of the tank (between Nodes 5 and 6), the radial gradient has decayed to about 0.5 °C.

A plot of the circumferential temperature differences at Node 6, as a function of time, is shown in Figure 14-15. The temperature differences are calculated between circumferential locations of 45° and 90°.

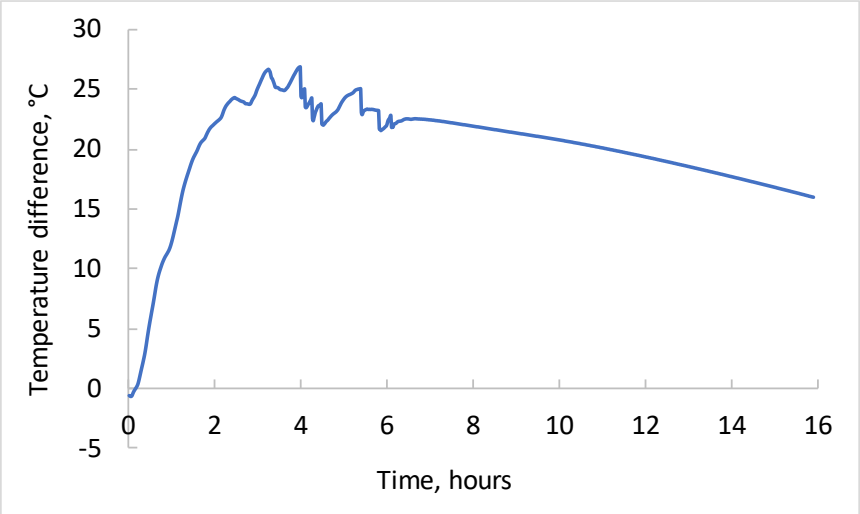

Figure 14-15 Differences in Floor Temperatures versus Time; Node 6 Between 45° and 90°

With reference to Figure 14-14, the radial temperature difference at Node 6 is less than 1 °C during the 16 hour time span of interest. However, the circumferential temperature difference at Node 6 is greater than 20 °C for most of the duration.

Similar to Figure 14-15, a plot of the circumferential temperature differences at Node 6, for circumferential locations of 90° and 135°, is shown in Figure 14-16.

The temperature differences in Figure 14-15 are essentially the mirror image of the temperature differences in Figure 14-16, which means that temperature differences between the 45° location and the 135° location are only a few °C.

The von Mises stresses in the floor at Node 6, generated by the circumferential temperature differences noted above, are shown in Figure 14-17. Throughout the calculation period, the stresses exceed the yield stress. If the material is routinely operating at or above the yield stress, then the creep life of the floor will be less than the 30-year life of the project.

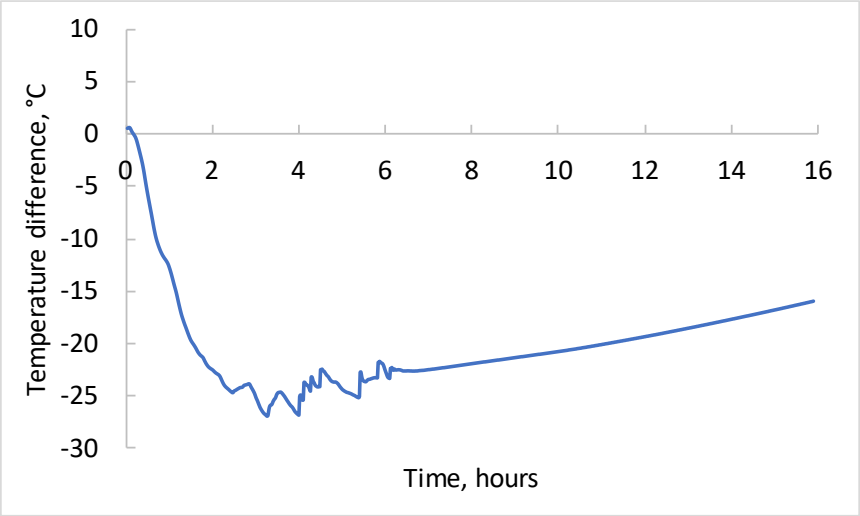

Figure 14-16 Differences in Floor Temperatures versus Time; Node 6 Between 90° and 135°

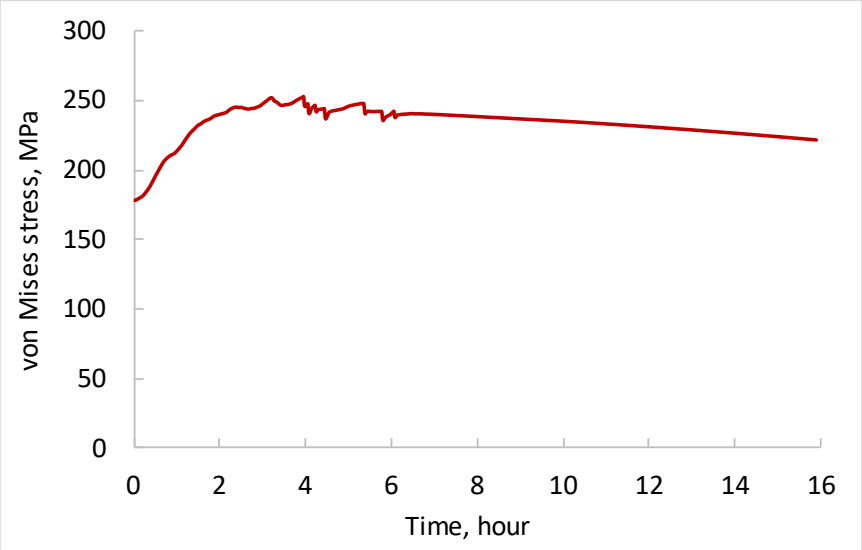

Figure 14-17 von Mises Stresses at Node 6

Several items can be noted from the discussion above:

- The analysis was conducted for only one day from the multiple days of operating data supplied to the study by the commercial project. Only one day of data were analyzed due to the lengthy computational time required (several weeks on a high performance computer)

- The day analyzed was selected to be representative of an average day with intermittent clouds. This day may, or may not, represent a worst-case condition for floor stresses

- At the start of the calculation, the stresses in the floor are taken to be equal to the stresses on the first day of commercial service. However, the calculation was developed based on plant operating data from (say) Day 905 of commercial service. During this 905 day period, the stresses are expected to evolve due to stress relaxation in the weld regions, plastic deformations associated with creep, plastic deformations generated by high friction forces coincident with changes in the inventory temperature, lateral movement of the tank due to non-isotropic thermal expansion and contraction, and vertical movement of the tank due to foundation settlement. The stress evolution over this 905 day period are unknown, and as such, the initial stress state for the calculation are also unknown. This necessarily introduces some level of uncertainty in the values shown in Figure 14-17.

The evolution of the floor stresses over months or years is difficult to determine, in large part due to the large computational requirements. Nonetheless, it is clear that even modest temperature differentials (25 to 30 °C) in the inventory, either radial or circumferential, can generate stresses that are nominally twice the allowable values discussed in Section 14.15.11.

14.12 Operator Actions

During receiver startup, the temperature of the salt leaving the receiver starts at the cold salt temperature (295 °C), and then increases to the normal design temperature (565 °C). Early in the startup process, salt is directed to the cold tank to prevent a noticeable decay in the inventory temperature of the hot tank. When the salt temperature in the downcomer reaches a defined crossover temperature, the flow is directed to the hot tank.

The crossover temperature is a function of the inventory temperature in the hot tank. A typical crossover temperature is 20 to 50 °C below the inventory temperature. Note that this phase of the startup process results in a small decay in the inventory temperature. However, the energy available in the salt at temperatures between the crossover temperature and the design temperature is still useful for electric energy production.

The decay in the inventory temperature is a function of the crossover temperature and the inventory level in the hot tank. The crossover temperature can be programmed in the DCS, and the control system will automatically open and close the tank diversion valves as necessary. However, as with most setpoints in the DCS, the operator is free to revise the setpoint. If the crossover setpoint is set to a low value, then additional thermal energy will be stored in the hot tank for electric energy production. During the project warranty and guarantee period, this can be an important consideration for the EPC contractor. However, the lower the setpoint, the greater the risk to the tank in terms of non-uniform temperature distributions, particularly in the floor, and the greater the potential for exceeding the limits from the vendor on the allowable rate of temperature change. Experience from more than one commercial project has shown that protecting the low cycle fatigue life of the tank often takes secondary importance to meeting the contractual requirements on energy production.

14.13 Cumulative Effects

As discussed above, plastic deformations in the floor could result from welding the floor plates, preheating the tank, and filling the tank with salt. The deformations may well take the form of buckles, or ridges, spanning a significant fraction of the diameter of the tank.

Once in commercial service, the tank will undergo a series of changes in level and changes in temperature. Some of these changes will place the floor into compression. If some of these loads cause the floor to yield, then the displacements are likely to appear as increases in the height of the ridges. The deformations can be compounded by local transient thermal stresses in the floor associated with receiver startups and receiver trips.

In tanks constructed from Type 347H, stress relaxation cracking will begin at the start of commercial service. The mechanism will progress at the highest rate at those locations with the largest residual stresses and the highest strains. The regions include the weld zones and the tops of the buckles.

At some point, 1) the progression of internal cracks and micro-voids generated by stress relaxation cracking, 2) in combination with cyclic compression / tension loads generated by friction, 3) in combination with a reduction in fatigue life at locations subject to plastic strains, 4) produces a crack at the top of the ridge. The crack is the source of the leak in the tank. This failure mechanism has been observed in a number of commercial projects.

It can be noted that ultrasonic examination of the welds in the floor and in the wall of a commercial tank has shown evidence of voids. The examinations were conducted after the tank had been in service for about 2 years. The formation of voids in 2 years is consistent with expected progression of stress relaxation cracking. If stress relaxation cracking is present, then strain localization at the grain boundaries can accelerate the damage due to low cycle fatigue.

14.14 Solutions

The question then arises: What solutions can be effected to prevent damage to the tank? Two approaches can be considered:

- A change in the tank design Codes
- Methods to reduce compressive loads on the floor.

14.14.1 Changes in the Tank Design Codes

Current Approach

To date, commercial tanks have been designed to the following combination of Standards and Codes:

- API Standard 650, Welded Steel Tanks for Oil Storage. However, the maximum design temperature in the Standard is 260 °C

- To overcome this limit, allowable material stresses are typically taken from Section II Part D Subpart 1A of the ASME Code for design temperatures above 260 °C

- Certain portions of the tank can operate at stresses greater than those listed in Section II. To ensure that the tank has a suitable fatigue life, the design by analysis requirements specified in Section VIII Division 2 are often adopted.

Stress Categories

The tank is subjected to a range of stress categories, including the following:

- Primary membrane stress, P_m, associated with static fluid pressures, operating pressures, and dead loads

- Local membrane stress, P_L, is a membrane stress typically generated by a discontinuity in the geometry

- Bending stress, P_b, produced, for example, by pressure applied to the central portion of a flat head

- Secondary stress, Q, produced by constrained thermal expansion or the bending stress at a structural discontinuity

- Peak stress, F, which does not cause any noticeable distortion but can be a source of a fatigue crack or a brittle fracture. An example is the thermal stress in the wall of a vessel caused by a rapid change in temperature.

Allowable Stress Values in Section VIII Division 2

In Section VIII Division 2, the allowable values for various combinations of stress categories include the following:

- Primary membrane stress $P_m = S$, where S is the value listed in Section II Part D Subpart 1. For Type 347H stainless steel at a temperature of 565 °C, a representative value for S is 117 MPa

- Local membrane stress $P_L = 1.5 * S$, or 234 MPa

- Local membrane stress P_L + Bending stress $P_b = 1.5 * S$, or 234 MPa

- Local membrane stress P_L + Bending stress P_b + Secondary stress Q = S_{PS}, where S_{PS} is the larger of 1) 3 * S from Section II, Part D, Table 5A, and 2) 2 * S_y (yield stress) from Section II, Part D, Table Y-1. For Type 347H stainless steel at a temperature of 565 °C, a representative value for S_{PS} is 352 MPa

- Local membrane stress P_L + Bending stress P_b + Secondary stress Q + Peak stress F = S_a, where S_a is alternating stress. The limit for the stress is obtained from a fatigue curve for the specified number of operating cycles, with corrections applied to the curve for mean stresses other than zero.

The values for the stresses are generally determined by finite element analyses.

Limitations of Section VIII Division 2

In the stress categories outlined in Section VIII Division 2, all of the allowable values are based on time-independent properties of the material. In particular, the effects of creep are not considered in the design.

In this design approach, the equipment is assumed to operate below the creep range by providing design margins against the following failure modes:

- Failure by plastic Instability or necking

- General structural collapse under a single application of limit load
- Time-independent buckling

- Incremental collapse or ratcheting under cyclic loading

- Fatigue under cyclic loading

- Fast fracture.

Nonetheless, preliminary calculations of the stresses in one commercial tank show values which are high enough (> 300 MPa) to 1) reduce the fatigue life to values less than the 30-year life of the project, and 2) initiate creep at the temperatures characteristic of a hot salt tank. Granted, none of the commercial tanks built to date have failed due to creep, but this may be due to a condition in which other failure mechanisms have reduced the life of the tank to values which are too short to allow significant quantities of creep to develop. In any event, all of the hot salt tanks built to date have failed in one way or another. As such, one could ask if the requirements in the Standards and Code sections noted above is the correct combination to use in the design and the analysis of the tank.

Alternate Design Codes

The requirements of Section III, Rules for Construction of Nuclear Facility Components, apply to materials in service at high temperatures.

Section III Division 1 Subsection NB provides rules for the design and the evaluation of pressure vessels, including the effects of fatigue. Nonetheless, the Subsection largely follows the design approach described for Section VIII Division 2. In addition, the effects of creep are largely avoided by limiting the maximum design temperature to 427 °C.

In contrast, Section III Division 1 Subsection NH provides rules for the design and the evaluation of pressure vessels, including the effects of both fatigue and creep. The Subsection applies to design temperatures up to 850 °C.

Operation at elevated temperature introduces time-dependent failure modes. The following six time-dependent failure modes are considered in the high-temperature design:

- Creep rupture under sustained primary loading
- Excessive creep deformation under sustained primary loading
- Cyclic creep ratcheting due to steady primary and cyclic secondary loading
- Creep-fatigue due to cyclic primary, secondary, and peak stresses
- Creep crack growth and nonductile fracture
- Creep buckling.

The evaluation process, compared to Section VIII Division 2, includes an additional set of stress values and factors: S_o, S_m, S_t, S_{mt}, K, and K_t. The derivations of the values and factors are described below.

S_o for Use in the Design Limits Calculation

S_o is the greater of the following two values:

- The maximum allowable stress value S in Section II Part D Table 1A. For Type 347H stainless steel at a temperature of 565 °C, the value is 110 MPa
- The S_m stress intensity at 300,000 hours in listed in Subsection HBB of the upcoming version of Section III Division 5, High Temperature Reactors. The text has yet to be published; however, publicly available inputs to the Section are available from Oak

Ridge National Laboratory, Pacific Northwest Laboratory, Argonne National Laboratory, and NUMARK Associates. The value for S_m is listed as 53 MPa in the ORNL report [30].

As such, the value for S_o is 110 MPa.

Time-Dependent Stress Value, S_t

In the design rules of Subsection NH, the material has assumed to reach a temperature where creep can produce deformations of the structure. S_t is a time-dependent allowable stress, and is defined as the lesser of the following parameters:

- 100 percent of the stress required to produce a permanent creep strain of 1 percent in a defined period. The allowable stress is determined through the use of a Larson Miller curve, which plots the stress as a function of the metal temperature and the logarithm of the operating period. An example for Type 316 stainless steel is shown in Figure 14-18.

  The estimated stress to produce a 1 percent strain in 100,000 hours is 105 MPa

- 80 percent of the minimum stress to initiate tertiary creep. The creep characteristics are often divided into three phases: primary; secondary; and tertiary. The primary phase is generally short, and shows a relatively rapid change in dimension with time. The secondary phase is typically much longer. As the material deforms, its cross sectional area will reduce. However, the material also strain hardens. The increase in the strength generally offsets the reduction in area, and the true stress value remains nominally constant. At some point in the process, the effects of strain hardening cease and the material enters the tertiary phase. Gross deformations appear, which is generally followed soon after by rupture. Using a separate Larson Miller plot, the allowable stress to initiate tertiary creep is 84 MPa for a time span of 100,000 hours

- 67 percent of the minimum stress to cause rupture. Using a separate Larson Miller plots, the allowable stress is 106 MPa for a time span of 100,000 hours.

As such, the value for S_t is 84 MPa.

Time-Independent Stress Value, S_m

S_m is the lesser of the following two values:

- 2/3 of the yield stress. For Type 347H stainless steel at a temperature of 565 °C, the value is 2/3 * 155 MPa = 103 MPa

[30] Ren, Weiju, et. al. (Oak Ridge National Laboratory, Oak Ridge, Tennessee), 'Technical Input for the Nuclear Regulatory Commission Review of the 2017 Edition of the ASME Boiler and Pressure Vessel Code, Section III, Division 5, High Temperature Reactors', Technical Letter Report ORNL/SPR-2020/1653, August 2020

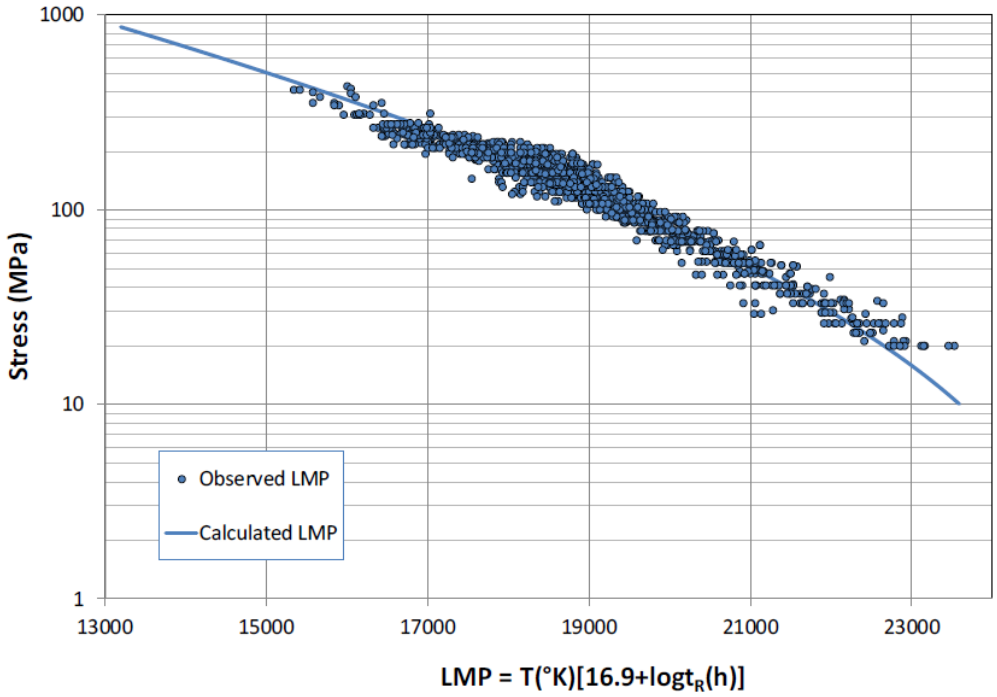

Figure 14-18 Larson Miller Diagram for the Stress to Develop 1 Percent Strain

- 1/3 of the tensile strength. For Type 347H stainless steel at a temperature of 565 °C, the value is 1/3 * 396 MPa = 132 MPa.

As such, the value for S_m is 103 MPa.

Lastly, S_{mt} is defined as the lesser of S_m (103 MPa) and S_t (84 MPa). As such, the value for S_{mt} is 84 MPa.

K has a value of 1.5 for shells and solid sections, and K_t is defined as (K + 1) / 2 = 1.25.

The allowable primary membrane stress, P_m, is equal to S_o = 110 MPa. The allowable sum of the local membrane stress, P_L, and the bending load, P_b, is equal to 1.5 * S_o = 165 MPa.

For the Level A and B Service Limits, the allowable primary membrane stress, P_m, is equal to S_{mt} = 84 MPa. The allowable sum of the local membrane stress, P_L, and the bending load, P_b, is equal to 1.5 * S_m = 154 MPa. The allowable sum of the local membrane stress, P_L, and the bending load, P_b, modified by the K_t factor is equal to S_t = 84 MPa.

Comparison of Section VIII Division 2 with Section III Subsection NH

Effects of Creep

The effects of creep are associated with operation at high temperatures, and the rate of creep is influenced by the stress. One of the contributions to the total stress can be a thermal stress produced by temperature gradients in the equipment.

In Section VIII Division 2, thermal stresses are treated as secondary stresses, and secondary stresses are not components in the design limit calculations involving the primary membrane stress, the local membrane stress, and the bending loads. As such, any creep generated by thermal stresses is not considered in the design calculations.

In contrast, Section III Subsection NH requires an analysis of the following:

- Deformations, based on either 1) a maximum allowable strain of 1 percent, or 2) the results from an inelastic analysis
- A creep-fatigue evaluation based on summations of the damages associated with the number of fatigue cycles and creep durations
- Buckling and instability criteria.

Allowable Stresses

In Section VIII Division 2, the highest numerical value for the allowable stress is S_{PS}, with a value of 352 MPa. In contrast, in Section III Subsection NH, the highest numerical value for the allowable stress is 1.5 * S_o (165 MPa). This value is about one-half of the design value from Section VIII Division 2.

To date, no commercial tanks have been designed and built to the requirements of Section III Subsection NH, and direct comparisons to commercial tanks are, to some degree, conjectural. Nonetheless, differences are likely to be present in the following areas:

- Design limit and fatigue calculations from a representative commercial project show peak stresses on the order of 220 MPa at the connection between the floor and the wall. The calculations are based on a coefficient of friction of 0.2 between the floor and the foundation. Evidence from other studies indicate that the coefficient is more likely to be in the range of 0.5 to 1.0. If the tank stress calculations were repeated with a higher coefficient of friction, it's not clear that the design could satisfy the requirements of Section III Subsection NH
- As discussed in Section 14.7, steady state radial temperature gradients in the floor on the order of 5 °C can produce thermal stresses in the floor approaching the allowable

value listed in Section II Part D Table 1A. In the design approach listed in Section VIII Division 2, these stresses are treated as secondary stresses, and do not influence the design limit calculations. In Section III Subsection NH, the thermal stresses in the floor will influence the creep and the fatigue assessments. This, in turn, may have an influence on the required design for the floor, which, in turn, would influence the buckling characteristics of the floor

- Based on the operating experience from a number of commercial tanks built to the requirements of API Standard 650, the vendor will often specify an allowable rate of temperature change. A representative value is 1 °C/min. However, operating data from the Crescent Dunes project has shown rates of change at least an order of magnitude higher. The fatigue damage associated with these rates of change has yet to be calculated. But, in future projects, the operating procedures must be specified in such a manner that the 30-year fatigue life of the tank can be satisfied.

Observations

Commercial tanks built to date have been designed using API Standard 650, Section II, and Section VIII Division 2. Essentially all of these tanks have developed leaks or other failures. Nonetheless, no studies have been conducted which demonstrate that this combination of design standards and codes, in combination of historical operating data on the tanks during transient conditions, has resulted in the tank failures. Similarly:

- Section III Subsection NH offers a more conservative set of design stresses and rules than Section VIII Division 2. However, no studies have been conducted which demonstrate that a tank, designed to the rules of Section III, would survive the life of the project

- The stresses in some portions of the tank, such as the wall and the roof, are generally predictable. As a result, it should be possible to estimate the creep and the fatigue life of these sections with an accuracy sufficient for a commercial project. In contrast, the stresses in the floor are not well understood, and the accuracies of the creep and fatigue calculations are generally unknown. As such, it may be possible to design the wall and the roof to the Codes typically used in previous commercial projects (i.e., API 650 and Section VIII Division 2), and adopt the more conservate design rules in Section III Division 5 for the floor.

Whichever combination of design rules is selected for the tank, the effect on the capital cost of the tank is likely to be modest. For example, in API Standard 650, the floor is essentially treated as a liquid boundary, and the thickness of the floor can be thin (i.e. 8 mm). However, following the rules of Section III Division 5, the allowable stresses associated with a creep and fatigue life of 30 years are relatively modest (~85 MPa), in which case the thickness of the floor may need to be double that of an API-style tank. Doubling the thickness of the floor increases the mass of steel in the tank by about 15 percent, which means, to a zeroth-order, that the

capital cost of the tank also increases by 15 percent. A cost increase of this order will have essentially no effect on the financial status of the project.

To some extent, the industry is faced with the following conundrum:

- Can a set of analyses be conducted that convinces the financial community that a tank designed to the requirements of Section III Division 5, or a comparable international Code, will have an availability of 99.99 percent?

- In an ideal case, a flat bottom tank experiences uniform friction forces around the circumference of the tank. However, industry experience indicates that this may not be the case, as lateral movement of a tank in a commercial project has been observed. If it is not possible to determine the actual distribution of friction forces on the floor, then it may not be possible to determine the actual stresses in the floor. If so, an alternate tank concept, one that avoids a flat floor on a flat foundation, may be required to reach an availability of 99.99 percent. However, there will be no industry experience with an alternate tank design, and this will necessarily incur some form of technical and financial risk to the Owner

- The best, and perhaps the only, method to prove which design codes are the correct codes, and which tank concept is the correct tank concept, is to design, fabricate, and test a full-size tank at a commercial project over a period of several years. However, it's not clear who would be prepared to fund such a development program.

14.14.2 Methods to Reduce Loads on the Floor

Multiple Tanks

The peak loads in the floor are, to some degree, a function of the tank diameter. Substituting two 50-percent capacity tanks, or three 33-percent capacity tanks, for one 100-percent capacity tank could reduce the loads in the floor to values below a yet-to-be-defined damaging threshold. The relationship between floor stresses due to friction and tank diameter are discussed in Section 14.10.4.

In addition, multiple tanks provide a degree of redundancy, and eliminate the single point of failure problem with one 100-percent capacity tank.

Nonetheless, the failure mechanisms in commercial tanks are not yet fully understood. Adopting smaller tanks may be a step toward a reliable design approach, but the maximum allowable tank dimensions have yet to be defined and demonstrated.

Radial Gradients

A few methods for controlling the radial temperature gradient in the floor include the following:

Insulation Design The radial temperature gradients can be reduced by changing the insulation design at the perimeter of the tank. This may consist of greater insulation thicknesses at the base of the tank, and the addition of insulation on the refractory ring wall beneath the wall. Nonetheless, a radial temperature gradient will still develop, and if the inventory reaches, or approaches, a stagnation condition, then damaging stresses in the floor will result.

Perimeter Heat Addition The radial gradient can also be reduced by some form of heat addition at the tank perimeter. The heat addition might take the form of radiant electric heaters, installed beneath the wall insulation. The principal liability would be a slow response time due to limited radiation heat fluxes from radiant heaters to the tank wall. Alternately, electric heaters could be embedded in the refractory ring wall. As above, the principal liability would be a slow response time due to the combination of a modest thermal conductivity, and a high thermal inertia, of refractory materials.

Multiple Distribution Headers An alternate approach to controlling the radial gradients is a dedicated distribution ring at the perimeter of the tank. Salt flow to the distribution ring would be supplied by recirculation from one of the hot salt pumps. The goal would be to move salt from the bulk inventory to the tank perimeter, and thereby provide forced convection heat transfer to compensate for the higher heat losses at the perimeter. The ability to move heat by forced convection is generally large relative to conduction heat transfer. As such, it should be a straightforward exercise to reduce the magnitude of the radial gradient.

On a related point, the hot salt tank at the 10 MWe Solar Two demonstration project did not use a distribution ring header near the floor. Instead, a series of spray nozzles, supported from the inside of the roof, introduced salt into the tank. The (flawed) goal of the nozzles was to prevent the mixing of salt from the receiver, at a temperature of 565 °C, with the bulk inventory in the tank, which would normally be at a temperature less than 565 °C. The intent was to intentionally stratify the inventory, and only send salt, at a temperature of 565 °C, to the steam generator. This approach, of course, reduced mixing within the inventory, which promoted undesirable vertical radial temperature gradients in the floor. However, adding salt to the top of the inventory, rather than introducing salt near the floor by a distribution header, effectively isolated the floor from any transient conditions in the downcomer. To what extent this reduced the local transient stresses in the floor is unknown. However, the hot tank operated safely, without leaks, during the 3-year test and evaluation period.

In principle, a commercial project could also replace the conventional distribution header near the floor with a series of spray nozzles, or some other flow distribution arrangement, located inside the roof. Thermal stratification will inevitably occur. However, the methods discussed above, and below, should be effective in limiting both the vertical and the horizontal stratification to acceptable levels.

Tank Scale Mixing Device An alternate method to control the radial and the circumferential temperature gradients is to provide some form of a mixing device that spans the full dimensions of the tank. This might consist of a vertical shaft located at the center of the tank. Two to four vertical perforated plates would be attached to the shaft. The horizontal dimension of the plate would be somewhat less than the radius of the tank, and the height of the plate

would be perhaps one half of the maximum liquid level. Rotating the shaft at a low speed, say 1 rpm, would keep the inventory mixed.

A second approach might be a perforated plate, with a diameter slightly less than the diameter of the tank. The plate would vertically traverse the depth of the inventory once every few minutes. Forcing a portion of the inventory to pass from the top of the plate to the bottom, and vice versa, would promote convection mixing at the perimeter of the tank.

It can be noted that the two approaches to whole-tank mixing are only conceptual, and additional design work is required to demonstrate that the concepts will work as intended. Nonetheless, the calculation of the floor stresses produced by radial temperature gradients (Section 14.7) and by circumferential temperature gradients (Section 14.11.2) indicate that intra-tank temperature differentials should be held to values no higher than perhaps 5 °C. It is unlikely that the static mixing generated by either one or two inlet distribution headers will satisfy a 5 °C limit, particularly at low flow rates or following a trip of the receiver. As a result, some form of active mixing device may be mandatory to protect the tank.

Friction Forces with a Tank Scale Mixing Device It can be noted that friction forces can develop in the floor, even with if the inventory temperatures are always isotropic. The effect occurs during startup of the receiver, as discussed in *Friction Forces*. As such, the use of a tank scale mixing device can help to control, but not fully eliminate, transient thermal stresses in the floor.

Cold Tank Diversion Valve Failure and Tank Scale Mixing Device On a related topic, the temperature distribution in the hot salt tank is determined by 1) conditions where the equipment (valves, instruments) operates as intended, and 2) conditions where the equipment does not operate as intended. One example of the latter is the following scenario:

- At the start an operating day, the hot tank is at the minimum level
- The receiver, after reaching normal operating conditions, trips. The receiver pumps are tripped. The circuit inlet control valves move to the 100 percent open position, and cold salt is supplied to the receiver from the pressurized inlet vessel
- The heliostat field, except for a limited number of heliostats providing a preheat flux, is defocused. The defocusing period requires about 60 seconds. During this period, the air pressure in the inlet vessel, and the salt flow rate to the receiver, follow an exponential decay
- The diversion valve in the downcomer, which directs flow to the cold salt tank, then malfunctions (fails to open). The temperature of the salt entering the hot tank decays from an initial value of 565 °C to the cold salt temperature of 295 °C at the projected rate of 360 °C/min.

The flow through the receiver is then stopped, and the receiver is drained. The temperature of the inventory in the hot tank, assuming perfect mixing, is shown in Figure 14-19.

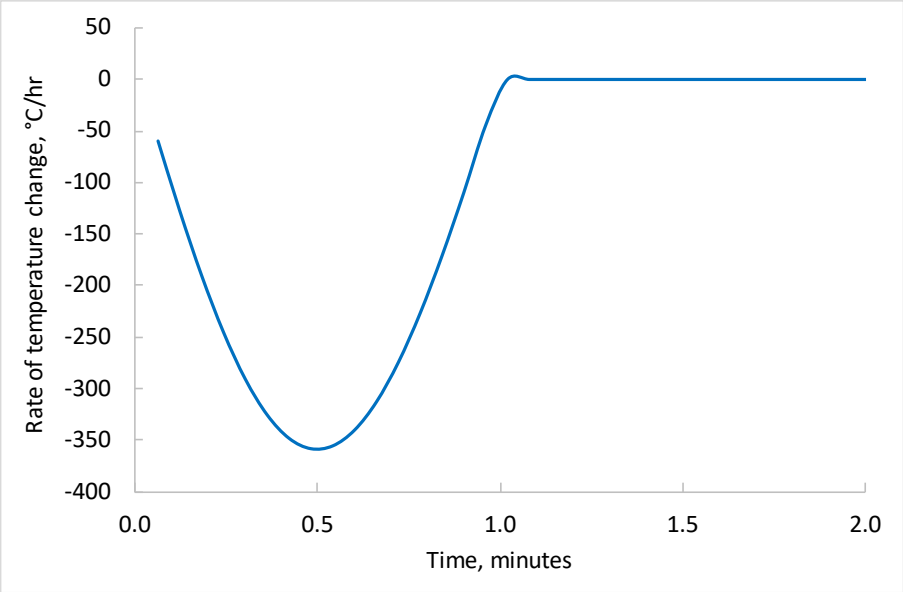

Figure 14-19 Hot Tank Temperature Following a Failure of the Cold Tank Diversion Valve

The peak cooling rate of -350 °C/hr is approximately 6 times the typical maximum rate allowed by the tank supplier. The stresses associated with this scenario have not been calculated, but local stresses above the yield value, and some loss in the fatigue life, would not be unexpected.

The failure of the cold tank diversion valve represents a single point failure, and would not be considered an improbable condition. As such, the design basis for the project should include this scenario, together with other potential single point failures, in an analysis of the fatigue life. If the analysis shows that damage to the tank can only be prevented (or meaningfully reduced) by some form of active mixing, then a mechanical mixer must be a feature of the tank design.

Friction Forces

During overnight hold periods, the temperature of the salt inventory in the tank decays. The tank thermally contracts, which places the floor in tension. Following the startup of the receiver, the temperature of the salt inventory increases. The tank starts to thermally expand, which 1) reduces the tensile stresses in the floor, and then 2) places the floor into compression. As discussed in Section 14.10.3, an increase in the inventory temperature of about 30 °C is sufficient to change the friction in the floor from the maximum tensile stress to the maximum compressive stress. The magnitude of the tensile or the compressive stress is directly proportional to the height of the salt in the tank.

During the plant design, finite element calculations of the stress in the floor should be developed for various combinations of temperature change, both positive and negative, and salt height. Allowable combinations are defined, such that the floor stresses satisfy the creep and the fatigue requirements. The allowable combinations are programmed into the

distributed control system in the form of permissives. The permissives provide two useful functions:

- The operator is not allowed to make ad hoc decisions regarding inventory temperature and level that could have a detrimental effect on the creep and the fatigue life of the floor

- Over the course of a day, the inventory temperatures increase to values as high as possible, consistent with the allowable stresses in the floor. This, in turn, maximizes the daily electric output of the Rankine cycle, without compromising the long-term availability of the storage system.

As discussed in Section 14.10.3, a static coefficient of friction of 0.3 between the floor and the foundation may be high enough to produce yield stresses near the center of the tank. The most common lubricant for commercial tanks is sand. One reference for data on friction coefficients between steel and sand is a paper Usegusi [31]. However, in general, there are little data on the coefficients for sand at high temperatures. If experiments show that the coefficients are greater than about 0.4, then sand may not be a suitable solid lubricant.

An alternative high temperature lubricant may be boron nitride. During construction, the boron nitride would be applied to the top of the foundation material (presumably refractory bricks) as a water/boron nitride suspension. However, there are no data on how long the boron nitride layer might survive. If the layer becomes eroded, it may be possible to renew the lubricant by injecting a water/boron nitride suspicion through an array of pipes installed at the top of the foundation. A series of experiments, at the full design temperature of the tank, would need to be conducted to demonstrate the feasibility of this approach.

An alternate solid lubricant is graphite. However, the galvanic potential between carbon and stainless steel is large. Pitting corrosion of the stainless steel is likely, which makes graphite a poor candidate.

14.15 Lifetime Assessment

The material in a tank is subjected to cyclic stresses, environmental effects (i.e., corrosion), and continuous stresses. The life of the material, N_f, is a function of the accumulated damage due to fatigue, corrosion, and creep, and can be represented as follows:

$$\frac{1}{N_f} = \frac{1}{N_f^{Fatigue}} + \frac{1}{N_f^{Oxidation}} + \frac{1}{N_f^{Creep}}$$

A range of considerations in evaluating the fatigue, the corrosion, and the creep lives of the tank are outlined in the sections below.

[31] Uesugi, Morimichi, et. al., (Department of Architectural Engineering, Chiba University, Japan), 'Friction Between Sand and Steel under Repeated Loading', Soils and Foundation Volume 29, No. 3, 127-137, September 1989, Japanese Society of Soils Mechanics and Foundation Engineering

14.15.1 Fatigue Assessment

The number of stress (or strain) cycles that a material can tolerate before fracture is a function of the material, the temperature, and the range of the stress (or strain). Fatigue data are typically generated for smooth bar samples, with a nominal cyclic strain rate of 0.001 in/in-sec.

Representative S-N (Stress-Number of cycles to failure) curves for Type 316 stainless steel are shown in Figure 14-20.

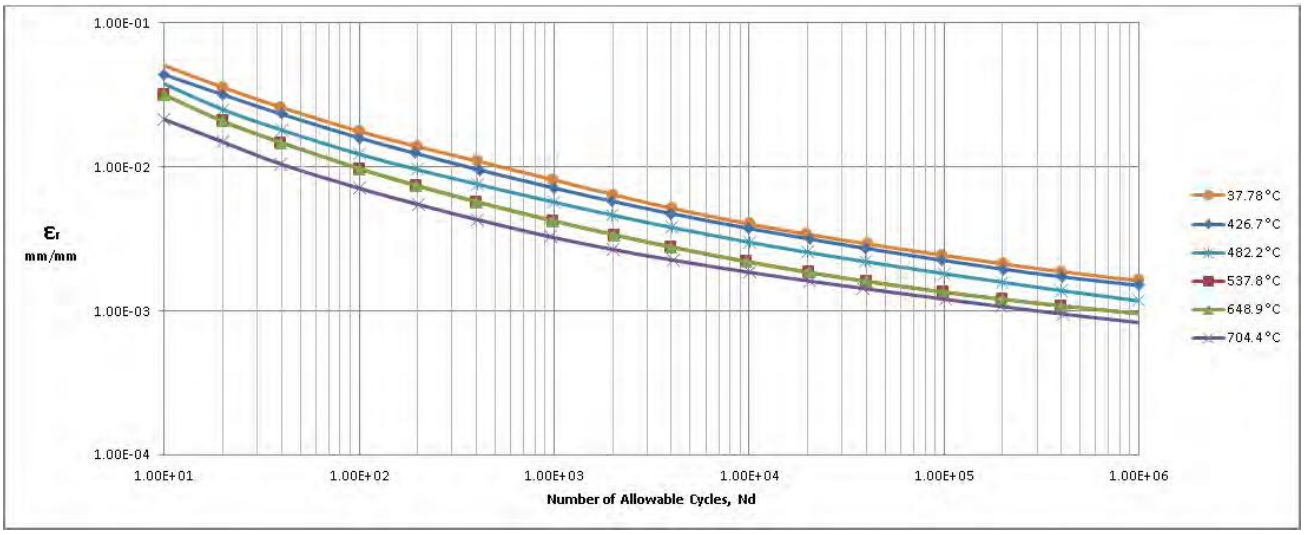

Figure 14-20 S-N Curves for Type 316 Stainless Steel

Nonetheless, and as might be expected, the material in a salt tank, particularly after welding, has markedly different fatigue characteristics than a smooth bar sample. The factors which influence the fatigue life include weld surface fatigue strength reduction factors, weld misalignment fatigue strength reduction factors, and fatigue life knockdown factors.

Weld Surface Fatigue Strength Reduction Factors

When a metal is welded, changes occur in the material properties, the grain structure, and state of stress. As might be expected, the fatigue properties in the weld region are generally inferior to the fatigue properties of the parent material. The fatigue properties of a weld, in turn, are influenced by the type of the weld, the surface condition, and the non-destructive examination methods. The effects are incorporated in the fatigue analysis by a fatigue strength reduction factor. The factor is a stress intensification value which accounts for the effect of a local structural discontinuity (stress concentration) on the fatigue strength. The factor is the ratio of the fatigue strength of a component without a discontinuity or weld joint to the fatigue strength of that same component with a discontinuity or weld joint. The factor is a multiplier on the alternating stress value used in the S-N curves; it is not a reduction factor on the fatigue life.

Fatigue strength reduction factors for a range of weld surface conditions are presented in Table 14-2. The weld quality levels are defined in Table 14-3.

Table 14-2 Weld Surface Fatigue Strength Reduction Factors - Table 1 of 2

Weld Condition	Surface Condition	Quality Levels (see Table 5.12)						
		1	2	3	4	5	6	7
Full penetration	Machined	1.0	1.5	1.5	2.0	2.5	3.0	4.0
	As-welded	1.2	1.6	1.7	2.0	2.5	3.0	4.0
Partial Penetration	Final Surface Machined	NA	1.5	1.5	2.0	2.5	3.0	4.0
	Final Surface As-welded	NA	1.6	1.7	2.0	2.5	3.0	4.0
	Root	NA	NA	NA	NA	NA	NA	4.0
Fillet	Toe machined	NA	NA	1.5	NA	2.5	3.0	4.0
	Toe as-welded	NA	NA	1.7	NA	2.5	3.0	4.0
	Root	NA	NA	NA	NA	NA	NA	4.0

In commercial tanks, the floor plates are typically welded using backing strips. The backing strips aid in the alignment of the welds between plates, which helps to reduce the fatigue strength reduction factors associated with weld misalignments (see Section *Weld Misalignment* below).

Code Guidelines

Section NH-3352(c) in Section III states *When Category B joints with backing strips not later removed are used, the suitability for cyclic operation shall be analyzed using a fatigue strength reduction factor of not less than 2 under conditions where creep effects are insignificant [NH-3211(c)]. For conditions where creep effects are significant, see NH-3353(b).* Category B joints are butt joints, which is the typical weld joint in a floor.

Further, Section NH-3352(e) states *Where partial penetration welds are used, a fatigue strength reduction factor of not less than 4 shall be used for any related fatigue and analysis under conditions where creep effects are insignificant [NH-3211(c)]. For conditions where creep effects are significant, see NH-3353(b).* Anecdotal evidence from the postmortem examinations of floors in commercial projects show evidence of misaligned welds with incomplete penetration.

As discussed in the section of this report titled *Comparison of Section VIII Division 2 with Section III Subsection NH*, creep effects in a hot salt tank are not likely to be insignificant. Along these lines, Section NH-3353(b) states *For meeting the analysis requirements of NH-3251 at elevated temperature weld regions, the assumed weld surface should model the most severe strain concentrations expected in the actual weld placed in service. This geometry may*

be prescribed on a drawing or may be recorded by prior observation. Prior observations of weld surface geometry can be visual; remote visual (e.g., using a borescope device or making a surface replica); or ultrasonic, based on a weld mockup test in which the same weld procedures are used on the same nominal pipe diameter and wall thickness, or based on a radiographic technique that is suitable for inspection of internal surfaces. (Section NH-33353(b) references *Welded Joints*, and the Section is likely applicable to joints other than piping connections.)

Table 14-3 Weld Surface Fatigue Strength Reduction Factors - Table 2 of 2

Fatigue-Strength-Reduction Factor	Quality Level	Definition
1.0	1	Machined or ground weld that receives a full volumetric examination, and a surface that receives MT/PT examination and a VT examination.
1.2	1	As-welded weld that receives a full volumetric examination, and a surface that receives MT/PT and VT examination
1.5	2	Machined or ground weld that receives a partial volumetric examination, and a surface that receives MT/PT examination and VT examination
1.6	2	As-welded weld that receives a partial volumetric examination, and a surface that receives MT/PT and VT examination
1.5	3	Machined or ground weld surface that receives MT/PT examination and a VT examination (visual), but the weld receives no volumetric examination inspection
1.7	3	As-welded or ground weld surface that receives MT/PT examination and a VT examination (visual), but the weld receives no volumetric examination inspection
2.0	4	Weld has received a partial or full volumetric examination, and the surface has received VT examination, but no MT/PT examination
2.5	5	VT examination only of the surface; no volumetric examination nor MT/PT examination.
3.0	6	Volumetric examination only
4.0	7	Weld backsides that are non-definable and/or receive no examination.

Notes:

1. Volumetric examination is RT or UT in accordance with Part 7.
2. MT/PT examination is magnetic particle or liquid penetrant examination in accordance with Part 7
3. VT examination is visual examination in accordance with Part 7.
4. See WRC Bulletin 432 for further information.

With floor plate thicknesses in the range of 6 to 8 mm, two weld passes would be typical. In terms of weld examination, the most problematic location would be the bottom of the root pass; i.e., the weld surface which is in contact with the top of the weld backing plate. Two problems can occur:

- Currently, there is no mechanism to visually examine the surface of this weld, looking for signs of the following:
    - Incomplete penetration or fusion
    - Oxidation. The quality of the weld will depend, in part, on the ability of the weld backing strip to capture and retain the cover gas (argon) in the weld zone. Any oxygen present in the weld zone can cause the filler material and the edges of the heat affected zone to oxidize. The result can be a weld with a high porosity and a low strength.

- There is a long total length of the welds to examine in a floor. Common non-destructive examinations typically include dye penetrant and vacuum box tests due to their speed and low cost. These examination methods can result in a low value for the weld quality presented in Table 14-3.

Based on these assessments, a weld surface fatigue strength reduction factor in the range of 2.5 to 4.0 can likely be justified.

Weld Misalignment Fatigue Strength Reduction Factors

Steel plates for the tank floor are typically fabricated to nominal dimensions for length, width, thickness, and flatness. Allowable tolerances on the dimensions are defined in ASTM A480, Standard Specification for General Requirements for Flat-Rolled Stainless and Heat-Resisting Steel Plate, Sheet, and Strip. For a floor plate which has a width of 2.5 m, a length of 12.0 m, and a thickness of 8 mm, the allowable tolerances include the following:

- Variation in thickness of -0.00 mm to +1.30 mm

- Panels cut by shearing
    - Variation in width of -0 mm to +20 mm
    - Variation in length of -0 mm to +75 mm

- Panels cut by water jet
    - Variation in width of -0 mm to +3.2 mm
    - Variation in length of -0 mm to +3.2 mm

- Variation in flatness of 14 mm.

When the panels are arranged on the foundation prior to welding, the tolerances will result in the following effects:

- The tops of all of the plates will not all be in the same horizontal plane

- The bottoms of all of the plates will not all be in the same horizontal plane

- The edges of the plates will not all be parallel.

As a consequence, some level of weld misalignment is inevitable.

The effects of weld misalignment on the fatigue life of a structure are discussed in Part 8, Assessment of Weld Misalignment and Shell Distortions, in API 579-1 / ASME FFS-1. The effects are calculated using the following expression:

$$\Delta S_p = \sigma_{ms}\left(1 + R_b^{pc} + R_b^{pa}\right) K_f$$

where ΔS_p is the range of primary plus secondary plus peak equivalent stress, MPa
σ_{ms} is the membrane stress from supplemental loads, MPa
R_b^{pc} is the adjustment factor for centerline misalignment, [ ]
R_b^{pa} is the adjustment factor for angular misalignment, [ ]
K_f is weld fatigue strength reduction factor, [ ].

Supplemental loads include, but are not limited to, the weight of the component, contained fluid, insulation or refractory; loads resulting from the constraint of free thermal expansion, thermal gradients or differences in thermal expansion characteristics; occasional loads due to wind, earthquake, snow, and ice; loads due both to environmental and operating conditions; reaction forces from fluid discharges; loads resulting from support displacements; and loads due to process upset conditions.

Equations for calculating the R_b factors are listed in Table 14-4.

Table 14-4 Equations for Calculating the R Factors in the Equation for ΔS_p

Type Of Misalignment	Equations For R_{bs}
Flat Plate – Centerline Offset (see Figure 8.2) (1)	$R_{bs}^{pc} = 6\left(\frac{e}{t_{1c}}\right)\left(1+\left(\frac{t_{2c}}{t_{1c}}\right)^{1.5}\right)^{-1}$ Limitations: $0.0 \le e \le t_{1c}$, $t_{2c} \ge t_{1c}$
Flat Plate – Angular Misalignment (see Figure 8.4) (1)	$R_{bs}^{pa} = 3\left(\frac{\delta}{t_c}\right) C_f$ where: $\delta = \frac{L\theta_p}{4}$ (θ_p *in radians*) $C_f = \left(\frac{2}{\beta}\right)\cdot\tanh\left[\frac{\beta}{2}\right]$ (*for fixed ends*) $C_f = \left(\frac{2}{\beta}\right)\cdot\tanh[\beta]$ (*for pinned ends*) $\beta = \frac{L}{t_c}\sqrt{\frac{3\sigma_m}{E_y}}$ (*in radians*) Limitations: $\theta_p \ge 0.0$
Note: The equation for R_b and R_{bs} are dimensionless.	

Centerline Misalignment

Centerline misalignment in flat plates with a butt weld is defined in Figure 14-21. 'P' is the applied load, 't' is the plate thickness, and 'e' is the weld offset.

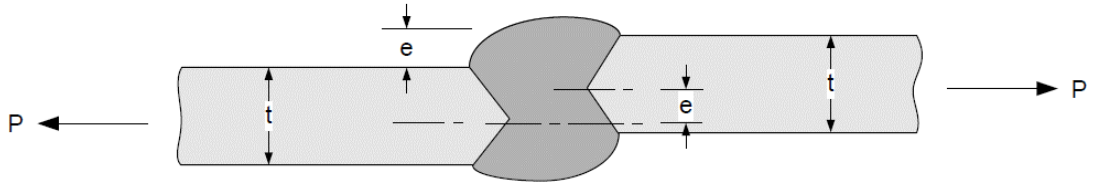

Figure 14-21 Centerline Offset Misalignment of Butt Welds in Flat Plates

Angular Misalignment

Angular misalignment in flat plates with a butt weld is defined in Figure 14-22. 'P' is the applied load, and Θ_p is the angular misalignment. The dimension 'L' is defined in Figure 14-23.

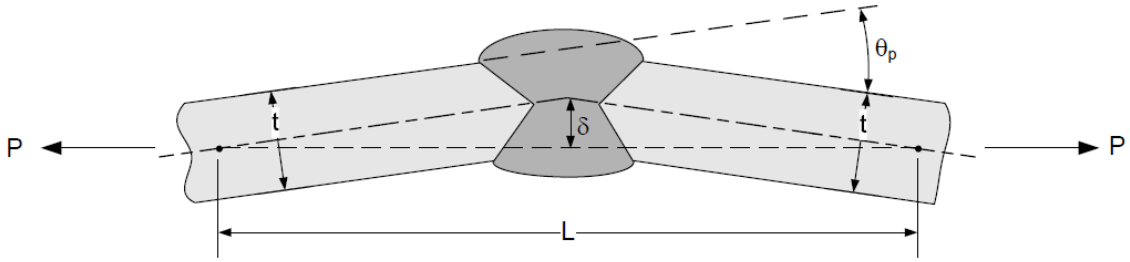

Figure 14-22 Angular Misalignment of Butt Weld Joints in Flat Plates

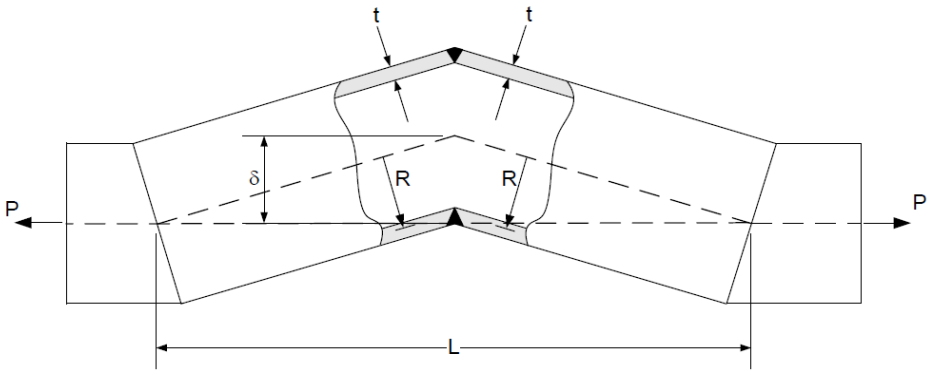

Figure 14-23 Definition of Dimension L in Figure 14-22

The calculated value for R_b^{pc}, the adjustment factor for centerline misalignment, for a range of offsets is shown in Figure 14-24.

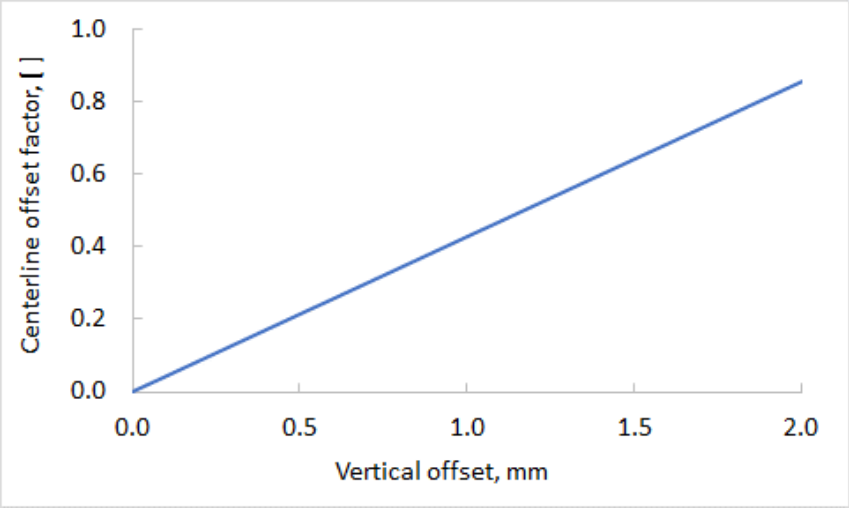

Figure 14-24 Adjustment Factor for Centerline Misalignment

The calculated value for R_b^{pa}, the adjustment factor for angular misalignment, for a range of angles is shown in Figure 14-25. For the purposes of the example, the sum of the supplemental loads is taken to be 200 MPa.

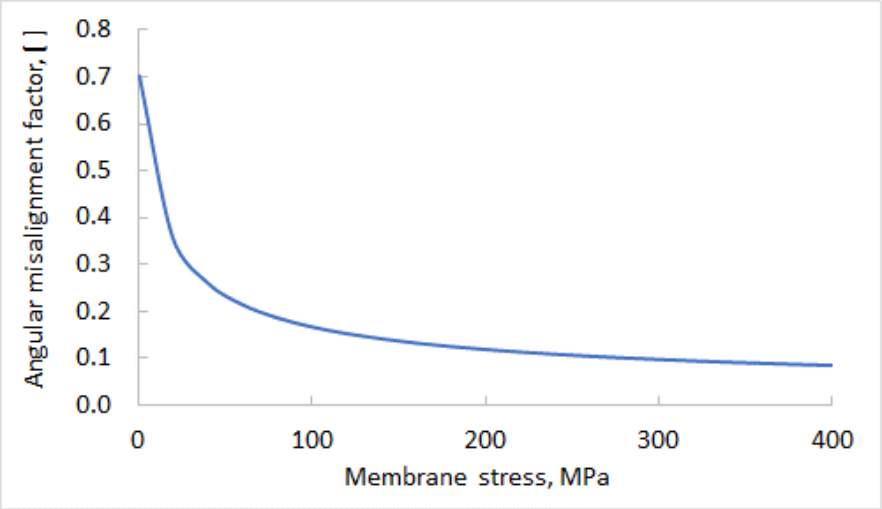

Figure 14-25 Adjustment Factor for Angular Misalignment

Representative Misalignment Factors

The centerline offsets and the angular misalignments in the tank in a commercial project likely span a fairly broad, and perhaps random, set of values. For the purposes of this discussion, the minimum centerline offset between adjacent plates is judged to be not less than 0.5 mm (1/64 in.). This is particularly so if the plate, as delivered, 1) deviates from flat by the maximum allowable value of 14 mm, and 2) the plate must be mechanically pushed flat against the foundation prior to welding. If the centerline offset is 0.5 mm, then the fatigue adjustment factor is on the order of 0.2.

Defining an angular misalignment is somewhat more problematic. With the plates arranged on the foundation, prior to welding, the angular misalignment should be zero. To start the welding process, the plates are tack-welded to one another, but this should not influence the angular misalignment. However, when Plate 1 is welded to Plate 2, the two plates start to form a domed shape. If the height of the dome, after welding, is 100 mm (see Section 14.5.2), then the out-of-plane angle at the edge of the plate is approximately $\tan^{-1}$(100 mm/1,250 mm) = 4.5 degrees, where 1,250 mm represents one-half of the width of the plate. When the tank is initially filled with salt, hydrostatic loads push the plates flat against the foundation. The bending stresses at the edges of the plates are equal to, or somewhat higher, than the yield stress. As such, most of the 4.5 degree angular misalignment disappears. However, some residual value of the stress will remain, which will retain some level of bending displacement at the edge. For purposes of the discussion, the residual bending misalignment is taken to be 0.25 degrees. If the stresses in the floor are in the range of 100 to 200 MPa, then the value for the angular misalignment factor is approximately 0.15.

With these representative factors, the weld fatigue strength reduction factor selected above in the Section titled *Weld Surface Fatigue* Strength Reduction Factors is further multiplied by a factor of (1 + 0.2 + 0.15) = 1.35. This would result in composite reduction factors in the range of 1.35 * 2.5 = 3.4 to 1.35 * 4.0 = 5.4.

It can be noted that increasing the thickness of the floor reduces the centerline offset misalignment factor (assuming that the vertical offset is maintained at 0.5 mm). However, the angular misalignment factor remains unchanged with a thicker floor.

Fatigue Strength Knockdown Factors

For areas not adjacent to welds, the fatigue life of commercial equipment is likely to be shorter than the fatigue life measured in smooth bar tests. The effect on the fatigue life, in areas not adjacent to welds, can be estimated using fatigue life knockdown factors. Several of these factors are outlined in Table 14-5. Unlike the fatigue strength reduction factors discussed in the sections above, the knockdown factor is a divisor on the smooth bar fatigue life, rather than a multiplier on the alternating stress.

The size effect factor accounts for equipment which has larger dimensions, and therefore has a shorter fatigue life, than the small samples typically used to develop fatigue data. Similarly, the surface finish effect accounts for equipment surfaces which are rougher, and therefore

have a shorter fatigue life, than smooth far samples. The data scatter factor accounts for the statistical nature of the smooth bar fatigue curves, and provides a degree of conservatism in the estimated life of the commercial equipment. Environmental effects are discussed below in the Section 14.15.2.

Table 14-5 Fatigue Life Knockdown Factors

Item	ASME	PVRC Working Group on S-N Data		PVRC Working Group on Evaluation Methods	
		Best Estimate Of Margin Needed	Conservative Estimate Of Margin Needed	Best Estimate Of Margin Needed	Conservative Estimate Of Margin Needed
Size Effect	2.5	1	1.2	1.0	1.2
Surface Finish	4 (1)	1.5	2	1.0	1.5
Data Scatter	2	2	2.5	2.0	2.5
Environmental Effects	4 (1)	2.5	4	---	---
Loading time history Effects	NC	1	1	1.0	2.5
Multi-Axial Stress Field	---	---	---	1.0	1.3
Sum	20	7.5	24	2.0	14.6

Notes:
1. Surface finish and environmental combined with a margin of 4.
2. From WRC 487, Table 1.

Using the factors in the column labeled ASME results, and an allowance for a surface finish factor of 1.5, results in an overall knockdown factor of 2.5 * 1.5 * 2 = 7.5.

14.15.2 Corrosion Assessment

Stainless steel, when exposed to salt, develops an outer corrosion layer. The layer consists of various nickel and iron oxides. The corrosion layer controls the principal corrosion mechanism for stainless steel, which is the diffusion of chromium from the metal into the salt.

In corrosion studies conducted at Sandia and at other laboratories, the corrosion coupons are typically free of internal and external stresses. However, under cyclic conditions, corrosion layers can develop when the material is at a high temperature and under compressive stress. During the balance of the cycle, the material can cool and the compressive stress can switch to a tensile stress. This can form microcracks in the oxide layer, which expose the parent material to an accelerated corrosion rate due to thinning, or the local removal, of the oxide layer.

This corrosion mechanism could occur in the floor of a hot tank due to a combination of 1) receiver start and stop cycles, 2) daily reversals in friction direction, and 3) changes in the stresses due to changes in the radial temperature gradient. If the floor is operating at stresses above than the yield stress, then the associated strains could be large enough to damage the outer oxide layer. This could change the shape of the corrosion rate-versus-time curve from parabolic (desired) to linear (not desired).

In general, the magnitude of this potential effect is largely unknown. Only after one or more commercial tanks have been in service for several years, and the inner surfaces examined for signs of non-uniform corrosion layers, can some form of an assessment be made.

14.15.3 Creep Assessment

WRC Bulletin 541

The Welding Research Council publishes Bulletin 541, Evaluation of Material Strength Data for Use in API Standard 530. Standard 530, in turn, is the Calculation of Heater-tube Thickness in Petroleum Refineries. The methods described in Bulletin 541 optimize the Larson-Miller Parameter (LMP) stress-rupture coefficients of the materials listed in API Standard 530.

The time to rupture, L [hours], is estimated by the following equation:

$$log_{10}[L] = \frac{LMP(\sigma)}{T} - C_{LMP}$$

where LMP is the Larson Miller parameter corresponding to the applied stress
σ is the applied stress, MPa
T is the absolute temperature, °K
C_{LMP} is a constant for the material, []

The stresses associated with times to rupture in the range of 1,000 hours to 1,000,000 hours are shown in Figure 14-26. The nominal life of the hot salt tank is 30 years, or 300,000 hours. The associated stress for both Type 316 / 316H and Type 347 H is a nominal 134 MPa.

To a first order, any permanent stress in the tank cannot exceed a value of 134 MPa; otherwise, that portion of the tank can fail due to rupture.

Project Omega

The assessment techniques developed under the Materials Properties Council (MPC) Project Omega program provide a method for estimating the remaining life of a component operating in the creep regime. A strain-rate parameter and multi-axial damage parameter (Omega) are used to predict the rate of strain accumulation, creep damage accumulation, and remaining time to failure as a function of stress state and temperature.

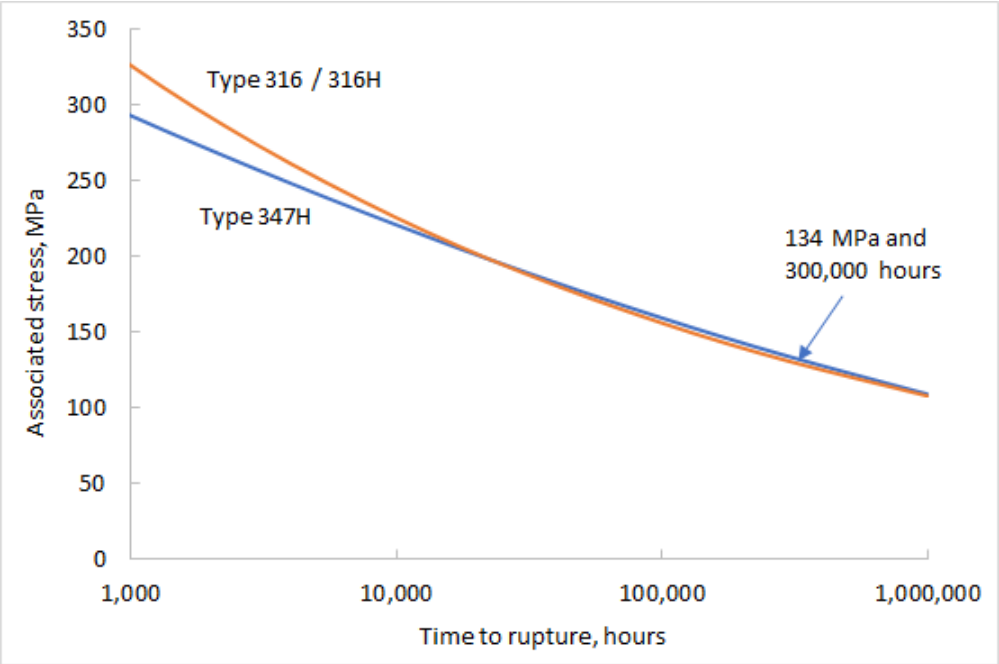

Figure 14-26 Bulletin 541 Time to Rupture and Stress For Type 316/316H and Type 347H

The equations are presented in Annex 10B - Material Data for Creep Analysis (Normative) in API 579-1 / ASME FFS-1. Equation coefficients for Type 347H are listed in Table 10B.1M, MPC Project Omega Creep Data (MPa, °C).

The stresses associated with times to rupture in the range of 1,000 hours to 1,000,000 hours are shown in Figure 14-27. With a creep rupture life of 300,000 hours, the associated stress for Type 347 H is a nominal value of 127 MPa.

The permanent stress in the tank cannot exceed a value of 127 MPa if the creep rupture life is to exceed 30 years.

14.15.4 Subset of Creep Assessment in Weld Regions

The coefficients for the Larson Miller equation (LMP(α), C_{LMP}) in WRC Bulletin 541 and in Project Omega are based on materials in the as-received condition; i.e., prior to welding. The value for C_{LMP} is typically taken as a constant for the material.

The value for C_{LMP} is obtained by plotting experimental creep data in log(time [hours]) versus 1/(Absolute Temperature[K]). An example for an austenitic stainless steel is shown in Figure 14-28 [32].

[32] Ghatak, A., and Robi, P. S. (Department of Mechanical Engineering, North Eastern Regional Institute of Science and Technology, Nirjuli, India), Modification of Larson–Miller Parameter Technique for Predicting Creep Life of Materials, Transactions of the Indian Institute of Metals, DOI 10.1007/s12666-015-0803-6, December 2015

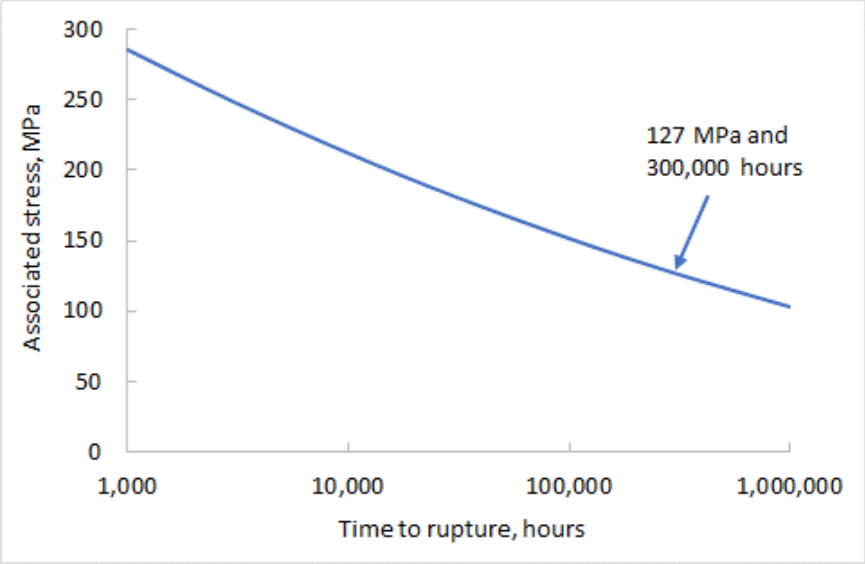

Figure 14-27 Project Omega Time to Rupture and Associated Stress For Type 347H

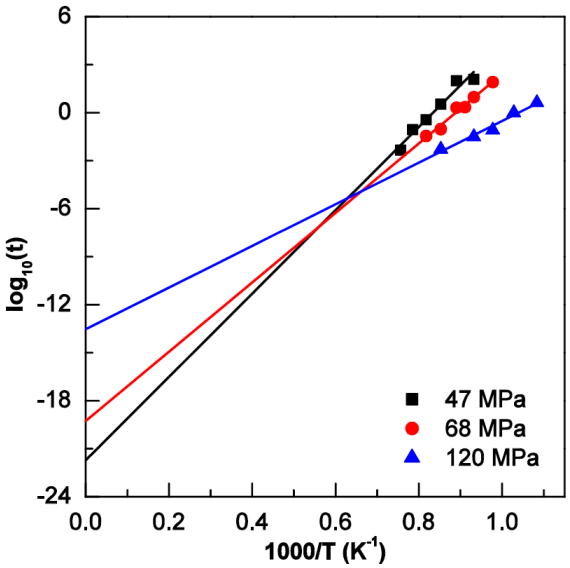

Figure 14-28 Graphical Calculation of Larson Miller Coefficient C_{LMP}

As noted in the Figure, the value for C_{LMP} is not a constant; it is a function of the applied stress.

During welding, residual stresses are developed in the weld region. The stresses are a function of the weld filler material, the heat input to the weld, the number of passes, and the location in the weld zone. The last item incorporates the fusion zone, the partially melted zone, and the heat affected zone.

The creep life will be a function of the sum of the operating stresses and the residual welding stresses. This implies that the Larson Miller coefficients will vary among the fusion zone, the partially melted zone, the heat affected zone, and the zones which are not welded. Further complicating the calculation of the creep life is the expected relaxation of the residual welding stresses over time, as shown in Table 14-1 Stress Relief as a Function of Temperature.

To account for the variation in C_{LMP} with stress, the authors in the referenced paper propose the following modified equation to estimate the creep lifetime:

$$log_{10}[L] = \frac{LMP(\sigma)}{T} - C_{LMP1} - C_{LMP2}\sigma$$

where LMP is the Larson Miller parameter corresponding to the applied stress
σ is the applied stress, MPa
T is the absolute temperature, °K
C_{LMP1} and C_{LMP2} are constants for the material, []

Ideally, different values for LMP(σ), C_{LMP1}, and C_{LMP2} would be developed for the fusion zone, the partially melted zone, the heat affected zone, and the zones which are not welded. However, the degree to which the ideal can be approached has yet to be determined. Specifically, the various coefficients are developed experimentally. Further, the accuracies of the coefficients are improved if the experiments are conducted at temperature representative of a commercial project; i.e., 600 °C. However, at these temperatures, creep lifetimes can be the order of tens of years if the stresses are modest (< 150 MPa). As a result, the uncertainties in the estimates of creep lifetime, particularly in the weld zones, are likely to remain high for at least the next generation of commercial projects.

14.15.5 Subset of Creep Assessment in Buckled Regions

In several commercial projects, the tank floors have developed buckles, with the buckles largely spanning the diameter of the tank. For the purposes of discussion, the thickness of the floor is taken to be 7 mm, and the inner radius of the plate at the top of the buckle is assumed to be 50 mm. Bending the floor in this shape generates a tensile strain of 0.065 on the top surface of the buckle, and a compressive strain of - 0.065 on the bottom surface of the buckle.

Using information from Section VIII, Division 2, Annex 3.D, for 300-series stainless steel at a temperature of 565 °C, a strain of 0.065 represents a true stress of approximately 260 MPa, as shown in Figure 14-29. The true stress and the true strain values include the effect of strain hardening.

It should be noted that the equations in Annex 3.D are applicable only for temperatures up to 482 °C. As such, the calculated stress of 260 MPa likely incurs some error. However, for the purposes of the discussion, the estimated stress should be the correct order of magnitude.

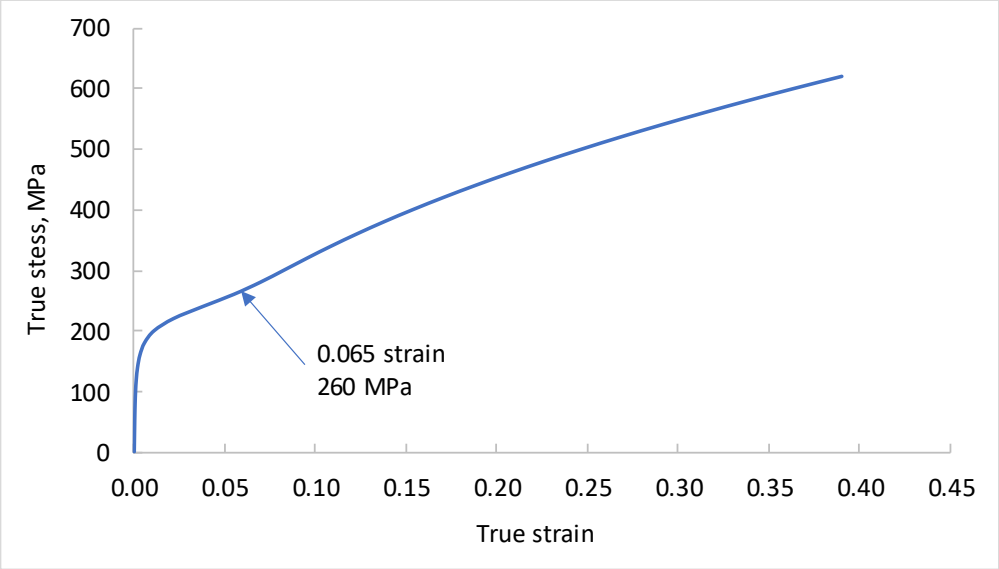

Figure 14-29 True Stress as a Function of True Strain for Type 347H at 565 °C

The inventory temperatures during commercial operation are well below the temperatures at which significant stress relaxation occurs (800 to 900 °C). As such, the calculated stress of 260 MPa is likely to persist for the life of the tank.

Using information for Larson Miller parameters from API 579-1 / ASME FFS-1, Table 10B.4M, the creep life as a function of stress for Type 347H at 565 °C can be calculated, as shown in Figure 14-30.

The calculated time to rupture is only several months if the tank is always operating at a temperature of 565 °C. However, in commercial projects, the temperature of the inventory is typically less than 565 °C due to the following effects:

- During overnight hold periods, the inventory level is typically low, and the temperature of the tank can decay by values in the range of 5 to 10 °C
- During receiver startup, salt is introduced into the tank at temperatures in the range of 500 to 565 °C.

If the annual average inventory temperature is 520 °C, rather than 565 °C, then the estimated creep life increases to some 26,000 hours. This period is a nominal 3 years, which is roughly consistent with the crack development times experienced at commercial projects.

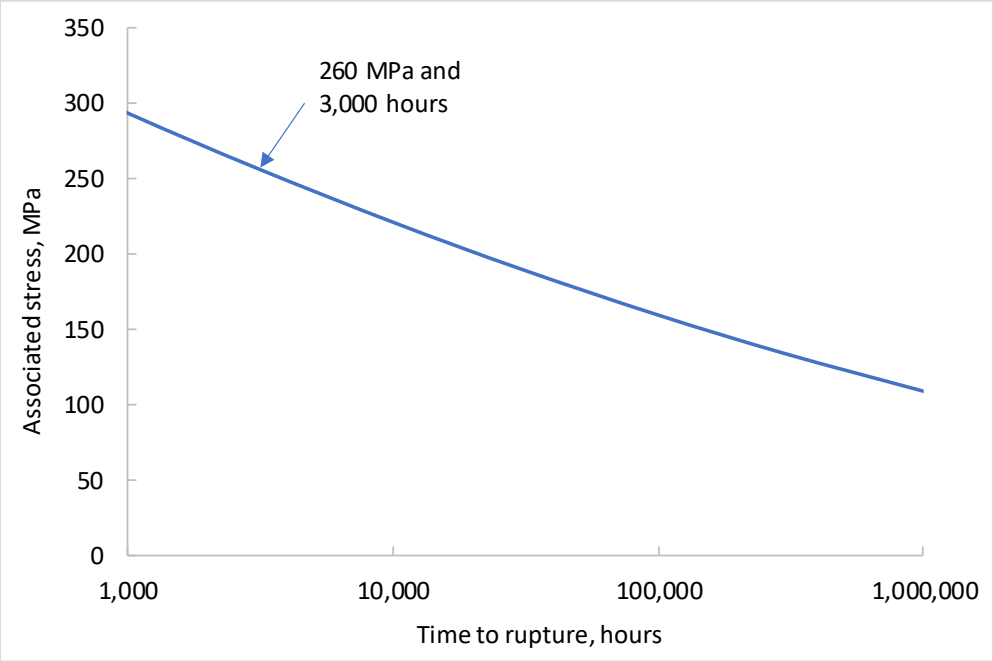

Figure 14-30 Time to Rupture as a Function of Stress for Type 347H at 565 °C

Clearly, the above calculations are only a zeroth-order analysis. The shape and the dimensions of the floor buckles in commercial projects, if present, are unique to each project. Further, the stresses in the buckled regions are also influenced by friction forces, thermal stresses generated by radial temperature gradients, and bending loads produced by hydrostatic loads. As such, it is difficult to accurately predict the creep life of a buckled region in the floor. Nonetheless, if the required creep life of the floor is 300,000 hours (30 years), then the stresses in the floor must be limited to about 127 MPa, as noted above in Section 14.15.3. A stress of 127 MPa is produced by a strain of 0.0015, which would be produced by a 'buckle' with a radius of about 2,400 mm. This represents a rather gentle curvature in the floor, which implies that even small permanent deformations of the floor could result in a creep life less than required.

14.15.6 Creep Assessment with Consideration of Residual Welding Stresses

Estimates of creep lifetimes can be developed using the methods outlined in Section 14.15.3; i.e., WRC Bulletin 541 and Project Omega. The coefficients in the equations are typically generated for materials as supplied from the mills; i.e., prior to cutting, fabrication, or welding.

When the floor plates are welded using the standard 347 filler material (E347-16 for SMAW, or ER347 for GTAW), residual welding stresses can reach peak values in the range of 350 to 500 MPa [33]. These values fall between the yield stress and the rupture limit at ambient temperature.

[33] Osorio, J. (National Renewable Energy Laboratory, Golden, Colorado), Failure Analysis for Molten Salt Thermal Energy Tanks for In-Service CSP Plants, DOE Award Number DE-EE00038475

It can be noted that different weld fillers are being investigated as an alternative to 347 to reduce residual stresses in this application. A common choice is ER16-8-2, which is often termed a lean austenitic. The principal benefit to ER16-8-2, compared with 347, is an increase in ductility, which allows a portion of the residual welding stresses to relax. However, qualifying filler materials can involve months to years of laboratory testing to verify the long term mechanical, corrosion, and chemical properties.

With a stress of 500 MPa, the estimated time to rupture for Type 347H stainless steel at a temperature of 25 °C is billions of years.

During preheating, the temperature of the tank is raised to approximately 300 °C. With a stress of 500 MPa, the creep life is reduced, but it is still in the range of thousands of years.

During commissioning, the temperature of the tank first reaches its design value of 565°C. With a stress of 500 MPa, the creep life is predicted to be only 5 hours. Clearly, tanks in commercial service have creep lifetimes longer than 5 hours, which means that a significant level of stress relaxation is occurring between the end of fabrication and the start of commercial service.

14.15.7 Relaxation of Residual Stresses Prior to Tank Commissioning

Tanks in commercial service are exhibiting lifetimes of at least 3 years. The sources of the failures are many and varied. Nonetheless, it is apparent that the creep life must exceed 3 years, as the tank failures to date are showing failure mechanisms other than creep.

As a bounding exercise, for Type 347H stainless steel at a temperature of 565 °C, the stress cannot exceed 200 MPa if the material is to reach a creep life of 26,000 hours (3 years). This implies that some form of stress relaxation is occurring, early in the commercial life of the tank, which reduces the peak stress by a nominal 60 percent; i.e., from 500 MPa to 200 MPa.

Residual stresses can be relaxed by thermal mechanisms, mechanical mechanisms, or a combination of the two.

Thermal Mechanisms

An increase in the metal temperature results in a decrease in the yield stress. When the yield stress decreases to the residual stress, the material plastically deforms. This, in turn, relieves a portion of the residual strain and relieves a portion of the associated stress. The degree of stress relaxation is a function of temperature and time, with the former the principal determinant.

The largest degree of relaxation occurs during solution annealing, when the metal is heated to about 1,050 °C. The residual stresses are reduced by some 95 percent; i.e., from 500 MPa to 25 MPa [34]. However, prior to the start of commercial service, tank temperatures are limited to

[34] Peckner, D. and Bernstein, I., Handbook of Stainless Steel, Chapter 4, Table 25, ISBN 0-07049147-X, 1977

a nominal 300 °C during preheating and initial filling. At 300 °C, the material undergoes only stress relief, and relaxation of the residual stresses is limited to about 30 percent (from 500 MPa to 350 MPa).

At a temperature of 300 °C, and at a stress of 350 MPa, the creep life is measured in billions of hours. As such, any creep damage which occurs during preheating can safely be ignored.

During commissioning, the temperature of the tank is raised from the preheat value of 300 °C to the design value of 565 °C. At a temperature of 565 °C, and at a stress of 350 MPa, the creep life is only 200 hours. Since the tanks in commercial projects are not suffering creep failures at 200 hours, additional relaxation of the residual stresses must be occurring during the heating period from 300 °C to 565 °C.

At temperatures in the range of 550 to 650 °C, the degree of stress relief is on the order of 35 percent. This implies that the peak residual stress is reduced to approximately 230 MPa (i.e., 0.65 * 350 MPa) at the start of commercial service. At a temperature of 565 °C, and at a stress of 230 MPa, the creep life is on the order of 7,000 hours. As above, the tanks are not suffering failures due to creep in the first year of service, and additional relaxation of residual stresses must be occurring before the start of commercial service.

Mechanical Mechanisms

Cyclic loading is a known mechanism for reducing residual stresses.

Late in the tank fabrication process, the floor is welded to the wall. The wall has a radial and a circumferential stiffness that is several orders of magnitude greater than the radial and tangential stiffness of the floor.

The tank, after fabrication but prior to preheating, undergoes some number of daily temperature cycles due to solar heating and nighttime cooling. The temperature of the wall will be out of phase with the temperature of the floor because 1) the heat transfer rate from the wall to the floor is low, and 2) the thermal inertia of the foundation, relative to thermal inertia of the wall, is essentially infinite. As such, the wall will place the floor into a number of compression and tension cycles, with a total of perhaps 100 to 200 cycles, depending on the project schedule. Some level of stress relief can be expected, but developing an accurate estimate is still likely to involve large uncertainties.

Summary

As noted above, commercial tanks have a creep life in excess of 26,000 hours. To achieve this life, the sum of the operating stresses and the residual stresses must be reduced from 230 MPa at the start of commercial service to values no higher than 200 MPa soon after the start of commercial service.

There is some combination of thermal and mechanical mechanisms, as yet undefined, which are at work to reduce the stress. Deciphering these mechanisms, and quantifying their effects, will be an important element in predicting the creep lifetime of the tank.

14.15.8 Required Relaxation of Residual Stresses to Achieve a 30-Year Creep Life

The tank has a design life of 25 to 30 years, which corresponds to 220,000 to 260,000 hours. Due to a range of uncertainties in the estimates of the operating and the residual stresses, a case could be made for some level of conservatism in the calculation of the creep life. As a point of departure, a design life of 300,000 hours could be adopted. At 565 °C, the corresponding allowable stress is 135 MPa.

For a commercial-size tank (35+ m diameter), the operating stresses, exclusive of residual stresses, are already in the range of 100 to 125 MPa. This implies that the residual stresses must be reduced by 75 to 90 percent to reach a creep life of 300,000 hours. However, as noted above, the degree of stress relief early in commercial service is only about 50 percent. Potential, and in some cases only partial, solutions to the problem of stress relief are outlined below.

Comprehensive Approach to Stress Relief

A post weld heat treatment on the tank, at the solution annealing temperature of 1,050 C, will almost completely remove the residual stresses (approximately 25 MPa remaining).

Practically speaking, solution annealing at a temperature of 1,050 °C, while maintaining the integrity of the tank shell, will be a challenging task. As outlined in the Code, it is preferable to heat the entire vessel in a closed furnace. However, this is not feasible for a large structure such as a tank, and alternative methods must be considered. The tank must either be internally heated, or different parts heated separately before joining, followed by local heat treatment of the remaining joints. In either case, the shell must be protected from damaging thermal gradients throughout the heating and cooling process.

Heat treatment of the wall may be relatively straightforward, as there are specialty contractors for this work. Nonetheless, the strength of the material at the annealing temperature will be quite low, and the wall may need to be temporarily reinforced to prevent plastic deformations.

The more problematic element is the floor. Achieving the required heating rates, the hold times, and the cooling rates may not be feasible due to the presence of the foundation. However, if the floor is elevated during fabrication, the heat treatment process is considerably more practical. Also, with the floor elevated, welding can be conducted from both above and below, which 1) eliminates the need for backing strips, and 2) reduces the heat input to the welds and the associated residual stresses.

It can be noted that in tanks designed to API 650 requirements, the principal function of the floor is to form a liquid boundary; i.e., it is not intended as a structural element. If welding results in changes to the metal chemistry, or the development of residual stresses, these

conditions are unlikely to affect the primary function of the floor. As such, post weld heat treating of the floor is not normally performed.

Conceptually, the post weld heat treatment of the wall and the floor might consist of the following steps:

1. The floor, in an elevated position, is welded, and local post weld heat treatments are conducted as the welds are completed. The process would be similar to the post weld heat treatment of pipe welds. (It should be noted that a successful local or global post weld heat treatment is not guaranteed. Stainless steels typically have sufficient uniaxial ductility to accommodate the plastic strains associated with stress relaxation. However, if the material is constrained, as it would be at the edges of adjoining plates, then strains can develop in multiple axes of the heat affected zones. Stainless steels with a high carbon content have a multiaxial failure ductility as low as 1 percent. The creep strain that occurs during the relaxation of the weld residual stresses could be sufficiently large to exceed the multiaxial failure ductility, and cracks could develop in the weld zone.)

2. The bottom course of the wall is assembled and welded.

3. The perimeter of the floor is welded to the bottom of the wall.

4. A post weld heat treatment is conducted on the bottom course. The heat treatment would incorporate the thick fillet weld connecting the floor to the bottom of the wall.

Heat treating the bottom course thermally expands the wall, which places the floor into tension. As long as the wall and the floor remain in the elastic range, then no new residual stresses will be imposed on the floor.

Approach to Partial Stress Relief

If solution annealing is impractical, it may be possible to achieve a sufficient degree of stress relief by heating the tank to an intermediate temperature, and then holding the tank at this temperature for an extended period.

The intermediate temperature should be one which reduces the yield strength as far as possible, but does not result in fundamental changes to the metal chemistry. For Type 347H stainless steel, a representative value might be 625 °C.

The preheating period for an empty tank (ambient to 300 °C) is nominally 30 days. In principle, the preheating temperature could be extended to 625 °C, and the preheating period could be extended to, as an example, 60 days.

An engineering analysis could be conducted to determine the optimum combination of temperature, time, degree of stress relief, and preheating cost.

Methods to Increase the Creep Life

One method for increasing the creep life is to reduce the tank temperature. For the purpose of the discussion, the tank design temperature is assumed to be reduced by 50 °C from the typical commercial value of 565 °C to a new value of 515 °C. With a creep life of 300,000 hours, the allowable stress increases to 200 MPa. If the operating stress, through careful tank design and process control, can be limited to 100 MPa, then the allowable residual stress can be 200 MPa - 100 MPa = 100 MPa. This, in turn, requires a stress relief of (230 MPa - 100 MPa) / 230 MPa = 55 percent. However, at a temperature of 515 °C, a stress relief of 55 percent is not assured, and the approach constitutes only a partial solution.

An alternate approach for increasing the creep life is to reduce both the tank design temperature and the design life. This necessarily requires the fabrication of replacement tanks during the project. For the purposes of the discussion, the design temperature is set to 515 °C and the design life is set to 10 years (100,000 hours). The allowable stress increases to 230 MPa. If the operating stress can be limited to 100 MPa, then the allowable residual stress can be 230 MPa - 100 MPa = 130 MPa. This, in turn, requires a stress relief of (230 MPa - 130 MPa) / 230 MPa = 40 percent. At a temperature of 515 °C, a stress relief of 40 percent cannot be guaranteed, and this approach only constitutes a partial solution.

Summary Observations

The estimates above of allowable residual stresses is only approximate because a full understanding of the operating stresses, and the degree of stress relief, in commercial tanks are not fully understood. Nonetheless, it is clear that sum of the operating stresses and the residual stresses could well exceed the allowable stresses associated with a creep life of 30 years. At some point, the solar industry may decide that some form of stress relief must be conducted if the tank is to achieve a creep life of 30 years.

14.15.9 Code Interpretation of Residual Stresses

The creep life is a function of the material, the temperature, and the stress. The last item includes operating stresses due to temperature gradients (self-restraint) and due to friction. However, the Code is somewhat ambiguous regarding the use of residual stresses in the creep analyses.

A review of Fitness-for-Service API 579-1 / ASME FFS-1 shows the following:

PART 9 - ASSESSMENT OF CRACK-LIKE FLAWS
ANNEX 9D - RESIDUAL STRESSES IN A FITNESS-FOR-SERVICE EVALUATION

9D.4.1 Post Weld Heat Treatment

If the type of PWHT cannot be established, the residual stress distribution for the as-welded condition shall be used in the assessment. If the weld joint is in a component operating in the

creep range (i.e. long-term operation), then the residual stress based on the PWHT condition may be used in the assessment.

PART 10 – ASSESSMENT OF COMPONENTS OPERATING IN THE CREEP RANGE

10.4.2.1 The Level 1 assessment for a component subject to a single design or operating condition in the creep range is provided below.
a) STEP 1 – Determine the maximum operating temperature, pressure, and service time the component is subject to. If the component contains a weld joint that is loaded in the stress direction that governs the minimum required wall thickness calculation, then 14ºC (25ºF) shall be added to the maximum operating temperature to determine the assessment temperature. Otherwise, the assessment temperature is the maximum operating temperature.

PART 14 - ASSESSMENT OF FATIGUE DAMAGE

14.8.3 Loading Time History
The loading time history showing the historical and assumed future start-up, normal, upset, and shut-down conditions should be reported. In addition, any additional loads and stresses considered in the assessment, e.g. stresses from supplement loads, thermal gradients and residual stresses.

PART 14 - ASSESSMENT OF FATIGUE DAMAGE

10.5.1.4 A sensitivity analysis should be performed as part of the assessment regardless of the method chosen.
b) Remaining life estimates in the creep range are sensitive to materials data, applied stresses, and corresponding temperature. Therefore, sensitivity studies should be performed to evaluate the interaction of these variables in regards to the remaining life prediction.

Summary Observations

The Fitness-for-Service Code provides some guidance regarding the use of residual welding stresses in the calculation of creep life. However, the texts in Parts 9 and 14 use terms such as 'may' and 'should', and as such, are not mandatory requirements. However, in Part 10, the term 'shall' is used. Nonetheless, adding 14 °C to the design temperature to account for creep damage may, or may not, result in an accurate lifetime assessment.

Operating stresses in the floor, due to temperature gradients and due to friction, are likely in the range of 100 to 125 MPa. For a 30-year tank life, the allowable creep stress is on the order of 130 MPa. This implies that residual stresses associated with welding must be quite low.

The Code is not specific regarding a mandatory requirement to include residual stresses in the assessment of creep. Nonetheless, it is clear that residual stresses must be included if the creep evaluation is to be accurate. As a minimum, the allowable residual stress will point to the degree of stress relief required to reach a 30-year tank life. To this end, a requirement to

include residual stresses, even if not mandated by the Code, should be included in the tank procurement specification.

14.15.10 Combined Fatigue and Creep Damage

A common approach to estimating the cumulative effect of successive fatigue cycles is Miner's Rule [35]. The approach is based on the following assumptions:

- The damage accumulated by the material during each cycle is a function only of the stress, σ
- For n cycles, the damage (or fraction of fatigue life) at the specified stress is

$$d = \frac{n}{N}$$

  where N is the number of cycles to the failure at the stress level σ.

- The damages, d_i, are added linearly, as follows:

$$D = \sum_{i=1}^{k} d_i = \sum_{i} \frac{n_i}{N_i}$$

- It is assumed that damage accumulates without the influence of one level on another. In this case, failure occurs when:

$$D = \sum_{i} \frac{n_i}{N_i} = 1$$

A similar approach can be used to estimate the cumulative effect of creep damage, with cycles (n) replaced by time (t).

As might be expected, the accumulation of fatigue damage reduces the ability of the material to accommodate creep damage. Allowable combinations of fatigue damage in conjunction with creep damage, for stainless steel and two ferritic steels, are shown in Figure 14-31.

14.15.11 Preliminary Lifetime Assessment

The sections above discuss methods for assessing the fatigue, the corrosion, and the creep lifetimes of the tank. However, quantitative assessments are not presented, as the calculation of stresses (steady state, transient, and cyclic) are beyond the scope of the Design Basis study.

[35] Lalanne, Christian, "Fatigue Damage, Mechanical Vibration and Shock Analysis, Third edition - Volume 4", Library of Congress Control Number 2014933740,ISTE Ltd and John Wiley & Sons, 2014

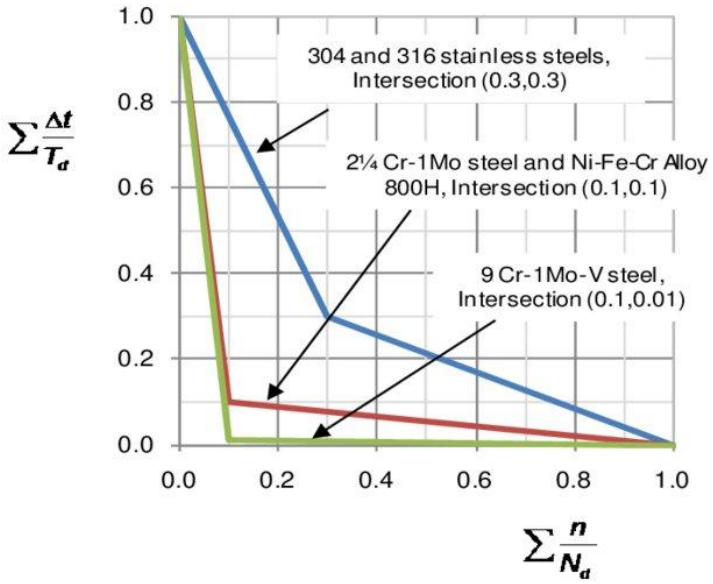

Figure 14-31 Allowable Combinations of Fatigue and Creep Damage

As a surrogate, representative values for the stresses have been developed from a Federal laboratory study evaluating the low cycle fatigue life of hot salt tanks [36]. Inputs to the computational fluid dynamics model are based on operating data from Crescent Dunes on the following parameters, each as a function of time:

- Downcomer flow rate and temperature
- Hot salt flow rate to the steam generator
- Inventory temperature and level.

Calculations of the floor temperatures, and the associated floor stresses, were developed for 3 representative days: clear; partly-cloudy; and intermittent clouds. The cycle of days are assumed to repeat, until a period of 30 years is reached.

Estimates of the cumulative fatigue damage, and the cumulative creep damage, were developed using the methods presented in ASME Section III, Division 1, Subsection NH and in API 579-1 / ASME FFS-1.

For floor radii between 0 and 75 percent of the tank radius, the creep and fatigue damage results are shown in Figure 14-32. For floor radii between 93 and 100 percent of the tank radius, the results are shown in Figure 14-33. In both figures, the combined fatigue and creep damage should remain beneath the limits defined by the red and the blue lines.

[36] Osorio, J. (National Renewable Energy Laboratory, Golden, Colorado), Failure Analysis for Molten Salt Thermal Energy Tanks for In-Service CSP Plants, DOE Award Number DE-EE00038475

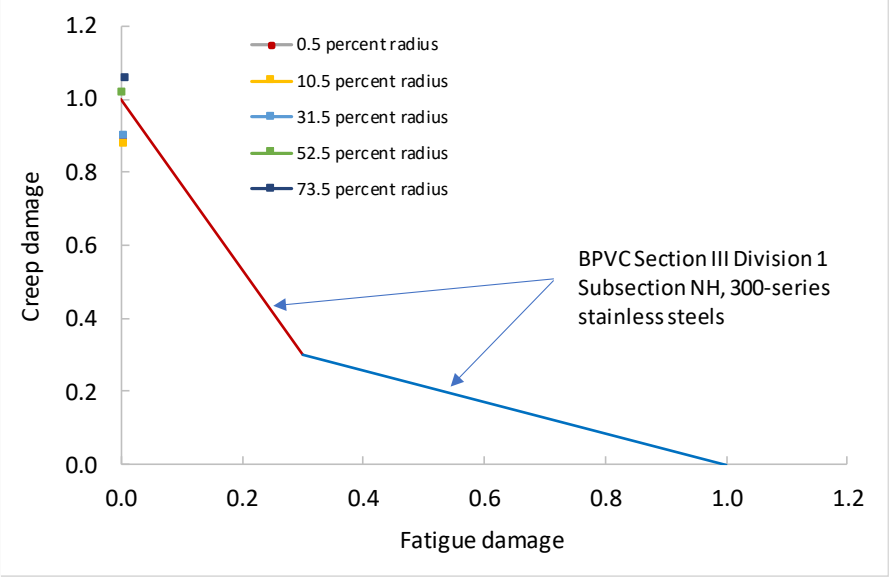

Figure 14-32 Combined Creep and Fatigue Damage for Tank Radii Less than 75 Percent

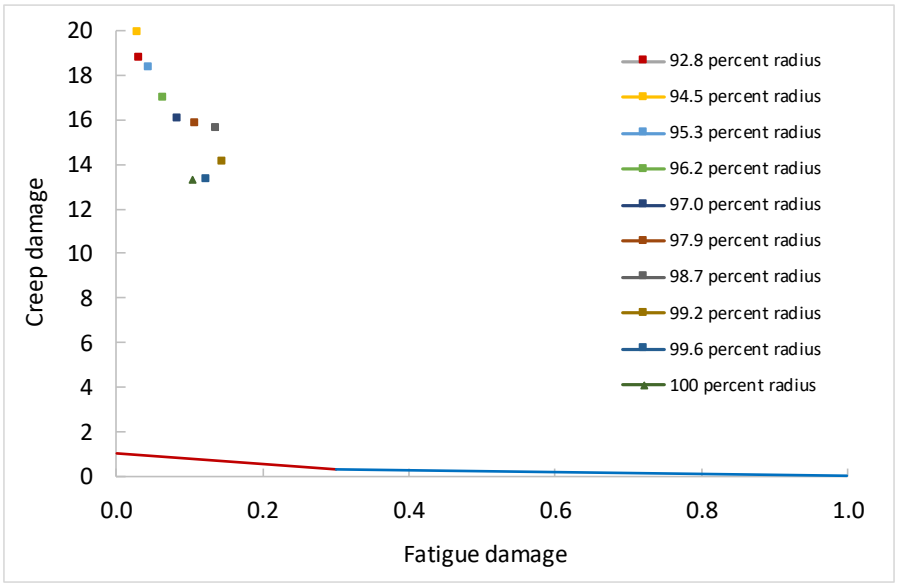

Figure 14-33 Combined Creep and Fatigue Damage for Tank Radii Greater than 93 Percent

For floor locations between 0 and 75 percent of the tank radius, the fatigue damage is minor; perhaps 1 percent of the allowable damage. Creep damage is in the range of 90 to 105 percent of the allowable damage, and lifetimes of the floor at these locations are projected to last the duration of the project.

In contrast, for floor locations between 93 and 100 percent of the tank radius, the cumulative fatigue damage is in the range of 2 to 15 percent of the allowable value, while the cumulative

creep damage is a factor of 10 to 20 times the allowable value. A review of the calculated floor stresses from the CFD / FEA model show values that are routinely above the yield value. In general, stresses in this range are inconsistent with a multi-decade creep lifetime.

The floor stresses are likely the result of a combination of 1) friction loads, and 2) self-restraint due to thermal stresses generated by radial temperature gradients. The relative contributions of the two effects are not yet known. Methods to reduce the stress values may involve some combination of the following:

- Limits on the maximum coefficient of friction between the floor and the foundation; i.e., certain materials in contact with the floor may be excluded from design consideration

- Constraints on tank operating procedures; i.e., if the tank level is W m, if the inventory temperature is X °C, and if the downcomer flow rate is Y kg/sec, then the receiver outlet temperature cannot exceed Z °C.

14.16 Material Selection

14.16.1 Stabilized and Non-stabilized Stainless Steel

Non-stabilized Stainless Steel

The hot salt tank at the 10 MWe Solar Two demonstration project was fabricated from Type 304H stainless steel. The tank operated at temperatures above 538 °C (1,000 °F). As such, the Code required the use of an 'H' grade of stainless steel, with a carbon content of at least 0.04 percent, to provide the required resistance to creep. However, the H grades of stainless steel are susceptible to a failure mechanism known as intergranular stress corrosion cracking if the following four conditions are met simultaneously:

1. Sensitization. The stainless steel becomes sensitized when the carbon in the steel reacts with chromium to form chromium carbide. At temperatures above 500 °C, the time required to form the chromium carbide is measured in hours. The chromium carbide preferentially forms at the grain boundaries, as there is space in the matrix to do so. With the chromium depleted at the grain boundaries, the material is susceptible to corrosion at the grain boundaries.

2. Tensile stresses. Tensile stresses can arise due to process conditions, or due to residual welding stresses.

3. Chlorides. The nitrate salt, depending on the purity, contains chlorides in the range of 0.05 to 0.4 percent.

4. Liquid water. The water acts both as a transport mechanism for the chlorides and as an electrolyte.

If all of these conditions are present, then corrosion-induced cracks can develop at the junctions between grain boundaries, and the cracks can then progress along the grain boundaries due to the tensile stresses. Interestingly, once the cracks start to appear, removing the liquid water does not halt the progression of the cracking.

Project Locations Near the Coast

Coastal locations are subject to salt spray from the ocean. Fabricating a tank from an H-grade of a non-stabilized stainless steel carries the risk of the tank developing intergranular stress corrosion cracking during the fabrication process. To minimize this risk, the Owner may elect to fabricate the tank from a stabilized stainless steel, and then accept the risk of stress corrosion cracking developing at some future date. In all likelihood, the Owner would need to make regular payments to a fund, which would be used to finance the construction of a second tank at some point in the future. The cost of the periodic payments would be reflected in the financial model for the project.

Project Locations in the Desert

For plants in a desert location, the risk of intergranular stress corrosion cracking developing during the fabrication stage of a tank constructed from a non-stabilized stainless steel is small. In addition, once the tank enters normal operation, the potential for intergranular stress corrosion cracking is nil. The first three of the four conditions noted above are present, but the operating temperatures of the tank preclude the presence of liquid water.

Nonetheless, if the tank must be drained for maintenance, and if the tank cools to ambient temperature, then there is the possibility of liquid water forming inside the tank due to moisture condensing from the air. Were intergranular stress corrosion cracking to begin, there would be no mechanism to halt the progression. In the worst case condition, the tank would need to be condemned.

Stabilized Stainless Steel

One method for reducing the potential for intergranular stress corrosion cracking is to use a stabilized stainless steel. A stabilized steel adds niobium (Type 347) or titanium (Type 321) as an alloying element. In Type 347, the niobium bonds with the carbon to form niobium carbide; in Type 321, the titanium bonds with the carbon to form titanium carbide. Both carbides reduce the free carbon in the matrix, which reduces the potential for forming chromium carbide. This, in turn, reduces the potential for intergranular stress corrosion cracking.

The solar industry has essentially adopted Type 347H for the fabrication material for the tanks, piping, pumps, and heat exchangers on the hot side (> 450 °C) of central receiver projects. Type 347H also offers higher strength at elevated temperatures than Types 304H and 316H. The higher strength translates to lower fabrication masses, and potentially reduced costs. Nonetheless, Type 347H is not a complete solution to the problem of intergranular stress corrosion cracking, as follows:

- During welding, the metal temperatures are high enough to dissolve the niobium carbide. This releases free carbon back into the matrix. As the weld cools, equilibrium considerations lead to a combination of niobium carbide, chromium carbide, and free carbon, depending on time-at-temperature and cooling rates. A common result is the preferential formation of chromium carbide at the edges of the heat affected zone. This leaves two thin zones, on either side of the weld, which become susceptible to intergranular stress corrosion cracking. The phenomenon is known as knife line attack.

- A post weld heat treatment can be performed, which raises the metal temperature high enough to dissolve both the chromium carbide and the niobium carbide. The metal is then held for a defined period at a defined temperature, which leads to the preferential formation of niobium carbide. The weld is then cooled rapidly through the temperature which preferentially forms chromium carbide. The high cooling rates can be achieved on piping, but cannot be effected on the thick metal sections in tanks, pumps, and heat exchangers.

- Welds with high residual stresses can be susceptible to a failure mechanism known as stress relaxation cracking. High residual stresses can result from thick metal sections with multiple welding passes, or from thin metal sections with long continuous weld lengths. This topic, discussed below in Section 14.16.2, is inherent characteristic of using niobium as an alloying element.

As such, Type 347H can reduce the potential for, but cannot eliminate the possibility of, intergranular stress corrosion cracking. Further, Type 347H introduces potential failure mechanisms not inherent in Type 304H and Type 316H.

Alternative Material Options

An alternative material option recently identified in research studies is found in the European standard for pressurized vessels EN10028-7. This material is stainless steel 1.4910 (X3CrNiMoBN17-13-3), which has a maximum service temperature of 600 °C.

The closest material to 1.4910 in the ASME Boiler and Pressure Vessel Code is Type 316LN (16Cr–12Ni–2Mo–N), which has a maximum service temperature of 427 °C.

Compared to 316LN, 1.4910 includes a 20 percent higher nickel content and the addition of small amounts of boron, and as such, is referred to as Type 316LNB.

Boron is added to improve the creep properties of the material. Recent studies indicate Type 316LNB has higher allowable 100,000-hour creep rupture stresses than Type 347H at temperatures in the range of 500 to 600 °C [37], and it has similar corrosion properties in nitrate

[37] M. Oum et al., "Therma 4910 for molten salt storage tanks: Improved stress relaxation cracking and high temperature properties", SolarPACES 2022, Albuquerque, NM, USA

salts [38]. More importantly, there is no niobium in the alloy, which reduces the potential for stress relaxation cracking, as discussed in Section 14.16.2.

For these reasons Type 316LNB is considered a potential material candidate to replace Type 347H; however, alternative failure mechanisms for the new material must be considered. The addition of nitrogen and boron to the alloy must be fully evaluated before considering Type 316LNB as the solution to all metallurgical challenges in the hot tank. Further tests should be conducted on weld samples to determine if the material is susceptible to stress relaxation cracking or other cracking phenomena.

Material Selection for Commercial Projects

The Type 304H stainless steel hot tank at Solar Two operated without failure during its brief 3-year test and evaluation period. However, the tank was never drained, and was never cooled to ambient temperature, for maintenance or repair. Similarly, an internal inspection of the Type 347H stainless steel hot tank at Crescent Dunes showed no signs of cracking, corrosion, or weld failures. However, evidence of stress relaxation cracking has been observed in other commercial projects.

The solar industry, in effect, must choose among potential tank materials, none of which offers a perfect solution:

- Type 304H, and to a lesser extent Type 316H, avoid the potential for stress relaxation cracking due to the absence of niobium. However, the materials are susceptible to intergranular stress corrosion cracking should the tank be exposed to liquid water. As such, if the tank is drained, and then cooled to ambient temperature, then the tank must be exposed to only dry air, without the possibility of moisture condensing from the air. One approach to accomplish this is to introduce only dry air into the interior of the tank. However, moisture could still condense on the outside of the tank. A potential solution is to introduce only dry, and heated, air into the tank such that the metal temperatures never fall below the dew point. To what extent this can be guaranteed by the maintenance company is perhaps an open topic

- Various industries have considered Type 316H as a potential alloy, but the nuclear industry in the past decades have reported hundreds of stress relaxation cracking failures in advanced gas cooled reactors [39]. In general, Type 316H is argued to have high susceptibility to stress relaxation cracking based on various industry failures and lab scale testing

- Type 347H reduces the potential for intergranular stress corrosion cracking, but introduces the potential for stress relaxation cracking. The cracking mechanism is a

[38] A. Bonk et al., "Thermal Energy Storage using Solar Salt at 620°C: How a reactive gas atmosphere mitigates corrosion of structural materials", SolarPACES 2022, Albuquerque, NM, USA
[39] Pickle, T. (Colorado School of Mines, Golden, Colorado, USA), et al, Evaluation of Alternative Base Materials for Mitigation of Stress Relaxation Cracking in Thermal Energy Storage Tanks, SolarPACES 2024, 30th International Conference on Concentrating Solar Power, Thermal, and Chemical Energy Systems

function of the metal thickness, the number of welding passes, the stress distribution, and the time / temperature history of the tank. If the development rate of the cracking can be predicted with the necessary accuracy, then it might be possible to fabricate a tank in Year 0 of the project, and then fabricate a replacement tank to be placed into service in, for example, Year 10 of the project. However, if the development rate of the cracking cannot be predicted with the required certainty, then the project may be obligated to build two tanks in Year 0 in preparation for an expected failure at an undefined time.

14.16.2 Stress Relaxation Cracking in Type 347H

As noted above, adding niobium to stainless steel results in the beneficial formation of niobium carbide. If the parent metal was never welded, then the material properties would be compelling for use in a solar project. However, welding, and the subsequent chemical reactions, introduce a range of undesirable characteristics.

Source of Cracking

The 3 main contributing factors are 1) susceptible microstructure, 2) residual stresses, and 3) elevated temperature in creep dominated regimes [40].

Susceptible Microstructure

The metallurgical mechanism contributing to cracking is believed to be the non-homogeneous precipitation of niobium carbonitrides (Nb (C,N)) in the grain interiors and at the grain boundaries. The material, in the as-received condition, has typically received a stabilizing heat treatment to homogenize the precipitates in the solid solution alloy. However, welding the material 1) dissolves many of the precipitates, 2) coarsens the grain structure, and 3) imposes a set of residual stresses. In the grain interiors, precipitation of the niobium carbonitrides occurs during elevated temperature service, or during post weld heat treatment. The precipitation mechanism, which is promoted by residual stresses, results in a fine grain structure with a high strength. In contrast, precipitation of the niobium carbonitrides at the grain boundaries results in a coarse grain structure due to a low coherency with the γ-austenite grain boundaries. The coarse structure at the grain boundaries has a lower strength than the fine grain structure within the grain boundaries. As a consequence, a zone develops between the grain interiors and the grain boundaries, and this zone is depleted of niobium carbonitrides. The depleted region is termed a precipitate free zone. A scanning electron microscope image of a precipitate free zone, which is on the order of a few microns wide, is shown in Figure 14-34 [41].

[40] E. C. B. Dillingh, A; Aulbers, A.P., "Stress Relaxation Cracking-Augmented Recommended Practice," TNO2016
[41] J. A. Siefert, J. P. Shingledecker, J. N. DuPont, and S. A. David, "Weldability and Weld Performance of Candidate Nickel based Superalloys for Advanced Ultra Supercritical Fossil Power Plants Part II: Weldability and Cross-weld Creep Performance," *Science and Technology of Welding and Joining,* vol. 21, pp. 397-428, 2016

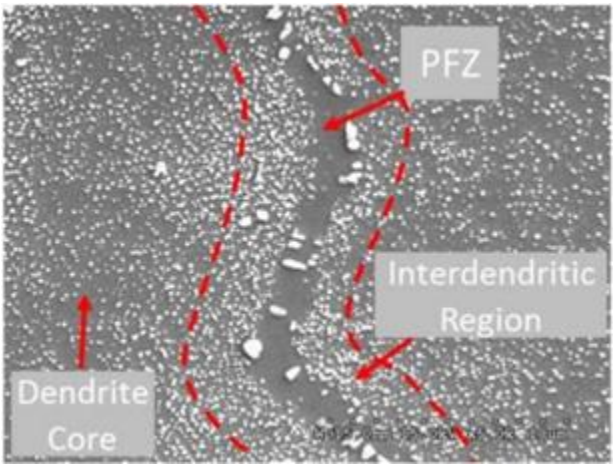

Figure 14-34 Image of a Precipitate Free Zone in the Weld Metal Near a Grain Boundary

It should be noted that the precipitation process occurs on the time scale of years.

Residual Stresses

During welding, the metal in the arc zone undergoes an increase in volume due to 1) the coefficient of thermal expansion, and 2) the change in phase from solid to liquid. After the weld is completed, the zone cools and shrinks. This places the top portion of the weld zone in tension, which is matched by compressive forces in the areas under and adjacent to the weld zone.
The magnitude of the residual welding stresses is a function of the following:

- Section thickness. For section thicknesses greater than about 3 mm, multiple welding passes are generally required. Adding a welding pass to an existing pass generally results in an increase in the residual stresses

- Weld length. Residual stresses are generally additive with weld length.

For thick metal sections (i.e., 50 mm), residual stresses can be as high as 500 to 600 MPa. For long weld lengths (> 1 m) in thin plates, residual stresses can reach values up to 600 to 700 MPa. The residual stress values noted here correspond to the material at ambient temperature.

Creep Characteristics

In commercial central receiver projects, the 300-series of austenitic stainless steels are selected for service on the hot side of the plant (565 °C) due, in part, to the creep resistance of the material.

During normal operation, material stresses are limited to ASME allowable values, which are generally in the range of 25 to 30 percent of the yield strength.

Due to the combination of a high resistance to creep and low operating stresses, the material exhibits limited creep produced by dislocations at the grain boundaries. As a result, the potential for the material to relieve residual stresses, welding or otherwise, is limited.

Stress Relaxation Cracking

The residual welding stresses, which, depending on the geometry, can fall in the range between the yield stress and tensile strength, do not relax due to creep. Concurrently, over a period of years, the material develops the precipitate free zones noted above. The zones have a low strength relative to the surrounding grain structure. The combination of high residual stresses and low strength causes the material to preferentially creep at the grain boundaries. Due to the high strains in these limited regions of low strength, the material starts to develop micro voids, which can then develop into cracks.

Since the highest residual stresses are typically below the surface of the weld, the cracks generally begin below the surface of the material and then progress out towards this surface. This leads to two undesirable characteristics:

- Subsurface cracks are difficult to locate
- Once the crack reaches the surface, and the crack is easy to locate; however, the crack has already likely progressed through the full thickness of the material.

Mitigation Measures

A range of mitigation measures are available to reduce the potential for stress relaxation cracking, including 1) conducting a post weld heat treatment, 2) selecting a weld filler material other than E347 (Type 347H), and 3) selecting a non-stabilized stainless steel for the tank.

Post Weld Heat Treatment

Post weld heat treatment offers two benefits for components prior to elevated temperature service: 1) reduction in residual stress, and 2) stabilization of the microstructure [42,43]. Some literature suggests a single heat treatment of 875 °C for a few hours is sufficient for reducing the susceptibility to stress relaxation cracking. However, a heat treatment near the solution temperature (> 1,050 °C) is needed for a complete stress relief and is recommended to retain the ductility in a highly restrained weld.

[42] J. R.D. Thomas, "HAZ Cracking in Thick Section of Austenitic Stainless Steels-Part 2," *Welding Journal,* 1984
[43] R. D. Thomas, Jr. and R. W. Messler, "Welding Type 347 Stainless Steel- An Interpretive Report," WRC Bulletin1997

A multi-step process for the post weld heat treatment could be the best option for preventing stress relaxation cracks in thick weldments, but the procedure must be carefully engineered to prevent relaxation cracking during heat treatment. Parameters such as the heating rates, hold times, temperatures, and quenching rates are all important parameters that influence the final stress state and the final microstructure. A three-step process consists of 1) an initial stress relief, 2) a solution heat treatment to dissolve the microstructure and effect a full stress relief, and 3) a stabilization heat treatment to form the desired precipitates.

1. The initial stress relief is recommended to reduce some of the initial stresses prior to ramping up to the solution temperature

2. The solution temperature helps to dissolve intergranular carbonitrides and reduces δ-ferrite by promoting the formation of γ-austenite in a predominantly two phase field (γ-Nb(C,N)). The reduction of the intergranular carbonitrides helps to minimize the precipitate free zones and allows for coarsening of intragranular Nb(C,N).

3. The final step of stabilization, initially developed by Morishige [44], is a step to further stabilize the microstructure by reducing the remaining free carbon through the nucleation and growth of Nb (C,N) using any of the remaining Nb. This helps to prevent the formation of chromium carbides ($M_{23}C_6$) during cooling.

Figure 14-35 shows an overlay of the three-step post weld heat treatment times and temperatures relative to precipitation C-curves for the formation of coarse niobium carbide, fine niobium carbide, and chromium carbide [45]. The three-step post weld heat treatment method has been used successfully in industry for decades.

Weld Filler Material

The principal candidate weld filler materials for a tank fabricated from Type 347H are the following:

- ER347H [46], which is essentially the tank material. It is an austenitic material, with ferrite numbers in the range of 2 to 9, with a typical value of 4.

- E16.8.2 [47], which is an austenitic material with a ferrite number of 1 to 6.

[44] N. Morishige, M. Kuribashi, H. Okabayashi, and T. Naiki, "On the Prevention of Service Failure in Type 347 Stainless Steel," presented at the Third International Symposium of the Japan Welding Society, 1978
[45] V. O. B. Messer, T Phillips, "Optimized heat treatment of 347 for high temperature application," *Corrosion,* 2004.
[46] Metronode Welding Consumables for High Temperature Alloys, Data Sheet C-11, 347H Stainless Steels, Metronode Products LTD, Surrey, KT16 9LL, March 2016
[47] Metronode Welding Consumables for High Temperature Alloys, Data Sheet C-12, 16.8.2 for High Temperature 3XXH Stainless Steels, Metronode Products LTD, Surrey, KT16 9LL, May 2019

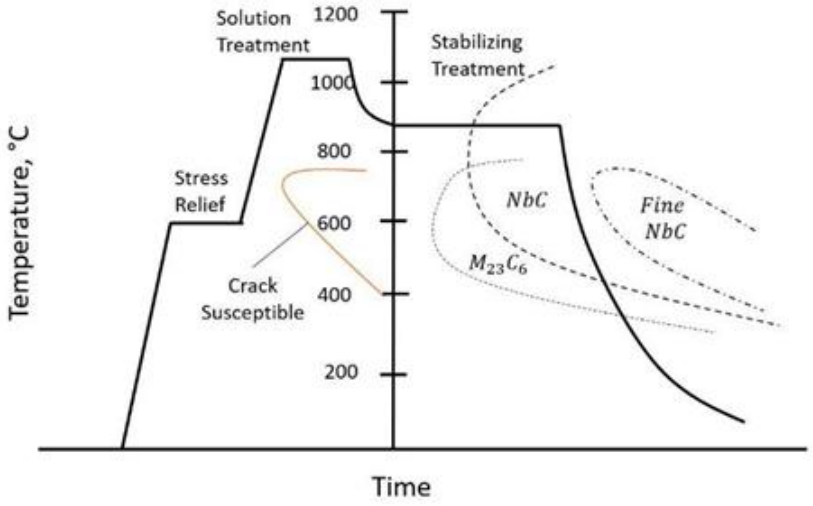

Figure 14-35 Three-Step Post Weld Heat Treatment Time and Temperature Schedule

For both of these consumables, bismuth-bearing constituents are held to very low levels (< 0.002 percent Bi) as required by API 582, Welding Guidelines for the Chemical, Oil, and Gas Industries.

E16.8.2 was developed as a more ductile alternative to 347H consumables to avoid failures in the heat affected zones of thick (> 12 mm) 347H base materials. The main benefit of E16.8.2 is reduced δ-ferrite, which is prone to transforming to a brittle σ phase.

The σ phase is a tetragonal crystal structure, with a precipitation temperature between 600 °C and 1,000 °C [48]. The structure is composed of various intermetallic compounds, including FeCr, FeMo, and $(FeNi)_x(CrMo)_y$. The σ phase can increase the hardness, and decrease both the toughness and the elongation, of steels.

The σ phase issues from the phase transformation of δ → σ (δ-ferrite to σ phase). When the Cr content is below 20 weight percent, the precipitation of the σ phase is not readily observable in austenitic stainless steels; however, the σ phase can be formed quickly when the Cr content is between 25 and 30 weight percent.

The addition of strong ferrite stabilizers other than Cr, such as Si and Mo, can also lead to the formation of the σ phase.

The δ-ferrite is a body centered cubic structure, in which Cr, Si, and Mo can efficiently diffuse. Further, the δ-ferrite regions, compared to the γ-austenitic regions, are rich in Cr. As such, the δ → σ phase transformation preferentially occurs in the δ-ferrite regions. Precipitation can also occur directly in the δ-ferrite particles.

[48] Hsieh, Chih-Chun, and Wu, Weite, (Department of Materials Science and Engineering, National Chung Hsing University, Taiwan), 'Overview of Intermetallic Sigma (σ) Phase Precipitation in Stainless Steels', International Scholarly Research Network, Volume 2012, Article ID 732471, January 2012

As such, reducing the δ-ferrite in the weld region offers the benefit of increased ductility, which improves the tolerance of strain localizations and mismatches in strengthening mechanisms.

Non-Stabilized Stainless Steels

The potential for stress corrosion cracking in a 300-series stainless steel is directly associated with the addition of niobium to the alloy. If niobium is not present, then the reprecipitation of niobium carbonitrides described above does not occur. This, in turn, results in a matrix which has 1) a more isotropic distribution of strength and ductility, and 2) a lower propensity for the development of internal cracks.

Nonetheless, the alternate candidate stainless steels, including Type 304H, Type 316H, and Type 304LNB, each of which have their own set of advantages and disadvantages. The topic is discussed in some detail in Section 14.16.1.

14.16.3 Stress Relaxation Cracking in Type 316LNB with Lean Austenitic Weld Filler

Type 316LNB is a low carbon version of Type 316, with additions of nitrogen and boron to provide resistance to creep similar to the properties of Type 316H. A recent study compared the resistance to stress relaxation cracking of Types 316LNB with Type 347H [49]. The weld filler material for Type 316LNB was a lean austenitic (ER16.8.2, 16 Cr - 8 Ni - 2 Mo), which has demonstrated improved toughness and thermomechanical properties compared to matching filler materials for Type 347H (347H-16).

Testing at 600, 700, and 800 °C show no cracking for the 22-hour test for Type 316 LNB with the ER16.8.2 filler material, while stress relaxation cracking is observed for alloy 347H with the matching filler material.

Future efforts will expand the test matrix, including longer times at 600 °C to simulate the conditions in a commercial tank. The planned work will also investigate the microstructural conditions needed for fracture, such as secondary phases in the partially melted weld zone.

In general, initial test results show that Type 316LNB is less prone to the development of stress relaxation cracking than Type 347H. However, additional testing is required to help predict the long term (30+ year) strength and ductility characteristics of the welded material in commercial service.

[49] Pickle, T. (Colorado School of Mines, Golden, Colorado, USA), et al, Evaluation of Alternative Base Materials for Mitigation of Stress Relaxation Cracking in Thermal Energy Storage Tanks, SolarPACES 2024, 30th International Conference on Concentrating Solar Power, Thermal, and Chemical Energy Systems

15. Nitrate Salt Steam Generators

15.1 Commercial Configuration

The Rankine cycles in essentially all solar projects use a single reheat design. Correspondingly, the steam generators in essentially all solar projects use separate heat exchangers for superheating, reheating, evaporation, and preheating. Separate heat exchangers are required due to 1) differences in the characteristics of latent heat transfer (evaporator) and sensible heat transfer (superheater, reheater, and preheater), and 2) different operating pressures (superheater and reheater).

A common approach to the fabrication of the heat exchangers is a U-tube bundle in a straight shell, with 2 passes on the shell side. The fluid on the shell side is typically salt. This is done for two reasons:

1. The high pressure fluid is the water/steam, and accommodating the high pressure fluid in tubes is easier to accomplish than accommodating the high pressure fluid in the shell

2. The salt in the heat exchanger can reasonably be expected to freeze at least once in the life of the project. If the salt is on the tube side, and freezes in the tubes, then the solid salt can form essentially immovable plugs. Thawing the tubes anywhere along the length of the frozen plug runs the risk of yielding the tube due to the nominal 4 percent increase in salt volume on thawing. If the freeze/thaw cycle is repeated, then there is the possibility of rupturing the tube. (This was the failure mechanism for the tube bundle in the kettle evaporator at the Solar Two demonstration project.) In contrast, if the salt is on the shell side, the thawing process begins by ensuring that the salt in the lines to and from the heat exchanger is liquid. Activating the electric heat tracing on the shell and the channel first melts the salt on the inner surface of the shell and the channel. Since the heat input from the heat tracing is typically a modest value, the initial mass of salt which melts is also a modest number. The volume change on thawing still occurs, but the liquid salt has an exit path through the salt lines. As such, the potential for plastically yielding the shell is low.

Most commercial heat exchangers use a flat tubesheet. During fabrication, the tubes are inserted into the tubesheet, the ends of the tubes are strength welded to the face of the tubesheet, and the tubes are then rolled into the tubesheet. The rolling operation occurs after the welding operation. This prevents any air which might be trapped in the gap between the tube and the tubesheet from heating and expanding into the weld region, which could produce a porous weld.

In some commercial projects, the evaporators use forced circulation, while other projects use natural circulation. The selection is largely the responsibility of the equipment supplier.

15.2 Heat Exchanger Location

Similar to the discussion in Section 11.2, Equipment Location for Oil-to-Salt Heat Exchangers in Parabolic Trough Projects, there is a range of options for the location of the steam generator heat exchangers.

In some commercial projects, the heat exchangers are located on an elevated platform between the storage tanks. The height of the platform is slightly above the mid-point height of the tanks. As such, the heat exchangers can drain to the tank with the lower liquid level.

In other projects, the steam generator is located at grade, and the heat exchangers drain to a tank located below grade. Drain pumps, located on the drain tank, pump salt from the drain tank back to the main storage tanks.

In general, locating the heat exchangers at grade is less expensive than locating the equipment on an elevated platform. However, locating a drain tank below grade is not an inexpensive option. Further, the drain tank must be heat traced on a continuous basis, and this represents a continuous auxiliary energy demand.

15.3 Cold Reheat Steam Electric Heater

Prior to turbine synchronization, live steam is sent to the condenser through the turbine bypass system. The system consists of a high pressure throttle valve, a steam attemperator, a low pressure throttle valve, and a second steam attemperator.

Early in the startup process, the temperature of the salt entering, and leaving, the superheater is approximately 290 °C. This results in a saturation pressure in both the evaporator and the superheater of about 74 bar.

With the bypass system in service, the steam from the superheater must be reduced in pressure to a value which can be accepted by the reheater. As such, the high pressure throttle valve reduces the pressure to the nominal design pressure of the reheater, which is about 32 bar. The corresponding cold reheat steam temperatures are in the range of 235 to 240 °C.

To provide an adequate margin against salt freezing at the cold end of the reheater, an electric steam heater is located downstream of the high pressure throttle valve and upstream of the cold end of the reheater. The capacity of the electric heater depends on the details of the startup sequence (i.e., steam flow rate and pressure versus time), but is typically on the order of several MWe.

15.4 Cyclic Operation

In a solar project, the steam generator, almost by definition, undergoes a daily startup and shut down cycle.

During overnight hold, cold salt is circulated through the steam generator. The salt is supplied by the cold salt attemperation pump, and the salt leaving the steam generator is returned to the cold salt tank. The heat input from the cold salt compensates for the heat losses from the heat exchangers and associated piping. The heat input also heats the makeup water added to the steam drum to compensate for steam and condensate losses in the Rankine cycle.

To start the steam generator, the hot salt pump is started, and hot salt is blended with cold salt from the attemperation pump at a point upstream of the superheater / reheater. Early in the startup process, the steam flows produced by the superheater and the reheater are not at temperatures high enough to admit to the turbine. The live steam and the hot reheat steam flows are attemperated and throttled, and the flow is then directed to the condenser through a turbine bypass system.

When the live and the reheat steam temperatures reach values which can be accepted by the turbine, a portion of the steam flow in the bypass system is sent to the turbine. The turbine is synchronized, and loaded to a value that will prevent a trip on reverse power. The steam flow in the bypass system is eventually stopped, with all of the steam flow now directed to the turbine.

The relative proportions of hot salt and cold salt at the mixing point upstream of the superheater / reheater are adjusted until the flow of cold salt reaches zero. The output of the turbine is adjusted by changing the speed of the hot salt pump.

To shut down the steam generator, the above process is essentially reversed.

The blending process of adding hot salt to cold salt is a consequence of the vendor limits on allowable rates of temperature change and thermal shock. Typical limits include a maximum rate of temperature change of 10 °C/min, and a maximum thermal shock (Fluid temperature - Metal temperature) of 60 °C. The limits are developed by the vendor to ensure that the heat exchangers have a low cycle fatigue life corresponding to at least 30 years of daily startup and shutdown cycles.

The vendor also specifies a minimum allowable flow rate on both the shell- and tube-sides. A typical value is 16 percent, which corresponds to a turndown ratio of 6:1. At low flow rates, the pressure drops on both the tube- and the shell-sides approach very low values. Local effects due to friction and buoyancy can then influence the flow distribution, which can produce stratified flow, channel flow, or both. If the flow distribution is not uniform, then the temperature distribution within the heat exchanger is also not uniform. Non-uniform temperature distributions can produce internal stresses which are non-uniform, unpredictable, and oscillating. These stresses may add to, or subtract from, the normal process stresses, which can lead to meaningful reductions in the low cycle fatigue life of the equipment.

15.5 Project Experience

15.5.1 Overnight Hold

The steady state heat losses through the insulation on the heat exchangers, and through the insulation on the steam generator piping, is a fraction of 1 percent of the design duty of the steam generator. However, the water and the steam leakage rates in the Rankine cycle can reach problematic levels if 1) the maintenance staff is not conscientiously repairing the steam and condensate leaks as they develop, and 2) tubes leaks in any of the heat exchangers result in steam being carried into the cold salt tank.

A condition can arise in which the energy in the flow of cold salt from the attemperation pump is not sufficient to compensate for the thermal demand of the steam generator; i.e., the temperature of the salt returning to the cold tank falls below the minimum operating temperature of 275 °C. The first line of defense is to add thermal energy to the drum by operating the electric water heaters that preheat the heat exchangers prior to filling with salt. The second line of defense is to add auxiliary steam to the drum from the auxiliary steam generator. The third line of defense is to blend a very small quantity of hot salt with the cold salt upstream of the superheater / reheater mixing station.

The first two approaches are straightforward to implement and to control, but both increase the auxiliary energy demand in the plant. The third uses energy collected by the receiver, but any energy withdrawn from the hot tank for temperature maintenance reduces the daily electric energy production. Further, the quantity of hot salt required is a small fraction of the flow capacity of the hot salt pump. This can lead to oscillations in the flow of salt from the hot pump, which, in turn, can lead to oscillations in the mixed salt temperature upstream of the superheater / reheater. Oscillations in the mixed salt temperature have been shown to lead to low cycle fatigue damage of the heat exchangers, particularly if the rates of temperature change exceed the vendor limit of 10 °C/min.

The solution to this problem is to generously size the electric water heaters in the steam generator, studiously repair any steam and condensate leaks in the Rankine cycle, and provide a means for artificially increasing the pressure drop on the salt side of the steam generator if the hot salt pump must be operated at a low flow rate.

15.5.2 Low Cycle Fatigue

A commercial project experienced multiple failures of the tube-to-tubesheet connections in the superheater in the first years of commercial service. A possible explanation for the common failure patterns is as follows:

1. During startup and shutdown, the rates of change in the temperature of the mixed salt entering the heat exchanger routinely exceeded the vendor limits. The rates of change were both positive and negative, producing, in effect, oscillations in the inlet temperature. The oscillations generated differential thermal expansions across the diameter of, and through the thickness of, the tubesheet.

2. The differential thermal expansion was exacerbated by the low steam flow rates, and the very low pressure drops, during startup and shutdown. Specifically, the steam flow tended to channel, favoring some tubes over others. This resulted in lower temperatures in some regions of the tubesheet, and higher temperatures in other regions.

3. The non-uniform thermal expansion caused flexing in the tubesheet, which over several thousand cycles, caused a relaxation in the friction forces in the rolled tube-to-tubesheet connections.

4. If the rolled connection is lost, then the tube-to-tubesheet welds must carry the loads associated with differential expansion between adjacent tubes, and the differential expansion between the tubes and the tubesheet. If the stresses are high enough, the welds can crack due to low cycle fatigue.

There is additional evidence that rapid changes in the temperature of high pressure heat exchangers can lead to failures of the tube-to-tubesheet connections. Specifically, the Solar One central receiver project used a superheated steam receiver, operating at nominal conditions of 100 bar and 540 °C. The thermal storage system consisted of a single tank thermocline, filled with a mixture of rock, sand, and mineral oil (Caloria HT-43). Energy was transferred from the receiver steam into the rock/sand mixture by circulating Caloria through an economizer, a steam condenser, and a steam desuperheater. Energy was transferred from the rock/sand mixture by circulating Caloria through an economizer, an evaporator, and a superheater.

To isolate the demineralized feedwater in the Rankine cycle from the Caloria in the storage system, the storage system charging and discharging heat exchangers used a double tubesheet design. Tube-to-tubesheet connections were by means of rolled joints; seal welds were not used. Leaks would be confirmed by the presence of either steam or Caloria in the intra-tubesheet space.

Within 400 hours, the tube-to-tubesheet joints started to leak [50]. Repairs were attempted by applying seal welds to the ends of the tubes and re-rolling the tubes into the tubesheets. However, the repairs were unsuccessful, and the storage system was essentially abandoned in place.

A post-failure finite element model of the heat exchanger, using a rate of temperature change of 9.6 °C/min, showed that the tube stresses at the rolled connections approached the yield value. If a material is operating at or near the yield stress under daily cycling conditions, the low cycle fatigue life is expected to be very short.

[50] S. E. Faas, et. al., (Sandia National Laboratories, Albuquerque, New Mexico), 10 MWe Solar Thermal Central Receiver Pilot Plant: Thermal Storage Subsystem Evaluation - Final Report, Sandia Report SAND86-8212, June 1986

15.5.3 Water Chemistry

High levels of O_2 can lead to accelerated corrosion rate, especially if the purity of the condensate and the feedwater purity is degraded by contamination (salts) passing through the demineralization system or from condenser cooling water in leakage. A deaerator can be used to control O_2 levels to the required values. Generally, for all-ferrous systems (those without copper tubing in heat exchangers) the desired levels are in the range of 5 ppb up to a maximum of 100 ppb.

Additionally, the pH of the feedwater is typically adjusted to a value of 9.4 or higher to reduce the solubility of protective oxides formed, and with adequate O_2 present, to support the formation of a stable layer of hematite on the water-side surfaces of the system. This is usually done by adding alkaline agents to the feedwater such as ammonium hydroxide, or ammonium hydroxide in combination with a neutralizing amine, such as ethanolamine.

At the Solar Two project, an examination of the water side of the preheater, after about 1 year of service, showed significant quantities of a loosely adherent deposit. An analysis showed the deposits to be magnetite. This is an undesirable condition, for the following reasons:

- Magnetite is a metal oxide, and due to its low thermal conductivity, deposits can reduce the heat transfer rates in the preheater and in the evaporator. Further, if the deposits form preferentially in some tubes and not others, this can lead to non-uniform flow distributions, non-uniform temperature distribution, and non-uniform stress distributions in the heat exchanger.

- Magnetite deposits are an indication of corrosion upstream of the evaporator. Depending on the water treatment approach selected for the project, the corrosion process generally accelerates if the pH is too low (< 9) and / or the dissolved oxygen levels are too low (< 5 ppb). This combination of pH and dissolved oxygen can occur in the feedwater if 1) the dosing of the alkaline agents is insufficient, and / or 2) the deaerator venting is too effective. Under two-phase conditions in the evaporator, low oxygen will always occur, and low pH may occur depending on local two-phase conditions and the alkaline agents applied.

- In the evaporator, oxide deposits can come out of suspension at the locations in the tubes where evaporation begins. If the evaporator uses austenitic tubes, then a passivation layer is expected to form on the tubes. However, defects or local variations in the passivation layer can lead to sensitization and pitting corrosion. Specifically, the chemical conditions under the deposits (sodium, chloride, sulfate, ammonia, and the resulting pH) can be different than the surrounding area. If so, a situation can develop in which the protective oxide passivation dissolves and active corrosion can initiate. In the case of pitting corrosion, this can become autocatalytic. Specifically, the dissolution of iron within the pit generates positive iron ions, which draw in and concentrate mobile, acidic ions, such as chlorides, within the pit.

- If the evaporator is a forced recirculation design, then oxide particles in the feedwater can damage the bearing, erode the impellers, and damage the shaft seals in the steam drum recirculation pumps.

Possible Sources of the Deposits

Hematite

Hematite (Fe_2O_3), in a hydrated form, is formed on carbon steel in an oxidizing environment, as follows:

$$Fe + 2\ H_2O \rightarrow Fe(OH)_2 + H_2$$

$$4\ Fe(OH)_2 + O_2 \rightarrow 2\ Fe_2O_3H_2O + 2\ H_2O$$

In general, hematite is a desirable form of iron oxide. It forms an adherent corrosion layer and isolates the parent metal from continued corrosion. It also exhibits a very low solubility in water compared to magnetite.

Magnetite

Magnetite (Fe_3O_4) is generally formed in a relatively reducing environment, through two different reactions:

$$3\ Fe(OH)_2 \rightarrow Fe_3O_4 + 2\ H_2O + O_2 \text{ (at temperatures above 50 °C)}$$

$$3\ Fe + 4\ H_2O \rightarrow Fe_3O_4 + 4\ H_2 \text{ (at temperatures above 150 °C)}$$

In general, magnetite is a less desirable form of iron oxide in flowing feedwater conditions (>100 °C), as 1) it forms a more soluble passivation layer than hematite in water, and 2) it is subject to damage mechanisms such as flow accelerated corrosion, particularly in turbulent locations operating at temperatures between 100 and 250 °C. Removal of the magnetite layer via flow accelerated corrosion exposes new material to the corrosion process. It also results in corrosion products moving through the system, where deposition may occur and lead to further damage mechanisms (e.g. accumulation of deposits in evaporator).

Water Chemistry Control

Although perhaps stating the obvious, the water treatment staff needs to maintain strict control over the water chemistry. The problem is more acute in plants which cycle each day, particularly if the vacuum is broken in the condenser each evening and the condensate in the hot well is exposed to oxygen. Further, the inline instruments for measuring pH and dissolved oxygen need to be maintained in good working order and to receive periodic calibrations.

In general, control of pH in high purity systems is best accomplished through conductivity control, as opposed to strictly relying on direct pH measurement. In addition, older dissolved

oxygen measurement technology relying on electrochemical potential measurements are less robust than optical methods employing luminescence technology. Application of 'smart' chemistry monitoring approaches, which incorporate instrumentation validation techniques, can further reduce the expertise required by the operating staff to maintain proper chemistry control.

If the experience from the Solar Two project, and from a range of commercial projects, are any indication, the water treatment system must be fully staffed, and water treatment specialists must be brought in on a periodic basis to review the effectiveness of the treatment system. Failure to satisfy each of these requirements will result in a significant negative effect on the plant availability.

15.5.4 Startup and Shutdown

A common steam generator arrangement in commercial projects consists of the following:

- Two 50-percent capacity steam generator trains
- Three 50-percent capacity hot salt pumps, discharging to a common header
- A common minimum flow recirculation valve for the three hot salt pumps
- Two 100-percent capacity cold salt attemperation pumps, discharging to a common header
- A common minimum flow recirculation valve for the two attemperation pumps
- Salt control valves, at the cold ends of the superheater and the reheater, for distributing the relative flows between the two heat exchangers
- A startup feedwater heater, located downstream of the last high pressure feedwater heater and upstream of the steam generator preheater.

The salt pump and discharge valve arrangement is shown in Figure 15-1, and the intra-heat exchanger salt valve arrangement is shown in Figure 15-2.

This arrangement reduces the number of control valves to a minimum, and likely offers the lowest cost piping arrangement. However, the arrangement carries a range of liabilities, as discussed in the following subsections.

Liability 1 - Sequential Startup

By placing the hot salt pumps on a common header, and placing the attemperation pumps on a common header, there is no method to start a second steam generator train if one train is already in service. To start the second train, the metal temperatures in the first train would need to be reduced to essentially the cold salt temperature to avoid thermally shocking the

second train. In effect, starting the second train must be postponed until the first train goes through it's normal daily shutdown.

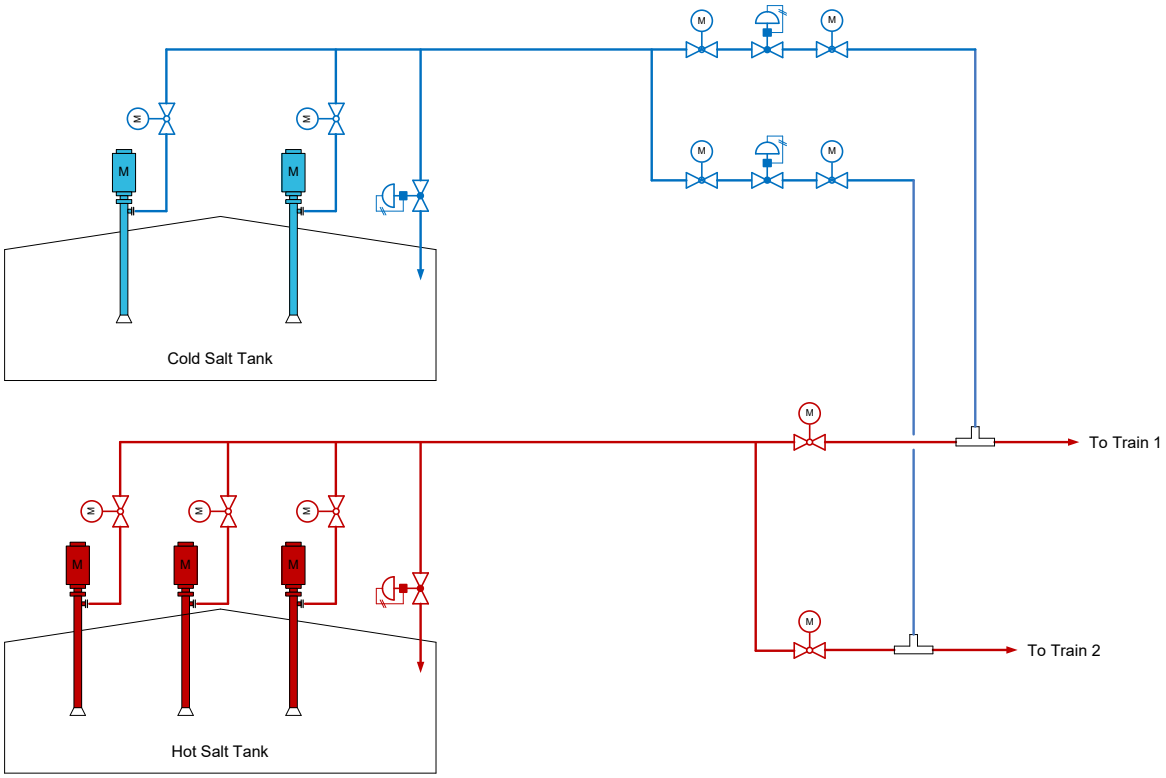

Figure 15-1 Salt Pump Arrangement in a Representative Commercial Project

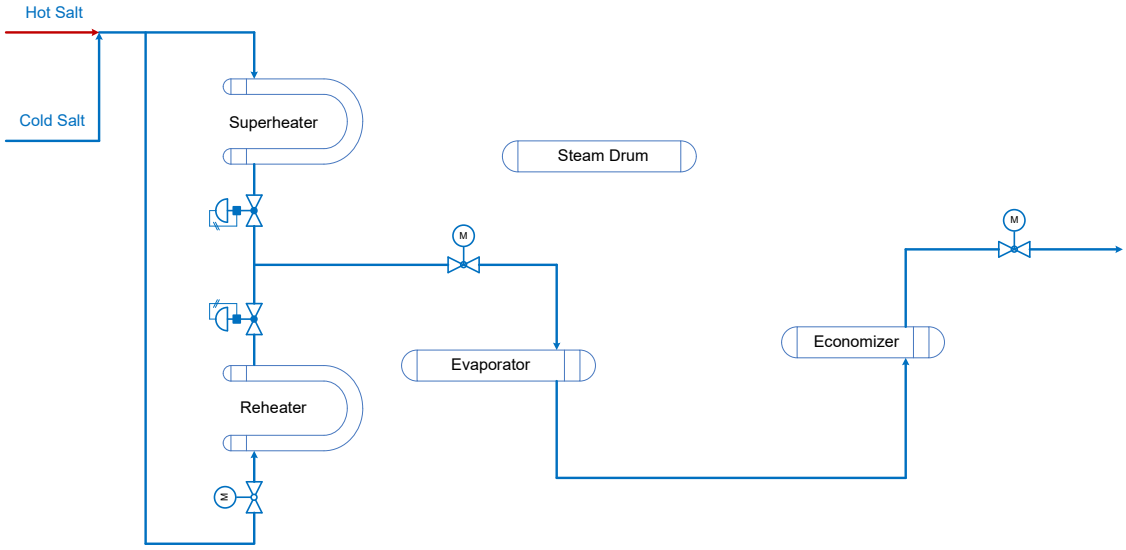

Figure 15-2 Intra-Heat Exchanger Salt Valve Arrangement

Liability 2 - Hot Salt Flow Control

The salt control valves downstream of the superheater and the reheater must have Cv values which are high enough to accommodate the design point flow rates with a reasonable pressure drop (< 1 bar). During startup, hot salt is blended with cold salt at the mixing station upstream of the superheater / reheater. The rate at which hot salt is added to cold salt must satisfy the vendor limit regarding the allowable rate of temperature change, which is nominally 10 °C/min. Using representative flow - head curves for the attemperation pump, the acceleration rate at which hot salt can be added to the cold salt is 0.0023 m^3/hr-hr (6 gal/min-min). A flow rate of 0.0023 m^3/hr is approximately 0.15 percent of the design flow rate from the hot salt pump. Further, early in the startup process, the salt flow rate to the steam generator is perhaps 15 percent of the design flow rate. As such, the pressure drop through the steam generator is on the order of 0.15^2 = 2 percent of the design pressure drop. To control the flow from the hot salt pump with this level of accuracy, in combination with a low discharge pressure, a backpressure must be imposed on the steam generator train. The backpressure is typically provided by the control valves downstream of the superheater and the reheater. However, these valves have reasonably large discharge coefficients, and to provide a meaningful backpressure on the system, the valves are forced to operate in the range of 2 to 4 percent open. Due to the low system pressures, the hot salt pump is already operating at the minimum speed. As such, all of the flow control adjustments during startup must be made by the control valves. As might be expected, the ability to adjust the flow in increments of 0.15 percent per minute is generally poor. The result is oscillations in the flow from the hot salt pump, which results in oscillations in the mixed salt temperature upstream of the superheater and the reheater. The oscillations can result in rates of temperature change which are a factor of 2 to 4 larger than the allowable rates.

Liability 3 - Salt Pump Recirculation Flow Control

The hot salt pumps and the attemperation pumps share a common pressure point at the mixing station upstream of the superheater / reheater. As such, the following parameters all influence one another:

- The discharge pressure of the hot salt pump
- Operating either one or two hot salt pumps
- The position of the minimum flow recirculation valve for the hot salt pump(s)
- The discharge pressure of the attemperation pump
- The position of the minimum flow recirculation valve for the attemperation pump

During the startup of the steam generator, the following characteristics apply:

- The pressure drop in the system is low

- The discharge pressures of the hot salt pump and the attemperation pump are both low

- The flow rate from the hot salt pump to the mixing station is low, which requires the minimum flow recirculation valve to control the (Mixing station flow) + (Recirculation flow)

- Depending on the speed range of the attemperation pump, the minimum flow recirculation valve for the attemperation pump can also be open to control the (Mixing station flow) + (Recirculation flow)

Under these conditions, the system flow stability can be marginal to poor. For example, to increase the flow of hot salt to the mixing station, the minimum flow recirculation valve for the hot pump can be closed slightly. Since the pressure drop in the steam generator flow path is different than the pressure drop in the hot salt pump recirculation line, a change in the recirculation valve position results in a change in the discharge pressure of the hot salt pump. This, in turn changes the effective discharge pressure of the attemperation pump, which changes the flow rate from the pump. In response, the minimum flow recirculation valve for the attemperation pump can change position to provide the required (Flow to the mixing station) + (Recirculation flow). The changes in the discharge conditions for the attemperation pump are then carried over to the hot salt pump, which normally results in a change in the recirculation valve position for the hot salt pump to provide the desired net hot salt flow to the mixing station. The system can then oscillate between two quasi-stable operating points, which results in oscillations in the mixed salt temperate at the mixing station.

Liability 4 - Minimum Steam Side Flow Rates

A typical vendor limit on the minimum allowable flow rate is 16 percent of the design flow rate.

If the design flow rate of the cold salt attemperation pump is 15 percent of the design steam generator flow rate, then operating the attemperation pump at 100 percent speed during overnight hold, and early in the startup process, satisfies the minimum flow requirement on the salt side of each of the heat exchangers.

Some projects use a recirculation pump between the steam drum and the cold end of the evaporator, and a separate recirculation pump between the steam drum and the cold end of the preheater. The flow capacities of each pump are greater than 15 percent of the design water flow rates, and operating the pumps early in the startup process ensures that the minimum water flow rates are always maintained in the evaporator and the preheater.

In contrast, steam flow is initiated in the superheater and in the reheater only when the blending of hot salt with cold salt begins. The steam flow rates begin at 0 percent, and increase with an increase in the flow rate of hot salt. As such, during each startup, the steam flow rates in both heat exchangers are necessarily below the minimum allowable flow rates. Due to the very low pressure drops at these flow rates, the flow distribution among the approximately 900 tubes is expected to be poor. Non-uniform flow distributions lead to non-

uniform temperature distribution, which, in turn, lead to unpredictable, and potentially damaging, stress distributions.

Liability 5 - Startup Feedwater Heater

Prior to turbine synchronization, the turbine extraction feedwater heaters are not in service. As such, the temperature of the feedwater leaving the last high pressure feedwater heater is nominally equal to the saturation temperature in the deaerator. This temperature is well below the freezing point of the salt. As such, the temperature of the feedwater supplied to the preheater must be increased to a value which is high enough to prevent salt solidification at the cold end of the preheater.

The same conditions apply once the turbine is synchronized, but with the turbine operating under part-load conditions.

A common approach to preheating the feedwater is to use a startup feedwater heater. The energy source for the startup heater is live steam, which has been throttled and attemperated.

This approach is very effective at preheating the feedwater, but it does incur a range of penalties, as follows:

- Using live steam for feedwater preheating is thermodynamically inefficient. Under part load turbine operating, the penalty in the Rankine cycle efficiency can range from 0.5 to 1.0 percentage points.

- The startup heater can undergo rapid changes in inlet steam flow. Although the steam flow is attemperated, the rates of change in the heater metal temperature can exceed typical commercial values; i.e., 10 °C/min. To what extent this influences the low cycle fatigue life of the heat exchanger is not yet known.

- The startup heater is used daily, and its operation is mandatory to start the steam generator. Further, one 100-percent heater is a typical design approach. As such, if the startup heater is not available, the plant incurs a forced outage.

- Starting the steam generator, synchronizing the turbine, and loading the turbine is an involved process. If the turbine trips due to a spurious control signal, the turbine can be quickly restarted once the trip is cleared. For this to occur, the steam generator must remain in operation; i.e., steam is dumped to the condenser through the bypass system. However, when the turbine trips, the extractions to the feedwater heaters are stopped, and the temperature of the feedwater leaving the last high pressure feedwater heater quickly decays. In response, the startup heater must be brought quickly into service. This produces a thermal shock on the tube side, in combination with a thermal shock on the shell side when live steam is introduced into the heater. To some degree, the low cycle fatigue life of the startup heater under thermal shock conditions is something of a commercial unknown.

15.6 Changes to the Equipment and the System Design

To avoid the problems experienced at a range of commercial projects, different approaches can be adopted regarding process design, fabrication techniques, and material selection.

15.6.1 Process Design

The goals of a revised process design are as follows:

- Allow the equipment to operate continuously at the 1-percent load case without affecting the low cycle fatigue life of the equipment. The 1-percent load case is an arbitrary requirement; i.e., it is no more applicable than the 2- or the 5-percent case. But if the process design, at 1 percent load, can protect the equipment against stress distributions that could reduce the low cycle fatigue life, then the process design can comprehensively protect the equipment over the full range of part- and full-load conditions

- Establishing uniform flow distributions, on both the shell- and the tube-sides of the heat exchangers throughout the full range of startup and shutdown conditions. Uniform flow distributions avoid the potential for non-uniform temperature distributions and the associated potential for damaging stress distributions.

Independent Trains

Even if two 50-percent steam generator trains are selected for a commercial project, each train should be independent of the other. Each train would consist of one 100-percent capacity hot salt pump, one 100-percent capacity attemperation pump, the steam generator heat exchangers, and a steam bypass system to the condenser. The salt pump arrangement is illustrated in Figure 15-3, and the intra-heat exchanger salt valve arrangement is shown in Figure 15-4. (Clearly, the analysis described below for two 50-percent independent trains can readily be extended to one 100-percent independent train.)

Independent trains allow either train to start at any time, regardless of the operating state of the other train. In addition, independent trains avoid a situation in which:

- Multiple pumps share a common discharge header

- Multiple pumps share a common minimum flow recirculation valve

- Multiple hot salt pumps, in parallel with multiple attemperation pumps, share a common mixing station upstream of the superheater / reheater.

The sharing of headers and mixing stations means that the discharge pressure of one pump influences the flow from any one, and perhaps more than one, of the other pumps operating in parallel.

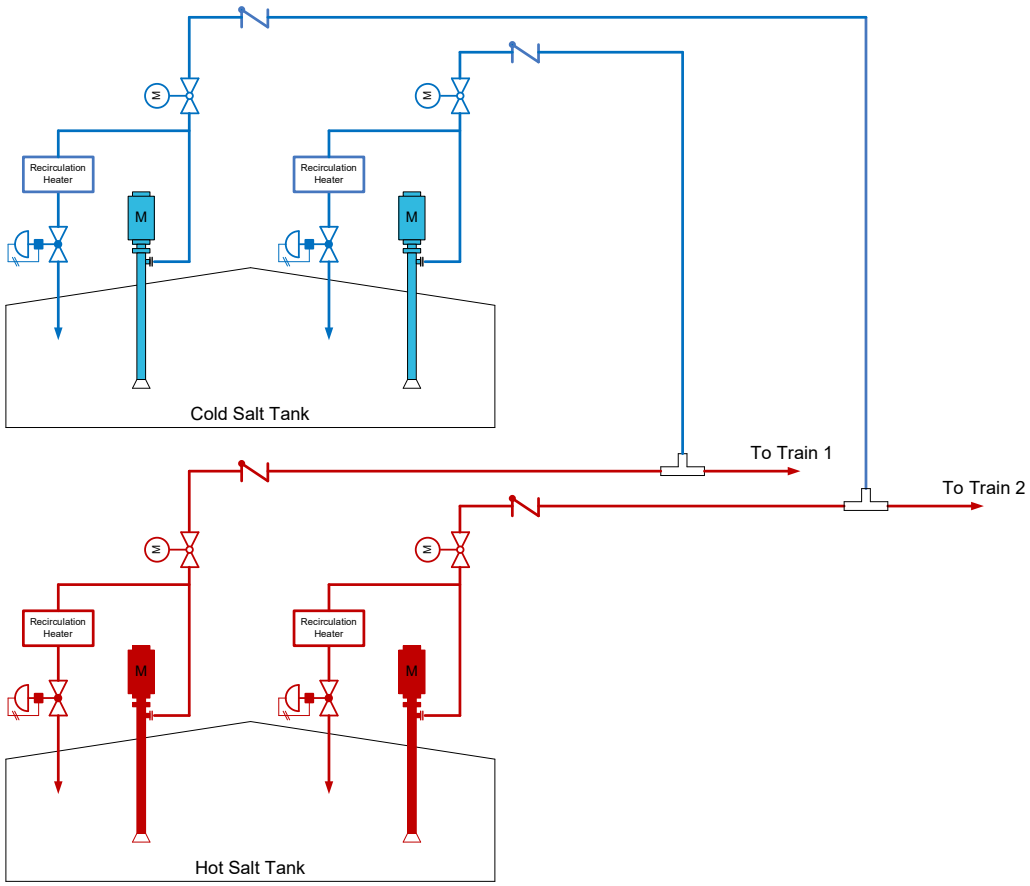

Figure 15-3 Salt Pump Arrangement with Independent Steam Generator Trains

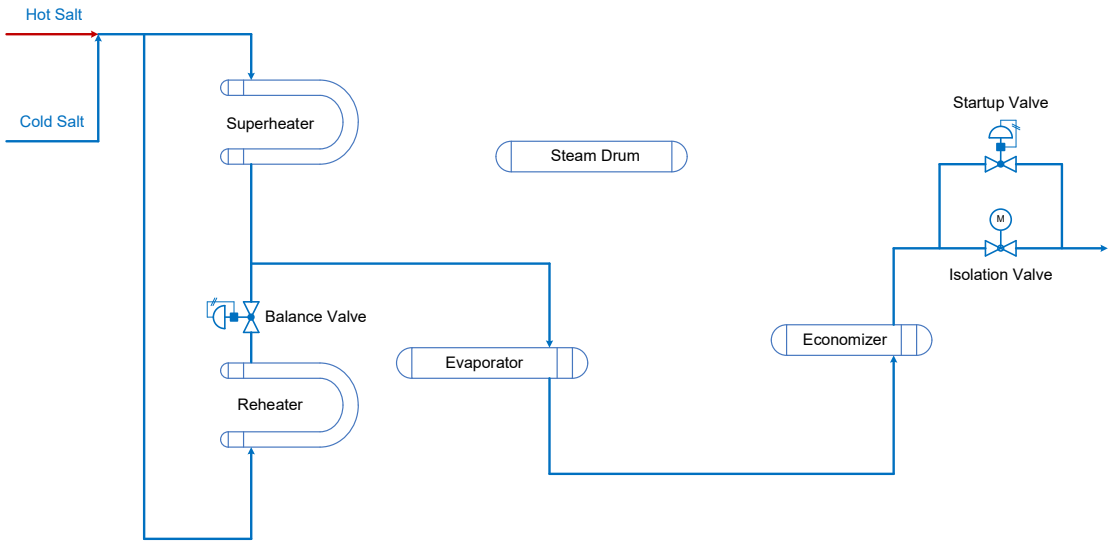

Figure 15-4 Intra-Heat Exchanger Salt Valve Arrangement

Further, it is recommended that a split-range startup salt valve be added in parallel to the normal isolation valve at the cold end of the preheater. With the isolation valve closed, the startup valve performs two important functions: 1) the valve adds an artificial pressure drop to the system, and 2) the hot salt pump and the cold salt pump now see a common discharge pressure. These function provide the following benefits:

- If the pressure drop in the system is increased, then the pumps are no longer obligated to operate at their minimum speeds. As such, varying the pump speed now becomes a potential means of system control. The value in this approach is that pump speeds can be both accurately measured and accurately controlled.

- If the head - flow characteristics of the pumps are well defined, and if the flow - pressure drop characteristics of the piping, the valves, and the heat exchangers are well defined, then it is possible to both calculate and to accurately control the relative flow rates of hot salt and cold salt. This, in turn, allows the salt temperature at the mixing station upstream of the superheater / reheater to be controlled by changing the relative speeds of the pumps.

- The control approach avoids the need to match the discharge pressures from the two pumps using signals from pressure transmitters, or to set the flow rates from the two pumps using signals from flow meters. The accuracy of salt pressure and flow instruments is generally too low to control an acceleration in the hot salt flow rate on the order of 0.0023 m^3/hr-hr.

- It is possible to select a discharge coefficient for the split range startup valve that allows the minimum flow recirculation valves for both the hot salt pump and the attemperation pump to be set to fixed positions for steam generator flow rates beginning with startup, through turbine synchronization, and then to an intermediate turbine load. As such, all of the system valves remain in fixed positions, and both of the salt pumps see a common discharge pressure, which reduces the potential for oscillations in the mixed salt temperature upstream of the superheater / reheater.

The above approach to steam generator system control during startup was successfully demonstrated at the Solar Two demonstration project [51].

Pump Redundancy

A spare hot salt pump, and a spare attemperation pump, would be stored in the site warehouse. The reliability of salt pumps has been excellent, and providing an installed redundant pump can be counterproductive to the plant availability. Specifically, each pump requires an isolation valve, a startup control valve, a check valve (see below), and a vent valve.

[51] Kelly, B (Bechtel National Inc., San Francisco, California), 'Lessons Learned, Project History, and Operating Experience of the Solar Two Project', Sandia Report SAND2000-2598, November 2000

Electric Salt Heaters in Minimum Flow Recirculation Lines

One example is the piping arrangement for the external electric salt heaters for the salt storage tanks. At one commercial project, two 100-percent salt heaters could receive salt from any of the 3 hot salt pumps in the hot tank, or salt from either of the 2 cold salt attemperation pumps in the cold tank. However, a total of 9 salt valves were required to either direct the flow as needed or to drain the equipment. In contrast, an alternate design would locate a separate electric heater in the minimum flow recirculation line for each of the salt pumps. Each heater would be located downstream of the minimum flow recirculation valve, and each heater would be located at an elevation above the salt tanks. The minimum flow valve would keep the electric heater flooded during operation, and the piping would be arranged such that the piping and the heater drain automatically when the pump is not in operation. Granted, a typical project might require 2 (or 3) hot salt pumps and 2 attemperation pumps, and as such, would require 4 (or 5) electric salt heaters. Further, the 4 (or 5) heaters could be more expensive than two 100-percent capacity heaters. However, the improvement in plant availability due to the elimination of 9 salt valves will more than offset the marginal cost of the smaller electric heaters. Plus, the use of salt heaters on each of the pumps provides essentially the same redundancy as the two 100-percent heaters in the example commercial project.

Pump Discharge Check Valves

Conventional swing check valves should be provided in the discharge lines on each of the salt pumps. During the early stages of the startup process, the required flow rate of hot salt is very small; something in the range of 2 to 20 m^3/hr. If the flow of hot salt were to be initiated by selecting a pump speed, and then opening an isolation valve in the pump discharge line, the likelihood that a flow as small as 2 m^3/hr could be established is very low. The more likely scenario is that one of the following conditions will occur:

- The discharge pressure of the hot salt pump is slightly too high, in which case the initial flow of hot salt is too high (20 m^3/hr).

- The discharge pressure of the hot salt pump is slightly too low, and cold salt starts to flow backwards towards the hot salt pump.

In either condition, it will not be possible to provide the required control of the mixed salt temperature at the entrance to the steam generator.

The best method for accomplishing this task is to provide a conventional swing check valve at the pump discharge. To initiate a flow, a hot salt pump speed is selected which provides a discharge pressure that is slightly below the cold salt pump discharge pressure. The differential pressure causes the hot salt pump check valve to close. (The pump is protected from overheating by the flow through the minimum flow recirculation line.) The speed of the hot salt pump is then increased in increments of 0.1 percent. The discharge pressure of the hot salt pump eventually rises to a value that is slightly greater than the cold salt pump discharge pressure, the check valve starts to open, and a very small, and stable, flow of hot salt is established.

The shutdown procedure for the steam generator is essentially the mirror image of the startup procedure. As such, the requirement for a check valve on the hot salt pump during startup is mirrored by a requirement for a check valve on the cold salt attemperation pump during shutdown.

15.6.2 Startup and Shutdown Procedures

A proposed heat exchanger and salt valve arrangement is shown in Figure 15-5. The startup valve adds an artificial pressure drop during startup and shutdown. Valve 1 and Valve 2 direct the flow of hot salt early in the startup, and late in the shutdown, process.

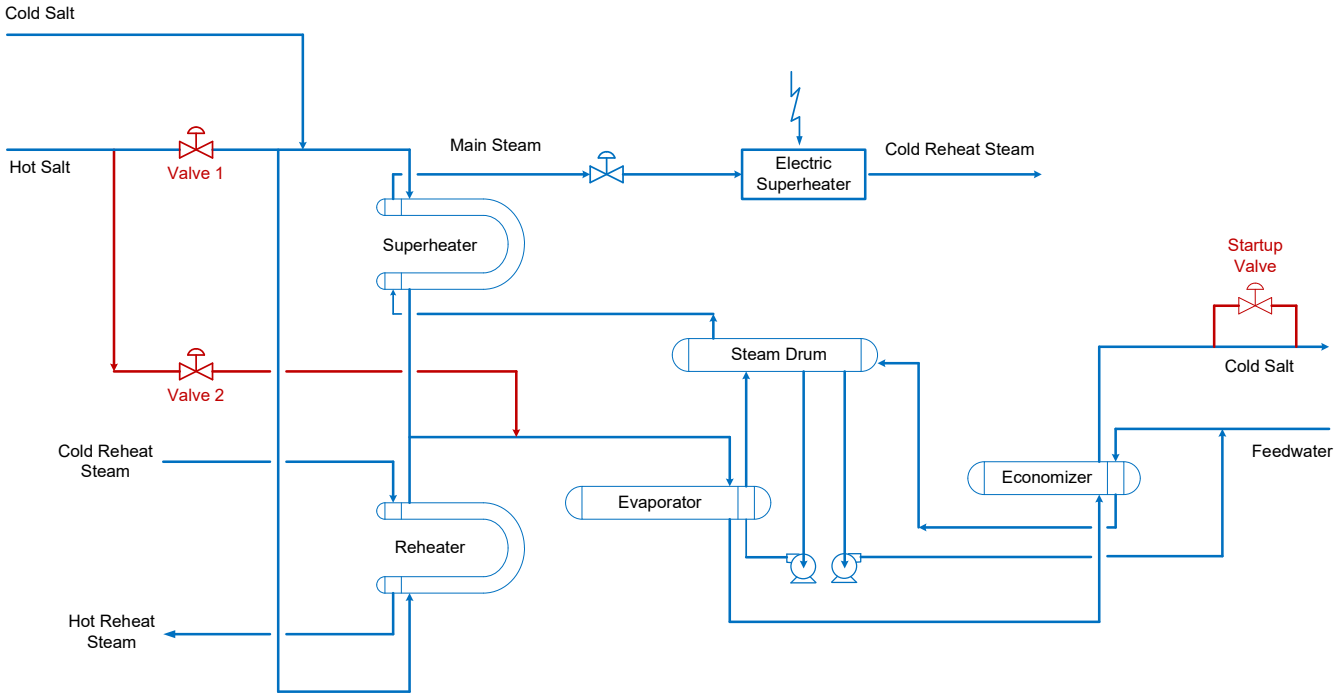

Figure 15-5 Steam Generator Heat Exchanger and Valve Arrangement

Early in the startup process, the temperature of the mixed salt upstream of the superheater / reheater is close to the cold salt temperature. As such, the temperature of the live steam at the hot end of the superheater is also close to the cold salt temperature. To ensure that the temperature of the salt at the cold end of the preheater does not challenge the salt freezing temperature, the saturation pressure in the steam drum is maintained at a nominal value of 100 bar. When live steam from the superheater at 100 bar is throttled to a pressure which can be accepted by the reheater (~ 30 bar), the temperature of the cold reheat steam can drop close to, or slightly below, the freezing temperature of the salt. To prevent salt from freezing at the cold end of the reheater, the temperature of the cold reheat steam is raised by means of an electric steam superheater.

Isothermal Steam Production

As discussed in Section 15.4, the steam flows in the superheater and in the reheater during startup necessarily span the range of 0 percent to the minimum flow rate allowed by the vendor (~ 16 percent). Low flow rates often produce poor flow distributions, which raise the possibility of undesirable temperature and stress distributions. However, if the heat exchanger is operating under isothermal conditions between flow rates of 0 and 16 percent on both the shell-side and the tube-side, then the potential for damaging stress distributions is largely eliminated.

One method for operating the superheater and the reheater under isothermal conditions is to establish a shell-side flow rate of cold salt at a temperature of 295 °C, and simultaneously establish a tube-side flow rate of steam at a temperature of 295 °C. The shell-side conditions are established by operating the cold salt attemperation pump at the design speed. The tube-side conditions are established by 1) selecting a set point pressure of 80 bar for the throttle valves in the steam bypass system to the condenser, and 2) supplying hot salt to a mixing station upstream of the evaporator, and 3) isolating the hot salt flow to the mixing station upstream of the superheater / reheater.

Step 0 - Overnight Hold

During overnight hold, cold salt is supplied to the steam generator, as shown in Figure 15-6. No steam production occurs, and the temperature of the salt passing through the heat exchangers decays only slightly due to the moderate heat losses from the heat exchangers and the system piping.

The recirculation pump from the steam drum to the cold end of the preheater is in service. Steam drum makeup water from the Rankine cycle combines with the recirculation flow at a point just upstream of the preheater. The direct contact heat exchange ensures that the relatively cold makeup water does not cause salt to solidify at the cold end of the preheater.

The startup salt valve at the cold end of the preheater is set to a position which provides the desired additional pressure drop for the salt pumps later in the startup process. A set of hydraulic calculations for a representative commercial project show that the startup valve can be set to a fixed position for Steps 0 through 4 discussed below.

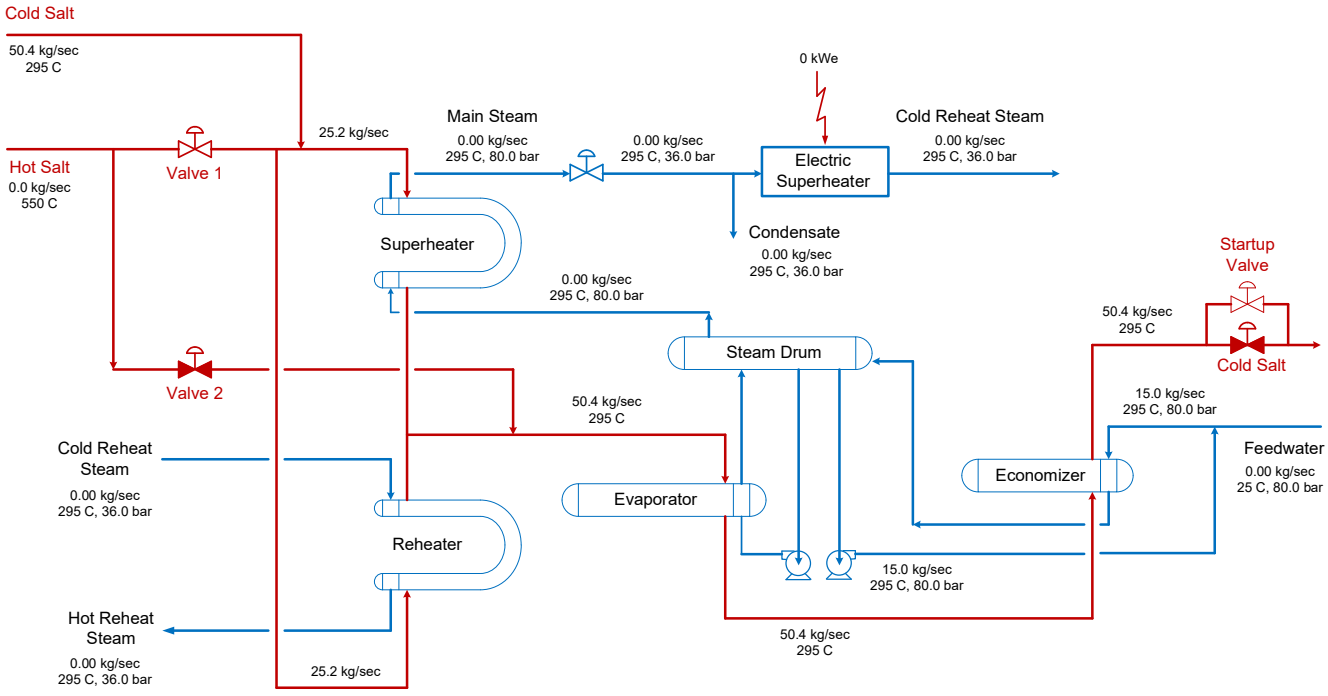

Figure 15-6 Step 0 - Overnight Hold

Step 1 - Isothermal Steam Production

The basic flow arrangement for the first step in this process is shown in Figure 15-7. The salt and steam flow rates are based on a nominal 125 MWe Rankine cycle with two 50-percent steam generator trains.

Cold salt, at a temperature of 295 °C, is supplied to the hot end of the superheater and to the hot end of the reheater. Simultaneously, saturated steam, at a temperature of 295 °C, is supplied to the superheater, and cold reheat steam, at a temperature of 295 °C, is supplied to the reheat. As such, no heat transfer occurs in either heat exchanger, and the temperature of the salt leaving both heat exchangers is 295 °C.

At the salt mixing station upstream of the evaporator, hot salt is added to the flows leaving the superheater and the reheater. This raises the temperature of the salt entering the evaporator to 428 °C, which provides the thermal energy required to 1) generate saturated steam, at a temperature of 295 °C, for delivery to the superheater and the reheater, and 2) establishes steam flow rates equal to 20 percent of the design flow rates in the both superheater and the reheater.

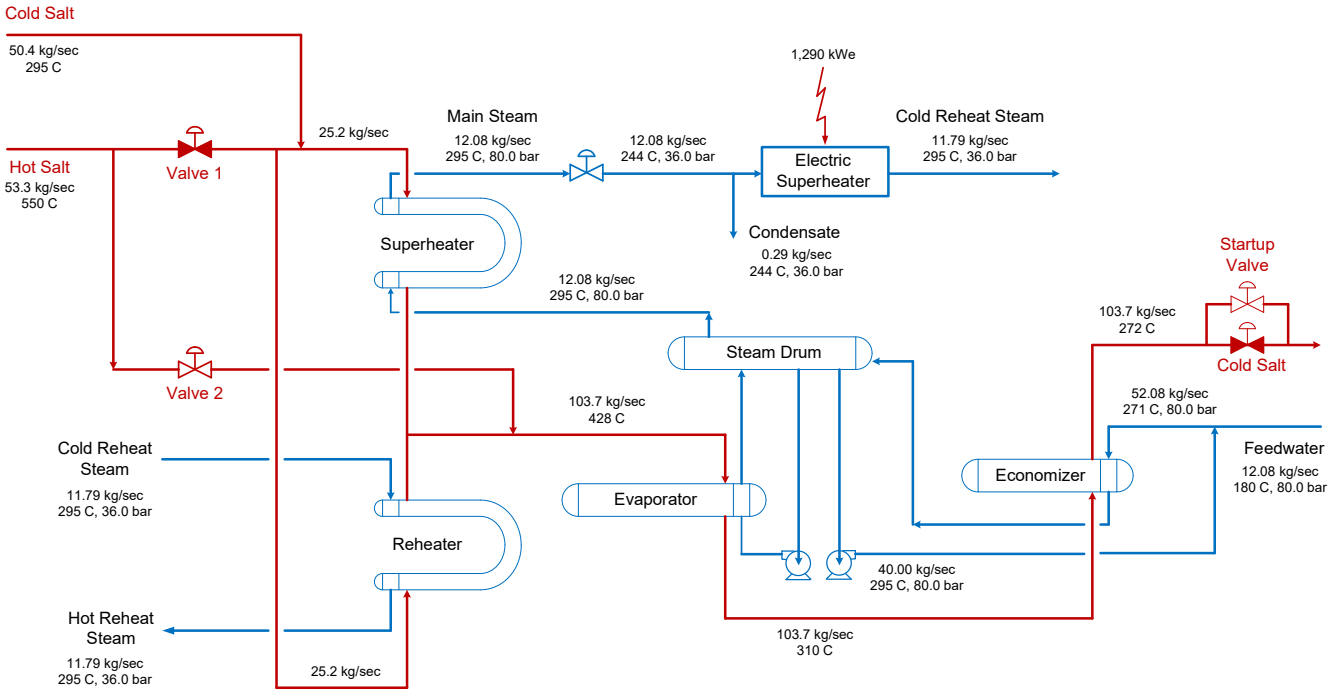

Figure 15-7 Step 1 - Isothermal Steam Production

The saturated steam pressure of 80 bar is established in the drum by the high pressure throttle valve in the steam bypass system to the condenser. A steam flow rate equal to 20 percent of the design flow rate is larger than the minimum required by the vendor (16 percent). However, the steam flow rate decays to 16 percent in the Step 2 below.

Throttling live steam, at a pressure of 80 bar, to the maximum pressure which can be accepted by the reheater (36 bar), results in a decrease of the steam temperature to the saturation temperature corresponding to 36 bar (244 °C). The quality of the steam leaving the high pressure throttle valve is on the order of 97 percent, and 0.3 kg/sec of condensate is removed in a trap prior to the steam entering the cold end of the reheater. To ensure that no heat transfer occurs in the reheater, the temperature of the cold reheat steam is increased to the cold salt temperature (295 °C) by means of a 1.3 MWe electric steam superheater.

The flow rate and temperature of the makeup water from the Rankine cycle are 12.1 kg/sec and 180 °C, respectively. The feedwater temperature assumes that auxiliary steam, at a nominal pressure of 10 bar, is supplied to the deaerator for preheating. The recirculation of saturated water from the drum to the cold end of the preheater raises the mixed feedwater temperature to a value of about 271 °C, which is high enough to prevent salt from freezing at the cold end of the preheater.

As a technical note, all commercial solar projects use an auxiliary steam generator for equipment preheating and to supply steam to the turbine shaft seals to establish a vacuum in the condenser. An auxiliary steam generator is required, as steam generator vendor generally

does not permit the use of the main evaporator for small steam flow rates over extended periods of time.

Superheated Steam Production

Step 2 - Switching the Salt Mixing Station

Once flows of 20 percent have been established on the tube-sides of the superheater and the reheater, the hot salt / cold salt mixing station is switched from a point upstream of the evaporator to the normal point upstream of the superheater / reheater, as shown in Figure 15-8.

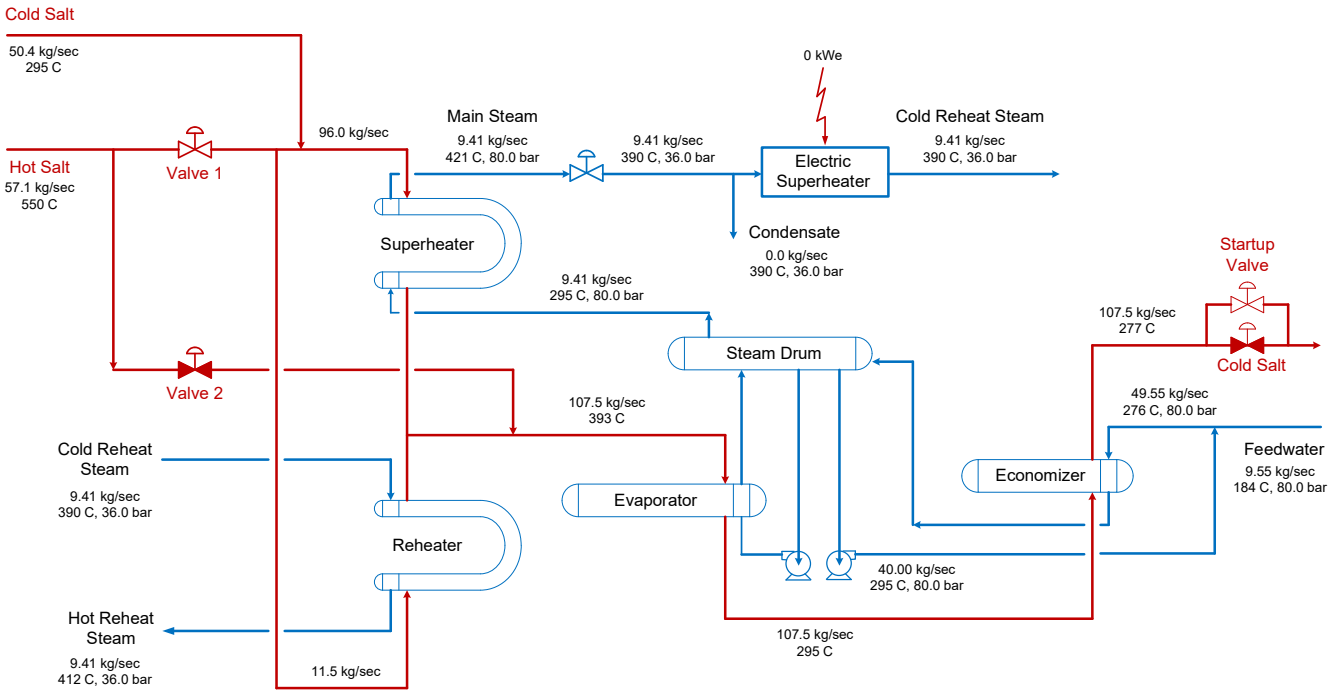

Figure 15-8 Step 2 - Live Steam and Hot Reheat Steam Production

The transition basically involves opening Valve 1 and closing Valve 2 at rates which keep the following sum a constant value: $Cv_{Valve\ 1} + Cv_{Valve\ 2}$. Under these conditions, no changes occur in either the hot salt or the cold salt flow rates, and the transition should be hydraulically stable. The rates at which Valve 1 and Valve 2 move are:

- Amenable to calculation, based on curves of Cv versus valve position
- Programmed in the DCS such that the mixed salt temperature at the hot end of the evaporator decreases at no more than the vendor limit of 10 °C/min

- Programmed in the DCS such that the mixed salt temperature at the hot end of the superheater / reheater increases at no more than 10 °C/min.

Moving the mixing station to a point upstream of the superheater / reheater raises the temperature of the salt entering both the superheater and the reheater. As such, heat transfer now begins in the superheater and in the reheater, which would normally increase the thermal demand on the steam generator. However, one of the goals of the transition is to maintain the cold salt and the hot salt flow rates fixed in both Step 1 and Step 2. With the flow rates fixed, the feedwater flow rate decreases to a new value of 9.55 kg/sec to offset the increased thermal demands of the superheater and the reheater. A feedwater flow rate of 9.55 kg/sec corresponds to the 16 percent minimum value specified by the vendor.

Step 3 - Turbine Synchronization

At the end of Step 2, the steam generator has nominal live steam and hot reheat steam flow rates of 16 percent, and live steam and hot reheat steam temperatures slightly above 410 °C. This combination of steam flow rate and temperature should be adequate to admit steam to the turbine under the conditions of a warm start, accelerate the turbine to synchronous speed, synchronize the turbine, and load the turbine to a value which is high enough to prevent a trip on reverse power. (If the turbine is undergoing a cold start or a hot start, then steam can be admitted to the turbine starting when the steam temperatures are lower than, or higher than, 410 °C, respectively.)

The steam supplied to the turbine is diverted from the turbine bypass system. Whatever steam is not required by the turbine continues to be bypassed to the condenser.

Step 4 – Low Load Operation

Once the turbine is synchronized, the extraction feedwater heaters are placed in service. However, saturated water from the steam drum continues to be recirculated to the cold end of the preheater to maintain the temperature of the salt at the cold end of the preheater at acceptable values.

To increase the thermal output of the steam generator, and to increase the live steam and the hot reheat steam temperature, the speed of the hot salt pump is increased. The increase in the discharge pressure of the hot pump will result in a decay in the flow rate from the attemperation pump. The rate at which the speed of the hot salt pump is increased is such that the mixed salt temperature at the hot end of the superheater / reheater satisfies the vendor limit of 10 °C/min.

At some point in this transition, the speed of the attemperation pump will need to be reduced. The rate at which the speed of the attemperation pump is reduced is such that the mixed salt temperature at the hot end of the superheater / reheater satisfies the vendor limit of 10 °C/min. Eventually, the flow rate from the attemperation pump stalls. A check valve on the discharge of the attemperation pump prevents a reverse flow through the pump. At this point, the

attemperation pump can be stopped, and only salt from the hot pump is supplied to the steam generator.

Once the steam generator trains reaches its design temperature profile (565 °C at the hot end of the superheater / reheater, and 295 °C at the cold end of the preheater), the salt isolation valve at the cold end of the preheater can be opened and the startup valve closed. Opening the isolation valve will reduce the pressure drop in the system, and the speed of the hot salt pump will need to be reduced to maintain a nominally constant flow rate of hot salt. It's unlikely that the valve transition can be accomplished without a change in the hot salt flow rate. However, even if the flow rate does change, the normal temperature profile along the steam generator has already been established, and the potential for thermally shocking the heat exchangers is very low.

Throughout Steps 1 through 4 above, the goals of the process design are as follows:

1. Avoid the use of pressure and flow measurements to set the relative flow rates of hot salt and cold salt. The accuracy of the pressure and flow instruments are inconsistent with the accuracy with which the flow rate of hot salt must be accelerated to satisfy the vendor limits on rates of temperature change.

2. During startup and shutdown, the salt-side pressure drops are very low. To reduce the potential for oscillations in the flow rates from pumps operating in parallel, the 1) the system pressure drop is artificially increased by means of a startup valve, and 2) the following valves are set to fixed positions: the startup valve at the cold end of the preheater; the minimum flow recirculation valve for the hot salt pump; and the minimum flow recirculation valve for the attemperation pump.

3. Process control inputs should be limited to those items which are accurate and reliable. In general, this limits the inputs to temperature measurements.

4. Process control outputs should be limited to those items which can be accurately measured and controlled. To a first order, this includes the speeds of the hot salt and the attemperation pump.

5. Items 2, 3, and 4 are satisfied if the mixed salt temperature to, and the thermal duty of, the steam generator are set by adjusting the relative speeds of the hot salt and the attemperation pumps.

6. During various stages of startup and shutdown, the flows from the hot salt and the attemperation pump will approach a value of zero. To prevent reverse flows through the pumps, conventional check valves should be provided in the discharge lines. A total of 4 swing check valves were used at the Solar Two demonstration project, and the valves proved to be reliable.

To shut down the steam generator, the turbine is brought to the minimum load, and then tripped to preserve the metal temperatures in preparation for the next startup. The steam generator is shut down in essentially a reverse of the 4 steps above.

15.6.3 Heat Exchanger Fabrication Techniques

A common joining technique for the tube-to-tubesheet connection is to strength weld the ends of the tubes to the face of the tubesheet, and then plastically deform the tubes into the tubesheets. However, there are alternate joining techniques that use welded connections.

Header / Coil

In conventional heat exchangers, the tubesheet must withstand the pressure differential between the shell- and the tube-side fluids. If the differential pressure is high, then the tubesheet must be thick (150 to 200 mm), as a flat plate is structurally inefficient when subjected to bending loads. However, thick metal sections are generally undesirable in equipment which must thermally cycle each day. The problems with transient stresses are compounded if thick metal sections are joined to thin metal sections.

A more efficient structure for withstanding a large differential pressure is a pipe section, particularly if the high pressure fluid is on the inside of the pipe. A section of pipe can act as a tubesheet, using the following arrangement:

- A series of holes are drilled along the length, and around the circumference, of the pipe
- Short, tapered nozzles are welded to the pipe at each hole
- The ends of the heat exchanger tubes are welded to the ends of the short nozzles.

The fabrication process is illustrated in Figure 15-9.

This fabrication approach offers three important advantages for equipment in cyclic service:

1. For a given differential pressure, the thickness of a pipe wall will be much less than the thickness of a flat tubesheet. Reducing the thickness of metal sections is generally beneficial in terms of controlling transient stresses.
2. All of the tube-to-tubesheet connections are welded. Leaks are much less likely to develop in a welded connection than in a friction connection.
3. The nozzles between the pipe and the tubes are tapered, which provides a transition in metal thickness. A tapered transition, rather than an abrupt transition as occurs between a flat tubesheet and a tube, reduces the transient thermal stresses.

Figure 15-9 Example of Header / Coil Heat Exchanger Fabrication [52]

Internal Bore Welding

In an internal bore welded design, tapered nozzles are machined from the face of a flat tubesheet. The ends of the tubes are then welded to the ends of the nozzle. Due to space limitations, the nozzle-to-tube butt welds are performed by a robotic welder inside the tube. A cross section example of the tubesheet and the welded connection is shown in Figure 15-10.

This fabrication approach offers many of the benefits associated with the header / coil design.

Allowable Rates of Temperature Change

Heat exchanger designs based on strength welding the tubes to the tubesheet, and then expanding the tubes into the tubesheet, have an allowable rate of temperature change of 8 to 10 °C/min, depending on the vendor.

Informal discussions with Aalborg CSP, a supplier of header / coil designs, indicate that allowable rates of temperature change are on the order of 12 to 13 °C/min.

The difference between the two allowable rates is not a large value. However, experience with commercial projects has shown that process designs have difficulties complying with a vendor limit of 10 °C/min. Relaxing the limit to 12 °C/min will not solve the problems with current process designs. However, revisions to the process design, as discussed above, in

[52] https://energetica-india.net/news/aalborg-csp-header-and-coil-technology-celebrates-its-10-years-leakage-free-anniversary

combination with higher allowable limits set by the vendor, should lead to needed improvements in steam generation system availability.

Figure 15-10 Example of an Internal Bore Welded Tube-to-Tubesheet Connection

15.6.4 Material Selection in the Evaporator

In a number of commercial projects, the tube material in the evaporator is Type 347H stainless steel. This material certainly provides the strength necessary for operation at both the normal salt inlet temperature of 450 °C, and the tube-side design temperature of 510 °C. Further, the tube material matches the materials in the tubesheet and in the shell, which simplifies the welding processes. Nonetheless, the choice of materials does not have unanimous concurrence [53]. For example, although the steam generator is not designed to ASME Section I requirements, Section I does not permit the use of stainless materials in evaporators due to the potential for stress corrosion cracking. Similarly, European norm EN12952-3, Water Side Boilers, does not permit the use of austenitic materials in boilers or in steam drums.

The stress corrosion mechanism is promoted by chlorides, caustic, or reduced sulfur which may be present in the feedwater. Further, stainless steel is susceptible to pitting corrosion if deposits accumulate on local portions of the surface but do not accumulate on portions adjacent to the deposits. The deposits can result from corrosion of the carbon steel components in the condensate system. The corrosion can result from poor control over the pH and the dissolved oxygen in the feedwater.

[53] Aalborg CSP, 'NE1 700 MW CSP Project, Material Selection for Evaporator Tubes, CT-SGS', Document 40088C-D156-00006, Revision A, December 2018

An alternate to Type 347H as the tube material is a ferritic alloy with a high chromium content, such as T91 [54]. This material offers acceptable corrosion resistance to salt at the normal operating conditions, and was successfully used in the first of two evaporators at the Solar Two demonstration project. Further, the material does not use nickel as an alloying elements; as such, it is largely immune to stress corrosion cracking mechanisms.

[54] Bradshaw, R. W. and Goods, S. H. (Sandia National Laboratories, Livermore, California), 'Corrosion of Alloys and Metals by Molten Nitrates', Sandia Report SAND2000-8727, August 2021

16. Valves in Salt Service

16.1 Valve Types

Isolation valves in salt service, including gate, ball, angle plug, swing check, and triple offset butterfly, will provide similar isolation characteristics to service in water. Similarly, control valves in salt service, including globe and angle plug, will provide similar control characteristics to service in water. However, not all types of valves are suitable for service in salt if the operating periods are measured in months to years.

Salt is an oxidizing material, and will develop oxide layers on all types of iron and nickel alloys. If the valve uses sliding surfaces, such as a gate valve or a ball valve, then oxide layers will develop on both the sliding and the stationary faces. Further, the oxide layers can mechanically bond to one another if the valve is not moved frequently; i.e., every few days. The corrosion process results in valve binding, even to the extent that the valve operators cannot develop the forces required to overcome the friction and the bonding forces. At the Solar Two demonstration project, the pneumatic actuator on an 8 in. ball valve developed forces high enough to plastically deform the valve stem, yet the valve remained in the open position.

In general, the only types of valves suitable for salt service are the ones where the plug moves perpendicular to the seat. The oxide layers still develop on the sealing surfaces. However, the oxide binding forces are lower if the surfaces move perpendicular to, rather than parallel to, one another. As such, the only suitable valve types are globe, angle plug, and triple offset butterfly. Nonetheless, it can be noted that some of the triple offset butterfly isolation valves at a commercial project developed internal leaks over a period of about 3 years. The source of the leakage was not fully identified, but it may be deformations of the valve bodies that are higher than expected due to the transmission of piping loads that are higher than expected. The solution for the commercial project was to replace the triple offset butterfly valves with valves which have a higher body rigidity; i.e., globe valves.

16.2 Stem Sealing

A common stem sealing material is graphite. The material is soft, which allows it to readily conform to the shape of the stem. Also, in the absence of an oxidizing environment, it is thermally stable. However, in salt service, the salt oxidizes the graphite to CO_2, and the packing eventually disappears.

At the Solar Two project, the recommended stem packing consisted of alternating layers of 1) Teflon washers, and 2) Inconel wire braids impregnated with graphite. Over time (weeks to months), the graphite in the braid oxidized, and the stem packings required periodic replacement of the Inconel braids. In general, this combination of packing materials was judged as marginally adequate. In subsequent commercial projects, other stem packing materials have been used, including various fluoropolymers, mica, and vermiculite. In some cases, the packing performed as intended, and in other cases, the packing developed leaks

almost immediately. In general, a robust packing material, with a longevity measured in years, has yet to be identified.

To this end, the only stem seal which has been shown to be effective in preventing a leak is a bellows seal. This, in turn, implies that the preferred valve types are limited to those which can use a bellows seal; i.e., valves with translating stems, such as globe and angle plug valves.

As might be expected, this approach has met with resistance in commercial projects:

- A bellows stem seal is much more expensive than a packing stem seal. Budgetary estimates from a study conducted for DOE indicate that adding a bellows stem seal can triple the cost of a valve

- For isolation service, large globe valves are more expensive than triple offset butterfly valves

- The bellows may, under specific sets if circumstances, rupture. These circumstances include moving the valve with frozen salt in the bellows, or exposing the bellows to high transient pressures generated by a leak in a heat exchanger.

Using bellows seals on valves will increase the capital cost of the project. However, the cost penalty can be reduced by developing process designs that minimize the use of valves. One example is the piping arrangement for storage tank recirculation heaters, discussed in Section 15.6.1. The cost penalty is also likely to be offset by an increase in plant availability. Leakage past the valve stem seals exposes the heat trace cables on the valve body and on the adjacent piping to salt. The cables operate at temperatures which are high enough (> 650 °C) to decompose the salt. Several of the decomposition products are various oxides, which aggressively corrode the outer metal covering on the heat trace cables. Corrosion lifetimes are often measured in weeks. Once the covering corrodes, the internal heating cables are exposed to moisture, and can fail in a matter of days. Failed cables lead to immovable valves and frozen salt piping, which can necessitate forced outages, lasting hours to days. A project economic analysis will often show that the marginal improvement in plant availability and revenue, due to a properly functioning heat trace system, justifies the marginal expense for bellows stem seals.

In a thermal storage system in a commercial parabolic trough project, the salt control valves used bellows stem seals. The valve vendor supplied an engineered insulation enclosure for the valve body and the bellows region. The enclosure included the requisite heat trace cables and control thermocouples. The valve, bellows, and insulated enclosure are operating at expected, with no stem sealing failures due to frozen salt in the bellows.

16.3 Triple Offset Butterfly Valves

In general, and particularly for large valves (> 18 in.), triple offset butterfly valves are less expensive than globe valves. Since the valve provides good sealing characteristics, there is a

motivation to use the valves wherever possible. Nonetheless, triple offset valves carry potential liabilities, as follows:

- Conventional stem packings, rather than bellows seals, must be used
- In large sizes, the valve bodies are not as rigid as those for globe valves. There have been instances in which large forces needed to be applied to piping to align the piping with the valve bodies. Once the welding was complete, the alignment forces were removed, which can result in a deformation of the triple offset valve body and a reduction in sealing effectiveness.

16.4 Isolation Valves

In the process design, careful consideration should be given to selection of globe, angle plug, and triple offset valves for isolation service. The detrimental effects on plant availability associated with leakage past valve stems should not be discounted. The selection of a valve with a bellows seal will likely increase the capital cost of the project, yet decrease the levelized energy cost.

16.5 Control Valves

For valve sizes of 20 in. and below, the preferred valve for control service is a globe valve with a bellows seal. For pipe sizes of 24 in. and above, there is a temptation to use a triple offset valve for control service due to cost considerations. However, the Cv versus percent open curves for triple offset valves show strong non-linear behavior, which can lead to difficulties in process control. If a control valve larger than 20 in. is required, the preferred option would be two 50-percent capacity globe valves with bellows seals.

16.6 Alternates to Globe and Triple Offset Butterfly Valves

The discussion above concentrates on the relative benefits and liabilities of globe valves and triple offset butterfly valves. However, alternate valve designs may also be available from commercial suppliers. Early in the project, discussions can be held between the project and potential valve suppliers to determine if alternate valve concepts could offer a suitable combination of structural rigidity, pressure drop, control linearity, hermetic stem sealing, and cost.

17. Piping in Salt Service

In parabolic trough projects using organic heat transfer fluids, both the cold salt and the hot salt piping will be carbon steel, with a typical specification of ASTM A106, Grade B or C.

In parabolic trough plants using inorganic heat transfer fluids, and in central receiver projects, the hot salt piping will be a 300-series stainless steel. The principal candidate materials include Type 304L, 316L, 304H, 316H, and 347H. The 'L' signifies a low carbon alloy, with a maximum carbon content of 0.02 percent. The 'H' signifies a high carbon alloy, with a minimum carbon content of 0.04 percent. Adding carbon to the alloy disrupts the lattice structure, which improves the resistance to creep.

The design temperature in both types of plants is above 538 °C. As such, if the allowable stress values for the piping are to be obtained from Subpart 1 in Section II D of the Code, then the 'H' grades of stainless steel will be required. For example, in Subpart 1, Type 304L is not permitted for equipment designed to Section III or to Section VIII Division 1 at temperatures above 427 °C due to the potential for dimensional changes due to permanent deformations. In contrast, ASME B31.3 lists allowable stresses for the 'L' grades of stainless steel piping for temperatures up to 815 °C.

17.1 Type 304H and Type 316H

At temperatures in the range of 500 to 600 °C, the carbon in Type 304H and Type 316H reacts with chromium to form chromium carbide. The carbide is preferentially formed at the grain boundaries, as there is space in the matrix to do so. This results in a reduction in the corrosion resistance of the alloy at the grain boundaries. If the alloy is exposed to a combination of chlorides (present in the salt), tensile stresses, and liquid water, then cracks can start to develop between the grain boundaries. Once the cracks start to develop, the process cannot be stopped, even if the liquid water is removed. This type of corrosion is known as intergranular stress corrosion cracking.

With the plant in normal service, the metal temperatures never fall far enough for the pipe to be exposed to liquid water. This, in and of itself, is enough to prevent intergranular stress corrosion cracking. However, the pipes can be exposed to liquid water if, during an outage, the equipment cools to ambient conditions, and then 1) it rains, or 2) nighttime temperatures fall below the dew point. Under these conditions, intergranular stress corrosion cracking can develop.

17.2 Type 304L and Type 316L

One method for reducing the potential for intergranular stress corrosion cracking is to use an 'L' grade of stainless steel. With a low carbon content, the potential to form chromium carbide is reduced. This, in turn, limits the depletion of chromium at the grain boundaries, which preserves the resistance to corrosion at the grain boundaries. However, the low carbon content reduces the resistance to creep, which can lead to dimensional changes due to permanent strains.

The allowable stresses for Types 304 L and 316L, at a temperature of 565 °C, are shown in Table 17-1. Also shown for reference are allowable stresses for Types 304H, 316H, and 347H.

Table 17-1 Allowable Stresses (MPa) for 300-Series Stainless Steel Piping at 565 °C

Type	Section II D, Subpart 1	B31.3
304L	Not permitted	43.4
316L	Not permitted	74.5
304H	85.5 [1], 69.6 [2]	84.1
316H	104.1 [1], 77.2 [2]	100.0
347H	111.7 [1], 92.4 [2]	117.9

Notes:
1. Use of these stresses may result in dimensional changes due to permanent strain.
2. Lower allowable stress to reduce the potential for dimensional changes.

The principal penalty to the use of an L-grade material for piping is a lower allowable stress, which translates to thicker wall sections. Since piping is typically priced on $/kg commodity basis, and since the unit prices for Types 304, 316, and 347 all fall within a similar range, selecting an L-grade material increases the cost of the piping by factors in the range of 20 percent to 150 percent.

It can be noted that there is some experience with the use of 304L for hot salt piping. At the Solar Two central receiver project, the design of the downcomer was developed using the properties of an H-grade stainless steel. However, the downcomer was fabricated using 304L, and the mismatch was discovered only after the downcomer had been installed. Rather than replace the downcomer with an H-grade material, the pipe stress analysis was repeated, but with iterations on the supports and the anchors until the stresses reached allowable values. During the (limited) 3-year life of the demonstration project, the downcomer operated as intended.

17.3 Type 347H

To avoid potential problems with intergranular stress corrosion cracking, most commercial projects have adopted Type 347H as the hot salt piping material. The alloy is essentially Type 304H with the addition of niobium. The niobium bonds with the carbon in the matrix to form niobium carbide. This reduces the quantity of free carbon available, which, in turn, reduces the potential for the formation of chromium carbide. If the chromium carbide concentration is reduced, then the potential for intergranular stress corrosion cracking is also reduced.

17.3.1 Knife Line Attack

Nonetheless, the alloy is not without its own set of problems. During welding, the metal temperatures are high enough to dissolve the niobium carbide. This makes available free carbon in the matrix. As the weld cools, the metal temperatures initially favor the reformation of niobium carbide. However, the weld typically cools at a rate that does not allow the equilibrium concentration of niobium carbide to form. Free carbon remains available in the matrix, which then allows chromium carbide to form as the weld continues to cool.

The welding process often results in 5 metal chemistry zones. Zones 1 and 5 are the original parent metal, to the left and to the right of the heat affected zone. Zone 3 is the center of the weld, where the concentration of niobium carbide is relatively high. Zones 2 and 4, which are in the heat affected zone, tend to have low concentrations of niobium carbide, but relatively high concentrations of chromium carbide. Zones 2 and 4 can then be susceptible to intergranular stress corrosion cracking in a phenomenon known as knife line attack. Knife line attack has been observed in Type 347H pipe fittings at the 10 MWe Solar Two demonstration project, and in Type 321H receiver tubes at a parabolic trough test facility in Spain.

17.3.2 Post Weld Heat Treatment of Type 347H

To reduce the potential for knife line attack, the weld can undergo a post weld heat treatment. The heat treatment involves the following steps:

- The residual weld stresses are partially relieved by raising the metal temperature to a nominal value of 650 °C. The goal is to reduce the potential for hot reheat cracking. Hot reheat cracking is a phenomenon in which the interior of the grain becomes strengthened by the precipitation of carbides during welding. Relaxation of residual stresses then occurs in the form of creep deformation at the grain boundaries, which can lead to cracking along the boundaries

- After a hold period for stress relaxation, the welds are solution annealed. The metal temperatures are raised high enough (~1,150 °C) to dissolve both the chromium carbide and the niobium carbide

- The metal temperature are held for a period which is long enough (~1 hour) for the equilibrium concentration of niobium carbide to form. This process reduces, but does not eliminate, all of the free carbon; i.e., there is an equilibrium concentration of niobium carbide, chromium carbide, and free carbon

- To reduce the potential for chromium carbide formation with the remaining free carbon, the weld zone is cooled rapidly through the temperature range which preferentially forms chromium carbide.

As might be expected, the heat treatment process is time consuming and not without expense. Further, the process is conducted outdoors, and if the time-temperature requirements cannot

be accurately met, then it is possible to develop cracks at the weld or to increase, rather than decrease, the concentrations of chromium carbides.

17.4 Project Decisions

The candidate piping materials, in order of probable commercial preference, are as follows:

- Type 347H: The material offers 1) the highest allowable stress among the 300-series stainless steels, which results in the lowest piping mass and installed costs, and 2) the addition of niobium to the alloy reduces the potential for intergranular stress corrosion cracking that can occur in the other H-grade stainless steels. The principal liability is a (relatively low) risk of knife line attack should the piping be exposed to liquid water.

- Type 304L / 316L: Due to the low carbon content, the material is largely immune to intergranular stress corrosion cracking, and due to the absence of niobium, the material is largely immune to knife line attack. The principal liabilities are relatively low allowable stresses, which result in an increase in the pipe mass and the installed cost.

- Type 304H / 316H: The allowable stresses for 304H / 316H are higher than the values for the L-grade materials, but somewhat less than the values for Type 347H. As such, the mass of the piping and the installed cost should fall between these cases. The principal liability is a susceptibility to intergranular stress corrosion cracking should the pipe be exposed to liquid water during a maintenance outage.

Type 347H may be the preferred piping material, for the reasons noted above. Nonetheless, the project must make a decision as to whether, or not, to perform a post weld heat treatment of the piping.

There is no mandatory requirement to perform a heat treatment, as the Code does not require the heat treatment of stainless materials. Further, anecdotal evidence from commercial projects indicates that the reliability and the availability of welds that receive a heat treatment are essentially the same as the reliability and the availability of welds that do not receive a heat treatment. Nonetheless, there may be a benefit to performing a heat treatment, as follows:

- Hot reheat cracking can occur in the heat affected zones of weld when reheated in the temperature range from 500 to 700 °C [55]. At this temperature, residual stresses due to welding relax by creep. The heat affected zone may not be able to accommodate this strain without cracking if the microstructure had been sufficiently altered during welding. Pipe temperatures above 565 °C are not expected during normal plant operation. However, metal temperatures in the range of 600 to 700+ °C can be expected if a heat trace circuit has a lengthy duty cycle of 100 percent due, for example, to a contactor sticking in the closed position. A post weld heat treatment might allow the welds in this

[55] Auzoux, Q., et al, (CEA Saclay DEN/DMN/SRMA Yvette, France), "Reheat cracking in austenitic stainless steel", 2001, https://www.osti.gov/etdeweb/servlets/purl/20401493

zone to avoid hot reheat cracking associated with an infrequent, but not unexpected, failure in the heat trace system.

- During the life of the project, the probability that the hot salt piping will be cooled to ambient temperature, and then opened to the ambient, during a maintenance outage is perhaps one-half to two-thirds. The exposure could result from repairs to a valve, inspection of a heat exchanger, or replacement of a pressure transmitter. During this time, liquid water could come into contact with the inside of the pipe due to rain, water leakage from a steam generator heat exchanger, or from ambient temperatures below the dew point. In addition, salt leakage from valve stem seals or from gaskets on pressure transmitters can expose both the insulation and the exterior of the pipe to salt. If the insulation is removed for replacement, liquid water can come into contact with the outside of the pipe due to rain or ambient temperatures below the dew point. In each case, a post weld treatment of the welds will reduce the potential for knife line attack at the edges of the welds.

In the final analysis, a post weld heat treatment can reduce the risk of hot reheat cracking and intergranular stress corrosion cracking. Nonetheless, in the absence of a post weld heat treatment, the potential for hot reheat cracking and intergranular stress corrosion cracking is generally regarded as low to moderate. The project will need to conduct a cost / benefit analysis to determine if the costs and the risks of post weld heat treatments justify the benefits of the heat treatments.

17.5 Pipe Maintenance

Once the plant enters commercial service, the salt piping, valves, and instruments will have been exposed to salt. When this equipment requires maintenance, the equipment will be cooled to ambient temperature. As such, the equipment can be exposed to liquid water if the metal temperature falls below the dew point, if it rains, or if the equipment is cleaned with water.

Carbon steel, in contact with nitrate compounds and liquid water, can develop stress corrosion cracking, as discussed above in Section 13.2. Stainless steel equipment, in contact with the chlorides in the salt, can develop intergranular stress corrosion cracking, as discussed in Section 14.16.1.

To reduce the potential for atmospheric condensation, the temperature of the equipment can be maintained above the dew point by means of portable electric or propane-fired air heaters. Temporary tarps or tents can limit the exposure of the equipment to rain. Further, water in any form, including distilled water, must not be used to remove residual salt from the equipment. If the equipment must be cleaned prior to further work, such as welding, then only mechanical methods should be used.

18. Electric Heat Tracing

The electric heat tracing uses mineral insulated cables, electronic contactors, and pulse width control.

18.1 Design Criteria

Heat tracing is an expensive item, and there is an economic incentive to install as little heating capacity as possible.

The absolute minimum capacity would be one which maintains the equipment at the salt melting temperature (240 °C) at the design minimum ambient temperature and at the design plant operating wind speed. However, any reduction in the output from the heat tracing, or any degradation in the insulation, will result in equipment temperatures below the freezing point of the salt.

Some commercial projects have adopted a piping design criteria based, in part, on maintaining a metal temperature of 275 °C at the minimum design ambient temperature. This criterion is, in effect, an infinite preheat period. As an example, a DN300 (12 in.) line with 125 mm (5 in.) of calcium silicate of insulation requires a heat input of 185 W/m to maintain a temperature of 275 °C at an ambient temperature of 10 °C. However, in a commercial project, the pipe insulation is subject to damage due, for example, to maintenance personnel walking on the pipe. If the insulation is compressed by 25 mm (1 in.), then the local thermal resistance is reduced, and the steady state temperature which can be maintained by the heat trace drops to 232 °C. Similarly, the insulation can develop gaps due to daily thermal expansion and contraction cycles. If the local effective thermal conductivity of the insulation increases by 20 percent, then the steady state temperature which can be maintained by the heat tracing falls to 230 °C. In either situation, if stagnant salt is present in the line, then local freezing can be expected. Further, the heat tracing can no longer raise the pipe metal temperature above the freezing point, and the line will remain plugged until repairs are made to the insulation. When the plant is new, the pipe insulation will provide the required thermal resistance, and the heat trace system will be judged to be adequate. However, as the plant ages, the pipe insulation will degrade, and availability problems with frozen salt lines will start to appear.

A more robust design criterion is a preheat period of, for example, 12 hours. Continuing with this example, preheating the pipe to 275 °C in 12 hours requires a heat input of 354 W/m, or nominally double the heat input if the preheat period is infinite. With a heat input of 354 W/m, the steady state temperature of the pipe increases from 275 °C, as above, to a new value of 516 °C. Further, if the insulation is compressed by 25 mm, then the steady state pipe temperatures can, in principle, be raised as high as 435 °C. Similarly, if the effective thermal conductivity of the insulation increases by 20 percent due to gaps in the insulation, then the pipe temperatures can be raised to a theoretical value of 430 °C. It's unlikely that the duty cycles of the heat trace system would be set so high as to produce pipe temperatures as high as 430 °C, but the available heating capacity would be sufficient to both prevent freezing and to thaw a line should freezing occur. As such, the heat trace system will be adequate both when the plant is new and after the plant has accumulated decades of commercial use.

For a specific project, the preheat time would be selected based on a range of parameters, including the definitions of the plant operating states, the heat trace zone boundaries, the defined transition times between operating states, the importance of a particular zone in terms of plant availability, the installed cost of the heat trace system, and the difficulties in accessing the heat trace zones for maintenance of both the cables and the pipe insulation.

In general, the optimum heat trace preheat period has yet to be identified. A preheat period of 8 hours provides a robust system, but likely results in a system which is more expensive than can be justified. However, the preheat period should not be more than 24 hours, as the margins against insulation degradation are likely insufficient if a commercial project is to reach its availability targets over a time span of decades.

18.2 Control Software Location

Essentially all heat trace suppliers provide a standalone, and often proprietary, programmable logic controller to control the duty cycles of the heat trace cables. The alternate control approach is to use the plant distributed control system for this function. In most commercial projects, the former approach is selected over the latter in terms of convenience, purchase price, and programming price. Nonetheless, the latter is generally preferred over the former, for the following reasons:

- The selection of which heat trace circuits, and the selection of the duty cycles for each circuit, can be readily adjusted based on the plant operating state. This, in turn, reduces the annual demand for auxiliary electric energy, and makes for more stable operating temperatures in each zone

- The control system data historian can be used for the analysis of the heat trace system and the diagnosis of temperature control problems

- Alarms are transmitted directly to the control system operator screens. This avoids the need for an operator to move from an operator station to the heat trace vendor's console to analyze an alarm. This, in turn, makes it more likely that prompt responses will be made to each alarm.

At the Solar Two demonstration project, the original heat trace system installation used a proprietary programmable logic controller supplied by the system vendor. However, modifications to the heat trace components were made over the course of the project, and the control responsibilities were shifted from the vendor equipment to the distributed control system. This arrangement incurred expenses for adding input / output points to the control system. However, the benefits of improved convenience for the operators, improved accuracy in maintaining the zone temperature set points, faster diagnoses of unusual system characteristics (such as valve leakage), and a reduction in auxiliary energy demand more than offset the marginal expense to the control system.

In a commercial project, incorporating the heat trace control into the distributed control system will involve a large number of input and output signals. This, in turn, will increase the cost of

the distributed control system. To reduce the change in price, a hybrid control approach may be possible, as follows:

The standard controller provided by the vendor receives inputs from the circuit thermocouples, compares the zone temperatures with the set point temperatures, and sends output signals to the contactors supplying electric power to the heat trace cables

The distributed control system contains the logic for changes to the set point temperatures, and the activation / deactivation of zones based on the plant operating mode

As mentioned in volume 2, all that can be achieved still maintaining vendor PLCs for control of circuits and temperature measurements, and having then a fiber optics communication link to DCS which can be used to send all signals in the PLC. The logics on set-point changes and zones activation/deactivation can reside in the DCS, and also the full historian with everything available in the PLC. The PLC would only have the logics for start/stop when temperature setpoint is reached, hysteresis, and errors management.

18.3 Cable Redundancy

Inquires with heat trace cable suppliers on the topic of cable failure rates indicate that the cables should last the life of the project. However, commercial experience has shown that cable lifetimes are often measured in years, rather than decades. The relatively short lifetimes can be due to the following effects:

- Flexing of the cables produced by the daily thermal expansions and contractions of the piping
- High operating temperatures if the circuit controls mistakenly operate the cables at a duty cycle of 100 percent for extended periods
- High operating temperatures if the zone control thermocouple is located in an incorrect position, or if the thermal insulation around the thermocouple is damaged.

Further, the cable lifetimes can as short as days or weeks if the cables are exposed to salt from a leaking valve stem or from a leaking instrument connection. The cables, when active, can produce surface temperatures in excess of 650 °C. At these temperatures, salt in contact with the cable will quickly decompose, producing NOx and various oxides. The oxides are particularly corrosive, and will corrode the common sheath materials of stainless steel and Inconel. After this happens, the heating elements are exposed to water vapor in the air, and the elements soon fail.

In many commercial projects, the design criteria for the heat trace system often include a provision for only 1 installed redundant cable, regardless of the pipe size and the number of active cables needed to satisfy the preheat requirements. However, if the lifetimes of the cables are measured in, under ideal circumstances, years, then most of the heat trace zones will be forced to switch to the redundant cable in the first years of plant operation. Further, the

zones will be unable to meet the heat trace design requirements starting in perhaps year 10 of commercial service. If a salt leak occurs, then the cable lifetimes can be two to three orders of magnitude shorter.

If a zone has only 1 redundant cable, then the loss of 2 cables on a small line (< 10 in.) means that the heat trace can no longer prevent the salt from freezing in a stagnant line. The loss of 2 cables on a large line means that the zone can no longer satisfy the required preheat time from ambient. In both cases, the only solution is to remove the insulation from the lines, replace the failed cables, and reinstall the insulation. Depending on the location of the zone, and the length of the zone, the repair process could require a forced outage lasting between 1 day to 2 weeks. For a nominal 125 MWe project, this could incur a loss in revenue of $150,000 to $2,000,000.

For a specific project, an economic analysis should be conducted to determine the optimum number of installed redundant cables. The analysis should include the following considerations:

- Experience with cable failure rates on commercial projects, rather than projected cable lifetimes offered by the heat trace supplier

- Susceptibility to a salt leak, including the number of valves in the zone, the type of stem seal on the valves (bellows or packing), and the number of instruments in the zone using flanged connections

- Zone location, zone dimension, and access for repair. For example, the riser and downcomer piping in the tower of a central receiver project generally have poor accessibility, and the number of redundant cables is likely to be a higher number than for a short zone consisting of horizontal piping at grade.

- Effect on the plant availability of a failed cable, including longer preheat periods for an empty line, or the thawing time for a frozen pipe

- Installed cost of redundant cables.

In general, the optimum number of installed redundant cables has yet to be identified, and the number is likely to be a function of the characteristics of the zone. Nonetheless, the following values for redundancy may, in the long run, prove be representative:

- 100 percent for zones 1) with valves using conventional stem packings, and 2) with instruments with flanged connections

- 50 percent for zones 1) with valves using bellows stem seals, and 2) without instruments.

18.4 Control Thermocouples

In many commercial projects, 2 thermocouples are installed in each zone for temperature monitoring and control. In some cases, one of the thermocouples is an installed spare. As such, the temperature measured at the thermocouple is taken to be the temperature along the entire length, and around the entire circumference, of the zone.

Clearly, this is a simplified version of the actual conditions. Depending on the pattern of the cables installed in the zone, and depending on the location of the control thermocouple, local zone temperatures can differ from the measured zone temperature by as little as 1 °C to more than 150 °C. These deviations can be above, or below, the zone set point temperature.

Further, if the control thermocouple of Zone 1 is close to Zone 2, then the control of the heat trace circuits in Zone 1 can be determined by the temperature in Zone 2. At one commercial project, this led to a situation in which the heat trace cables, on a section of carbon steel piping, operated with a duty cycle of 100 percent. Within a few weeks, the pipe section failed. A postmortem examination estimated that metal temperatures exceeded 500 °C, which produced rapid oxidation of the steel.

In general, using 1, or in some cases 2, thermocouples for zone temperature control may not be adequate. The number of thermocouples should be based on the following:

- For long zones downstream of isolation valves, vent valves, drain valves, and pressure relief valves, multiple thermocouples are useful for identifying leakage patterns and the potential for frozen plugs

- For long zones with multiple pipe supports and anchors, multiple thermocouples are useful for identifying local areas with low pipe temperatures due to the higher heat losses at the supports and the anchors

- For short zones connected to other short zones, multiple thermocouples are useful for controlling each zone independently of the adjacent zones

- For carbon steel lines, multiple thermocouples are useful for identifying local areas with metal temperatures above the set point value. This, in turn, reduces the potential for overheating and damage due to corrosion.

Adding thermocouples, including the wiring back to the DCS, is not without expense. However, the ability to analyze the temperature profiles throughout a zone has proven to be useful in preventing local freezing, preventing local overheating, and in diagnosing the events leading to an outage.

Thermocouples should be added to a zone until the marginal cost of the thermocouple exceeds the marginal revenue associated with the expected increase in plant availability.

19. Significant Accomplishments and Conclusions

19.1 Parabolic Trough Projects using Organic Heat Transfer Fluids

Scores of commercial parabolic trough projects, using organic working fluids and nitrate salt thermal storage, have been constructed in Europe, Africa, and the United States. The plants have largely met the availability targets stated in the performance models, and are generally viewed as commercially successful.

Further refinements to the plant designs are likely to be limited to identifying optimum designs for the salt valves, the electric heat tracing, and the salt instruments.

19.2 Parabolic Trough Projects using Inorganic Heat Transfer Fluids

The preferred heat transfer fluid in trough projects using inorganic working fluids is the industry standard mixture of sodium nitrate and potassium nitrate. The salt permits collector field outlet temperatures as high as 520 °C, which, compared to trough projects using organic working fluids, reduces the unit cost of thermal storage and increases the efficiency of the Rankine cycle. However, this working fluid has not been adopted for commercial projects. The principal risk is frozen salt in the piping headers and in the heat collection elements. Methods have been demonstrated for freeze recovery; however, the time required for complete recovery ranges from weeks to months, depending on the capacity of the thawing equipment.

In general, projects using inorganic fluids can, in principle, offer a modest reduction in the levelized cost of energy compared to projects using organic fluids. However, much or all of the benefit can be erased if freezing in the collector field occurs more than once every several years.

19.3 Central Receiver Projects

Commercial central receiver plants (outside of China) have largely failed to meet the annual availability targets stated in the plant performance models. The largest contributor to the low availability values has been leaks in the hot salt storage tanks.

The tanks are typically designed to a combination of API 650 (general tank geometry), ASME Section II (allowable material stresses), and ASME Section VIII Division 2 (low cycle fatigue). Under Section VIII Division 2, allowable stresses can be as high as 300+ MPa, and simultaneously satisfy a fatigue life of 30 years. However, design temperatures are high enough (500+ °C) to initiate creep in stainless steel, yet Section VIII Division 2 does not consider damage mechanisms due to creep.

As an alternate approach, ASME Section III Division 5 can be adopted as the design basis. This Section includes assessments of the combined effects of fatigue damage and creep damage. Interestingly, to satisfy a creep lifetime of 30 years, operating stresses must be limited to about 120 MPa. This is a significant reduction from the stresses permitted under Section VIII Division 2, and this should improve the availability of the hot tank.

20. Path Forward

The technology discussions reflect the state of the art in 2025. Some design features noted in the report are industry standards. One example is the use of binary nitrate salt as the storage medium in parabolic trough plants using thermal storage. Due to favorable operating and economic experience, the industry standards are unlikely to change for future commercial projects.

In contrast, essentially all of the hot salt tanks in commercial central receiver projects (outside of China) have experienced some form of failure. The sources of the failures are varied, and include 1) buckling of the floor due to compressive stresses generated by radial and circumferential temperature gradients, 2) high compressive stresses in the floor due to friction associated with thermal expansion, 3) stress relaxation cracking of Type 347H stainless steel, and 4) selection of design codes (Section VIII Division 2) which evaluates damage due to fatigue but does not consider damage due to creep.

The level of understanding of the failure mechanisms in hot salt tanks is an order of magnitude better than the level of understanding in the previous round of commercial plant development. However, at the time of this report, a complete understanding of the failure mechanisms is not known. Fortunately, additional analyses of hot salt tanks are currently underway at government laboratories, commercial solar plant developers, and commercial nuclear plant developers. Ideally all, but more likely only some, of the results of the analyses will be made available in public forums. Nonetheless, the most valuable contributions to developing a reliable tank design are derived from fabricating, commissioning, and operating a tank at a commercial size. Naturally, much of the experience with the next round of installations will be treated as proprietary by the project developers. Nonetheless, some design and performance information will be shared due to the industry grapevine and to personnel changes among engineering companies.

As outlined in the Statement of Project Objectives, one of the goals of the Design Basis Document project is to revise and update the text as additional information becomes available. New information is expected to be available not only on hot salt tank designs but also on topics (as examples) 1) steam generator fabrication methods, 2) steam generator startup and shutdown procedures, 3) impedance heating of heat collection elements in parabolic trough plants using inorganic heat transfer fluids, 4) nitrate salt instruments, and 5) post weld heat treatment of Type 347H stainless steel piping. Revisions and additions to the Design Basis text could be conducted as an extension to the existing contract with Solar Dynamics, or as a new contract issued to an engineering contractor with salt experience.

21. Products

Conference Proceedings, Papers, and Presentations

- DOE Webinar: Design Basis Document / Owner's Technical Specification for Nitrate Salt Systems in CSP Projects, May 2022
  Presentation: https://doi.org/10.2172/2587401

- Hypothesis of Sources of Failures in Hot Salt Tanks at Central Receiver Projects, SolarPACES 2022 Conference, Albuquerque, New Mexico, September 2022
  Paper: https://doi.org/10.52825/solarpaces.v1i.635
  Presentation: https://doi.org/10.2172/2587379

- Current Molten Salt Tanks at 560 °C: Challenges and Developing Solutions. Panel presentation on Thermal Energy Storage for Electricity and Industrial Heat Applications, ASME 17th International Conference on Energy Sustainability, July 2023
  Presentation: https://doi.org/10.2172/2587385

- DOE Virtual Receiver and Reactor Workshop: Nitrate Salt Receivers, February 2024
  Presentation: https://doi.org/10.2172/2587387

- 2024 SETO Peer Review: Design Basis Document / Owner's Technical Specification for Nitrate Salt Systems in CSP Projects, March 2024
  Poster: https://doi.org/10.2172/2587398

Technical Reports

Revisions 0 of the 3 volumes in the Design Basis Document / Owner's Technical Specification for Nitrate Salt Systems in CSP Projects can be found at: https://doi.org/10.2172/2587356 and https://www.solarynllc.com/csp-plant-technologies.

22. Project Team and Roles

The project team, and the principal participants, include:

- Solar Dynamics: Bruce Kelly and Luca Imponenti
- Electric Power Research Institute: Thomas Sambor and Steven Kung
- Malta: Benjamin Bollinger, Samar Shah, and Tian Ong

The division of responsibility among the project team is as follows:

- Task 1 - Table of Contents: Solar Dynamics lead; EPRI and Malta support
- Task 2 - Functional Requirements: EPRI lead; Solar Dynamics and Malta support
- Task 3 - Operating Modes and Transitions Between Modes: EPRI lead; Solar Dynamics and Malta support
- Task 4 - Risk Analysis: EPRI lead; Solar Dynamics and Malta support
- Task 5 - Operating Requirements: EPRI lead; Solar Dynamics and Malta support
- Task 6 - Functional / Prescriptive Specifications: Solar Dynamics lead; EPRI and Malta support
- Task 7 - Current State of the Art: Solar Dynamics lead; EPRI and Malta support
- Task 8 - Alternate Designs: Solar Dynamics lead; EPRI and Malta support
- Task 9 - Industry Review: EPRI lead; Solar Dynamics and Malta support
- Task 10 - Diversity, Equity, and Inclusion Plan: Deleted from scope of work
- Task 11 - Final Report and Public Dissemination: Solar Dynamics lead; EPRI and Malta support

23. References

Literature references are cited in the footnotes.